Department of Biomedical and Biotechnological Sciences
University of Catania School of Medicine

International PhD Program in Neuroscience
XXXI Cycle

Walter Gulisano

A renewed vision for Amyloid-β and tau in Alzheimer's disease pathophysiology

Ph.D. THESIS

Coordinator: *Prof. Salvatore Salomone*

Tutor: *Prof. Agostino Palmeri*

Co-Tutor: *Prof. Daniela Puzzo*

Academic Year 2017-18

Index

Synopsis

The aim of this thesis was to study the pathogenetic mechanisms underlying Alzheimer's disease (AD), a neurodegenerative disorder affecting the elderly and characterized by memory loss, personality changes and cognitive dysfunction leading to dementia.

I will discuss the main projects in which I participated aimed at understanding the role of the main molecular interactors involved in AD pathogenesis, i.e. Amyloid-beta peptide (Aβ) and tau protein, on hippocampal synaptic plasticity and memory in animal models. After reviewing the pathophysiological models that have been developed so far, our general purpose was to study novel aspects of Aβ and tau involvement in physiological and pathological conditions to give a different interpretation of the disease.

The present thesis is divided into different sections, as follows:

1. The *General Introduction* provides a comprehensive overview on the role of Aβ and tau in both physiology and pathology. The purpose is to summarize the state of the art, reporting the main discoveries that have driven and inspired the research projects included in this thesis (Gulisano et al, J Alzh Dis, 2018).

2. *Chapters 1-3* focus on the physiological and pathological role of Aβ. In particular:

- *Chapter 1* reports a study performed to understand whether different aggregation status (monomers vs. oligomers), concentrations (200 nM vs. 200 pM) and isoforms (Aβ40 vs Aβ42) of the peptide exert a beneficial or detrimental effect on hippocampal synaptic plasticity and memory (Gulisano et al, Neurobiol Aging, 2018).
- *Chapter 2* reports a study aimed at understanding the relationship between Aβ and cGMP and the underlying molecular mechanisms during hippocampal

synaptic plasticity and memory in physiological conditions (Palmeri et al., J Neurosci, 2018).

- *Chapter 3* reports a pre-clinical study in which the increase of cGMP and cAMP obtained by a treatment with sub-efficacious doses of phosphodiesterase inhibitors was able to revert the AD phenotype in animal models of AD (Gulisano et al., Neuropharm, 2018).

3. *Chapter 4 and 5* focus on the role of tau and its interaction with Aβ. In particular:

- *Chapter 4* reports a study showing that an acute exposure to extracellular tau oligomers is able to impair synaptic plasticity and memory. Here, the interaction between Aβ and tau was also studied by evaluating the effect of a combination of subthreshold doses of Aβ and tau oligomers (Fa' et al., Sci Rep, 2016).
- *Chapter 5* reports a study focusing on the role of Amyloid precursor protein (APP) as a common target mediating the detrimental effects of Aβ and tau on synaptic plasticity and memory (Puzzo et al., eLife, 2017).

4. A *General Discussion* will summarize the relevance of these findings giving new insights into possible future directions.

General introduction

"The saddest aspect of life right now
is that science gathers knowledge
faster than society gathers wisdom."
Isaac Asimov

Preface

Alzheimer's disease (AD) is a neurodegenerative disorder clinically characterized by dementia, defined as a deficit of memory function and at least one other cognitive domain (language, praxis, gnosis, executive function, judgment, and abstract thought) as well as functional impairment, without alteration of the state of consciousness. In the last decades, AD has gained rising attention for its growing prevalence in aging populations, with 46.8 million people affected by the pathology worldwide, a number expected to increase up to 74.7 million in 2030 and 131.5 million in 2050. Besides representing a serious health and social problem, the disease causes exorbitant costs for the healthcare system estimated as 604 billion dollars in 2010 that represented a 35.4% increase in only 5 years[1,2]. Despite the numerous efforts to counteract the disease, no therapies have so far proven to prevent AD onset or progression. To date, data from thousands of basic, pre-clinical, and clinical studies have identified amyloid-β peptide (Aβ) and tau protein as the key actors in the pathophysiology of AD, mainly because of their deposition in the characteristic histopathological brain lesions, the senile plaques for Aβ and the neurofibrillary tangles (NFTs) for tau, and the increase of their soluble forms in the brain of AD patients. However, therapeutic approaches aimed to decrease Aβ levels that have been attempted so far, have failed. Similarly, tau-based clinical trials have not yet produced positive findings.

The overall goal of this chapter is to provide a critical assessment of the literature on mechanisms underlying disease occurrence and progression. Specifically, we will revisit studies on Aβ and tau, as well as on their interaction, discussing the amyloid hypothesis - that has dominated the AD field in the last 25 years - and the role of tau protein.

Amyloid-β peptide and Alzheimer's disease: more than one century of research

Aβ derives from a complex cleavage of APP, a type I single-pass transmembrane protein constituted by 639–770 amino acids in humans, and highly expressed in the central nervous system where it exerts a variety of physiological functions[3]. APP is initially cleaved by α-secretase or β-secretase, generating soluble and carboxyterminal fragments (CTF). α-secretase activity leads to the formation of sAPPα and CTF83, whereas β-secretase generates sAPPβ and CTF99. Then, γ-secretase intervenes, further cleaving CTF83 and CTF99, generating the intracellular peptide AICD/AID (amyloid intracellular domain) and a small p3 peptide from CTF83, and AICD/AID and Aβ from CTF99. Based on this biochemical processing, the cascade initiated by α-secretase has been considered neuroprotective when compared with the β-secretase cleavage, leading to the amyloidogenic cascade and the formation of Aβ[4]. Based on the γ-secretase site of cutting, different isoforms of Aβ can be generated, composed of 38–43 amino acids. Aβ40 is the predominant species, whereas Aβ42 is present at lower concentrations but has received more attention in the AD field due to its high propensity to form aggregates. However, in the brain of AD patients, Aβ38 and truncated forms at N-terminal region, i.e., Aβ15, Aβ16, and Aβ17, have been also detected[5]. Aβ is undoubtedly the most studied protein in AD and its putative role in the pathogenesis of the disease has oriented drug development and clinical trials for several decades.

But how and why did the AD amyloidogenic theory emerge? From a historical perspective, it was at the beginning of the last century when Alois Alzheimer and other European neuropsychiatrists, e.g., Gaetano Perusini, attributed a nosographic identity to a form of "mental" disorder characterized by memory loss, hallucinations, and disorientation. At that time, the most influent personalities in psychiatry, Sigmund Freud and Emilin Kraeplin, fervently disputed on the origin of psychiatric illness, respectively emphasizing the role of the psyche or of organic and genetic factors. The mind/brain diatribe led several scientists to seek for the "material" causes of mental diseases. In this context, Alzheimer and Perusini, strongly supported by Kraeplin,

observed that the psychiatric symptoms of dementia could be correlated to peculiar histological lesions in postmortem brains. In the autopsy of the first described AD patient, Auguste Deter, cortical atrophy, neurons filled with neurofibrils, and extracellular miliary foci of an unknown substance were observed. After Alzheimer's death, research studies on the disease were few until the 1980s, when epidemiological studies revealed an increase of patients affected by primary dementia.

It was during these years that key discoveries were made, fated to influence research in the field until today. Based on Alzheimer's histological descriptions, Aβ and tau were recognized as the main components of extracellular foci (senile plaques) and intracellular neurofibrils (NFTs), respectively[6–8]. In the same period, the first genetic mutation linked to dementia was identified on chromosome 21 coding for the APP[9]. This autosomal dominant disease was responsible for early onset AD (EOAD) characterized by high levels of Aβ. Other genetic mutations were identified in Familiar Alzheimer's disease (FAD), involving genes responsible for Aβ production such as presenilin 1 (PS1) on chromosome 14, which mutation is the most common cause of EOAD, and presenilin 2 (PS2) on chromosome 1. Consistent with these findings, the presence of AD-like pathology in patients affected by Down's syndrome, due to a trisomy of chromosome 21, reinforced the idea that the increase of Aβ played a major role in AD pathogenesis. Based on these data, in 1995 the first mouse model of AD carrying an APP mutation was engineered[10] and, over time, different models for pre-clinical studies have been generated based on the most common mutations observed in FAD[11]. These findings contributed to the excitement around the "Amyloid Cascade Hypothesis"[12–14], recognized as the pathogenic mechanism underlying AD. Because insoluble fibrils of Aβ were present in AD plaques, and could be formed in vitro from synthetic Aβ, they have dominated the scene until a fundamental breakthrough confirmed by several in vitro and in vivo studies indicated that soluble forms of Aβ were also present in the brain[15,16]. Aβ soluble aggregates range from monomers to oligomers (molecular aggregates consisting of a few monomer units) and pre-clinical studies confirmed that dimers, trimers, tetramers, dodecamers, and high molecular weight oligomers were all able to induce neurotoxic effects as well as to induce an

immediate impairment of synaptic plasticity, and in particular of hippocampal long-term potentiation (LTP), thought to be the electrophysiological correlate of memory (for a review on the role of Aβ oligomers, see[17]). Moreover, Aβ oligomer presence in human cerebrospinal fluid (CSF) could be already recognized decades before AD onset[18]. These data led to the formulation of another theory, the "Oligomer Hypothesis"[19–21], according to which Aβ oligomers but not monomers or fibrils were responsible for synaptic dysfunction and memory loss in AD[21,22]. This further influenced AD drug discovery so that new therapies aimed at specifically targeting Aβ oligomers were developed in addition to those clearing Aβ plaques. Unfortunately, while the "Oligomer Hypothesis" is still a matter of investigation, and data are being gathered to test the grounds of its premises, the clinical failure of most of the anti-Aβ drugs has strongly destabilized this concept. Clinical trials to date show that, despite successful results obtained in animal models of AD, anti-Aβ drugs have not yet been shown to modify cognition in humans although they might be able to reduce plaque or amyloid burden. So far (based on Medline database search and Clinical-Trials.gov): 1) active immunization (i.e., AN-1792, CAD-106, and vanutide cridificar) have not proven effective and several side effects were reported; 2) passive immunization with monoclonal antibodies bapineuzumab, solanezumab, crenezumab, and gantenerumab have not yet succeeded, and although a recent clinical trial with aducanumab has shown a dose-dependent reduction of Aβ plaques, the study was not sufficiently powered to detect clinical changes and the drug is undergoing further investigation[23]; and 3) a number of clinical trials with drugs aimed at preventing Aβ formation by inhibiting β- or γ- secretases have also failed or were interrupted; among these, the γ-secretase inhibitors semagacestat and avagacestat did not show efficacy, and actually induced mildworsening in cognition and severe side effects, whereas the EPOCH trial with the newest β-secretase inhibitor verubecestat was stopped for the lack of any positive effect. Notwithstanding these discouraging results, several scientists are still developing anti-Aβ therapies, convinced that the failure of Aβ tailored drugs might relate to the particular drugs chosen, inadequate dosage, or the fact that treatment was started in a late phase of the disease when Aβ-induced damage cannot be reversed.

This chapter is written, in turn, with the belief that a careful evaluation of the knowledge in the AD field is due prior to further investing resources with anti-Aβ therapies. Evidences that have been underestimated for a long time are now gaining ground, questioning the way in which the actual role of Aβ in AD pathogenesis is currently thought. First, late onset AD (LOAD), representing 95% of AD cases, is not linked to genetic anomalies leading to a direct overproduction of Aβ, as in FAD, although the phenotype might be comparable. However, pre-clinical studies on AD mouse models have been almost entirely performed on mice presenting FAD-like mutations leading to an increase of Aβ. Second, we know since the 1990s that there is no correlation between Aβ deposition and clinical degree of dementia among affected individuals[24–27], and plaques might occur in the brains of individuals with no sign of dementia[26,28,29]. Third, recent studies have suggested that plaque formation might be a reactive process[30] with a protective role by decreasing oligomer levels[31]. Fourth, a vast literature claims that Aβ exerts a physiological role in the CNS interfering with neuronal growth, neurotransmitter release, synaptic function, and memory formation[32,33]. Indeed, our group and others have previously demonstrated that administration of low concentrations of oligomeric Aβ positively modulate synaptic function[34–36] and, conversely, blocking endogenous Aβ in the healthy brain resulted in an impairment of synaptic plasticity and memory[35,37]. Finally, even Aβ concentration per se has become a relative concept, as the persistence of a low picomolar Aβ concentration in extracellular fluids provides for detrimental outcomes in synaptic plasticity[38]. In conclusion, taking into account almost one century of research, it emerges that the Aβ model of AD is insufficient[39,40] and needs to be reconsidered[33].

A revaluated player in Alzheimer's disease pathogenesis: Tau protein

As described above, the intricate story of Aβ and tau began with the brain of Auguste Deter, but most of the research efforts have been directed toward Aβ. Recently, the discontent generated by too many anti-Aβ therapy failures has induced several groups to re-focus on tau. Tau is a microtubule-associated protein originally described as a heat stable protein essential for microtubule assembly and stabilization[41]. It is present in the human brain in six main isoforms, deriving from the alternative splicing of exons 2, 3, and 10 of microtubule-associated protein tau (MAPT) gene. This process appears to be of particular interest for exon 10 splicing which determines the presence of tau isoforms containing 3- (3R) or 4-repeats (4R) of a ∼32 amino acid sequence in the microtubule binding domain (MBD)[42]. Moreover, the splicing process of exons 2 and 3 determines the number of 29-residue near-amino-terminal inserts which results in isoforms containing 0, 1, or 2 inserts (0N, 1N, 2N)[43]. Both R and N repeats are capable of microtubule-binding and assembly-promoting activity, whereas the flanking regions are more likely involved in binding processes[44,45]. In the last decades, many studies have demonstrated tau physiological involvement at different subcellular localizations: 1) at axonal level, by regulating axonal elongation, maturation and transport[46–49]; 2) in dendrites, participating in synaptic plasticity[50,51]; and 3) in nucleus, maintaining the integrity of genomic DNA, cytoplasmic and nuclear RNA[52,53]. From a functional point of view, tau can be divided in four different regions consisting of a N-terminal domain, a proline-rich domain, a MBD, and a C-terminal domain[54–56]. The N-terminal domain is rich with negative charges devoted to separation of different microtubules by electrostatic repulsion when tau is bound to a certain microtubule[45,57,58]. Interestingly, the C-terminal domain, besides its key role in regulation of microtubule polymerization induction and interaction with plasma membranes[59–62], creates an overall asymmetry in the molecule contributing to this microtubule spacing function thanks to its neutral charge. The proline-rich domain and the MBD with their multiple aminoacidic acceptor

residues are more involved in interactions with different signaling proteins, which can be scaffolded by tau or can modify tau conformational status and activity itself[54]. The presence of multiple binding sites confers to tau many interaction possibilities in regards to cell signaling. The flanking region of MBD contains the majority of phosphate acceptor residues, and the phosphorylation of these sites is relevant for regulating microtubule polymerization[63–66], regulation of axonal transport[67] and neurotransmitter receptors[68,69], interference with vesicles trafficking[70] and apolipoprotein E[71], interaction with Src-family kinases[62,72–75], and many others[54–56].

The multiple roles of tau in neuronal physiology have been widely studied and, undoubtedly, a fine regulation is needed to maintain tau structure and function. Accordingly, a wide range of neurodegenerative disorders known as tauopathies have been recognized and classified with respect to the predominant species of tau that accumulates: 1) 3R tauopathies (i.e., Pick's disease); 2) 4R tauopathies (i.e., corticobasal degeneration and progressive supranuclear palsy); and 3) 3R + 4R tauopathies (i.e., AD)[42]. Biochemical studies have demonstrated that deposition of insoluble tau aggregates in NFTs depends upon a dysregulated phosphorylation process of the flanking regions of tau. In fact, while two phosphates per molecule of tau are normally present[76], analysis of tau from AD brains has revealed the presence of about eight phosphates per molecule of tau[77]. For this reason, tau phosphorylation abnormalities have been linked to misfolding and deposition of the protein in the diseased brain[78]. Although tau has been defined as a "natively unfolded" protein with a low tendency to aggregation[79], phosphorylation of certain residues or detachment from microtubules[79–81] might change its conformational status and consequently its aggregation propensity. However, the undefined structure of tau in solution has precluded crystallographic analyses leaving a lack of knowledge about the protein structure[82]. Moreover, notwithstanding electron microscopic visualization of tau bound to microtubules demonstrated a linear alignment lengthwise to the protofilament ridges, the protein structure keeps holding a disordered state[83,84]. Interestingly, when in a solution, tau spontaneously tends to modify its conformation in favor of a paperclip-like structure that might prevent its aggregation[55,82], unlike Aβ that has a high tendency

to aggregate in a solution due to its biochemical properties. Thus, alterations of tau (i.e., hyperphosphorylation, truncated forms) could inhibit the constitution of the paperclip-like structure leading to paired helical filament (PHF) and NFT formation[85]. In this context, tau hyperphosphorylation has been widely studied and the sequence hyperphosphorylation→PHFs→NFTs linked to AD, even if it is unlikely to represent by itself the main pathogenic event for several reasons. First, tau phosphorylation has been demonstrated to be responsible for aggregation only when occurring at certain residues[86], whereas in other sites it has the opposite effect thus preventing aggregation[80]. Moreover, tau hyperphosphorylation is not a prerogative of AD, since it occurs in several other conditions such as hypothermia[87], starvation[88], chronic stress[89], and anesthesia[90,91]. Interestingly, the amount of PHFs and NFTs is slightly related to the severity of neuronal damage and cognitive impairment in humans. Experiments on regulatable mouse models of tauopathy demonstrated that a variant of human tau with the pro-aggregant mutation ΔK280 developed synaptic and memory impairment as well as tau hyperphosphorylation and pre-tangle formation. However, when the proaggregant tau was turned off, synaptic deficit was rescued even if insoluble tau was still present[92]. Other studies on transgenic mice expressing mutant tau (P301L mutation), which could be suppressed with doxycycline, demonstrated that behavioral impairment and neuronal loss were recovered when suppressing transgenic tau, whereas NFTs accumulation continued[93]. Moreover, in the P301S model of tauopathy, synaptic damage and cognitive impairment occurred before the emergence of NFTs[94]. Some authors also reported that, in vitro, abnormally phosphorylated tau can sequester normal tau into tangles of filaments, leading to the hypothesis that tau accumulation into PHFs might initially be neuroprotective until it starts compromising neuronal function as a space-occupying lesion[95]. The observations that synaptic and memory impairment is not mediated by NFTs, and that insoluble deposition of tau might be a compensatory protective mechanism suggested that synaptic failure might be sought in soluble oligomeric species of tau, resembling the “Oligomeric Hypothesis” already formulated for Aβ. Soluble tau was found to be most acutely toxic in animal models of tauopathy[93,94,96]. Most importantly, increases in granular tau oligomer levels occur

before NFTs form and before individuals manifest clinical symptoms of AD, suggesting that increases in tau oligomer levels may represent a very early sign of brain aging and AD[97]. We have recently demonstrated that an acute exposure to tau oligomers (but not monomers) both in vitro and in vivo is detrimental to LTP and memory[98]. Noteworthy, this toxic effect was exerted by a different preparation of oligomeric tau, i.e., recombinant tau 4R/2N, tau derived from AD patients, tau derived from hTau mice[98]. These results are in agreement with other observations reporting that tau oligomers 1) impair synaptic function and memory in wild type mice[99], 2) correlate with cognitive impairment in rTg4510 mice[100], and 3) accelerate pathology in hTau mice[101]. Pre-clinical findings have been confirmed by studies on humans showing the increase of oligomeric forms of tau in the brain of AD patients compared to controls, occurring before NFT formation and clinical symptoms[97]. Interestingly, tau oligomers have been also found in other tauopathies such as progressive supranuclear palsy, dementia with Lewy bodies, and Huntington's disease[101–103].

These aspects should be taken into account when designing new drugs targeting tau to avoid the same issues already experienced with anti-Aβ treatments. Notwithstanding the increase of tau oligomers in the AD brain and CSF, drugs aimed at inhibiting tau aggregation or dissolving existing aggregates, i.e., methylthioninium chloride and its second-generation derivatives such as TRx0237, have not been proven efficacious in clinical trials. A Phase II study with TRx0237 was terminated after a few months for "administrative" reasons, whereas Phase III studies have reported negative results on cognitive improvement (see clinicaltrials.gov for details). However, it is not clear whether these drugs actually inhibit tau aggregation in humans. Also, this makes us wonder whether the increase of tau oligomers in AD patients should be better considered as a pathogenic marker of the disease rather than a target of therapeutic strategies.

Aβ and tau oligomers: a game at the synapse resulting in memory impairment

How do Aβ and tau induce memory loss? According to most of the studies, the answer should be sought at the synapse. Although cortical atrophy and synaptic loss have been reported in AD brains, mainly due to a structural damage imputable to plaques and tangles in a later stage of the disease, a subtle effect exerted by soluble forms of Aβ and tau at the synapse seems to be the earlier event underlying memory loss[98,99,104,105]. Several studies have demonstrated that administration of different preparations of oligomeric Aβ and tau (synthetic, from transgenic mice, from AD brains) impaired synaptic plasticity and memory. The role of soluble oligomers also emerged in studies performed on AD mouse models, since synaptic and memory dysfunction was present before the appearance of plaques or tangles[17,106]. In vitro and in vivo studies have shown that Aβ and tau derange molecular signaling pathways crucial for synaptic plasticity at both pre- and post-synaptic sites. Both Aβ and tau interfere with the transcription factor cAMP response element-binding protein (CREB), whose phosphorylation at Ser133 is thought to be one of the fundamental events in memory formation[107–109]. In particular, Aβ inhibits the physiological increase of CREB phosphorylation during LTP[110–112], causing a downregulation of both the NO/cGMP/PKG and the cAMP/PKA pathways, two cascades converging on CREB. Tau overexpression and hyperphosphorylation was also found to be accompanied by a reduction of CREB phosphorylation at Ser133, mediated by a decrease of phosphorylation of NR2B (Tyr1472)[113]. Moreover, synaptic plasticity and memory impairment caused by h-tau overexpression was reported to be related to nuclear dephosphorylation/inactivation of CREB[114]. Interestingly, these findings were validated in humans affected by AD showing a decrease in CREB and phospho-CREB levels in hippocampus[115–119]. Aβ and tau also target other molecules upstream of CREB, among which the Ca2+/calmodulindependent protein kinase II (CaMKII), another key molecule needed for LTP and memory formation[120]. CaMKII is dysregulated in the hippocampus of AD mouse models and patients (for a review,

see[121]) and it has been demonstrated that Aβ oligomers interfere with its phosphorylation leading to AMPA receptor dysfunction[122–124]. On the other hand, evidences for the interaction tau-CaMKII have been reported since the late 1980 s in works analyzing the ability of CaMKII to induce an AD-like tau phosphorylation[125,126]. CaMKII phosphorylates tau at different sites and this might prevent tau binding to microtubule[127] and modify tau structure leading to PHFs formation[128]. Indeed, CaMKII colocalizes with tau mRNA, PHFs, NFTs in AD brains (for a review, see[121]). Recently, in a drosophila model of tauopathy, suppression of tau phosphorylation at Ser262/356 inhibited tau toxicity through a mechanism involving calcium homeostasis dysregulation driven by CaMKII[129]. The deleterious effects of Aβ and tau also involved BDNF, a critical factor linked to neuronal survival and function that is needed for synaptic plasticity and memory. A decrease of BDNF levels in serum and brains of AD patients correlates with cognitive impairment, and BDNF polymorphisms have been proposed to be involved in AD pathogenesis[130]. Moreover, several in vitro and in vivo studies have confirmed that Aβ-induced LTP and cognitive dysfunction are associated with a reduction of BDNF levels[130]. Recently, a loss of BDNF has been also reported in THY-Tau22 and P301L mouse models of tau pathology[131,132].

Taken all together, these findings suggest that restoring synaptic-related molecules and second messenger systems regulating memory mechanisms might be a viable therapeutic strategy to counteract AD[112]. Most importantly, these data point at common synapse-related mechanisms affected by both Aβ and tau during memory impairment.

Aβ and tau activity dependent secretion, neuronal uptake, and spreading of the disease

Because Aβ and tau interfere with the synaptic machinery, another relevant subject of investigation has been to determine whether they act via extracellular or intracellular mechanisms. Based on the localization of insoluble deposits, for several years Aβ has been considered an extracellular protein and tau an intracellular one. However, it is now clear that this rigid vision is no more applicable, since both Aβ and tau can be found inside and outside neurons. Notwithstanding most of the studies have been performed on models of disease, the extra- and intracellular presence of Aβ and tau is the result of a physiological dynamic process in which the two proteins are secreted at the synapse and internalized by neurons. A relevant body of data has supported the hypothesis that neurons are able to secrete Aβ in an activity dependent fashion. In vitro studies performed by applying drugs that decrease (i.e., tetrodotoxin or high magnesium) or increase (i.e., picrotoxin) neuronal activity have shown a concomitant decrease or increase of Aβ secretion in organotypic slices overexpressing human APP Swedish mutation[133]. An in vivo approach by using microdialysis also revealed an increase of Aβ levels in the brain interstitial fluid concomitant to the increase of synaptic activity[134] or paralleling the neurological status[135]. An increase of Aβ secretion has also been found during learning in healthy wild-type mice[37]. Based on the fact that synaptic activity stimulates Aβ secretion, and that extracellular Aβ is known to reduce synaptic plasticity, it has been proposed a theory according to which an increase of synaptic (and cognitive) activity is linked to AD pathogenesis. However, although an increase of brain activity in AD could be supported by data indicating hyperexcitability in transgenic mice and human AD patients[136,137], this activity-dependent role of Aβ should be better viewed as a physiological mechanism occurring within the healthy brain, especially because levels of Aβ secreted during activity are in the picomolar range and are not neurotoxic[34,37,138]. Thus, the high increase of extracellular Aβ during AD might be due to a derangement of this physiological loop or it could be a consequence of degeneration of neurons that have previously accumulated Aβ at

intracellular level (for a review, see[139]). Whether the impairment of synaptic function is directly mediated by these high extracellular Aβ levels or by Aβ accumulated inside neurons, is still a matter of debate.

Surely, these two pools are strictly interconnected, since extracellular Aβ induced the accumulation of intracellular Aβ by stimulating APP processing[140] or by a direct APP-mediated internalization[141]; in turn, intracellular Aβ disrupts synaptic transmission and plasticity[142]. Interestingly, tau also undergoes the same dynamic flux characterized by activity-dependent secretion and neuronal internalization. Indeed, application of KCl or glutamate to cultured neurons resulted in an increase of tau secretion[98,143] mediated by AMPA receptor activation[143]. In vivo studies reported an increase of tau in brain interstitial fluid when stimulating neurons with high K+ perfusion, or after stimulation of the N-Methyl-d-aspartic acid (NMDA) receptors, or picrotoxin administration[144]. An increase of tau secretion also paralleled the increase of glutamate release induced by an antagonist of metabotropic glutamate receptors 2/3[144]. The phenomenon was further confirmed in different cultured neural cell lines where extracellular tau levels were modified proportionally to synaptic activity[145]. On the other hand, several pre-clinical studies have demonstrated that exogenously applied tau can increase of Aβ secretion in organotypic slices be internalized by neurons[98,146–149] and glial cells[150–152] with different mechanisms involving bulk endocytosis[149], binding to heparan sulfate proteoglycans[153] or to APP[141]. Activity dependent secretion and neuronal uptake of Aβ and tau have been related to the spread of the disease throughout the brain, a process known as spreading which refers to the capability of neurotoxic proteins to diffuse from a neuron to another, expanding the disease from a restricted area to the entire brain. This type of dissemination, defined as “trans-synaptic spreading”, is thought to occur among different brain areas functionally connected[154,155] and is supported by observations on postmortem AD brains as well as by clinical studies exploiting computerized x-ray tomography (CT) and magnetic resonance imaging (MRI) techniques, that allow tracing different neuropathological markers such as atrophy of certain brain areas, brain ventricles enlargement, and deposition of amyloid plaques and NFTs (for a review, see[78]). However, it should be pointed out that imaging

biomarkers like fluorodeoxyglucose in PET scans are associated to discrete difficulties in data interpretation, as they are also positive in Suspected Non-Alzheimer Disease Pathophysiology (SNAP)[156]. Evidence for AD spreading and progression throughout the cortex was reported more than 30 years ago, based on tangle distribution in the proximity of the same pyramidal neurons that give connectivity to other brain areas[157]. At the present day, neither the cause that initiates spreading nor its underlying mechanisms have been identified, but useful information has come from pre-clinical studies. Notwithstanding tau has been under the spotlight for many years, one of the first evidence of spreading in AD dates back to the 1990 s and involves Aβ[158,159]. When trying to unravel the causes of Aβ diffusion, studies have often focused on the first area affected in AD, the medial temporal lobe, and in particular, the entorhinal cortex (EC). EC superficial layer is susceptible to Aβ-dependent neurodegeneration, and this can negatively affect its primary afferent regions resulting in a disruption of the whole circuitry in both mouse models and AD patients[160,161]. Consistently, an increase of mutant APP in layer II/III neurons of EC has been shown to elicit a molecular and functional disruption in the CA1 area of the hippocampus with presence of soluble Aβ in the dentate gyrus, Aβ deposits in the performant pathway, and epileptiform activity in the parietal cortex[162]. Further studies in mutant human APP (mhAPP) mice have reported an age-dependent progressive deterioration of synaptic plasticity and memory spreading from the EC to the hippocampus[163], a phenomenon mediated by microglial RAGE activation and subsequent increase in p38MAPK phosphorylation[163]. Consistently, other studies reported the capability of reactive microglia in secreting Aβ through microvesicles, which in turn would promote Aβ toxicity to neurons through their axons[164–166]. Accordingly, other supporting evidences indicate that after administration of fluorescent oligomeric Aβ to neurons, a higher percentage of the protein was found surrounding neurons, and this process needed the presence of differentiated neuritis to occur[167]. Cell-to-cell transfer mechanism has been reported for different Aβ species (i.e., oAβ1–42 TMR, oAβ3(pE)–40TMR, oAβ1–40TMR, and oAβ11–42TMR), and this prion-like spreading was attributed to an insufficient activity of cellular clearance degradation systems[168]. Another mechanism proposed for Aβ

spreading relies on the presence of tunneling nanotubes (TNTs) consisting of cellular membrane extensions creating a direct connection between cells[169]. TNTs have been demonstrated to mediate highspeed transfer of Aβ among neurons, through a p53/EGFR/Akt/PI3K/mTOR pathway that, in turn, would trigger F-actin polymerization promoting TNTs formation[170]. However, Aβ has been shown to be secreted by neurons through exosomes[171] that could be internalized and stored from the acceptor neuron as lysosomal vesicles through a macroautophagy mediated mechanism[167,172]. In any case, despite these numerous evidences, there is not a uniform consensus about the causes or mechanisms underlying Aβ spreading. On the other hand, a growing body of evidence refers to tau spreading as a prion-like propagation, which fascinatingly occurs in different directions among the many forms of tauopathies[173]. Also, tau pathology is likely to begin in EC then move to the hippocampus, and ultimately invading the cortex, following an overlapping path existing among functionally connected areas[55,154,155,174]. These evidences are consistent with data coming from studies on non-human primates in which bilateral lesions of EC induce a functional impairment of declarative memory accompanied by long-lasting hypometabolism in temporal and parietal lobes, demonstrating a functional connection starting from EC[175]. Accordingly, in a transgenic mouse model differentially expressing pathological human tau in EC (EC-tau), the localization of tauopathy was investigated at different time points, demonstrating a progression of the pathology through anatomically and functionally connected brain areas[155]. Interestingly, in vivo chemogenetic stimulation of EC in EC-tau mice induced additional pathology in synaptically connected areas (e.g., dentate gyrus)[145]. Consistent with this finding, tau has been found in exosomes that might lead to its diffusion to adjacent cells[176,177]. Further work demonstrated that cell-to-cell contact was not necessarily needed for tau spreading in vitro given that the administration of neuronal-derived tau media to neuronal cultures was sufficient for tau transfer and internalization, even though it is not known whether tau in the media was vesicle bound or free[145]. Other studies suggested that pathologic tau requires TNTs to be transferred from a neuron to another one[178]. However, whether the mechanism underlying tau propagation is mediated by

TNTs, non-vesicular direct translocation or through secretory lysosomes into extracellular space[159,176,179,180] is still under investigation. Another interesting feature of tau transmission is the possibility that it can move both anterogradely and retrogradely, meaning that it can be internalized both at the somatodendritic compartment and axon terminals, and can be transported in either direction to disseminate tauopathy[149,159]. While spreading is involved in the progression of the disease among functionally connected brain areas, the transition from oligomers to insoluble deposits has been described as a "nucleation dependent protein polymerization" and explains the pattern of aggregate formation[181] for proteins with high tendency to organize in β-sheet conformation as for Aβ, tau, or α-synuclein[182]. This process, known as seeding, involves a nucleation phase and a growth phase. In the nucleation phase, the nucleus formation requires the assembly of misfolded monomers, a thermodynamically unfavorable process remarkably dependent on protein concentration[158,183,184]. The latter influences the lag time defined as the period before aggregates detection. In fact, supersaturated solutions can drastically shorten the nucleus formation time from years to microseconds[158]. After the nucleus formation, the critical concentration is reached, and a further addition of monomers occurs leading to polymerization, representing the growth phase. Interestingly, if a preformed nucleus, or seed, is added to a solution containing normally folded monomers, an immediate polymerization occurs. This phenomenon is defined as seeding[158,181] and can be distinguished as homologous or heterologous[181,185]. While homologous seeding involves monomers of the same type, heterologous seeding or cross-seeding takes place when a nucleus formed by a certain misfolded protein promotes polymerization of a different protein[181,185]. A large body of evidence supports this cross-seeding among tau, α-synuclein and TDP-43[186]. Some studies in which spreading of tau pathology was significantly accelerated by injecting pre-aggregated Aβ into mouse brain[187,188] suggested the possibility of Aβ and tau cross-seeding. Consistently, a protein interaction study by surface plasmon resonance demonstrated an affinity constant of tau for Aβ which was almost 1000-fold higher than for tau toward itself[189]. Moreover, confocal immunohistochemical imaging of AD brains showed intracellular aggregates

in which Aβ and tau coexisted in the same structure[189]. Also, a recent work showed that tau fibrillization can be induced in a cell-free assay by adding pre-aggregated Aβ, and that Aβ provide an efficient seed to induce tau cross-seeding and a consequent spreading of tau pathology in vivo[190]. In conclusion, seeding and spreading of Aβ and tau and their dynamic flux across the membrane characterized by activity-dependent secretion and neuronal internalization are crucial for the progression of the disease. Most importantly, the commonalities displayed by both Aβ and tau with respect to these phenomena are intriguing and suggest that soluble forms of the two molecules are involved in similar mechanisms of disease etiopathogenesis.

References

1. Martin Prince, A. *et al.* World Alzheimer Report 2015 The Global Impact of Dementia An Analysis of prevalence, Incidence, cost and Trends. (2015).
2. Wimo, A. *et al.* The worldwide costs of dementia 2015 and comparisons with 2010. *Alzheimers. Dement.* **13,** 1–7 (2017).
3. Muller, U. C. & Zheng, H. Physiological Functions of APP Family Proteins. *Cold Spring Harb. Perspect. Med.* **2,** a006288–a006288 (2012).
4. Zhang, Y., Thompson, R., Zhang, H. & Xu, H. APP processing in Alzheimer's disease. *Mol. Brain* **4,** 3 (2011).
5. Mawuenyega, K. G., Kasten, T., Sigurdson, W. & Bateman, R. J. Amyloid-beta isoform metabolism quantitation by stable isotope-labeled kinetics. *Anal. Biochem.* **440,** 56–62 (2013).
6. Glenner, G. G. & Wong, C. W. Alzheimer's disease: Initial report of the purification and characterization of a novel cerebrovascular amyloid protein. *Biochem. Biophys. Res. Commun.* **120,** 885–890 (1984).
7. Glenner, G. G. & Wong, C. W. Alzheimer's disease and Down's syndrome: Sharing of a unique cerebrovascular amyloid fibril protein. *Biochem. Biophys. Res. Commun.* **122,** 1131–1135 (1984).
8. Grundke-Iqbal, I. *et al.* Microtubule-associated protein tau. A component of Alzheimer paired helical filaments. *J Biol Chem* **261,** 6084–6089 (1986).
9. Levy, E. *et al.* Mutation of the Alzheimer's disease amyloid gene in hereditary cerebral hemorrhage, Dutch type. *Science* **248,** 1124–6 (1990).
10. Games, D. *et al.* Alzheimer-type neuropathology in transgenic mice overexpressing V717F b-amyloid precursor protein. *Lett. to Nat.* **373,** 523–527 (1995).
11. Puzzo, D., Gulisano, W., Palmeri, A. & Arancio, O. Rodent models for Alzheimer's disease drug discovery. *Expert Opin. Drug Discov.* **10,** 703–711 (2015).
12. Hardy, J. & Allsop, D. Amyloid deposition as the central event in the aetiology of Alzheimer's disease. *Trends in Pharmacological Sciences* **12,** 383–388 (1991).
13. Hardy, J. & Higgins, G. Alzheimer's disease: the amyloid cascade hypothesis. *Science (80-.).* **256,** 184–185 (1992).
14. Hardy, J., Duff, K., Hardy, K. G., Perez-Tur, J. & Hutton, M. Genetic dissection of Alzheimer's disease and related dementias: amyloid and its relationship to tau. *Nat. Neurosci.* **1,** 355–8 (1998).
15. Wisniewski, T., Ghiso, J. & Frangione, B. Alzheimer's disease and soluble A beta. *Neurobiol. Aging* **15,** 143–52 (1994).
16. Lambert, M. P. *et al.* Diffusible, nonfibrillar ligands derived from A 1-42 are potent central nervous system neurotoxins. *Proc. Natl. Acad. Sci.* **95,** 6448–6453 (1998).
17. Walsh, D. M. & Selkoe, D. J. Aβ oligomers - A decade of discovery. *J. Neurochem.* **101,** 1172–1184 (2007).
18. Fukumoto, H. *et al.* High-molecular-weight beta-amyloid oligomers are elevated in cerebrospinal fluid of Alzheimer patients. *FASEB J.* **24,** 2716–2726 (2010).
19. Hardy, J. & Selkoe, D. J. The Amyloid Hypothesis of Alzheimer ' s Disease : Progress and Problems on the Road to Therapeutics. *Science (80-.).* **297,** 353–357 (2002).
20. Ferreira, S. T. & Klein, W. L. The Aβ oligomer hypothesis for synapse failure and memory loss in Alzheimer's disease. *Neurobiol. Learn. Mem.* **96,** 529–43 (2011).
21. Ripoli, C. *et al.* Effects of different amyloid β-protein analogues on synaptic function. *Neurobiol. Aging* **34,** 1032–1044 (2013).
22. Attar, A. *et al.* Protection of primary neurons and mouse brain from Alzheimer's pathology by molecular tweezers. *Brain* **135,** 3735–3748 (2012).
23. Sevigny, J. *et al.* The antibody aducanumab reduces Aβ plaques in Alzheimer's disease. *Nature* **537,** 50–56 (2016).
24. Terry, R. D. *et al.* Physical basis of cognitive alterations in alzheimer's disease: Synapse loss is the major correlate of cognitive impairment. *Ann. Neurol.* **30,** 572–580 (1991).

25. Arriagada, P. V *et al.* Neurofibrillary tangles but not senile plaques parallel duration and severity of Alzheimer's disease. *Neurology* **42,** 631–639 (1992).
26. Dickson, D. W. *et al.* Correlations of synaptic and pathological markers with cognition of the elderly. *Neurobiol. Aging* **16,** 285–298 (1995).
27. Sloane, J. A. *et al.* Lack of correlation between plaque burden and cognition in the aged monkey. *Acta Neuropathol.* **94,** 471–478 (1997).
28. Katzman, R. *et al.* Clinical, pathological, and neurochemical changes in dementia: A subgroup with preserved mental status and numerous neocortical plaques. *Ann. Neurol.* **23,** 138–144 (1988).
29. Delaere, P. *et al.* Large amounts of neocortical beta A4 deposits without neuritic plaques nor tangles in a psychometrically assessed, non-demented person. *Neurosci Lett* **116,** 87–93 (1990).
30. Reitz, C. Alzheimer's disease and the amyloid cascade hypothesis: a critical review. *Int. J. Alzheimers. Dis.* **2012,** 369808 (2012).
31. Cheng, I. H. *et al.* Accelerating amyloid-beta fibrillization reduces oligomer levels and functional deficits in Alzheimer disease mouse models. *J Biol Chem* **282,** 23818–23828 (2007).
32. Puzzo, D. & Arancio, O. Amyloid-β peptide: Dr. Jekyll or Mr. Hyde? *J. Alzheimers. Dis.* **33 Suppl 1,** S111-20 (2013).
33. Puzzo, D., Gulisano, W., Arancio, O. & Palmeri, A. The keystone of Alzheimer pathogenesis might be sought in Aβ physiology. *Neuroscience* **307,** 26–36 (2015).
34. Puzzo, D. *et al.* Picomolar amyloid-beta positively modulates synaptic plasticity and memory in hippocampus. *J. Neurosci.* **28,** 14537–45 (2008).
35. Morley, J. E. *et al.* A physiological role for amyloid-β protein: Enhancement of learning and memory. *J. Alzheimer's Dis.* **19,** 441–449 (2010).
36. Lawrence, J. L. M. *et al.* Regulation of presynaptic Ca2+, synaptic plasticity and contextual fear conditioning by a N-terminal betaamyloid fragment. *J Neurosci* **34,** 14210–14218 (2014).
37. Puzzo, D. *et al.* Endogenous amyloid-β is necessary for hippocampal synaptic plasticity and memory. *Ann. Neurol.* **69,** 819–30 (2011).
38. Koppensteiner, P. *et al.* Time-dependent reversal of synaptic plasticity induced by physiological concentrations of oligomeric Aβ42: an early index of Alzheimer's disease. *Sci. Rep.* **6,** 32553 (2016).
39. Glass, D. J. & Arnold, S. E. Some evolutionary perspectives on Alzheimer's disease pathogenesis and pathology. *Alzheimers. Dement.* **8,** 343–51 (2012).
40. Herrup, K. The case for rejecting the amyloid cascade hypothesis. *Nat. Neurosci.* **18,** 794–799 (2015).
41. Weingarten, M. D., Lockwood, A. H., Hwo, S. Y. & Kirschner, M. W. A protein factor essential for microtubule assembly. *Proc. Natl Acad. Sci. USA* **72,** 1858–1862 (1975).
42. Dickson, D. W., Kouri, N., Murray, M. E. & Josephs, K. A. Neuropathology of frontotemporal lobar degeneration-tau (FTLD-tau). *J. Mol. Neurosci.* **45,** 384–9 (2011).
43. Liu, C., Götz, J. & Gotz, J. Profiling murine tau with 0N, 1N and 2N isoform-specific antibodies in brain and peripheral organs reveals distinct subcellular localization, with the 1N isoform being enriched in the nucleus. *PLoS One* **8,** e84849 (2013).
44. Trinczek, B., Biernat, J., Baumann, K., Mandelkow, E. M. & Mandelkow, E. Domains of tau protein, differential phosphorylation, and dynamic instability of microtubules. *Mol. Biol. Cell* **6,** 1887–902 (1995).
45. Kar, S., Fan, J., Smith, M. J., Goedert, M. & Amos, L. A. Repeat motifs of tau bind to the insides of microtubules in the absence of taxol. *EMBO J.* **22,** 70–7 (2003).
46. Dawson, H. N. *et al.* Inhibition of neuronal maturation in primary hippocampal neurons from tau deficient mice. *J. Cell Sci.* **114,** 1179–1187 (2001).
47. Vershinin, M., Carter, B. C., Razafsky, D. S., King, S. J. & Gross, S. P. Multiple-motor based transport and its regulation by Tau. *Regul. by Tau. Proc Natl Acad Sci U S A* **104,** 87–92 (2007).
48. Yuan, A., Kumar, A., Peterhoff, C., Duff, K. & Nixon, R. A. Axonal transport rates in vivo are unaffected by tau deletion or overexpression in mice. *J. Neurosci.* **28,** 1682–1687 (2008).
49. Ittner, L. M., Ke, Y. D., Götz, J. & Gotz, J. Phosphorylated Tau interacts with c-Jun N-terminal kinase-interacting protein 1 (JIP1) in Alzheimer disease. *J. Biol. Chem.* **284,** 20909–20916

(2009).
50. Frandemiche, M. L. *et al.* Activity-Dependent Tau Protein Translocation to Excitatory Synapse Is Disrupted by Exposure to Amyloid-Beta Oligomers. *J. Neurosci.* **34,** 6084–6097 (2014).
51. Qu, X. *et al.* Stabilization of dynamic microtubules by mDia1 drives Tau-dependent Aβ1-42synaptotoxicity. *J. Cell Biol.* **216,** 3161–3178 (2017).
52. Sultan, A. *et al.* Nuclear tau, a key player in neuronal DNA protection. *J. Biol. Chem.* **286,** 4566–4575 (2011).
53. Violet, M. *et al.* A major role for Tau in neuronal DNA and RNA protection in vivo under physiological and hyperthermic conditions. *Front. Cell. Neurosci.* **8,** 84 (2014).
54. Morris, M., Maeda, S., Vossel, K. & Mucke, L. The many faces of tau. *Neuron* **70,** 410–426 (2011).
55. Wang, Y. & Mandelkow, E. Tau in physiology and pathology. *Nat. Rev. Neurosci.* **17,** 22–35 (2015).
56. Arendt, T., Stieler, J. T. & Holzer, M. Tau and tauopathies. *Brain Res. Bull.* **126,** 238–292 (2016).
57. Mukhopadhyay, R. & Hoh, J. H. AFM force measurements on microtubule-associated proteins: the projection domain exerts a long-range repulsive force. *FEBS Lett.* **505,** 374–378 (2001).
58. Amos, L. A. Microtubule structure and its stabilisation. *Org. Biomol. Chem.* **2,** 2153 (2004).
59. Brandt, R. & Lee, G. Functional organization of microtubule-associated protein tau. Identification of regions which affect microtubule growth, nucleation, and bundle formation in vitro. *J. Biol. Chem.* **268,** 3414–9 (1993).
60. Maas, T., Eidenmüller, J. & Brandt, R. Interaction of Tau with the Neural Membrane Cortex Is Regulated by Phosphorylation at Sites That Are Modified in Paired Helical Filaments. *J. Biol. Chem.* **275,** 15733–15740 (2000).
61. Eidenmuller, J. *et al.* Phosphorylation-mimicking glutamate clusters in the proline-rich region are sufficient to simulate the functional deficiencies of hyperphosphorylated tau protein. *Biochem J* **357,** 759–767 (2001).
62. Reynolds, C. H. *et al.* Phosphorylation regulates tau interactions with Src homology 3 domains of phosphatidylinositol 3-kinase, phospholipase C[gamma]1, Grb2, and Src family kinases. *J. Biol. Chem.* **283,** 18177–18186 (2008).
63. Lee, G., Neve, R. L. & Kosik, K. S. The microtubule binding domain of tau protein. *Neuron* **2,** 1615–24 (1989).
64. Butner, K. A. & Kirschner, M. W. Tau protein binds to microtubules through a flexible array of distributed weak sites. *J. Cell Biol.* **115,** 717–30 (1991).
65. Goode, B. L. *et al.* Functional interactions between the proline-rich and repeat regions of tau enhance microtubule binding and assembly. *Mol. Biol. Cell* **8,** 353–65 (1997).
66. Mukrasch, M. D. *et al.* Sites of tau important for aggregation populate {beta}-structure and bind to microtubules and polyanions. *J. Biol. Chem.* **280,** 24978–86 (2005).
67. Xia, D., Li, C. & Götz, J. Pseudophosphorylation of Tau at distinct epitopes or the presence of the P301L mutation targets the microtubule-associated protein Tau to dendritic spines. *Biochim. Biophys. Acta - Mol. Basis Dis.* **1852,** 913–924 (2015).
68. Cardona-Gómez, G. P. *et al.* Estrogen dissociates Tau and alpha-amino3-hydroxy-5-methylisoxazole-4-propionic acid receptor subunit in postischemic hippocampus. *Neuroreport* **17,** 1337–1341 (2006).
69. Miyamoto, T. *et al.* Phosphorylation of tau at Y18, but not tau-fyn binding, is required for tau to modulate NMDA receptor-dependent excitotoxicity in primary neuronal culture. *Mol. Neurodegener.* **12,** 41 (2017).
70. Ebneth, A. *et al.* Overexpression of tau protein inhibits kinesin-dependent trafficking of vesicles, mitochondria, and endoplasmic reticulum: implications for Alzheimer's disease. *J. Cell Biol.* **143,** 777–94 (1998).
71. Strittmatter, W. J. *et al.* Isoform-specific interactions of apolipoprotein E with microtubule-associated protein tau: implications for Alzheimer disease. *Proc. Natl. Acad. Sci. U. S. A.* **91,** 11183–6 (1994).
72. Brandt, R., Léger, J., Lee, G., Leger, J. & Lee, G. Interaction of tau with the neural plasma

membrane mediated by tau's aminoterminal projection domain. *J Cell Biol* **131,** 1327–1340 (1995).
73. Bhaskar, K., Yen, S. H. & Lee, G. Disease-related modifications in tau affect the interaction between Fyn and Tau. *J. Biol. Chem.* **280,** 35119–35125 (2005).
74. Lee, G. Tau and src family tyrosine kinases. *Biochim. Biophys. Acta - Mol. Basis Dis.* **1739,** 323–330 (2005).
75. Qi, H. *et al.* Nuclear Magnetic Resonance Spectroscopy Characterization of Interaction of Tau with DNA and Its Regulation by Phosphorylation. *Biochemistry* **54,** 1525–1533 (2015).
76. Kanemaru, K., Takio, K., Miura, R., Titani, K. & Ihara, Y. Fetal-type phosphorylation of the tau in paired helical filaments. *J. Neurochem.* **58,** 1667–1675 (1992).
77. Köpke, E. *et al.* Microtubule-associated protein tau. Abnormal phosphorylation of a non-paired helical filament pool in Alzheimer disease. *J. Biol. Chem.* **268,** 24374–24384 (1993).
78. Smith, A. D. Imaging the progression of Alzheimer pathology through the brain. *Proc. Natl. Acad. Sci. U. S. A.* **99,** 4135–7 (2002).
79. Mukrasch, M. D. *et al.* Structural polymorphism of 441-residue tau at single residue resolution. *PLoS Biol.* **7,** e34 (2009).
80. Schneider, A., Biernat, J., von Bergen, M., Mandelkow, E.-M. M. & Mandelkow, E.-M. M. Phosphorylation that detaches tau protein from microtubules (Ser262, Ser214) also protects it against aggregation into Alzheimer paired helical filaments. *Biochemistry* **38,** 3549–3558 (1999).
81. von Bergen, M. *et al.* Assembly of tau protein into Alzheimer paired helical filaments depends on a local sequence motif ((306)VQIVYK(311)) forming beta structure. *Proc. Natl. Acad. Sci. U. S. A.* **97,** 5129–34 (2000).
82. Jeganathan, S., von Bergen, M., Brutlach, H., Steinhoff, H. J. & Mandelkow, E. Global hairpin folding of tau in solution. *Biochemistry* **45,** 2283–2293 (2006).
83. Al-Bassam, J., Ozer, R. S., Safer, D., Halpain, S. & Milligan, R. A. MAP2 and tau bind longitudinally along the outer ridges of microtubule protofilaments. *J. Cell Biol.* **157,** 1187–1196 (2002).
84. Goux, W. J. *et al.* The formation of straight and twisted filaments from short tau peptides. *J. Biol. Chem.* **279,** 26868–75 (2004).
85. Wegmann, S., Medalsy, I. D., Mandelkow, E., Muller, D. J. & Müller, D. J. The fuzzy coat of pathological human Tau fibrils is a two-layered polyelectrolyte brush. *twolayered polyelectrolyte brush. Proc Natl Acad Sci* **110,** E313–E321 (2013).
86. Vega, I. E. *et al.* Increase in tau tyrosine phosphorylation correlates with the formation of tau aggregates. *Brain Res. Mol. Brain Res.* **138,** 135–144 (2005).
87. Planel, E. Alterations in glucose metabolism induce hypothermia leading to tau hyperphosphorylation through differential inhibition of kinase and phosphatase activities: implications for Alzheimer's disease. *J. Neurosci.* **24,** 2401–2411 (2004).
88. Yanagisawa, M., Planel, E., Ishiguro, K. & Fujita, S. C. Starvation induces tau hyperphosphorylation in mouse brain: implications for Alzheimer's disease. *FEBS Lett.* **461,** 329–333 (1999).
89. Sotiropoulos, I. *et al.* Stress acts cumulatively to precipitate Alzheimer's disease-like tau pathology and cognitive deficits. *J. Neurosci.* **31,** 7840–7 (2011).
90. Le Freche, H. *et al.* Tau phosphorylation and sevoflurane anesthesia. *Anesthesiology* **116,** 779–787 (2012).
91. Whittington, R. A., Bretteville, A., Dickler, M. F. & Planel, E. Anesthesia and tau pathology. *Prog. Neuro-Psychopharmacology Biol. Psychiatry* **47,** 147–155 (2013).
92. der Jeugd A, V. *et al.* Cognitive defects are reversible in inducible mice expressing pro-aggregant full-length human Tau. *Acta Neuropathol.* **123,** 787–805 (2012).
93. Santacruz, K. Tau suppression in a neurodegenerative mouse model improves memory function. *Science (80-.).* **309,** 476–481 (2005).
94. Yoshiyama, Y. *et al.* Synapse Loss and Microglial Activation Precede Tangles in a P301S Tauopathy Mouse Model. *Neuron* **53,** 337–351 (2007).
95. Alonso, A., Zaidi, T., Novak, M., Grundke-Iqbal, I. & Iqbal, K. Hyperphosphorylation induces

self-assembly of tau into tangles of paired helical filaments/straight filaments. *Proc. Natl Acad. Sci. USA* **98,** 6923–6928 (2001).
96. Leroy, K. *et al.* Early axonopathy preceding neurofibrillary tangles in mutant tau transgenic mice. *Am. J. Pathol.* **171,** 976–992 (2007).
97. Maeda, S. *et al.* Increased levels of granular tau oligomers: An early sign of brain aging and Alzheimer's disease. *Neurosci. Res.* **54,** 197–201 (2006).
98. Fa, M. *et al.* Extracellular tau oligomers produce an immediate impairment of LTP and memory. *Sci Rep* **6,** 39 (2016).
99. Lasagna-Reeves, C. A. *et al.* Tau oligomers impair memory and induce synaptic and mitochondrial dysfunction in wild-type mice. *Mol. Neurodegener.* **6,** 39 (2011).
100. Berger, Z. *et al.* Accumulation of pathological tau species and memory loss in a conditional model of tauopathy. *J. Neurosci.* **27,** 3650–62 (2007).
101. Gerson, J. *et al.* Tau Oligomers Derived from Traumatic Brain Injury Cause Cognitive Impairment and Accelerate Onset of Pathology in Htau Mice. *J. Neurotrauma* **33,** 2034–2043 (2016).
102. Sengupta, U. *et al.* Tau oligomers in cerebrospinal fluid in Alzheimer's disease. *Ann. Clin. Transl. Neurol.* **4,** 226–235 (2017).
103. Vuono, R. *et al.* The role of tau in the pathological process and clinical expression of Huntington's disease. *Brain* **138,** 1907–1918 (2015).
104. Selkoe, D. J. Alzheimer's Disease Is a Synaptic Failure. *Science (80-.).* **298,** 789–791 (2002).
105. Selkoe, D. J. Soluble oligomers of the amyloid β-protein impair synaptic plasticity and behavior. *Behavioural Brain Research* **192,** 106–113 (2008).
106. Guerrero-Muñoz, M. J., Gerson, J. & Castillo-Carranza, D. L. Tau Oligomers: The Toxic Player at Synapses in Alzheimer's Disease. *Front. Cell. Neurosci.* **9,** 464 (2015).
107. Silva, A. J., Kogan, J. H., Frankland, P. W. & Kida, S. CREB AND MEMORY. *Annu. Rev. Neurosci.* **21,** 127–148 (1998).
108. Lonze, B. E. & Ginty, D. D. Function and regulation of CREB family transcription factors in the nervous system. *Neuron* **35,** 605–23 (2002).
109. Carlezon, W. A., Duman, R. S. & Nestler, E. J. The many faces of CREB. *Trends Neurosci.* **28,** 436–45 (2005).
110. Vitolo, O. V *et al.* Amyloid beta -peptide inhibition of the PKA/CREB pathway and long-term potentiation: reversibility by drugs that enhance cAMP signaling. *Proc. Natl. Acad. Sci. U. S. A.* **99,** 13217–21 (2002).
111. Puzzo, D. *et al.* Amyloid-beta peptide inhibits activation of the nitric oxide/cGMP/cAMP-responsive element-binding protein pathway during hippocampal synaptic plasticity. *J. Neurosci.* **25,** 6887–97 (2005).
112. Teich, A. F. *et al.* Synaptic Therapy in Alzheimer's Disease: A CREB-centric Approach. *Neurotherapeutics* **12,** 29–41 (2015).
113. Xie, M. *et al.* The Involvement of NR2B and tau Protein in MG132-Induced CREB Dephosphorylation. *J. Mol. Neurosci.* **62,** 154–162 (2017).
114. Yin, Y. *et al.* Tau accumulation induces synaptic impairment and memory deficit by calcineurin-mediated inactivation of nuclear CaMKIV/CREB signaling. *Proc. Natl. Acad. Sci. U. S. A.* **113,** E3773-81 (2016).
115. Pugazhenthi, S., Wang, M., Pham, S., Sze, C.-I. & Eckman, C. B. Downregulation of CREB expression in Alzheimer's brain and in Aβ-treated rat hippocampal neurons. *Mol. Neurodegener.* **6,** 60 (2011).
116. Yamamoto-Sasaki, M., Ozawa, H., Saito, T., Rösler, M. & Riederer, P. Impaired phosphorylation of cyclic AMP response element binding protein in the hippocampus of dementia of the Alzheimer type. *Brain Res.* **824,** 300–3 (1999).
117. Yamamoto, M. *et al.* Reduced immunoreactivity of adenylyl cyclase in dementia of the Alzheimer type. *Neuroreport* **7,** 2965–70 (1996).
118. Bartolotti, N., Bennett, D. A. & Lazarov, O. Reduced pCREB in Alzheimer's disease prefrontal cortex is reflected in peripheral blood mononuclear cells. *Mol. Psychiatry* **21,** 1158–66 (2016).
119. Yamamoto, M. *et al.* Ca2+/CaM-sensitive adenylyl cyclase activity is decreased in the

Alzheimer's brain: possible relation to type I adenylyl cyclase. *J. Neural Transm.* **104,** 721–32 (1997).
120. Fink, C. C. & Meyer, T. Molecular mechanisms of CaMKII activation in neuronal plasticity. *Curr. Opin. Neurobiol.* **12,** 293–9 (2002).
121. Ghosh, A. & Giese, K. P. Calcium/calmodulindependent kinase II and Alzheimer's disease. *Mol Brain* **8,** 78 (2015).
122. Zhao, D., Watson, J. B. & Xie, C.-W. Amyloid beta prevents activation of calcium/calmodulin-dependent protein kinase II and AMPA receptor phosphorylation during hippocampal long-term potentiation. *J. Neurophysiol.* **92,** 2853–8 (2004).
123. Gu, Z., Liu, W. & Yan, Z. {beta}-Amyloid impairs AMPA receptor trafficking and function by reducing Ca2+/calmodulin-dependent protein kinase II synaptic distribution. *J. Biol. Chem.* **284,** 10639–49 (2009).
124. Whitcomb, D. J. *et al.* Intracellular oligomeric amyloid-beta rapidly regulates GluA1 subunit of AMPA receptor in the hippocampus. *Sci. Rep.* **5,** 10934 (2015).
125. Baudier, J. & Cole, R. D. Phosphorylation of tau proteins to a state like that in Alzheimer's brain is catalyzed by a calcium/calmodulin-dependent kinase and modulated by phospholipids. *J. Biol. Chem.* **262,** 17577–83 (1987).
126. Baudier, J. & Cole, R. D. Interactions between the microtubule-associated tau proteins and S100b regulate tau phosphorylation by the Ca2+/calmodulin-dependent protein kinase II. *J. Biol. Chem.* **263,** 5876–83 (1988).
127. Singh, T. J. *et al.* Calcium/calmodulin-dependent protein kinase II phosphorylates tau at Ser-262 but only partially inhibits its binding to microtubules. *FEBS Lett.* **387,** 145–148 (1996).
128. Steiner, B. *et al.* Phosphorylation of microtubuleassociated protein tau: Identification of the site for Ca2(+)-calmodulin dependent kinase and relationship with tau phosphorylation in Alzheimer tangles. *EMBO J* **9,** 3539–3544 (1990).
129. Oka, M. *et al.* Ca2+/calmodulin-dependent protein kinase II promotes neurodegeneration caused by tau phosphorylated at Ser262/356 in a transgenic Drosophila model of tauopathy. *J. Biochem.* **162,** 335–342 (2017).
130. Song, J.-H., Yu, J.-T. & Tan, L. Brain-Derived Neurotrophic Factor in Alzheimer's Disease: Risk, Mechanisms, and Therapy. *Mol. Neurobiol.* **52,** 1477–1493 (2015).
131. Burnouf, S. *et al.* NMDA receptor dysfunction contributes to impaired brain-derived neurotrophic factorinduced facilitation of hippocampal synaptic transmission in a Tau transgenic model. *Aging Cell* **12,** 11–23.e907. (2013).
132. Jiao, S.-S. *et al.* Brain-derived neurotrophic factor protects against tau-related neurodegeneration of Alzheimer's disease. *Transl. Psychiatry* **6,** e907 (2016).
133. Kamenetz, F. *et al.* APP processing and synaptic function. *Neuron* **37,** 925–37 (2003).
134. Cirrito, J. R. *et al.* Synaptic Activity Regulates Interstitial Fluid Amyloid-β Levels In Vivo. *Neuron* **48,** 913–922 (2005).
135. Brody, D. L. *et al.* Amyloid-beta dynamics correlate with neurological status in the injured human brain. *Science* **321,** 1221–4 (2008).
136. Scala, F. *et al.* Intraneuronal Aβ accumulation induces hippocampal neuron hyperexcitability through A-type K+ current inhibition mediated by activation of caspases and GSK-3. *Neurobiol. Aging* **36,** 886–900 (2015).
137. Vossel, K. A. *et al.* Seizures and Epileptiform Activity in the Early Stages of Alzheimer Disease. *JAMA Neurol.* **70,** 1158 (2013).
138. Palmeri, A. *et al.* Amyloid-β Peptide Is Needed for cGMP-Induced Long-Term Potentiation and Memory. *J. Neurosci.* **37,** 6926–6937 (2017).
139. Tampellini, D. Synaptic activity and Alzheimer's disease: A critical update. *Front. Neurosci.* **9,** 1–7 (2015).
140. Tampellini, D. *et al.* Synaptic Activity Reduces Intraneuronal A , Promotes APP Transport to Synapses, and Protects against A -Related Synaptic Alterations. *J. Neurosci.* **29,** 9704–9713 (2009).
141. Puzzo, D. *et al.* LTP and memory impairment caused by extracellular Aβ and Tau oligomers is APP-dependent. *Elife* **6,** (2017).

142. Ripoli, C. *et al.* Intracellular accumulation of amyloid-β (Aβ) protein plays a major role in Aβ-induced alterations of glutamatergic synaptic transmission and plasticity. *J. Neurosci.* **34,** 12893–903 (2014).
143. Pooler, A. M., Phillips, E. C., Lau, D. H. W., Noble, W. & Hanger, D. P. Physiological release of endogenous tau is stimulated by neuronal activity. *EMBO Rep.* **14,** 389–394 (2013).
144. Yamada, K. *et al.* Neuronal activity regulates extracellular tau in vivo. *J. Exp. Med.* **211,** 387–393 (2014).
145. Wu, J. W. *et al.* Neuronal activity enhances tau propagation and tau pathology in vivo. *Nat. Neurosci.* **19,** 1085–92 (2016).
146. Frost, B., Jacks, R. L. & Diamond, M. I. Propagation of Tau Misfolding from the Outside to the Inside of a Cell. *J. Biol. Chem.* **284,** 12845–12852 (2009).
147. Guo, J. L. & Lee, V. M. Seeding of normal Tau by pathological Tau conformers drives pathogenesis of Alzheimer-like tangles. *J. Biol. Chem.* **286,** 15317–15331 (2011).
148. Guo, J. L. & Lee, V. M. Y. Neurofibrillary tangle-like tau pathology induced by synthetic tau fibrils in primary neurons over-expressing mutant tau. *FEBS Lett.* **587,** 717–723 (2013).
149. Wu, J. W. *et al.* Small Misfolded Tau Species Are Internalized via Bulk Endocytosis and Anterogradely and Retrogradely Transported in Neurons. *J. Biol. Chem.* **288,** 1856–1870 (2013).
150. Luo, W. *et al.* Microglial internalization and degradation of pathological tau is enhanced by an anti-tau monoclonal antibody. *Sci. Rep.* **5,** 11161 (2015).
151. Bolós, M., Perea, J. R. & Avila, J. Alzheimer's disease as an inflammatory disease. *Biomol. Concepts* **8,** 37–43 (2017).
152. Piacentini, R. *et al.* Reduced gliotransmitter release from astrocytes mediates tau-induced synaptic dysfunction in cultured hippocampal neurons. *Glia* **65,** 1302–1316 (2017).
153. Holmes, B. B. *et al.* Heparan sulfate proteoglycans mediate internalization and propagation of specific proteopathic seeds. *Proc. Natl Acad. Sci. USA* **110,** E3138–E3147 (2013).
154. Braak, H. & Del Tredici, K. Alzheimer's pathogenesis: is there neuron-to-neuron propagation? *Acta Neuropathol.* **121,** 589–595 (2011).
155. Liu, L. *et al.* Trans-Synaptic Spread of Tau Pathology In Vivo. *PLoS One* **7,** e31302 (2012).
156. Jack, C. R. *et al.* Suspected non-Alzheimer disease pathophysiology — concept and controversy. *Nat. Rev. Neurol.* **12,** 117–124 (2016).
157. Pearson, R. C., Esiri, M. M., Hiorns, R. W., Wilcock, G. K. & Powell, T. P. Anatomical correlates of the distribution of the pathological changes in the neocortex in Alzheimer disease. *Proc. Natl. Acad. Sci. U. S. A.* **82,** 4531–4 (1985).
158. Jarrett, J. T. & Lansbury, P. T. Seeding 'one-dimensional crystallization' of amyloid: a pathogenic mechanism in Alzheimer's disease and scrapie? *Cell* **73,** 1055–8 (1993).
159. Lv, Z.-Y., Tan, C.-C., Yu, J.-T. & Tan, L. Spreading of Pathology in Alzheimer's Disease. *Neurotox. Res.* **32,** 707–722 (2017).
160. Palop, J. J. *et al.* Neuronal depletion of calcium-dependent proteins in the dentate gyrus is tightly linked to Alzheimer's disease-related cognitive deficits. *Proc. Natl. Acad. Sci. U. S. A.* **100,** 9572–7 (2003).
161. Scarmeas, N. *et al.* Seizures in Alzheimer Disease. *Arch. Neurol.* **66,** 992–7 (2009).
162. Harris, J. A. *et al.* Transsynaptic progression of amyloid-β-induced neuronal dysfunction within the entorhinal-hippocampal network. *Neuron* **68,** 428–41 (2010).
163. Criscuolo, C. *et al.* Entorhinal Cortex dysfunction can be rescued by inhibition of microglial RAGE in an Alzheimer's disease mouse model. *Sci. Rep.* **7,** 42370 (2017).
164. Joshi, P. *et al.* Microglia convert aggregated amyloid-β into neurotoxic forms through the shedding of microvesicles. *Cell Death Differ.* **21,** 582–593 (2014).
165. Prada, I. *et al.* A new approach to follow a single extracellular vesicle–cell interaction using optical tweezers. *Biotechniques* **60,** 35–41 (2016).
166. Söllvander, S. *et al.* Accumulation of amyloid-β by astrocytes result in enlarged endosomes and microvesicle-induced apoptosis of neurons. *Mol. Neurodegener.* **11,** 38 (2016).
167. Nath, S. *et al.* Spreading of neurodegenerative pathology via neuron-to-neuron transmission of beta-amyloid. *J Neurosci* **32,** 8767–8777 (2012).
168. Domert, J. *et al.* Spreading of amyloid-β peptides via neuritic cell-to-cell transfer is dependent

on insufficient cellular clearance. *Neurobiol. Dis.* **65,** 82–92 (2014).
169. Rustom, A., Saffrich, R., Markovic, I., Walther, P. & Gerdes, H.-H. Nanotubular Highways for Intercellular Organelle Transport. *Science (80-.).* **303,** 1007–1010 (2004).
170. Wang, Y., Cui, J., Sun, X. & Zhang, Y. Tunnelingnanotube development in astrocytes depends on p53 activation. *Cell Death Differ* **18,** 732–742 (2011).
171. Rajendran, L. *et al.* Alzheimer's disease beta-amyloid peptides are released in association with exosomes. *Proc. Natl. Acad. Sci. U. S. A.* **103,** 11172–7 (2006).
172. Zheng, L. *et al.* Macroautophagy-generated increase of lysosomal amyloid β-protein mediates oxidant-induced apoptosis of cultured neuroblastoma cells. *Autophagy* **7,** 1528–45 (2011).
173. Sanders, D. W. *et al.* Distinct tau prion strains propagate in cells and mice and define different tauopathies. *Neuron* **82,** 1271–88 (2014).
174. Braak, H. & Braak, E. Neuropathological stageing of Alzheimer-related changes. *Acta Neuropathol.* **82,** 239–259 (1991).
175. Meunier, M., Bachevalier, J., Mishkin, M., Murray, E. A. & Chavoix, C. Effects on visual recognition of combined and separate ablations of the entorhinal and perirhinal cortex in rhesus monkeys. *J. Neurosci.* **13,** 5418–32 (1993).
176. Saman, S. *et al.* Exosome-associated Tau Is Secreted in Tauopathy Models and Is Selectively Phosphorylated in Cerebrospinal Fluid in Early Alzheimer Disease. *J. Biol. Chem.* **287,** 3842–3849 (2012).
177. Asai, H. *et al.* Depletion of microglia and inhibition of exosome synthesis halt tau propagation. *Nat. Neurosci.* **18,** 1584–1593 (2015).
178. Gousset, K. *et al.* Prions hijack tunnelling nanotubes for intercellular spread. *Nat. Cell Biol.* **11,** 328–336 (2009).
179. Simón, D. *et al.* Tau Overexpression Results in Its Secretion via Membrane Vesicles. *Neurodegener. Dis.* **10,** 73–75 (2012).
180. Dujardin, S. *et al.* Ectosomes: A New Mechanism for Non-Exosomal Secretion of Tau Protein. *PLoS One* **9,** e100760 (2014).
181. Morales, R., Moreno-Gonzalez, I. & Soto, C. Cross-seeding of misfolded proteins: implications for etiology and pathogenesis of protein misfolding diseases. *PLoS Pathog.* **9,** e1003537 (2013).
182. Soto, C. Unfolding the role of protein misfolding in neurodegenerative diseases. *Nat. Rev. Neurosci.* **4,** 49–60 (2003).
183. Hofrichter, J., Ross, P. D. & Eaton, W. A. Kinetics and mechanism of deoxyhemoglobin S gelation: a new approach to understanding sickle cell disease. *Proc. Natl. Acad. Sci. U. S. A.* **71,** 4864–8 (1974).
184. Chothia, C. & Janin, J. Principles of protein-protein recognition. *Nature* **256,** 705–8 (1975).
185. Morales, R., Green, K. M. & Soto, C. Cross currents in protein misfolding disorders: interactions and therapy. *CNS Neurol. Disord. Drug Targets* **8,** 363–71 (2009).
186. Spires-Jones, T. L., Attems, J. & Thal, D. R. Interactions of pathological proteins in neurodegenerative diseases. *Acta Neuropathol.* **134,** 187–205 (2017).
187. Gotz, J. *et al.* Formation of neurofibrillary tangles in P301l tau transgenic mice induced by Abeta 42 fibrils. *Science (80-.).* **293,** 1491–1495 (2001).
188. Bolmont, T. *et al.* Induction of Tau Pathology by Intracerebral Infusion of Amyloid-β-Containing Brain Extract and by Amyloid-β Deposition in APP × Tau Transgenic Mice. *Am. J. Pathol.* **171,** 2012–2020 (2007).
189. Guo, J.-P., Arai, T., Miklossy, J. & McGeer, P. L. Abeta and tau form soluble complexes that may promote self aggregation of both into the insoluble forms observed in Alzheimer's disease. *Proc. Natl. Acad. Sci. U. S. A.* **103,** 1953–8 (2006).
190. Vasconcelos, B. *et al.* Heterotypic seeding of Tau fibrillization by pre-aggregated Abeta provides potent seeds for prion-like seeding and propagation of Tau-pathology in vivo. *Acta Neuropathol.* **131,** 549–69 (2016).

Chapter 1: The effect of Amyloid-β peptide on synaptic plasticity and memory is influenced by different isoforms, concentrations, and aggregation status

Gulisano W[1], Melone M[2], Li Puma DD[3], Tropea MR[1], Palmeri A[1], Arancio O[4], Grassi C[5], Conti F[6], Puzzo D[7].

[1]Department Biomedical and Biotechnological Sciences, University of Catania, Catania, Italy. [2]Department Experimental and Clinical Medicine, Section of Neuroscience and Cell Biology, Università Politecnica delle Marche, Ancona, Italy; Center for Neurobiology of Aging, INRCA IRCCS, Ancona, Italy. [3]Institute of Human Physiology, Università Cattolica Medical School, Rome, Italy. [4]Taub Institute for Research on Alzheimer's Disease and the Aging Brain, Columbia University, New York, NY, USA. [5]Institute of Human Physiology, Università Cattolica Medical School, Rome, Italy; Fondazione Policlinico Universitario A. Gemelli, Rome, Italy. [6]Department Experimental and Clinical Medicine, Section of Neuroscience and Cell Biology, Università Politecnica delle Marche, Ancona, Italy; Center for Neurobiology of Aging, INRCA IRCCS, Ancona, Italy; Foundation for Molecular Medicine, Università Politecnica delle Marche, Ancona, Italy. [7]Department Biomedical and Biotechnological Sciences, University of Catania, Catania, Italy.

In: Neurobiol Aging. 2018 Jul 18;71:51-60.
doi: 10.1016/j.neurobiolaging.2018.06.025.

Abstract

The increase of oligomeric amyloid-beta (oAβ) has been related to synaptic dysfunction, thought to be the earliest event in Alzheimer's disease (AD) pathophysiology. Conversely, the suppression of endogenous Aβ impaired synaptic plasticity and memory, suggesting that the peptide is needed in the healthy brain. However, different species, aggregation forms and concentrations of Aβ might differently influence synaptic function/dysfunction. Here, we have tested the contribution of monomeric and oligomeric Aβ42 and Aβ40 at 200 nM and 200 pM concentrations on hippocampal LTP and spatial memory. We found that, when at 200 nM, oAβ40, oAβ42 and monomeric Aβ42 impaired LTP and memory, whereas only oAβ42 200 pM enhanced synaptic plasticity and memory and rescued the detrimental effect due to depletion of endogenous Aβ. Interestingly, quantification of monomer-like and oligomer-like species carried out by transmission electron microscopy revealed an increase of the monomer/oligomer ratio in the oAβ42 200 pM preparation, suggesting that the content of monomers and oligomers depends upon the final concentration of the solution.

Introduction

Progressive accumulation of amyloid-beta peptide (Aβ) in brain regions involved in cognition has been considered a main pathogenic event in Alzheimer's disease (AD). The multifaceted pathological role of this protein spans from its deposition in the characteristic senile plaques, a histological hallmark of AD, to the synaptotoxic effect of oligomers leading to memory dysfunction[1]. On the other hand, low physiological concentrations of Aβ have neurotrophic and neuroprotective properties[2], and exert a positive modulatory function on synaptic plasticity and memory[3]. Several studies aimed at understanding whether these opposite Aβ effects are due to different concentrations, species or aggregation forms of the peptide, as this might represent a crucial aspect to clarify when and how Aβ physiological function switches toward pathology.

Aβ is a β-sheet–forming protein with a high propensity to form aggregates, such as oligomers, protofibrils, and fibrils. Typically, Aβ peptides are composed of 39–43 amino acids and, among these, Aβ40 is the most represented form (about 60% of total Aβ) that, however, has a less propensity to aggregate[4]. The aggregation rate seems to be related to the amino acids at the C terminus[5], giving Aβ42 the higher propensity to form oligomers, which have been related to AD neuronal dysfunction[6]. Different types of oligomers seem to correlate with cognitive decline in AD[7,8] and are present in the human brain or cerebrospinal fluid (CSF) decades before AD onset[9,10].

Because Aβ is thought to be secreted in a monomeric form, it is common to ascribe its physiological properties to monomers[11]. However, in the normal healthy brain, the concentration of soluble Aβ has been estimated in the picomolar range with species ranging from monomers to higher molecular weight oligomers[12–14]. Thus, a certain degree of oligomerization also occurs in physiological conditions for both Aβ40 and Aβ42.

Although several studies have investigated the effects of different forms and aggregation states of soluble Aβ responsible for its toxic actions in AD, few studies have evaluated these aspects under physiological conditions. We have previously

demonstrated that Aβ42 exerts an opposite effect on long-term potentiation (LTP) and memory, depending on its concentration[15]. Interestingly, both the positive and negative Aβ42 effects were attributable to a preparation containing monomers and oligomers, suggesting that oligomeric forms of Aβ are involved in normal synaptic plasticity other than synaptic dysfunction.

Here, we aimed to clarify the effects of different isoforms, concentrations, and aggregation status of the peptide on synaptic plasticity and memory.

Results

Oligomeric and monomeric human Aβ42 and Aβ40 exert a different effect on hippocampal long-term potentiation

We first aimed to clarify whether the positive/negative effects of Aβ on LTP, that is, the cellular surrogate of memory[16], were mediated by Aβ42 and/or Aβ40 in monomeric and/or oligomeric forms. Based on previous works[13,17,18], different preparations of Aβ were prepared and characterized by using WB analysis (Fig. 1A). We used (1) a fresh preparation of Aβ42 or Aβ40 enriched in monomers, named mAβ42 and mAβ40; and (2) an aged preparation of Aβ42 or Aβ40 enriched in oligomers, named oAβ42 and oAβ40. The presence of different bands corresponding to monomers (4.5 kDa), dimers (9 kDa), trimers (13.5 kDa), and tetramers (18 kDa) confirmed that although oligomers are prevalent in oAβ42 solution, they are also present in a small quantity in mAβ42. As for oAβ40 solution, it contains lower levels of oligomers compared with oAβ42, whereas only monomers and few dimers are detectable in mAβ40 preparation.

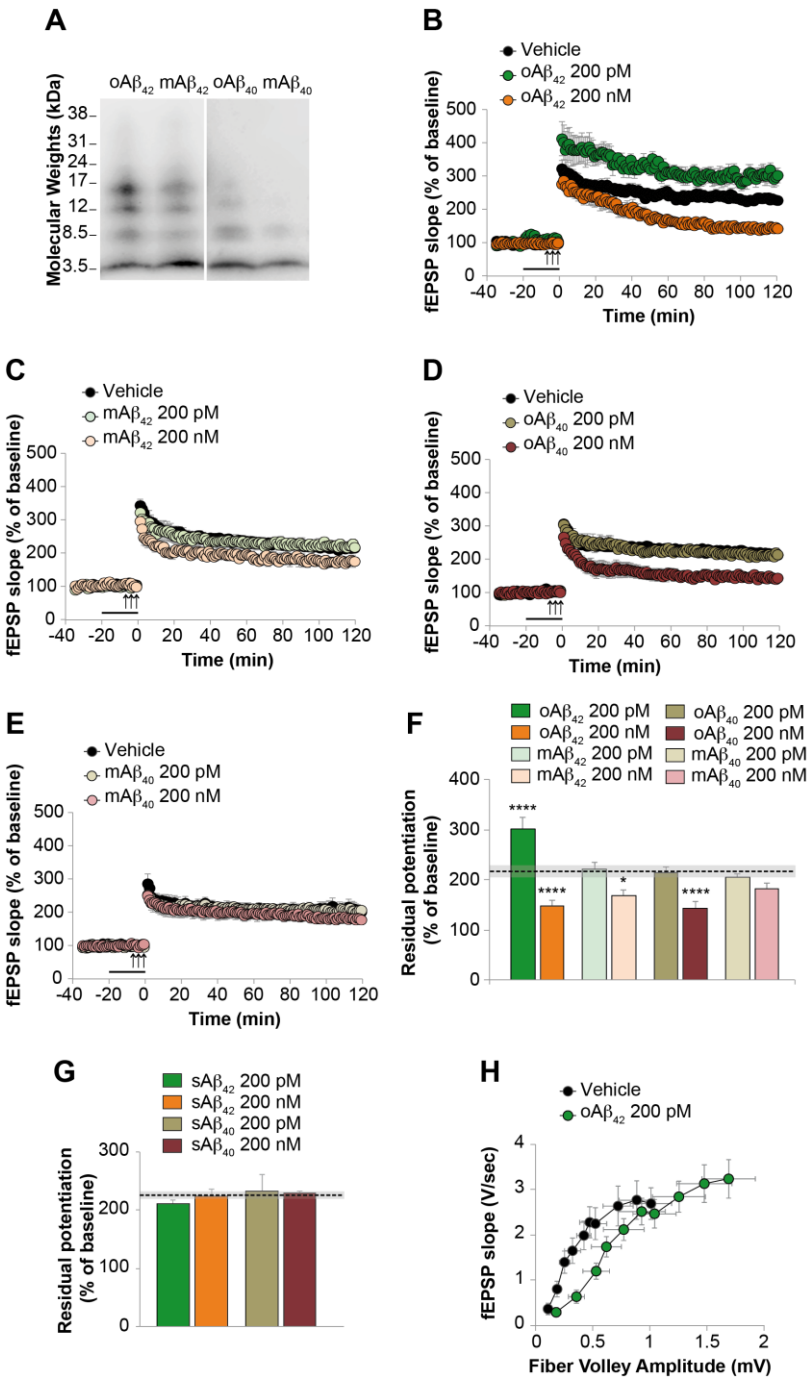

Fig. 1. LTP is impaired by nM concentrations of oAβ42, oAβ40, and mAβ42, whereas it is enhanced by pM concentrations of oAβ42. (A) WB analysis of 200 nM different human Aβ solutions shows different bands corresponding to monomers, dimers, trimers, and tetramers. (B) Hippocampal slices perfused for 20 minutes before a strong tetanic stimulation show an improvement of LTP with 200 pM oAβ42, but an impairment with 200 nM oAβ42, (C) 200 nM mAβ42, or (D) 200 nM oAβ40 (n = 7 slices for each condition from 6 to 7 animals). (E) mAβ40 does not affect LTP either at 200 pM or 200 nM (n = 7 slices for each condition from 5 to 6 animals). Arrows indicate tetanus delivery and horizontal bar

Aβ perfusion. (F) Graph shows the residual potentiation obtained by averaging the last 5 recording time points of LTP (from 116th to 120th min after tetanus) from slices treated as in (B–E). Dotted line with shadow area represents the average ±SEM of residual potentiation in tetanized vehicle-treated slices. (G) Scrambled Aβ42 or Aβ40 at 200 nM or 200 pM does not affect LTP compared with tetanized slices treated with vehicle (n = 5 slices for each condition from 4 to 5 animals). (H) oAβ42 200 pM does not modify fEPSP slope but induces an increase of fiber volley amplitude during BST assessment. Data expressed as average ±SEM. **** $p < 0.0001$; * $p < 0.05$. Abbreviations: BST, baseline synaptic transmission; fEPSP, field excitatory postsynaptic potential; LTP, long-term potentiation; mAβ, monomeric amyloid-beta; oAβ, oligomeric amyloid-beta; SEM, standard error mean.

Because oAβ42 in the nM range is known to inhibit LTP without affecting BST, we investigated the effect of 200 pM oAβ42 on BST. Although fEPSP slope was not modified by 200 pM oAβ42, we found a significant increase of fiber volley amplitude ($F(1,18) = 4.746$; $p = 0.043$; Fig. 1G).

Thus, only administration of exogenous 200 pM oAβ42 was capable to induce an increase of hippocampal LTP, whereas 200 nM oAβ42, mAβ42, or oAβ40 impaired it. oAβ42 at 200 pM concentration also enhanced fiber volley amplitude.

Oligomeric and monomeric human Aβ42 and Aβ40 exert a different effect on hippocampal-dependent spatial memory

Because LTP represents the molecular correlate of learning and memory[16], we next assessed the effects of different preparations of synthetic human Aβ in hippocampal-dependent memory tested by MWM, a widely used behavioral task to study spatial learning and reference memory[19]. We implanted guide cannulas into the dorsal hippocampi and, after 1-week recovery, animals (n = 10 for each condition) underwent intrahippocampal injections of Aβ preparations as previously described [15].

During the first 3 days, mice were trained to find a platform hidden beneath the surface of the water and latency, that is, the time needed to reach the platform, was recorded. ANOVA for repeated measures showed a significant difference among groups ($F(4,45) = 5.145$; $p = 0.002$). When analyzing the last point of the spatial learning curve, mice treated with 200 pM oAβ42 needed less time to find the hidden platform compared with vehicle-infused mice with a significant difference in the sixth session ($p = 0.034$;

Fig. 2A). On the contrary, mice treated with oAβ42 200 nM showed an impairment of spatial learning because they spent more time to find the platform compared with vehicle-treated mice in the sixth session (p = 0.001; Fig. 2A). Treatment with mAβ42 at low concentration did not influence latency, whereas when at 200 nM, mAβ42 was capable of impairing spatial learning (p = 0.049; Fig. 2A).

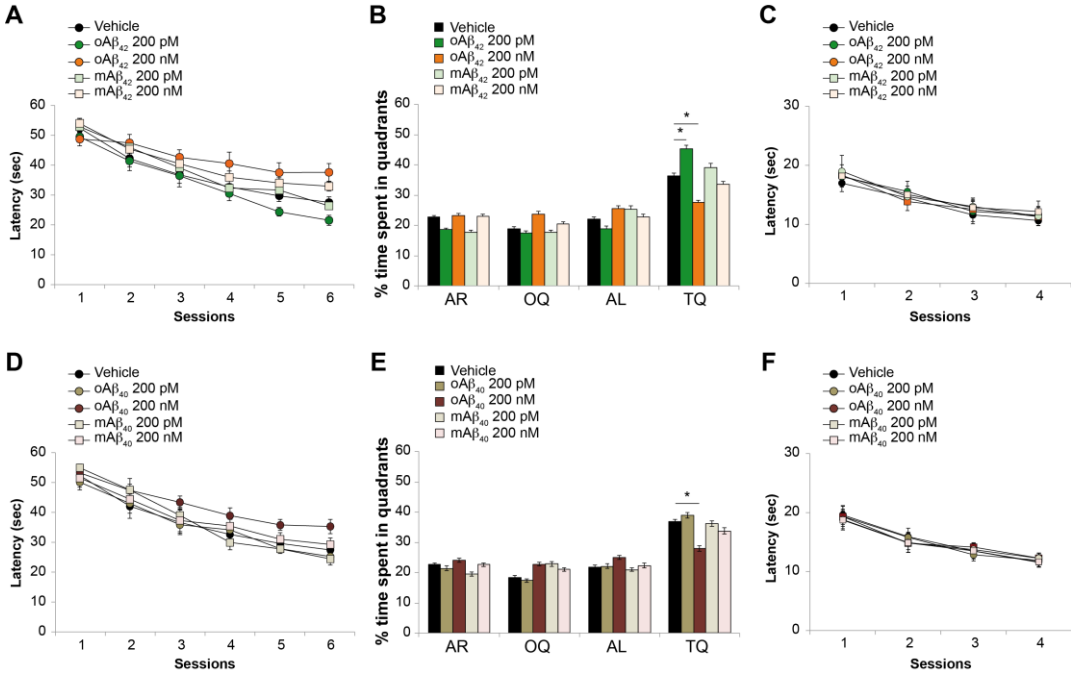

Fig. 2. High concentrations of oAβ42 and oAβ40 impair spatial learning and reference memory, whereas only low concentrations of oAβ42 enhance cognition. (A) Bilateral intrahippocampal injections of 200 nM oAβ42 and mAβ42 20 minutes before training increase the time to reach the platform in the MWM test. Conversely, latency is decreased in mice injected with 200 pM oAβ42, whereas 200 pM mAβ42 does not affect spatial learning. (B) The probe trial shows that administration of 200 nM or 200 pM oAβ42 induces a reduction or an increase of the % of time spent in TQ, respectively. mAβ does not affect reference memory regardless of the concentration used. (C) The visible platform trial does not reveal significant differences in the latency to reach the platform among groups. (D) Infusions of 200 nM oAβ40 20 minutes before training increase the time to reach the platform in the MWM test, whereas other Aβ40-based solutions do not affect latency. (E) The probe trial confirms that only 200 nM oAβ40 affects reference memory because it induces a reduction of the % of time spent in TQ. (F) The visible platform trial does not reveal significant differences among groups. Data expressed as average ±SEM. * $p < 0.05$. Abbreviations: AR, adjacent right; AL, adjacent left; mAβ, monomeric amyloid-beta; oAβ, oligomeric amyloid-beta; MWM, morris water maze; OQ, opposite quadrant; SEM, standard error mean; TQ, target quadrant.

Then, we assessed reference memory with the probe test, performed during the fourth day. The platform was removed and mice were allowed to search for 60 seconds. The

amount of time spent in each quadrant of the maze was evaluated. In each experimental group, we first compared the time spent in the TQ, where the platform was located during training, with other quadrants to verify whether mice had reference memory. All the groups spent significantly more time in the TQ compared with other quadrants ($p < 0.0001$), except when mice were treated with 200 nM oAβ42 ($p = 0.188$; Fig. 2B). Planned comparison indicated that mice treated with 200 pM oAβ42 spent more time in exploring the TQ ($p = 0.027$ vs. vehicle), whereas mice treated with 200 nM oAβ42 spent less time in exploring the TQ ($p = 0.048$ vs. vehicle), confirming the opposite effects of low and high doses of oAβ42 in reference memory (Fig. 2B). No differences were recorded in mice treated with 200 pM mAβ42 or 200 nM mAβ42, although the latter impaired LTP and spatial learning. A visible platform trial did not reveal any significant difference in the time to reach the platform among the groups during the 4 sessions of the task ($F(4,45) = 0.282$; $p = 0.888$; Fig. 2C).

Spatial learning was different among mice previously treated with different preparations of Aβ40 ($F(4,45) = 5.052$; $p = 0.002$). In the sixth trial, mice treated with 200 nM oAβ40 spent more time to find the hidden platform ($p = 0.008$ vs. vehicle; Fig. 2D), whereas no differences were found among treatments with other Aβ40 and vehicle ($p > 0.05$). Analyses of the probe trial showed that reference memory was impaired only in animals treated with oAβ40 200 nM that spent the same amount of time in TQ versus other quadrants ($p = 0.075$), whereas mice treated with vehicle or other Aβ40 preparations were able to remember the location of the platform (time spent in TQ vs. other quadrants: $p < 0.001$; Fig. 2E).

Planned comparison confirmed that 200 nM oAβ40 induced a reduction of the time spent in TQ ($p = 0.027$ vs. vehicle; Fig. 2E), whereas other preparations were ineffective ($p > 0.05$).

A visible platform trial did not reveal any significant difference in the time to reach the platform among the groups during the 4 sessions of the task ($F(4,45) = 0.077$; $p = 0.989$; Fig. 2F).

Thus, administration of exogenous 200 nM oAβ40 impaired spatial learning and reference memory, whereas other Aβ40 preparations did not influence it.

Endogenous oligomers of Aβ42 are needed for synaptic plasticity and memory

After the evaluation of the effects induced by exogenous administration of human Aβ per se, we aimed to clarify the role of endogenous Aβ in synaptic plasticity. To achieve a suppression of all the endogenous Aβ species, we used a monoclonal antibody (M3.2 mAb) able to recognize rodent Aβ40 and Aβ42 with high affinity[20–22] and specificity[23–25]. Thus, we performed rescue experiments by treating hippocampal slices with M3.2 mAb concurrently with different preparations of 200 pM human Aβ, not recognized by the rodent antibody. We first confirmed that perfusion of hippocampal slices with M3.2 mAb (2 μg/mL) for 20 minutes before tetanizing Schaffer collateral fibers inhibited CA3/CA1 LTP ($n = 6/6$ slices from 5/4 mice; $F(1,10) = 47.954$; $p < 0.0001$ vs. vehicle; Fig. 3A). Rescue experiments ($n = 6$ slices from 4-5 mice for each condition) showed that only 200 pM oAβ42 was able to restore the M3.2 mAb-induced LTP deficit ($F(1,10) = 35.069$; $p < 0.0001$ vs. M3.2 mAb; $F(1,10) = 0.331$; $p = 0.578$ vs. vehicle), whereas other preparations were ineffective (M3.2 mAb + mAβ42: $F(1,10) = 0.720$; $p = 0.413$; M3.2 mAb + oAβ40: $F(1,10) = 1.383$; $p = 0.267$; M3.2 mAb + mAβ40: $F(1,10) = 0.444$; $p = 0.520$; vs. M3.2 mAb; Fig. 3A). Analyses of residual potentiation of the last 5 recording time points confirmed that only 200 pM oAβ42 rescued the M3.2-induced impairment of LTP ($F(5,30) = 26.522$; $p < 0.001$ among all; Bonferroni's $p = 0$ for M3.2 mAb vs. vehicle and M3.2 mAb + oAβ42 vs. M3.2 mAb; Fig. 3B).

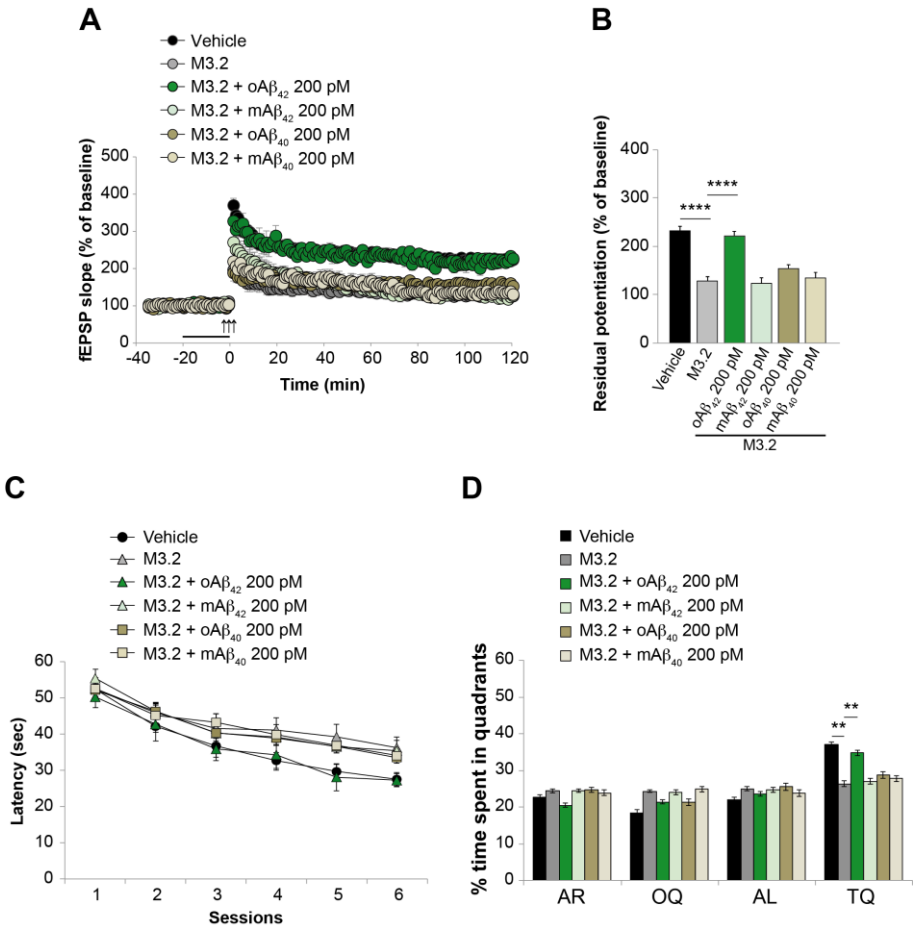

Fig. 3. **oAβ42 200 pM rescues the reduction of LTP and memory induced by depletion of endogenous Aβ.** (A) The reduction of LTP induced by 20 minutes perfusion with the antimurine Aβ monoclonal antibody M3.2 mAb (2 μg/μL) is rescued by a concomitant perfusion with 200 pM oAβ42 ($p = 0$), but not mAβ42, oAβ40, or mAβ40. Arrows indicate tetanus delivery and horizontal bar drugs perfusion. (B) Graph bars represent the residual potentiation (average of the last 5 recording time points). (C) Bilateral intrahippocampal injections of M3.2 mAb (2 μg/mL, in a final volume of 1 μL over 1 minute) 20 minutes before the session increase latency in the MWM test. Concomitant perfusion with oAβ42 200 pM rescues spatial learning, normalizing the time needed to find the hidden platform. Conversely, 200 pM mAβ42, oAβ40, or mAβ40 administration is not able to restore the M3.2 mAb-induced increase of latency. (D) The probe trial shows a reduction in time spent in TQ in mice treated with M3.2 mAb compared with vehicle. Memory is normal when mice are infused with M3.2 mAb and 200 pM oAβ40, but not mAβ42, oAβ40, or mAβ40. Data expressed as average ±SEM. **** $p < 0.0001$; ** $p < 0.005$. Abbreviations: AR, adjacent right; AL, adjacent left; LTP, long-term potentiation; mAβ, monomeric amyloid-beta; oAβ, oligomeric amyloid-beta; MWM, morris water maze; OQ, opposite quadrant; SEM, standard error mean; TQ, target quadrant.

We then focused on the role of endogenous Aβ in memory. As for electrophysiological experiments, mice (n = 10 for each condition) were treated with M3.2 mAb (2 μg/μL in a final volume of 1 μL over 1 minute) or vehicle. Twenty minutes after

intrahippocampal injections, mice underwent MWM. As previously demonstrated, we confirmed that blocking endogenous Aβ impaired spatial learning and reference memory. A significant difference was found analyzing the overall training among groups ($F(5,54) = 4.380$, $p = 0.002$). In particular, analyses of the last session showed that mice previously treated with M3.2 mAb spent a longer time to find the hidden platform compared with vehicle-infused mice ($p = 0.007$; Fig. 3C). The probe trial showed that reference memory was impaired in M3.2 mAb-treated animals as they spent the same time in TQ versus other quadrants ($t(18) = 0.920$, $p = 0.370$); consistently, the time spent in TQ was significantly different when compared with that of vehicle-infused mice ($p = 0.001$ vs. vehicle; Fig. 3D).

To understand whether different species and aggregation status of the peptide specifically mediated the learning impairment, mice were infused with 200 pM oAβ42, mAβ42, oAβ40, or mAβ40, in addition to M3.2 mAb. Consistently with our electrophysiological findings, only 200 pM oAβ42 was capable to rescue behavioral deficits both during the hidden training ($p = 0.006$ vs. M3.2 mAb; $p = 0.448$ vs. vehicle; Fig. 3C) and the probe trial (TQ vs. other quadrants: $t(18) = 6.897$, $p < 0.0001$; % time spent in TQ: $p = 0.006$ vs. M3.2 mAb; $p = 0.448$ vs. vehicle; Fig. 3D). Conversely, mAβ42, oAβ40, or mAβ40 did not rescue M3.2 mAb-induced spatial learning and reference memory. In fact, the memory deficit persisted in the hidden test during the fifth and the sixth session ($p > 0.05$ when comparing M3.2 mAb + mAβ42 or oAβ40 or mAβ40 vs. M3.2 mAb; Fig. 3C), and the probe trial ($p > 0.05$ when comparing TQ vs. other quadrants in mice treated with M3.2 mAb + mAβ42 or oAβ40 or mAβ40; $p > 0.05$ when comparing % time spent in TQ between in M3.2 mAb vs. M3.2 mAb + mAβ42 or oAβ40 or mAβ40; Fig. 3D).

The content of oligomers and monomers depends on the concentration of Aβ solutions

Given that only oAβ42 was able to either stimulate or impair LTP and memory depending on concentration, we investigated whether this biphasic effect was

associated with a difference in Aβ total concentration and/or changes in the relative content of monomers and oligomers.

A preliminary sodium dodecyl sulfate–polyacrylamide gel electrophoresis of the 2 synthetic preparations confirmed that when at 200 pM, both monomers and oligomers were present although in different proportions (Fig. 4A).

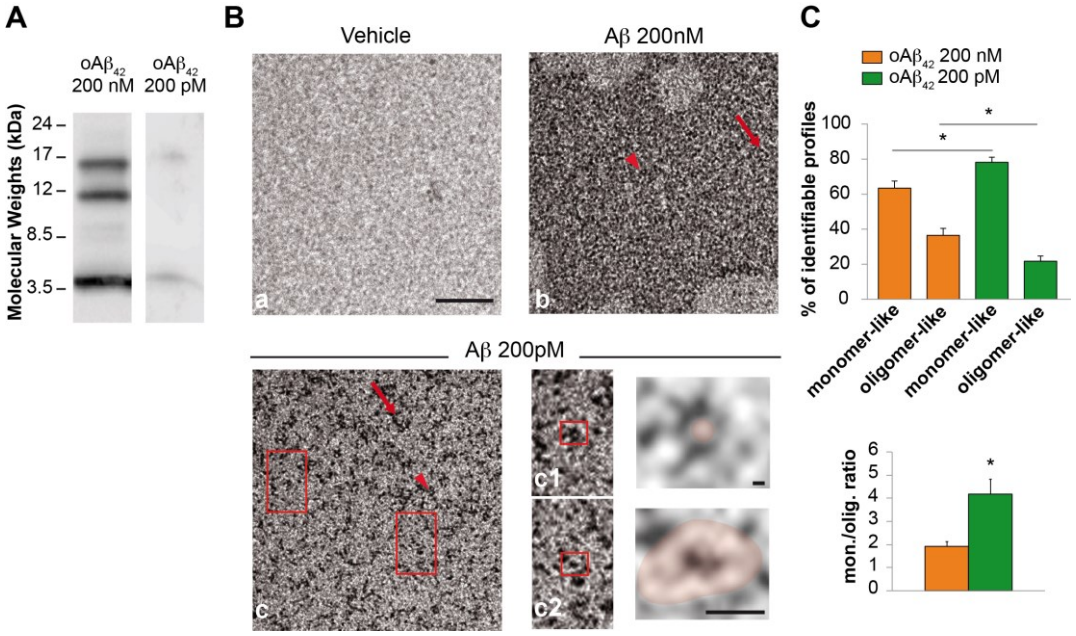

Fig. 4. oAβ42 synthetic preparations at 200 nM and 200 pM show a different content of monomers and oligomers. (A) WB of synthetic human 200 pM oAβ42 shows the presence of both monomers and oligomers. (B) TEM showing ultramicroscopic fields of grids incubated with vehicle, 200 nM or 200 pM solutions of oAβ42 and processed with negative staining technique. In b and c, arrowheads and arrows indicate monomer-like and oligomer-like elements, respectively. Enlarged framed regions showing representative examples of a monomer-like (round shape and diameter ≤ of 5 nm; c1) and an oligomer-like element (oval shape and diameter ≥ of 10 nm; c2). Colored shadows in c1 and c2 resemble the round and oval shape of monomer-like and oligomer-like elements, respectively. Bars: 100 nm for a, b, d; 1 nm for c1 subpanel; and 5 nm for c2 subpanel. (C) The % of identifiable monomers is higher, whereas the % of identifiable oligomers is lower in the 200 pM versus the 200 nM oAβ42 solution. Monomers/oligomers ratio is higher in the 200 pM solution. Data expressed as mean ± SEM. * $p < 0.05$. Abbreviations: oAβ, oligomeric amyloid-beta; SEM, standard error mean; TEM, transmission electron microscopy; WB, western blot.

TEM carried out by negative staining technique[26] was then performed to visualize oAβ42 solutions at 200 nM and 200 pM. Both preparations exhibited negatively stained Aβ with variable size and morphology resembling monomer-like (round shape and

diameter ≤ of 5 nm) and oligomer-like (oval shape and diameter ≥ of 10 nm) profiles of Aβ (Fig. 4B). Quantification of monomer-like and oligomer-like species showed that 200 nM and 200 pM solutions displayed different proportions of monomers and oligomers (Fig. 4C). In particular, comparisons of monomer-like and oligomer-like species of the 2 preparations revealed that the percentage of identifiable monomer-like elements in 200 pM solution was significantly higher than that in 200 nM solution (78.21 ± 2.88 vs. 63.49 ± 4.00%; Mann-Whitney test: $p = 0.018$), whereas the percentage of identifiable oligomer-like species was significantly lower in 200 pM solutions than that in 200 nM solutions (21.78 ± 2.88 vs. 36.50 ± 4.00%; $p = 0.018$), as confirmed by the increase of the monomers/oligomers ratio in 200 pM oAβ42 solution (1.91 ± 0.22 vs. 4.17 ± 0.65; Mann-Whitney test: $p = 0.005$). Thus, the content of monomer and oligomer forms depended on Aβ concentration.

Discussion

This work was inspired by previous observations indicating that Aβ exerts an opposite effect on synaptic plasticity and memory depending on its concentration[15]. Here we have demonstrated that this Aβ biphasic effect is influenced by different isoforms or aggregation status of the peptide.

While it is commonly accepted that high levels of Aβ42 oligomers are detrimental for synaptic activity[27], monomeric forms of Aβ42 are thought to exclusively have neuroprotective functions[11]. However, in this article, we showed that when at high concentration, Aβ42 monomers impair synaptic plasticity and memory. This suggests that monomers are also able to exert a neurotoxic action when at high concentrations, in agreement with findings suggesting a role for monomers in AD[28,29]. Although we cannot exclude that the few oligomers present in our mAβ42 preparations might be responsible of the synaptotoxic effect, or that mAβ42 might undergo further oligomerization once injected into the hippocampus, our data suggests that caution is needed when designing anti-Aβ therapies exclusively directed against oligomers sparing monomers, as they might not be a safe and effective strategy as expected.

We then studied the effects of Aβ40, which is known to be the most represented Aβ species in the brain but with low propensity to oligomerize[5]. In our experimental conditions, 200 nM oAβ40 impaired synaptic plasticity and memory, whereas when monomers prevailed (mAβ40), the solution was ineffective. Thus, oAβ40 was capable of inhibiting LTP in a comparable manner to what observed for oAβ42, suggesting an isoform effect, even if the oAβ40 solution contains lower levels of oligomers in respect to oAβ42. Although we cannot affirm that oAβ40 oligomers are more toxic than those of oAβ42, it appears that Aβ solutions inducing a greater LTP impairment (oAβ42 and oAβ40) contain a higher amount of dimers, as shown in Fig. 1A. Conversely, mAβ42, which induces a weaker neurotoxic effect, contains few dimers and a higher quantity of trimers and tetramers. This is consistent with previous studies reporting a different oligomerization behavior for Aβ40 and Aβ42, with a distinct distribution of low order oligomers due to differences in their dimer equilibrium structures[30]. Photoinduced cross-linking of unmodified proteins experiments showed that Aβ42 tends to form "paranuclei" (e.g., pentamers and examers) which, in turn, can oligomerize to generate structures of higher order. Conversely, Aβ40 does not form paranuclei and is more prone to exist as a mixture of monomers, dimers, and tetramers, rather than trimers and larger oligomers[31,32], as confirmed by studies exploiting ion mobility coupled with mass spectrometry[33]. Dimers and tetramers thus represent a key aggregation status for Aβ40 due to their stability and resistance to further monomer or dimer addition in the tetrameric state. This might be related to the fact that Aβ40 has a more closed planar angle in the tetrameric form compared with Aβ42. Consequently, the latter is able to add another monomer to its tetrameric structure leading to pentameric paranuclei formation[33]. Based on these observations, we can speculate that dimers are mainly responsible of the negative effect exerted by oAβ40 on synaptic plasticity and memory. Accordingly, Aβ40 dimerization increased β-strand propensity and toxicity[7] and Aβ dimers have been recognized as the smallest oligomeric species increasing in the AD brain[34,35]. Moreover, a recent work has evidenced that an increased production of soluble Aβ dimers, but not monomers, plaques or other forms of insoluble Aβ, is sufficient to exert a detrimental effect on synaptic plasticity and memory in TgDimer

mice[36]. In any case, the oligomerization and the consequent toxicity of the peptide might be altered by different physicochemical conditions and further works, out of the scope of the present article, are needed to better understand the different effects exerted by single Aβ aggregates in synaptic plasticity and memory.

On the other hand, when studying the positive effect of Aβ at picomolar concentrations, we found that only 200 pM oAβ42 enhanced LTP and memory, in agreement with previous findings[13], whereas oAβ40 or monomer enriched solutions, that is, mAβ42 and mAβ40, did not exert any effect. Interestingly, oAβ42 also exerted an enhancing effect on fiber volley amplitude, which is an index of presynaptic recruitment, in agreement with previous works indicating that low concentrations of oAβ42 enhances neurotransmitter release[13,37]. Consistently, the suppression of LTP and memory induced by the murine anti-Aβ antibody M3.2 mAb, was specifically rescued by 200 pM oAβ42[24,38,39], excluding that mAβ42 or Aβ40 at these conditions and concentrations played a role in synaptic plasticity and memory in the healthy brain.

Thus, our study highlighted a different contribution of soluble Aβ in synaptic plasticity and memory depending on its species, aggregation state, and concentration. This is a crucial point, considering that soluble Aβ aggregates extracted from AD brains are highly heterogeneous and it is not clear whether synthetic preparations used for in vitro and in vivo research reproduced the physicochemical characteristics of Aβ in the human brain. Our functional results might be due to the structural differences between Aβ42 and Aβ40. In fact, the difference in Aβ42 and Aβ40 monomeric structures are thought to induce oligomers formation via different pathways, resulting in larger Aβ42 oligomers. However, whether this different oligomeric conformation is responsible for the different effects exerted by our preparations is unknown and out of the scope of the present article. Here, we can confirm that Aβ42 is much prone to oligomerization, consistently with previous studies demonstrating that the presence of 2 additional amino acid residues at Aβ42 C terminus confers more rigidity to the peptide structure stimulating oligomers formation[5]. Moreover, our experience indicates that, in a 200 nM solution, the quantity of oligomers increased after few hours of incubation in ACSF and that the oligomerization process is faster at RT. To exclude that the detection of

oligomers was due to the presence of sodium dodecyl sulfate, which has been shown to enhance ex vivo aggregation of Aβ[40], we have performed WB in nondenaturating nonreducing conditions and confirmed our findings by TEM analyses.

Notably, in our conditions, both monomers and oligomers are present when synthetic Aβ42 or Aβ40 were dissolved in ACSF, even if in different proportions. Indeed, the dynamic rearrangement of monomers/oligomers in the physiological brain environment is still a matter of debate[41]. The most diffuse opinion is that Aβ is secreted in monomeric form during synaptic activity, which strengthens the idea to restrict its physiological effects to monomers. On the other hand, the aggregation state is likely to depend on different physicochemical characteristics that are not perfectly reproducible in in vivo and in vitro studies[27]. However, some works have demonstrated that a certain degree of oligomerization is likely to occur whenever the peptide is present in a solution at 37 °C and pH 7.4[42], as in the physiological brain environment. On the contrary, recent studies performed by single-molecule fluorescence imaging have evidenced that Aβ remained in monomeric forms up to a 3 μM concentration, which is much higher than the one detected in AD brains, leading to the conclusion that, when present, oligomers should be released as such and are not the result of monomers aggregation[43]. TEM analyses confirmed that our oAβ42 preparations contained both monomers and oligomers, although their quantity depended on the final concentration of the solution with an increase of the monomers/oligomers ratio when at 200 pM concentration. This, together with the biphasic effect exerted by oAβ42, raises 2 major points: (1) the presence of oligomers is inversely proportional to the concentration of the solution; (2) the presence of oligomers, even if limited, is necessary for Aβ to exert its positive effect on the synapse, challenging the theory that oligomers only have a deleterious effect. Intriguingly, oligomers have been detected in the CSF and brain of healthy people throughout life[10], with a prevalence of trimers during childhood and adolescence, when plastic changes are highly effective.

As for monomers, our findings suggest that (1) in our experimental conditions, it is not possible to obtain a pure monomeric preparation, in contrast with previous studies[11]; (2) Aβ42 solutions enriched in monomers impaired synaptic plasticity and memory

when at high concentrations, whereas they do not elicit any effect when at low physiological concentrations. This does not exclude that they might exert a physiological function through different mechanisms, for example by interfering with cellular mechanisms aimed at controlling apoptosis, survival, and energetic metabolism of the cell.

Conclusion

Our findings have demonstrated that the presence of oligomers is crucial either in physiological or pathological conditions. Intriguingly, we have previously demonstrated that exposure to 200 pM Aβ42 exerts opposite effects depending on the time of exposure, with short exposures enhancing synaptic plasticity and memory, and longer exposures reducing them[37]. Thus, it is plausible that Aβ42 oligomers are not toxic per se but only when present in excessive quantities or for a prolonged time.
Although we cannot exclude that different methods of Aβ preparation or different concentrations might induce different effects on synaptic plasticity, these findings should be taken into consideration either when studying the physiological role of the peptide or designing therapies targeting Aβ in AD.

Disclosure statement

The authors have no actual or potential conflicts of interest.

Acknowledgements

This work was supported by University of Catania intramural funding to D.P and A.P., PRIN 2015H4K2CR, UNIVPM PSA 2017 to F.C and NIH grant R01AG049402 to O.A.

Materials and methods

Animals

All experiments involving animals were approved by University of Catania (#327/2013-B, #119–2017-PR) and Columbia University (#AC-AAAO5301) in accordance with the respective regulations of local Institutional Animal care and Use Committee. Wild-type (C57Bl/6J) mice were obtained from breeding colonies kept in the animal facilities at University of Catania and Columbia University. Mice were maintained in stable hygrometric and thermic conditions (50%; 21 °C ± 1 °C) on 12 hours light/dark cycle with ad libitum access to food and water. Males and females were used in a sex-balanced fashion (5 males and 5 females; averaged weight: 30.5 ± 0.14 vs. 25.07 ± 0.18) for each condition described in behavioral experiments. Males were used for electrophysiological experiments. We used 5–7 slices for each LTP recording from 5 to 7 different animals as reported for each experiment in the result section. All mice used in our experiments were 3–6 months old.

Aβ preparation

Aβ was prepared as previously described[15,17,18]. Briefly, the lyophilized peptide (American Peptide, Sunnyvale, CA, USA) was suspended in 1,1,1,3,3,3-hexafluoro-2-propanol (Sigma, St. Louis, MO, USA) to 1 mM. After the complete evaporation of 1,1,1,3,3,3-hexafluoro-2-propanol to allow complete monomerization, the Aβ film was dissolved in dimethyl sulfoxide (DMSO; Sigma), sonicated for 15 minutes, aliquoted, and stored at −20 °C. Different protocols were used to obtain preparations of Aβ42 or Aβ40 enriched in monomers (mAβ42 and mAβ40) or oligomers (oAβ42 and oAβ40). For mAβ42 and mAβ40, the DMSO-Aβ solution was diluted in artificial CSF (ACSF) immediately before use to the final concentration (200 pM and 200 nM). For oAβ42 and oAβ40, the DMSO-Aβ solution was incubated in PBS at 4 °C for 12 hours and 1 week, respectively, to allow oligomerization. These oligomerized Aβ solutions were then diluted in ACSF to the final concentration, calculated based on the MW of the monomeric peptides. The oligomerization status of these solutions was routinely tested by western blot (WB) analysis. Scramble Aβ42 and Aβ40 (AnaSpec Inc, San Jose, CA, USA) were prepared following the same procedure.

WB analysis of Aβ preparations

Aβ solutions, prepared as described previously, were incubated for 20 minutes at 29 °C to reproduce electrophysiological conditions. After this step, NuPAGE LDS sample buffer 4× was added and the samples were separated on 10%–20% Novex Tricine precast gels (Invitrogen) according to the manufacturer's protocol. Gels were transferred to 0.2 mm nitrocellulose membranes (Amersham Biosciences, Buckinghamshire, UK). Membranes were blocked for 1 hour, at room temperature (RT), in a solution of 5% nonfat dry milk in Tris-buffered saline containing 0.1% Tween-20 before incubation overnight at 4 °C with the mouse monoclonal antibody 6E10 (1:1000; Covance, Princeton, NJ, USA). Membranes were washed 3 times with Tris-buffered saline containing 0.1% Tween-20 and then incubated with the horseradish peroxidase-conjugated Ig antimouse antibody (1:2500; Cell Signaling Technology Inc, Danvers, MA, USA) at RT for 1 hour. In another series of experiments, only oAβ42 at the final concentrations of 200 nM and 200 pM was assessed by WB following the same procedure. Development was done by using the SuperSignal West Femto Maximum Sensitivity Substrate (Thermo Scientific, Waltham, MA, USA). Immunoblots were documented by using UVItec Cambridge Alliance. Molecular weights were estimated using Rainbow Molecular Weight Markers (GE Healthcare Life Sciences).

Electrophysiological recordings

Extracellular electrophysiological field recordings were performed on 400 μm transverse hippocampal slices as previously described[13]. After cutting procedure by using a manual tissue chopper, slices were transferred to a recording chamber and perfused (1–2 mL/min) with ACSF (composition in mM: 124.0 NaCl, 4.4 KCl, 1.0 Na2HPO4, 25.0 NaHCO3, 2.0 CaCl2, 2.0 MgCl2, 10.0 Glucose) kept at 29 °C and continuously bubbled with an O2/CO2 mixture at 95% and 5%. After 120 minutes recovery, field excitatory postsynaptic potentials (fEPSPs) were recorded in CA1 stratum radiatum by a glass electrode filled with ACSF in response to Schaffer collaterals stimulation by a bipolar tungsten electrode. Baseline synaptic transmission (BST) was assessed by a 5–35 V stimulus delivery and plotted as fEPSP slope against afferent volley amplitude. Baseline was recorded every minute, by stimulating at a voltage able to evoke a response of 35% of the maximum evoked response in BST. LTP was induced by a theta-burst stimulation, that is, 3 TBS trains delivered with a 15 seconds inter-train interval with each train consisting in 10 × 100 Hz bursts with 5 pulses per burst with a 200-ms interburst interval, at the test pulse intensity. Recordings were performed and analyzed in pClamp 10 (Molecular Devices, Sunnyvale, CA, USA).

Infusion technique

Cannulas were implanted as previously described[44]. Anesthesia was induced with an association of Tiletamine + Zolazepam (60 mg/kg) and Medetomidine (40 μg/kg). Mice were implanted with a 26-gauge guide cannula into the dorsal hippocampi (coordinates from bregma: posterior = 2.46 mm, lateral = 1.50 mm to a depth of 1.30 mm). After 6–8 days of recovery, drugs were bilaterally injected in a final volume of 1 μL over 1 minute through infusion cannulas that were connected to a microsyringe by a polyethylene tube. During infusion, animals were handled gently to minimize stress. After infusion, the needle was left in place for another minute to allow diffusion. In some animals, after behavioral studies, a solution of 4% methylene blue was infused for localization of infusion cannulas.

Behavioral studies

Morris Water Maze (MWM) experiments were performed as described[45]. The apparatus consisted of a plastic maze filled with water maintained at about 25 °C and made opaque to hide the submerged platform by the addition of nontoxic white paint. The submerged platform was located in the south-west quadrant and left there throughout the tests. Spatial cues were placed on the 4 cardinal points of the maze. We first assessed spatial learning by placing animals into the pool where they learned to locate the hidden platform beneath the surface of the water. Mice were trained for 3 days (2 daily sessions held 4 hours apart). Each session consisted of three 1-minute trials. For each trial, mice started from a different, randomly chosen quadrant. The time taken to reach the hidden submerged platform (latency) was recorded. After this acquisition training, on the fourth day, the platform was removed to perform the probe test. This allowed evaluating the retention of spatial memory. One session consisting of four 1-minute probe trials separated by 5 seconds was performed. The maze was divided into 4 quadrants: the target quadrant (TQ) previously containing the platform; the adjacent left, the adjacent right, and the opposite quadrant. The percent time spent in each quadrant was recorded and analyzed with a video tracking system (Netsense srl, Catania, Italy), and the performances of the 4 probe trials were averaged. On the fifth and sixth day, visual, motor, and motivation skills were tested in 2 sessions/day (each consisting of three 1-minute trials) by measuring the time taken to reach a visible platform (randomly positioned in a different place each time) marked with a green flag.

Transmission electron microscopy for Aβ visualization

For Aβ visualization, carbon-coated copper 200 mesh grids were processed according to negative stained technique with 2% uranyl acetate[26,46,47]. Briefly, grids were incubated for 20 minutes with 5 μL of oAβ42 200 nM, 200 pM, and vehicle (2 grids for each condition), then washed with boiled filtered distillated water and then exposed for 30 seconds to 2% uranyl acetate. After air-dried, grids were examined in a blinded manner, with a Philips CM10 electron microscope coupled to a MegaView-II high resolution CCD camera (Soft Imaging System, Germany). Electron microscopical fields were captured at an original magnification of 34,000, 64,000 and 92,000×. For quantification of Aβ monomer-like and

oligomer-like elements in Aβ 200 nM and 200 pM preparations, 200 nm × 200 nm subfields (n = 8) were randomly selected from 34,000× original acquisitions (n = 2). According to previous electron microscopy visualization of Aβ[26], negatively Aβ stained was deciphered by the presence of an electrondense contour displaying a variable morphology. Based on the shape and on the estimated internal diameter, monomer-like elements (round shape and diameter ≤ of 5 nm) and oligomer-like elements (oval shape and diameter ≥ of 10 nm[26] were noted and counted. Diameters of recognizable elements were calculated by using Image J software.

Statistics

All experiments were performed by operators blind with respect to treatment. Data were expressed as mean ± standard error mean (SEM). Statistical analysis was performed by using different tests, based on preliminary analyses of normal distribution. We have used (1) analysis of variance (ANOVA) for repeated measures to analyze LTP for 120 minutes of recording after tetanus and curves of spatial learning (independent variables time and treatment, with treatment as main effect); (2) 1-way ANOVA with Bonferroni's post hoc correction for LTP residual potentiation (treatment as main effect); (3) 1-way ANOVA with LSD post hoc correction for latency in the sixth MWM trial and percentage of time spent in TQ in the probe test; and (4) paired t-test to analyze percentage of time spent in TQ versus non-TQ quadrants. Given the non-normal distribution of data obtained in transmission electron microscopy (TEM) experiments (assessed by D'Agostino & Pearson normality) comparison between the monomer-like and oligomer-like elements of Aβ 200 nM and 200 pM was made by Mann-Whitney test. SigmaPlot 12.0, Systat 9 and GraphPad Prism 7 software were used. The level of significance was set at $p < 0.05$.

References

1. Walsh, D. M. & Selkoe, D. J. Aβ oligomers - A decade of discovery. *J. Neurochem.* **101,** 1172–1184 (2007).
2. Vandersteen, A. *et al.* A comparative analysis of the aggregation behavior of amyloid-β peptide variants. *FEBS Lett.* **586,** 4088–93 (2012).
3. Puzzo, D. & Arancio, O. Amyloid-β peptide: Dr. Jekyll or Mr. Hyde? *J. Alzheimers. Dis.* **33 Suppl 1,** S111-20 (2013).
4. Vandersteen, A. *et al.* A comparative analysis of the aggregation behavior of amyloid-b peptide variants. *FEBS Lett* **586,** 4088–4093
5. Sgourakis, N. G., Yan, Y., McCallum, S. A., Wang, C. & Garcia, A. E. The Alzheimer's peptides Abeta40 and 42 adopt distinct conformations in water: a combined MD / NMR study. *J. Mol. Biol.* **368,** 1448–57 (2007).
6. Jarrett, J. T. & Lansbury, P. T. Seeding 'one-dimensional crystallization' of amyloid: a pathogenic mechanism in Alzheimer's disease and scrapie? *Cell* **73,** 1055–8 (1993).
7. Ono, K., Condron, M. M. & Teplow, D. B. Structure-neurotoxicity relationships of amyloid beta-protein oligomers. *Proc. Natl. Acad. Sci. U. S. A.* **106,** 14745–50 (2009).
8. Roychaudhuri, R., Yang, M., Hoshi, M. M. & Teplow, D. B. Amyloid beta-protein assembly and Alzheimer disease. *J. Biol. Chem.* **284,** 4749–53 (2009).
9. Fukumoto, H. *et al.* High-molecular-weight beta-amyloid oligomers are elevated in cerebrospinal fluid of Alzheimer patients. *FASEB J.* **24,** 2716–2726 (2010).
10. Lesné, S. E. *et al.* Brain amyloid-β oligomers in ageing and Alzheimer's disease. *Brain* **136,** 1383–98 (2013).
11. Giuffrida, M. L. *et al.* Beta-amyloid monomers are neuroprotective. *J. Neurosci.* **29,** 10582–7 (2009).
12. Giedraitis, V. *et al.* The normal equilibrium between CSF and plasma amyloid beta levels is disrupted in Alzheimer's disease. *Neurosci. Lett.* **427,** 127–31 (2007).
13. Puzzo, D. *et al.* Picomolar amyloid-beta positively modulates synaptic plasticity and memory in hippocampus. *J. Neurosci.* **28,** 14537–45 (2008).
14. Schmidt, S. D., Nixon, R. A. & Mathews, P. M. *ELISA method for measurement of amyloid-b levels. Amyloid Proteins*. (Humana Press, New Jersey).
15. Puzzo, D., Privitera, L. & Palmeri, A. Hormetic effect of amyloid-β peptide in synaptic plasticity and memory. *Neurobiol. Aging* **33,** 1484.e15-24 (2012).
16. Bliss, T. V & Collingridge, G. L. A synaptic model of memory: long-term potentiation in the hippocampus. *Nature* **361,** 31–9 (1993).
17. Ripoli, C. *et al.* Effects of different amyloid β-protein analogues on synaptic function. *Neurobiol. Aging* **34,** 1032–1044 (2013).
18. Stine, W. B., Dahlgren, K. N., Krafft, G. A. & LaDu, M. J. In vitro characterization of conditions for amyloid-beta peptide oligomerization and fibrillogenesis. *J. Biol. Chem.* **278,** 11612–22 (2003).
19. Puzzo, D., Lee, L., Palmeri, A., Calabrese, G. & Arancio, O. Behavioral assays with mouse models of Alzheimer's disease: practical considerations and guidelines. *Biochem. Pharmacol.* **88,** 450–67 (2014).
20. Morales-Corraliza, J. *et al.* In vivo turnover of tau and APP metabolites in the brains of wild-type and Tg2576 mice: greater stability of sAPP in the beta-amyloid depositing mice. *PLoS One* **4,** e7134 (2009).
21. Morales-Corraliza, J. *et al.* Immunization targeting a minor plaque constituent clears β-amyloid and rescues behavioral deficits in an Alzheimer's disease mouse model. *Neurobiol. Aging* **34,** 137–45 (2013).
22. Wesson, D. W., Morales-Corraliza, J., Mazzella, M. J., Wilson, D. A. & Mathews, P. M. Chronic anti-murine Aβ immunization preserves odor guided behaviors in an Alzheimer's β-amyloidosis model. *Behav. Brain Res.* **237,** 96–102 (2013).
23. Palmeri, A. *et al.* Amyloid-β Peptide Is Needed for cGMP-Induced Long-Term Potentiation and

Memory. *J. Neurosci.* **37,** 6926–6937 (2017).
24. Puzzo, D. *et al.* Endogenous amyloid-β is necessary for hippocampal synaptic plasticity and memory. *Ann. Neurol.* **69,** 819–30 (2011).
25. Ricciarelli, R. *et al.* A novel mechanism for cyclic adenosine monophosphate-mediated memory formation: Role of amyloid beta. *Ann. Neurol.* **75,** 602–7 (2014).
26. Ahmed, M. *et al.* Structural conversion of neurotoxic amyloid-beta(1-42) oligomers to fibrils. *Nat. Struct. Mol. Biol.* **17,** 561–7 (2010).
27. Hayden, E. Y. *et al.* Inhibiting amyloid β-protein assembly: Size-activity relationships among grape seed-derived polyphenols. *J. Neurochem.* **135,** 416–30 (2015).
28. Guglielmotto, M. *et al.* Aβ1-42 monomers or oligomers have different effects on autophagy and apoptosis. *Autophagy* **10,** 1827–43 (2014).
29. Manassero, G. *et al.* Beta-amyloid 1-42 monomers, but not oligomers, produce PHF-like conformation of Tau protein. *Aging Cell* **15,** 914–23 (2016).
30. Côté, S., Laghaei, R., Derreumaux, P. & Mousseau, N. Distinct dimerization for various alloforms of the amyloid-beta protein: Aβ(1-40), Aβ(1-42), and Aβ(1-40)(D23N). *J. Phys. Chem. B* **116,** 4043–55 (2012).
31. Bitan, G., Lomakin, A. & Teplow, D. B. Amyloid beta-protein oligomerization: prenucleation interactions revealed by photo-induced cross-linking of unmodified proteins. *J. Biol. Chem.* **276,** 35176–84 (2001).
32. Bitan, G. *et al.* Amyloid beta -protein (Abeta) assembly: Abeta 40 and Abeta 42 oligomerize through distinct pathways. *Proc. Natl. Acad. Sci. U. S. A.* **100,** 330–5 (2003).
33. Bernstein, S. L. *et al.* Amyloid-β protein oligomerization and the importance of tetramers and dodecamers in the aetiology of Alzheimer's disease. *Nat. Chem.* **1,** 326–31 (2009).
34. Mc Donald, J. M. *et al.* The presence of sodium dodecyl sulphate-stable Abeta dimers is strongly associated with Alzheimer-type dementia. *Brain* **133,** 1328–41 (2010).
35. Shankar, G. M. *et al.* Amyloid-β protein dimers isolated directly from Alzheimer's brains impair synaptic plasticity and memory. *Nat. Med.* **14,** 837–842 (2008).
36. Müller-Schiffmann, A. *et al.* Amyloid-β dimers in the absence of plaque pathology impair learning and synaptic plasticity. *Brain* **139,** 509–25 (2016).
37. Koppensteiner, P. *et al.* Time-dependent reversal of synaptic plasticity induced by physiological concentrations of oligomeric Aβ42: an early index of Alzheimer's disease. *Sci. Rep.* **6,** 32553 (2016).
38. Garcia-Osta, A. & Alberini, C. M. Amyloid beta mediates memory formation. *Learn. Mem. (Cold Spring Harb. NY)* **16,** 267–272 (2009).
39. Morley, J. E. *et al.* A physiological role for amyloid-β protein: Enhancement of learning and memory. *J. Alzheimer's Dis.* **19,** 441–449 (2010).
40. Esparza, T. J. *et al.* Soluble Amyloid-beta Aggregates from Human Alzheimer's Disease Brains. *Sci. Rep.* **6,** 38187 (2016).
41. Bemporad, F. & Chiti, F. Protein misfolded oligomers: experimental approaches, mechanism of formation, and structure-toxicity relationships. *Chem. Biol.* **19,** 315–27 (2012).
42. El-Agnaf, O. M., Mahil, D. S., Patel, B. P. & Austen, B. M. Oligomerization and toxicity of beta-amyloid-42 implicated in Alzheimer's disease. *Biochem. Biophys. Res. Commun.* **273,** 1003–7 (2000).
43. Nag, S. *et al.* Nature of the amyloid-beta monomer and the monomer-oligomer equilibrium. *J. Biol. Chem.* **286,** 13827–33 (2011).
44. Puzzo, D. *et al.* LTP and memory impairment caused by extracellular Aβ and Tau oligomers is APP-dependent. *Elife* **6,** (2017).
45. Puzzo, D. *et al.* F3/Contactin promotes hippocampal neurogenesis, synaptic plasticity, and memory in adult mice. *Hippocampus* **23,** 1367–82 (2013).
46. Booth, D. S., Avila-Sakar, A. & Cheng, Y. Visualizing proteins and macromolecular complexes by negative stain EM: from grid preparation to image acquisition. *J. Vis. Exp.* **135,** 1631–5 (2011).
47. Picou, R., Moses, J. P., Wellman, A. D., Kheterpal, I. & Gilman, S. D. Analysis of monomeric Abeta (1-40) peptide by capillary electrophoresis. *Analyst* **135,** 1631–5 (2010).

Chapter 2: Amyloid-β peptide is needed for cGMP-induced long-term potentiation and memory

Palmeri A[1], Ricciarelli R[2], Gulisano W[1], Rivera D[2], Rebosio C[3], Calcagno E[2], Tropea MR[1], Conti S[4], Das U[5], Roy S[5,6], Pronzato MA[2], Arancio O[4], Fedele E[7,8], Puzzo D[9].

[1]Department of Biomedical and Biotechnological Sciences, Section of Physiology, University of Catania, 95123 Catania, Italy.[2]Department of Experimental Medicine, Section of General Pathology, School of Medical and Pharmaceutical Sciences, University of Genoa, 16132 Genoa, Italy. [3]Department of Pharmacy, Section of Pharmacology and Toxicology, School of Medical and Pharmaceutical Sciences, University of Genoa, 16148 Genoa, Italy. [4]Department of Pathology and Cell Biology & The Taub Institute, Columbia University, New York, New York, 10032. [5]Department of Pathology and Department of Neurosciences, University of California, San Diego, La Jolla, California 92093. [6]Department of Pathology and Department of Neuroscience, University of Wisconsin, Madison, Wisconsin 53705, and [7]Department of Pharmacy, Section of Pharmacology and Toxicology, School of Medical and Pharmaceutical Sciences, University of Genoa, 16148 Genoa, Italy, [8]Center of Excellence for Biomedical Research, University of Genoa, 16132 Genoa, Italy. [9]Department of Biomedical and Biotechnological Sciences, Section of Physiology, University of Catania, 95123 Catania, Italy.

In: J Neurosci. 2017 Jul 19;37(29):6926-6937.

doi: 10.1523/JNEUROSCI.3607-16.2017.

Abstract

High levels of amyloid-β peptide (Aβ) have been related to Alzheimer's disease pathogenesis. However, in the healthy brain, low physiologically relevant concentrations of Aβ are necessary for long-term potentiation (LTP) and memory. Because cGMP plays a key role in these processes, here we investigated whether the cyclic nucleotide cGMP influences Aβ levels and function during LTP and memory. We demonstrate that the increase of cGMP levels by the phosphodiesterase-5 inhibitors sildenafil and vardenafil induces a parallel release of Aβ due to a change in the approximation of amyloid precursor protein (APP) and the β-site APP cleaving enzyme 1. Moreover, electrophysiological and behavioral studies performed on animals of both sexes showed that blocking Aβ function, by using anti-murine Aβ antibodies or APP knock-out mice, prevents the cGMP-dependent enhancement of LTP and memory. Our data suggest that cGMP positively regulates Aβ levels in the healthy brain which, in turn, boosts synaptic plasticity and memory.

Introduction

Synaptic plasticity is a multifaceted property of the brain that dynamically modifies neuronal activity following adequate stimuli. Plastic changes have been related to learning and memory, defined as the ability of an organism to modify its behavior through experience and to retain this information over time. Molecular mechanisms underpinning synaptic plasticity and memory have been widely studied in the last decades and the scientific community has mostly focused on long-term potentiation (LTP), a form of long-lasting synaptic strengthening thought to be the electrophysiological correlate of memory. In this regard, it is well established that the second messengers cyclic adenosine monophosphate (cAMP) and cyclic guanosine monophosphate (cGMP) play a crucial role in LTP signal transduction mechanisms, and are involved in both memory induction and maintenance/consolidation processes[1–4]. As a matter of fact, several studies have focused on the potential use of phosphodiesterase inhibitors (PDE-Is) for their ability to enhance cyclic nucleotide levels and memory in healthy conditions and in neurological disorders characterized by synaptic and memory deficits, such as Alzheimer's disease (AD)[5–15]. This is consistent with the hypothesis that downregulation of cyclic nucleotide levels during aging and neurodegenerative disorders might be related to cognitive decline[16,17]. High levels of amyloid-β (Aβ) downregulate both the cAMP and cGMP pathways and, on the other hand, the increase of cyclic nucleotides by PDE-Is is capable of modifying Aβ levels[6,8–10,18–23]. Interestingly, upregulation of cGMP levels by PDE5-Is decreased Aβ load in transgenic models of AD[9,22,24] and in models of physiological aging[10], whereas it induced a slight increase of Aβ in young healthy mice[10]. This dichotomy might be interpreted in light of the peculiar double-role of Aβ, which is present at high concentrations in AD brains where it exerts a synaptotoxic effect, and at low picomolar concentrations in healthy brains where, on the contrary, it mediates physiological mechanisms underlying learning and memory (for review, see[25,26]). Indeed, administration of human Aβ at low picomolar concentrations, resembling its physiological content in the brain[27,28], has been found to enhance LTP and memory in

healthy mice[27,29–31]. Furthermore, Aβ is physiologically released during neuronal activity[32,33] and it is needed for normal synaptic plasticity and memory[28]. Considering the key role of both cGMP and Aβ in LTP and memory, and their reciprocal relationships, here we sought to examine how they interact in physiological conditions. Our findings revealed that cGMP causes an increase in Aβ levels by modifying β-site APP cleaving enzyme-1 (BACE-1) and amyloid precursor protein (APP) approximation. Furthermore, blocking the endogenous Aβ function prevented the well known cGMP-dependent enhancement of LTP and memory. These results suggest a possible novel mechanism according to which cGMP acts upstream of Aβ by stimulating its production. Aβ, in turn, is responsible for the enhancement of LTP and memory.

Results

The increase of cGMP increases Aβ levels

We first investigated whether cGMP elevation affects Aβ secretion in N2a cells. N2a cells were treated with 100 μm sildenafil, vardenafil[13], or vehicle for 1 h. The intracellular content of cGMP was measured by a cGMP-specific EIA assay, whereas Aβ42 levels in the conditioned medium were measured by ELISA. We confirmed that treatment with the PDE5-Is induced an increase of intracellular cGMP content in N2a cells compared with vehicle ($F(2,6) = 12.746$, $p = 0.007$; Fig. 1A). This was particularly evident for vardenafil, which was able to determine a 23.36 ± 5.75-fold induction in cGMP content ($t(4) = 3.883$, $p = 0.018$). The cGMP increase stimulated Aβ42 secretion in N2a cells (1.4-fold increase, $t(4) = 3.933$, $p = 0.017$ for sildenafil and twofold increase, $t(4) = 5.678$, $p = 0.005$ for vardenafil; Figure 1A). Thus, the increase in cGMP content paralleled the increase of Aβ42 levels ($F(2,6) = 18.936$, $p = 0.003$). Pearson's correlation coefficient between the PDE5-I–induced cGMP and Aβ42 was equal to 0.97, confirming a very strong relationship between the two events.

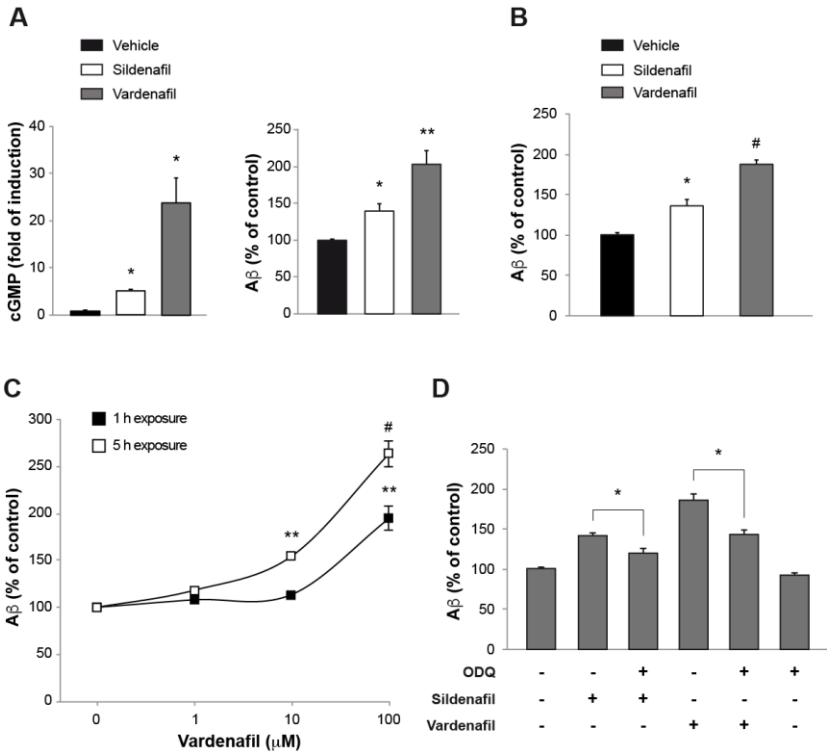

Figure 1. cGMP increase stimulates Aβ secretion. A, Vardenafil and sildenafil stimulate Aβ secretion in N2a cells. A treatment with 100 μm sildenafil or vardenafil for 1 h increases intracellular cGMP levels compared with vehicle (fold-induction in cGMP content: sildenafil = 5.17 ± 0.34; vardenafil = 23.36 ± 5.75; $p < 0.05$). ELISA measurement of Aβ42 in conditioned media reveals that the increase in cGMP levels induces a parallel increase of Aβ secretion (Aβ levels percentage of control: sildenafil = 139 ± 9.84%, $p < 0.05$; vardenafil = 202 ± 17.92% of control, $p < 0.005$). B, A treatment with vardenafil and sildenafil increases Aβ42 levels in rat hippocampal slices. In particular, sildenafil induces an increase equal to 136 ± 7.57% of control and vardenafil an increase equal to 187.3 ± 7.75% of control. C, Dose–response curve for the effect of different concentrations of vardenafil on Aβ42 levels after 1 h (1 μm: 108.5 ± 2.5% of control; 10 μm: 113.5 ± 0.5% of control; 100 μm: 194.33 ± 12.90% of control) or 5 h (1 μm: 118.33 ± 3.17% of control; 10 μm: 154.33 ± 2.84% of control; 100 μm: 262.66 ± 13.86% of control). *$p < 0.05$; **$p < 0.005$; #$p < 0.0001$. D, The guanylyl cyclase inhibitor ODQ reduces Aβ secretion induced by sildenafil (120.3 ± 6.33% vs 142.33 ± 2.40 of control) and vardenafil (145.33 ± 4.63% vs 186.26 ± 7.28 of control), but does not change Aβ42 basal levels (93.9 ± 3.59% of control). Data are mean ± SEM.

Next, we validated findings from N2a cells using a different system, the hippocampus, a region of the brain with remarkable plastic characteristics of the kind that are required for learning and memory. Rat hippocampal slices were incubated for 1 h with 100 μm sildenafil or vardenafil and then the conditioned medium was analyzed for Aβ42 content. A significant difference was found in slices treated with PDE5-Is with respect to controls ($F(2,6) = 57.575$, $p < 0.0001$), confirming the increase of Aβ42 levels after

treatment with sildenafil ($t(4) = 4.548$, $p = 0.010$; Fig. 1B) or vardenafil ($t(4) = 13.462$, $p < 0.0001$; Fig. 1B) observed in N2a cells. Together, these findings indicate that cGMP increase induces Aβ42 secretion in N2a cells and hippocampal slices, with vardenafil being more effective than sildenafil in determining this effect (vardenafil vs sildenafil in N2a cells: $t(10) = 5.136$, $p < 0.0001$; in slices: $t(4) = 5.241$, $p = 0.006$).

These results prompted us to perform a dose–response curve to evaluate the minimum dose of vardenafil capable of stimulating Aβ42 secretion. N2a cells were treated for 1 h with vardenafil at different concentrations ranging from 1 to 100 μm. The increase of Aβ42 levels was significant after a treatment with vardenafil at 100 μm, whereas no differences were detected at 1 or 10 μm (ANOVA for the dose–response curve: $F(3,14) = 58.153$, $p < 0.0001$; Bonferroni's $p < 0.001$ for vardenafil 100 μm vs other conditions; Fig. 1C). A prolonged exposure to vardenafil revealed a time- and concentration-dependent increase of Aβ42 levels (two-way ANOVA for time and treatment: $F(3,22) = 10.461$, $p < 0.0001$). After 5 h of exposure to the drug there was a significant difference from control ($F(3,8) = 98.320$, $p < 0.0001$) with a concentration of both 10 μm (Bonferroni's $p = 0.005$) and 100 μm (Bonferroni's $p < 0.0001$; Fig. 1C).

Because the intracellular cGMP concentration reflects a fine balance between cyclic nucleotide production by soluble guanylyl cyclase (sGC) and degradation by PDEs, we further investigated the involvement of cGMP on Aβ42 secretion in N2a cells treated with the sGC inhibitor [1H-[1,2,4]oxadiazolo-[4, 3-a]quinoxalin-1-one] (ODQ). As expected, the increase of Aβ42 levels induced by sildenafil and vardenafil was significantly reduced by ODQ pretreatment (50 μm) ($t(4) = 3.248$, $p = 0.031$ compared with sildenafil; $t(4) = 4.740$, $p = 0.009$ compared with vardenafil; Figure 1D) which, however, did not alter, per se, the Aβ42 basal levels ($t(6) = 1.447$, $p = 0.198$; Fig. 1D). Thus, when cGMP production was inhibited by ODQ, neither vardenafil nor sildenafil were capable of increasing Aβ levels, confirming a direct dependency between cGMP and Aβ production.

cGMP does not modify APP expression

Because Aβ is produced by APP cleavage[34], we examined whether the increase of cGMP might affect APP expression. N2a cells were treated with vardenafil and then processed for total protein extraction followed by immunoblot analysis performed with an antibody directed against the N-terminus of APP (22C11). Vardenafil did not modify APP full-length expression at different concentrations (1–100 μm; $F(3,8) = 1.401$, $p = 0.312$) and time-exposures (1–5 h; $F(3,8) = 1.472$, $p = 0.294$; Fig. 2A,B). We also evaluated APP full-length expression in hippocampal slices, but no changes were detected after treatment with vardenafil or sildenafil ($F(3,8) = 2.562$, $p = 0.157$; Fig. 2C). Thus, the cGMP-induced increase of Aβ was not due to an increase of full-length APP.

cGMP stimulates Aβ production by increasing APP/BACE-1 convergence in endolysosomal compartments

Considering that BACE-1 cleavage of APP is a prerequisite for Aβ formation, we evaluated the effect of vardenafil on the enzymatic activity of BACE-1. To this end, we tested the proteolytic activity of BACE-1, extracted from N2a cells treated with 100 μm vardenafil, on a secretase-specific substrate that releases fluorescence after its cleavage. Under these experimental conditions, the activity of BACE-1 on the exogenous synthetic substrate was unmodified ($t(10) = 1.365$, $p = 0.199$; Fig. 2D).

Next, we examined whether cGMP affects APP-BACE-1 approximation by direct visualization of the substrate-enzyme interaction in cells. Toward this, we used the Optical Convergence of APP and BACE-1 (OptiCAB) assay[35], based on the bimolecular fluorescence complementation of Venus protein fragments[36].

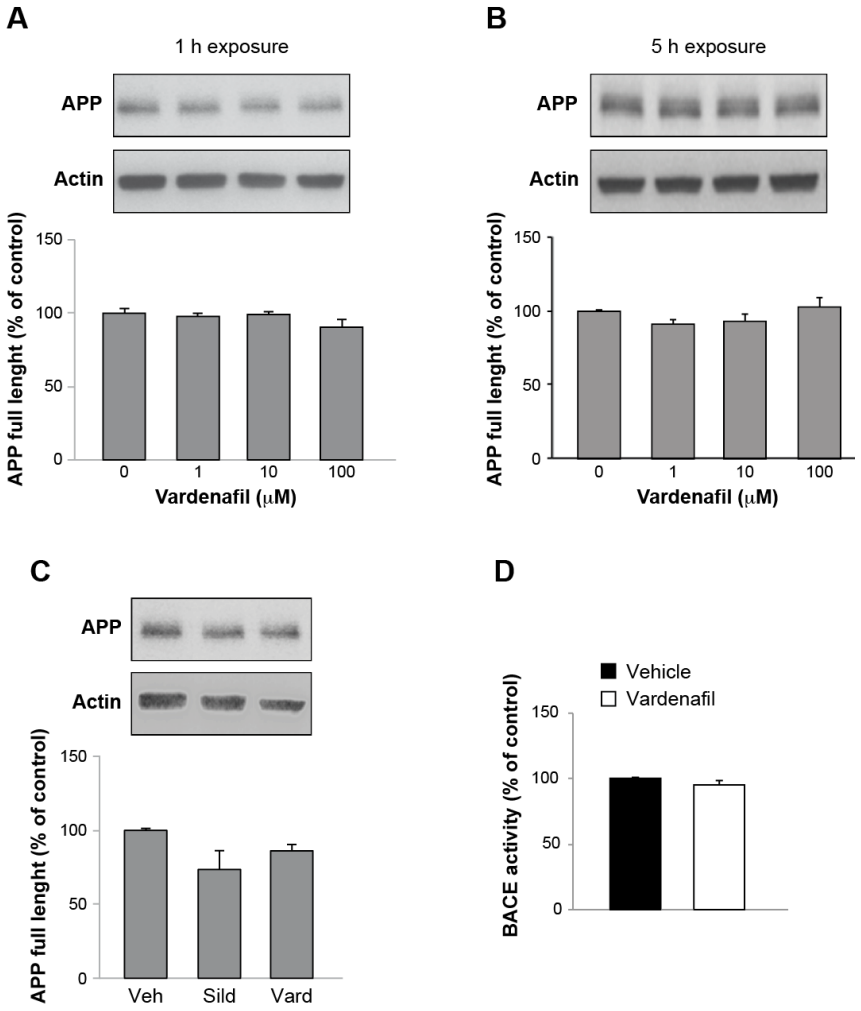

Figure 2. cGMP increase does not modify APP expression. A, B, A treatment with vardenafil at different concentrations ranging from 1 to 100 μm does not modify APP full-length expression in N2a cells neither after 1 h (A) nor after 5 h (B) exposure. C, A treatment with 100 μm sildenafil or vardenafil does not modify APP full-length expression in hippocampal slices. Top, Immunoblots; bottom, results of the relative densitometric scan. D, The proteolytic activity of BACE-1 on a secretase-specific exogenous substrate is not modified by treatment of N2a cells with 100 μm vardenafil. Data are mean ± SEM.

As described in Figure 3A, APP was tagged to the N-terminal fragment of the Venus protein (VN) and BACE-1 was tagged to the complementary C-terminal fragment of Venus (VC). The principle of this assay is that interaction between APP:VN and BACE-1:VC fragments reconstitutes the Venus protein, making it fluorescent[35].

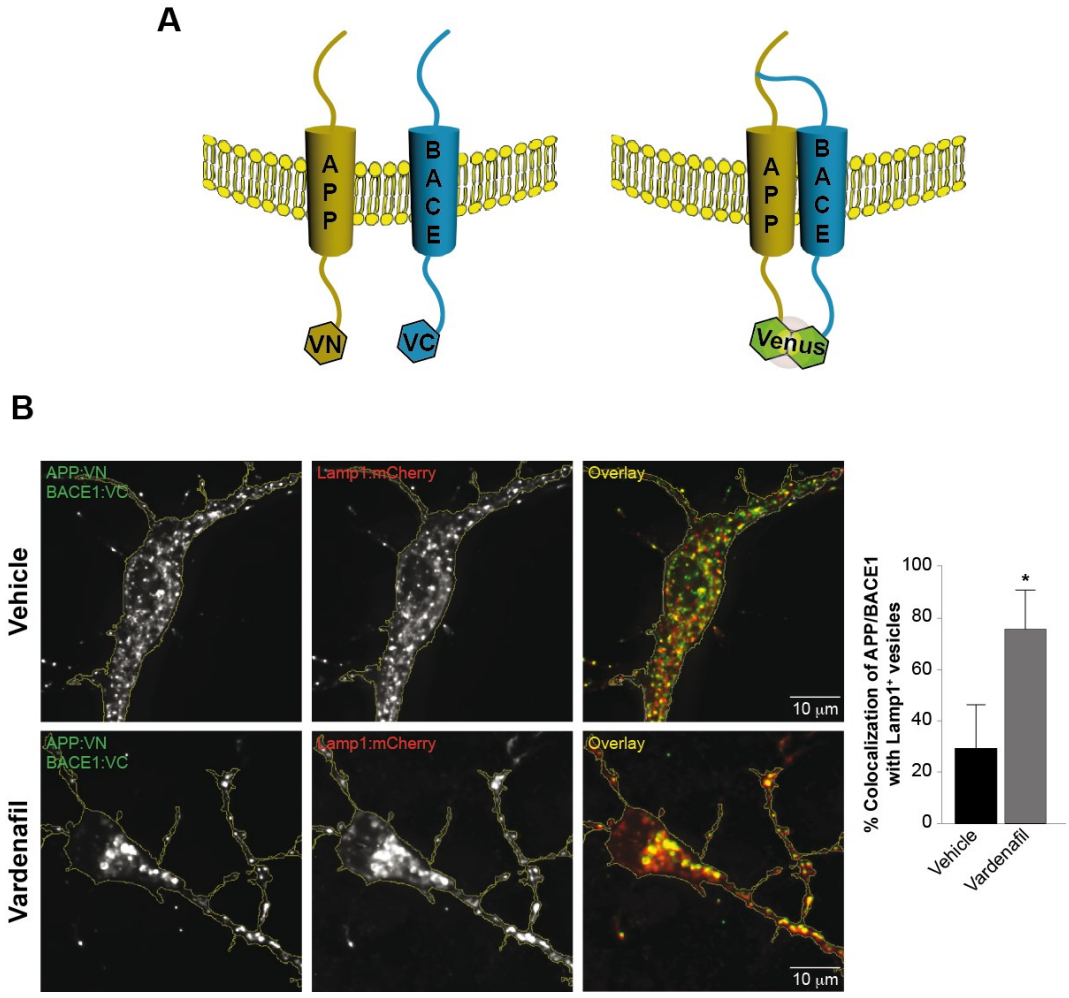

Figure 3. cGMP induces APP and BACE-1 interaction in the late endosome/lysosomes. A, Graphical representation of OptiCAB assay used to detect APP-BACE-1 interactions. APP and BACE-1 are respectively tagged with the VN and the VC fragment of Venus protein. When APP interacts with BACE-1 Venus fluorescence is reconstituted (Venus fluorescence, right). B, Fluorescence of cultured neurons expressing APP:VN, BACE-1:VC, Lamp1:mCherry, and treated with 100 μm vardenafil or vehicle control for 16 h. Note the increase (78.27 ± 8.97%) in the colocalization of Venus-positive puncta indicating APP/BACE-1 interaction with Lamp1, a late endosome/lysosome marker, compared with DMSO (vehicle)-treated control set (28.82 ± 10.12%). n = 10–12 neurons for each condition. *$p < 0.05$. Data are mean ± SEM.

It was recently shown that the vast majority of APP and BACE-1 interactions take place in the recycling endosomes in the somatodendritic compartments of primary cultured neurons[35]. Interestingly, after cotransfecting the neurons with APP:VN, BACE-1:VC

and Lamp1:mCherry, a late endosome/lysosome marker, we observed a significant increase in the colocalization of Venus puncta with the Lamp1-positive organelles in the presence of 100 μm vardenafil ($t(4) = 3.396$; $p = 0.027$; Fig. 3B).

Aβ is required for cGMP-induced late-LTP

cGMP signaling has been demonstrated to play a pivotal role in LTP and synaptic plasticity[2,3,37]. A tetanic stimulation of presynaptic fibers results in a transient increase in cGMP[38], which is responsible for the enhancement of synaptic plasticity. Drugs enhancing cGMP levels are able to convert short-lasting early phase LTP (e-LTP) into a long-lasting form of LTP, called late-LTP (l-LTP)[4]. We therefore confirmed that the increase of cGMP levels by PDE5 inhibition was capable of converting e-LTP into l-LTP when Schaffer collateral fibers of hippocampal slices are stimulated in vitro with a weak tetanic stimulation including a theta burst stimulation consisting of four-pulse bursts at 100 Hz, with the bursts repeated at 5 Hz for 10 times and an intensity of stimulation for the individual pulses equal to ∼35% of the maximum evoked response[4,9,39].

Slices were perfused with 50 nm sildenafil[9] or 10 nm vardenafil[4] for 10 min before tetanus. Both sildenafil and vardenafil produced a robust l-LTP lasting at least 3 h (ANOVA for repeated measures of the post-tetanic time points: sildenafil: $F(1,12) = 40.218$, $p < 0.0001$; vardenafil: $F(1,12) = 32.115$, $p < 0.0001$, both compared with vehicle + weak tetanus; Figure 4A), whereas vehicle-treated slices showed lower amounts of LTP fading at ∼1 h. The PDE5-I–induced LTP was similar to LTP induced through a strong tetanic stimulation in which, instead of providing only one theta burst stimulation, we administered three trains of theta bursts with an intertrain interval of 15 s (sildenafil: $F(1,10) = 3.070$, $p = 0.110$; vardenafil: $F(1,12) = 0.181$, $p = 0.678$, both compared with vehicle + strong tetanus; Figure 4A).

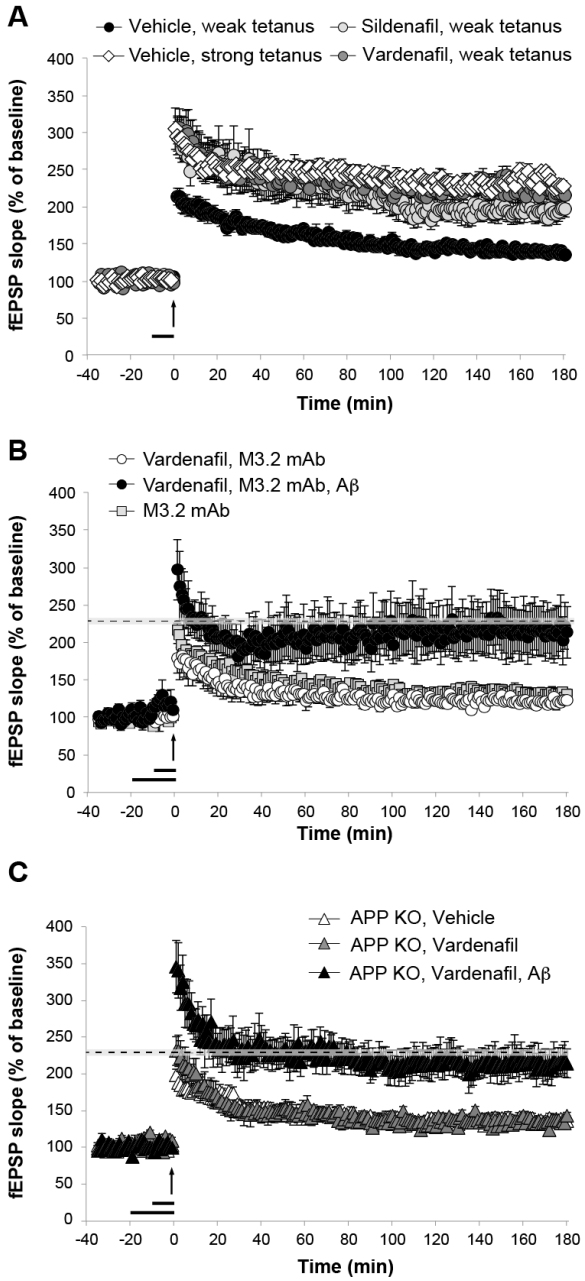

Figure 4. cGMP-induced conversion of e-LTP into l-LTP requires Aβ. A, Perfusion of hippocampal slices with 50 nm sildenafil or 10 nm vardenafil for 10 min before a weak tetanus is able to convert e-LTP in l-LTP (vehicle: n = 7; 134.96 ± 4.19% of baseline slope 180 min after tetanus; sildenafil: n = 5; 196.72 ± 11.11% of baseline slope; vardenafil: n = 7; 214.86 ± 11.75% of baseline slope). The PDE5-I–induced l-LTP is comparable to l-LTP evoked by a strong tetanus (n = 7; 227.41 ± 6.79% of baseline slope 180 min after tetanus). B, A concomitant perfusion with a monoclonal anti-Aβ antibody (M3.2 mAb; 2 µg/ml) for 20 min before a weak tetanus suppresses the vardenafil-enhancing effect on LTP (n = 7; 123.25 ± 4.60% of baseline slope 180 min after tetanus). Vardenafil-induced l-LTP is rescued by perfusion with human Aβ42 (200 pm) in slices concurrently treated with M3.2 (n = 8; 213.51 ± 34.17% of baseline slope 180 min after tetanus). C, 200 pm Aβ42 rescues the vardenafil-induced l-LTP in slices obtained from APP KO mice (n = 7/7; 143.27 ± 10.69% of baseline slope 180 min after tetanus vs 214.47 ± 19.68% of baseline slope 180 min after tetanus). The horizontal bar indicates the period during which

drugs are added to the bath solution. The arrow indicates tetanus delivery. The shaded areas in B and C correspond to the average potentiation (dotted line) and the SE range in slices treated with vehicle + strong tetanus as in A. Data are mean ± SEM.

Because a relatively high concentration of vardenafil (100 μm) was applied to slices for 1 h to produce a significant increase in Aβ levels, we performed additional experiments to study the effect of vardenafil at 100 μm on LTP induced by a strong tetanus. We found that a treatment with vardenafil 100 μm was capable of inducing a significant increase in LTP compared with vehicle-treated slices (360.90 ± 33.95 vs 227.41 ± 6.79% of baseline; $F(1,12) = 28.692$, $p < 0.0001$ comparing vehicle + strong tetanus vs 100 μm vardenafil + strong tetanus; data not shown).

Given that the experiments shown in Figure 1 demonstrated cGMP-induced Aβ secretion, and in previous studies we have proved that low picomolar concentrations of Aβ are capable of enhancing LTP[27,29], we wanted to verify whether the cGMP-induced conversion of e-LTP in l-LTP depends upon Aβ. To this end, we examined whether vardenafil was still capable of inducing l-LTP after depletion of endogenous murine Aβ. Hippocampal slices were treated with a monoclonal antirodent Aβ antibody (M3.2 mAb; 2 μg/ml) for 20 min before the weak tetanus[39]. M3.2 antibody is a monoclonal antibody with a selective affinity for murine Aβ, which has been fully characterized in previous studies for its capability to block Aβ in both physiological and pathological conditions[40–42]. Moreover, in those studies and in previous experiments performed in our laboratory[28], control IgG antibodies (i.e., IgG2a isotype-matched control antibody that does not bind to any rodent proteins) have been used to demonstrate the specificity of M3.2 for rodent Aβ.

Here, when we blocked endogenous Aβ with M3.2, vardenafil was no longer capable of eliciting l-LTP ($F(1,12) = 48.135$, $p < 0.0001$ compared with vardenafil + weak tetanus; $F(1,12) = 183.422$, $p < 0.0001$ compared with vehicle + strong tetanus; Figure 4B). Importantly, M3.2 mAb alone did not modify early-LTP induced by a weak tetanus ($F(1,12) = 2.712$, $p = 0.125$, compared with vehicle + weak tetanus; Fig. 4B), excluding that M3.2 blocked potentiation per se, as occurring when blocking endogenous Aβ before a strong stimulation used to induce l-LTP[28]. Thus, an antirodent

Aβ antibody, which sequesters the endogenously produced peptide, prevented the well known potentiating effects of vardenafil on LTP, suggesting that endogenous Aβ is needed for this effect to occur.

M3.2 mAb also recognizes β-CTF, soluble APP α, and full-length APP. Thus, it might exert an effect independent of Aβ depletion by binding to other targets. To further support the involvement of Aβ in the cGMP-induced LTP, we performed rescue experiments with exogenous human Aβ42, which is not recognized by the M3.2 mAb. In fact, in the presence of M3.2 (sequestering vardenafil-induced endogenous Aβ production), exogenously added human Aβ was able to restore l-LTP to the same level of that observed in the absence of the antibody ($F(1,13) = 0.410$, $p = 0.533$ compared with vardenafil + weak tetanus; $F(1,13) = 0.740$, $p = 0.405$ compared with vehicle + strong tetanus; Figure 4B). This rescue experiment demonstrated that the abolishment of the cGMP-induced LTP was specifically due to the lack of Aβ.

To further confirm these findings with an independent strategy, we provided genetic evidence for the involvement of Aβ in cGMP-induced synaptic plasticity increase. We performed additional experiments using APP KO mice that do not produce Aβ. When hippocampal slices from these animals were perfused with vardenafil, the drug failed to enhance LTP ($F(1,12) = 28.846$, $p < 0.0001$ compared with WT slices treated with vardenafil + weak tetanus; $F(1,12) = 77.172$, $p < 0.0001$ compared with WT slices treated with vehicle + strong tetanus; Figure 4C). Moreover, addition of 200 pm human synthetic Aβ42 was capable of eliciting l-LTP in APP KO slices treated with vardenafil ($F(1,12) = 0.126$, $p = 0.729$ compared with WT treated with vardenafil + weak tetanus; $F(1,12) = 0.514$, $p = 0.487$ compared with WT treated with vehicle + strong tetanus; Figure 4C). Together these findings demonstrate that Aβ is required for the cGMP-induced conversion of e-LTP into l-LTP.

Aβ is required for cGMP-induced memory

The electrophysiological results prompted us to evaluate whether Aβ is required for cGMP-induced memory. To this end we used WT and APP KO mice. We studied

recognition memory by the ORT, a task based on the natural tendency of rodents to explore unfamiliar objects, which relies on the integrity of hippocampus and parahippocampal regions[43]. After 3 d of habituation, mice underwent training (T1) in which they were presented with two identical objects for 3 min. Right after T1 animals were treated with vehicle or vardenafil (1 mg/kg, i.p.;[4]). After 24 h (T2), animals were put back in the arena containing the "familiar" object (the same as in T1) and the "novel" object. Mice were allowed to explore the objects for 3 min and exploration time was recorded and scored. WT mice treated with vehicle showed the natural forgetting, due to the short time exposure in T1 and the long 24 h interval between T1 and T2. Indeed, there was no difference between the percentage time spent exploring the novel object and that spent exploring the familiar object in WT vehicle-treated animals ($t(22) = 0.698$; $p = 0.492$; Fig. 5A). As previously demonstrated[4], treatment with vardenafil produced memory because animals spent more time exploring the novel object in T2 ($t(22) = 5.538$; $p < 0.0001$; Fig. 5A). As for the LTP experiments, this effect was not present in APP KO littermates. ($t(24) = 0.845$; $p = 0.407$; Fig. 5A). Analyses of D confirmed a difference among groups ($F(3,45) = 3.446$, $p = 0.024$) and indicated that only WT mice treated with vardenafil recognized the familiar object (Bonferroni's $p = 0.02$) because their D significantly differed from 0 ($t(12) = 0.597$; $p = 0.561$; Fig. 5B). No differences were detected in latency to approach the novel object for the first time ($F(3,45) = 0.359$, $p = 0.783$; Fig. 5C) and in total exploration time ($F(3,45) = 0.762$, $p = 0.521$; Fig. 5D), suggesting that the treatment did not modify anxiety and motor activity. Together, these experiments demonstrate that cGMP-induced memory cannot be evoked in APP KO mice.

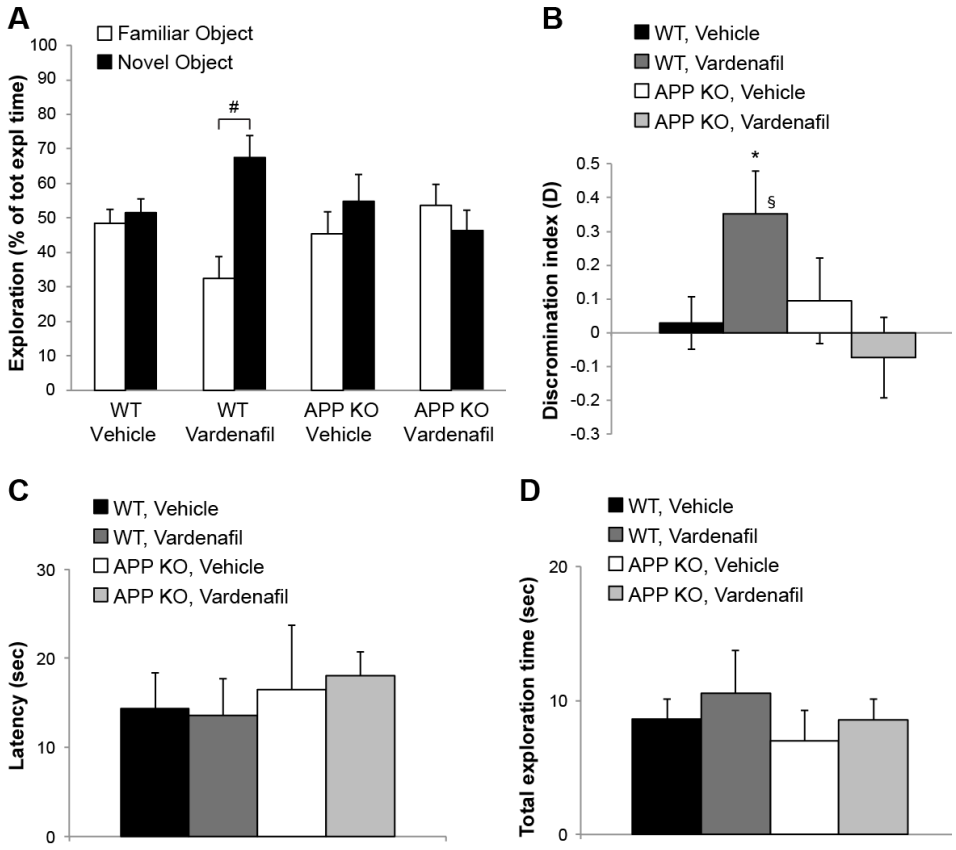

Figure 5. cGMP-induced recognition memory is not present in APP KO mice. A, Exploration times of familiar and novel object during T2 (after a 24 h retention interval) show that WT mice treated with vardenafil spend longer time exploring the novel object (n = 12; 65.45 ± 6.34 vs 32.43 ± 6.34% of total exploration time). Conversely, vardenafil is not able to evoke memory in APP KO mice (n = 13; 46.32 ± 5.93 vs 53.67 ± 5.93% of total exploration time). WT and APP KO mice treated with vehicle spend the same amount of time exploring the familiar and the novel object (WT: n = 12; 51.47 ± 3.9 vs 48.52 ± 3.9% of total exploration time; APP KO: n = 12; 54.72 ± 7.87 vs 45.27 ± 7.87% of total exploration time), confirming the physiological forgetting due to the shorter exposition in T1. B, Analyses of the D confirm that vardenafil-induced enhancement of recognition memory is not evoked in APP KO mice. C, Latency to first approach to the novel object and (D) total exploration time are comparable in the four groups of mice. *$p < 0.05$; #$p < 0.0001$; §difference from 0. Data are mean ± SEM.

Discussion

From the early 1990s, Aβ has been found to be a physiological product of cellular metabolism, but studies on the mechanisms underlying its production and degradation have mainly aimed at better understanding the pathophysiology of AD. However, there is a growing body of evidence suggesting that Aβ regulates synaptic function and

memory in the healthy brain[25,44,45]. To understand the mechanism by which this occurs, we have investigated the role of cGMP in the phenomenon because the cyclic nucleotide is involved in synaptic plasticity and memory[1–3]. Our data show that increase in cGMP levels, obtained by using the PDE5-Is sildenafil or vardenafil, induces a parallel increase of Aβ secretion in two different models, N2a cells and rat hippocampal slices. This effect was reduced when cells were pretreated with ODQ, a selective inhibitor of sGC, confirming that Aβ production is regulated by cGMP.

Considering that our previous reports indicated that cAMP influences APP synthesis[35,39,46,47], we first investigated whether cGMP modifies APP expression, but we did not find any change in APP levels both in N2a cells and hippocampal slices treated with vardenafil. A possible explanation for this finding is that we measured total APP full-length which is present in several cell compartments (endoplasmic reticulum, trans-Golgi network, etc.), and therefore any change in local APP expression might have gone undetected, especially in light of increasing evidence indicating that BACE1 cleavage of APP, the rate-limiting step in Aβ production[34], occurs predominantly in the endolysosomal compartment (for review, see:[48,49]). Therefore, we hypothesize that the enhancement of Aβ production by vardenafil involves processing of a fraction of the precursor protein that does not significantly impact the levels of total APP. Consistent with this scenario, we found that the cGMP increase does not induce a generic activation of BACE-1, but rather stimulates APP and BACE-1 to converge in the endolysosomal compartment where amyloidogenic processing is favored. Recent reports on the distinct distribution of amyloidogenic enzymes in late endosome/lysosomes corroborate our observation[35,50]. Moreover, these results are consistent with previous studies demonstrating that a treatment with the PDE5-I sildenafil induces a slight increase of Aβ without affecting APP full-length expression in healthy mice[10].

It could be argued that the cGMP-induced increase of Aβ levels might be harmful, because high concentrations of Aβ are commonly associated with the characteristic impairment of cognition in AD. Yet, the Aβ increase that we detected in our studies is in the picomolar range, a concentration known to produce physiological positive

effects[27]. Our findings might also appear controversial in light of most of the scientific literature recommending the use of PDE-Is to reduce Aβ levels. However, these studies have been performed in models of Aβ hyper-production, i.e., AD transgenic animals[9,22,24]. Thus, it could be feasible to hypothesize that cGMP exerts opposite effects in physiological or pathological conditions characterized by low or high levels of Aβ, respectively. In this context, it is also interesting to note that either Aβ or cGMP behave in a hormetic fashion[29,51], stimulating or inhibiting cellular functions based on the applied dose. Other studies have found that NO donors, such as sodium nitroprusside, bidirectionally modulates APP processing depending upon the concentration used[52]. On the other side, it has been shown that high concentrations of Aβ determine a decrease of cGMP in different cell and animal models[18,19,53,54]. Intriguingly, in patients diagnosed with mild AD, cognitive impairment and CSF Aβ42 levels were significantly associated with a decrease in cGMP content[55]. An overview of these findings might suggest the existence of a physiological feedback cGMP-Aβ axis, i.e., the increase of cGMP stimulates Aβ production that, in turn, inhibits cGMP production via a negative feedback mechanism. This hypothesis might justify the reduction of cGMP induced by an abnormal increase of Aβ levels, and the reduction of Aβ levels after a chronic administration of cGMP-enhancing drugs such as PDE-Is.

Hippocampal LTP can be induced through several tetanization protocols including the θ-burst stimulation. A weak tetanus leads to e-LTP, which lasts ∼1 h and is protein synthesis independent, whereas a strong tetanus leads to l-LTP, which lasts longer and is protein or RNA synthesis dependent[56]. Here, we have found that elevation of cGMP levels transforms e-LTP into l-LTP. This finding is consistent with the observation that the NO/cGMP signaling, first thought to be involved only in e-LTP, plays a role also in l-LTP[1–4]. Moreover, this observation is consistent with the observation that stimulation of the NO/cGMP signaling participates to memory formation and consolidation[4,5,12].

Considering that we and others have previously demonstrated that Aβ is also needed for LTP and memory formation[28], and it has a positive modulatory effect on these phenomena when administered at physiological concentrations[27,30,31], we wanted to

investigate whether the cGMP-induced LTP and memory was related to Aβ production. Here we show that vardenafil-induced enhancement of synaptic plasticity and memory requires Aβ to occur. Indeed, removing Aβ by immunological (anti-Aβ antibodies) or genetic (APP KO) manipulation prevents the cGMP-dependent enhancement of LTP and memory. This is consistent with previous data showing that when blocking Aβ function with an APP siRNA or a monoclonal anti-Aβ antibody, LTP induced by a strong tetanus was impaired, but it could be rescued by administration of 200 pm Aβ that should restore the physiological content of the peptide in the brain[28]. When a higher concentration of Aβ (300 pm) was added together with the anti-Aβ antibody, LTP was further enhanced compared with vehicle-treated slices. However, in the same work[28] we demonstrated that young APP KO present normal LTP, consistent with other studies showing that APP KO mice present abnormalities in neuronal morphology and LTP at 12–15 months of age, whereas younger mice are normal[57]. This might be due to compensation mechanisms that are known to occur in genetically modified animals. Here, we used young APP KO mice that do not produce Aβ but still have a normal LTP. In this way, the fact that vardenafil was not able to induce l-LTP in APP KO mice could not be attributable to an impairment of l-LTP per se.

In rescue experiments, exogenous human Aβ was able to restore l-LTP in slices treated with an anti-rodent Aβ antibody, confirming that Aβ was needed for the vardenafil-induced l-LTP. It is interesting to note that, as in previous works[27–29], we have used a solution of human Aβ containing both monomers and oligomers to rescue the l-LTP impairment due to an inhibition of endogenous murine Aβ, that is thought to be less prone to oligomerize. Thus, one might interpret our results through an effect of Aβ monomers. However, it should be taken into account that oligomers cannot be excluded in light of some recent studies showing that also murine Aβ might form aggregates and deposits. For example, it has been shown that SAMP8 mice present an increase of murine Aβ42 oligomers[58] and that murine Aβ overproduction might produce deposits similar to human AD plaques[59].

As for the behavioral experiments, APP KO mice lack not only Aβ, but also all the other APP proteolytic fragments that could be responsible, at least in theory, for the

effects induced by vardenafil on memory. However, these results completed a series of experiments demonstrating that: 1) by enhancing cGMP, PDE5 inhibitors increase Aβ levels in an ODQ-sensitive manner; and 2) the effect of vardenafil on hippocampal LTP, the generally accepted electrophysiological correlate of memory formation and consolidation, is abrogated by antirodent Aβ antibody, but it can be rescued by addition of exogenous human Aβ. Therefore, our behavioral analysis supports the hypothesis that cGMP stimulates Aβ production, which is instrumental for cGMP to boost hippocampal LTP and memory.

Similar to the current findings showing that Aβ is required for cGMP-induced hippocampal l-LTP and memory, we previously reported that increasing endogenous cAMP through PDE4 inhibition also requires Aβ to enhance hippocampal LTP[39]. The fact that cGMP and cAMP are known to cooperate in synaptic plasticity and memory processes and that both act through Aβ production lays the basis for a novel interpretation of synaptic mechanisms that deserve further investigation in the future.

In conclusion, we have found a tight relationship between cGMP and Aβ, demonstrating that cGMP acts upstream of Aβ by regulating its secretion, a sine qua non for LTP and memory to work in physiological conditions. Our findings might be useful to better understand the mechanism of action of drugs increasing cGMP levels, such as PDE5-Is, that might enhance cognition via a positive modulation of Aβ in the healthy brain. Most importantly, these experiments stress the relevance of fully understanding the physiological role(s) of Aβ to design effective and safe approaches to AD therapy, as Aβ lowering treatments might lead to memory worsening instead of amelioration.

Footnotes

This work was supported by the Alzheimer's Association (IIRG-09-134220 to D.P.), the University of Catania (Progetto di Ricerca d'Ateneo to A.P.), the University of

Genoa (Progetto di Ricercad'Ateneo to E.F. and R.R.), and the National Institutes of Health (NS049442/NS092045 to O.A.).

The authors declare no competing financial interests.

Materials and methods

Ethics Statement

All the experimental procedures were in accordance with the European and Italian guidelines for the care of laboratory animals and the Italian legislation on animal experimentation, and were approved by the institutional ethical committee. All efforts were made to minimize animal suffering and to use the minimum number of animals necessary to produce reliable results.

Drugs preparation and administration

Vardenafil and sildenafil were obtained from Sigma-Aldrich. ODQ was purchased from Tocris Bioscience. All chemicals were first dissolved in DMSO and then diluted in the appropriate medium for N2a cells and hippocampal slices, in ACSF for electrophysiological experiments, and in saline solution (NaCl 0.9%) for behavioral experiments, immediately before use. Final concentrations were chosen based on previous studies[4,5]. For electrophysiological studies, we used exogenous human synthetic Aβ42 to perform rescue experiments. Aβ42 (American Peptide) was prepared as previously described[27]. Briefly, the lyophilized peptide was suspended in 100% 1,1,1,3,3,3-hexafluoro-2-propanol (HFIP) (Sigma-Aldrich) to 1 mm. HFIP was allowed to evaporate, and the resulting clear peptide film was stored at −80°C. The film was added to DMSO (Sigma-Aldrich) and sonicated for 10 min. Aβ42-DMSO aliquots were prepared and stored at −20°C. Twenty-four hours before the use, one aliquot was diluted to the final concentration in artificial CSF (ACSF; for the composition see below) and incubated at 4°C for 24 h to allow oligomerization. As in our previous works[27–29], we have chosen to use this synthetic Aβ preparation, containing both monomers and oligomers, to reproduce the physiological brain environment where a certain degree of oligomerization is likely to occur[27]. Concentrations of Aβ42 were calculated based on the molecular weight of its monomeric peptide. Moreover, preliminary experiments ensured that scramble Aβ42 (AnaSpec) did not exert any effect, as previously demonstrated[27].

Aβ42 evaluation in cell cultures and hippocampal slices

Mouse N2a cells were grown in 50% DMEM, 50% OptiMEM, with 0.1 mm nonessential amino acids, 1% penicillin-streptomycin mixture, and 5% fetal bovine serum. They were treated for 1 or 5 h with vehicle or drugs, as indicated. Transverse rat hippocampal slices (250 μm) were obtained using a McIlwain tissue chopper. Slices were incubated for 1 h at 37°C into 2 ml of a physiological solution continuously aerated with 95% O2 and 5% CO2 in the presence of PDE5-Is as indicated. Aβ42 released into supernatant media from cultured cells and hippocampal slices was measured by Aβ1–42 ELISA (Wako Chemicals GmbH).

cGMP enzymatic immunoassay

Quantification of intracellular cGMP was performed with DetectX Direct Cyclic GMP Enzyme Immunoassay Kit (Arbor Assay), following the manufacturer's protocol. cGMP levels were calculated according to the standard curves prepared on the same enzymatic immunoassay (EIA) plates.

Immunoblot analysis
APP protein expression was evaluated in N2a cells and hippocampal slices. Cells were processed for total protein extraction as previously reported[47]. Hippocampal slices were homogenized in 0.6 ml of ice-cold buffer containing 1% complete protease inhibitor, 1% Triton X-100, 25 mm Tris HCl, 25 mm NaF, 1 mm EDTA, 0.5 mm EGTA, sonicated for 30 s, and centrifuged at 10,000 × g for 10 min at 4°C. The supernatant was centrifuged a second time at 10,000 × g for 10 min and then used for APP immunoblot assay, performed according to standard methods. As primary antibodies, we used a monoclonal mouse anti-human APP (22C11,1 μg/ml; Millipore Bioscience Research Reagents) and a monoclonal mouse anti-human β-actin (clone AC-15, 1:10,000; Sigma-Aldrich). Anti-mouse secondary antibodies were coupled to horseradish peroxidase (GE Healthcare). Proteins were visualized with an enzyme-linked chemiluminescence detection kit according to the manufacturer's instructions (GE Healthcare). Chemiluminescence was monitored by exposure to film and the signals were analyzed under non-saturating condition with an image densitometer (Bio-Rad).

BACE activity
The activity of BACE in N2a cells was determined using the β-Secretase Activity Fluorimetric Assay kit from BioVision, according to the manufacturer's protocol. The method is based on the BACE-dependent cleavage of a secretase-specific peptide conjugated to the fluorescent reporter molecules EDANS and DABCYL, which results in the release of a fluorescent signal that can be detected on a fluorescence microplate reader (excitation at 355 nm/emission at 510 nm). The level of secretase enzymatic activity is proportional to the fluorometric reaction.

APP-BACE Interaction assay
Primary hippocampal neurons were cultured from postnatal day (P)0–P1 CD1 mice and transiently transfected with Lipofectamine 2000 as described previously[46]. Briefly, neurons were dissociated and plated on poly-d-lysine-coated glass-bottom dishes from Mattek at a density of 50,000 cells/cm2, and maintained in neurobasal/B27 medium with 5% CO2 and 80% humidity. On DIV10, neurons were transfected with APP:VN, BACE1:VC, and Lamp1:mCherry (1.2 μg/ml) DNA, as previously described[35]. After 6 h, neurons were incubated with DMSO or vardenafil for 16 h and fixed in 4% PFA. Images were acquired using an Olympus IX81 inverted epifluorescence microscope. Z-stack images were captured using a 100× objective (imaging parameters: 0.339 μm z-step, 500 ms exposure and 1 × 1 binning). Captured images were deconvolved (Huygens, Scientific Volume Imaging B.V.) and subjected to a maximum intensity projection.

Animals
We used 3- to 4-month-old C57BL/6J wild-type (WT) and APP KO (B6.129S7-Apptm1Dbo/J) mice from a colony kept in the animal facility of the University of Catania, and adult Sprague-Dawley rats from a colony kept in the animal facility of the University of Genoa. The animals were maintained on a 12 h light/dark cycle (lights on at 6:00 A.M.) in temperature and humidity-controlled rooms; food and water were available ad libitum.

Electrophysiology
Electrophysiological recordings were performed as previously described[4,39] on male animals. Briefly, transverse hippocampal slices (400 μm) were cut and transferred to a recording chamber where they were maintained at 29°C and perfused with ACSF (in mm: 124.0 NaCl, 4.4 KCl, 1.0 Na2HPO4, 25.0 NaHCO3, 2.0 CaCl2, 2.0 MgCl2; flow rate 2 ml/min)

continuously bubbled with 95% O2 and 5% CO2. Field extracellular recordings were performed by stimulating the Schaeffer collateral fibers through a bipolar tungsten electrode and recording in CA1 stratum radiatum with a glass pipette filled with ACSF. A 15 min baseline was recorded every minute at an intensity that evoked a response ∼35% of the maximum evoked response. LTP was induced through either a weak or a strong tetanus. The weak tetanus consisted of a theta burst stimulation including bursts of four 1 ms pulses at 100 Hz, with the bursts repeated at 5 Hz for 10 times and an intensity of stimulation for the individual pulses equal to ∼35% of the maximum evoked response. The strong tetanus was similar to the weak tetanus. However, instead of providing only one theta burst stimulation, three trains of theta bursts were administered with an intertrain interval of 15 s. Responses were recorded for 3 h after tetanization and measured as field EPSP slope expressed as percentage of baseline. The results were expressed as mean ± SEM.

Object recognition test

The object recognition test (ORT) was performed as previously described[4] in sex-balanced WT mice. To allow mice to familiarize with the environment and the injection, mice underwent 3 d of handling, observation by the experimenter, and habituation to the arena and the injection. Animals were put in the arena (white plastic box 50 × 35 × 15 cm) and exposed to two different objects (changing from day to day). After 5 min of habituation, they received intraperitoneal injection of saline solution and were put back in their home cage. On the fourth day mice underwent the ORT training session (T1). Animals were put in the arena containing two identical objects (glass vases) placed in the central part of the box, equally distant from the perimeter. The animal was given 3 min to explore the environment and objects. Immediately after, T1 animals received an intraperitoneal injection of vardenafil (1 mg/kg). Twenty-four hours after T1, the mouse was put back in the arena to perform the test (T2). In this second trial, lasting 3 min, one familiar object (used in T1) was replaced by a novel object (ceramic cup). The time spent exploring the objects was scored using a personal computer by an experimenter who was blinded to the conditions tested. We opted for a delay interval of 24 h, at which under normal, nontreated circumstances, no discrimination between the objects occurs (natural forgetting), which allows for an improvement of long-term memory performance following drug treatment. Animal exploration, defined as the mouse pointing its nose toward the object from a distance not >2 cm, was evaluated in T2 to analyze: (1) time of exploration of each object and total time of exploration of the two objects expressed as percentage exploration of the novel and percentage exploration of the familiar object, (2) discrimination (D) index calculated as “exploration of novel object minus exploration of familiar object/total exploration time”, (3) latency to first approach to novel object, and (4) total exploration time.

Statistical Analyses

All data were expressed as mean ± SEM. Statistical analysis was performed by using Systat software. Normal distribution was prior evaluated by Kolmogorov–Smirnov test ($p > 0.05$). We used unpaired t test, one-way and two-way ANOVA with Bonferroni post hoc. Pearson's correlation was used to correlate Aβ42 and cGMP levels. For LTP we used ANOVA with repeated measures comparing 180 min of recording after tetanus. For ORT we used one-way ANOVA with Bonferroni post hoc for comparisons among groups, paired t test to compare exploration of the novel versus the familiar object in the same mouse, one-sample t test to compare D with zero. The level of significance was set at $p < 0.05$.

References

1. Bernabeu, R., Schmitz, P., Faillace, M. P., Izquierdo, I. & Medina, J. H. Hippocampal cGMP and cAMP are differentially involved in memory processing of inhibitory avoidance learning. *Neuroreport* **7,** 585–8 (1996).
2. Son, H. *et al.* The specific role of cGMP in hippocampal LTP. *Learn. Mem.* **5,** 231–45
3. Lu, Y. F., Kandel, E. R. & Hawkins, R. D. Nitric oxide signaling contributes to late-phase LTP and CREB phosphorylation in the hippocampus. *J. Neurosci.* **19,** 10250–61 (1999).
4. Bollen, E. *et al.* Improved long-term memory via enhancing cGMP-PKG signaling requires cAMP-PKA signaling. *Neuropsychopharmacology* **39,** 2497–2505 (2014).
5. Prickaerts, J. *et al.* Effects of two selective phosphodiesterase type 5 inhibitors, sildenafil and vardenafil, on object recognition memory and hippocampal cyclic GMP levels in the rat. *Neuroscience* **113,** 351–61 (2002).
6. Gong, B. *et al.* Persistent improvement in synaptic and cognitive functions in an Alzheimer mouse model after rolipram treatment. *J. Clin. Invest.* **114,** 1624–34 (2004).
7. Sakurai, H. *et al.* Effects of cilostazol on cognition and regional cerebral blood flow in patients with Alzheimer's disease and cerebrovascular disease: a pilot study. *Geriatr. Gerontol. Int.* **13,** 90–7 (2013).
8. Puzzo, D. *et al.* Amyloid-beta peptide inhibits activation of the nitric oxide/cGMP/cAMP-responsive element-binding protein pathway during hippocampal synaptic plasticity. *J. Neurosci.* **25,** 6887–97 (2005).
9. Puzzo, D. *et al.* Phosphodiesterase 5 inhibition improves synaptic function, memory, and amyloid-beta load in an Alzheimer's disease mouse model. *J. Neurosci.* **29,** 8075–86 (2009).
10. Puzzo, D. *et al.* Effect of phosphodiesterase-5 inhibition on apoptosis and beta amyloid load in aged mice. *Neurobiol. Aging* **35,** 520–31 (2014).
11. Rutten, K. *et al.* The selective PDE5 inhibitor, sildenafil, improves object memory in Swiss mice and increases cGMP Levels in hippocampal slices. *Behav. Brain Res.* **164,** 11–16 (2005).
12. Rutten, K., Basile, J. L., Prickaerts, J., Blokland, A. & Vivian, J. A. Selective PDE inhibitors rolipram and sildenafil improve object retrieval performance in adult cynomolgus macaques. *Psychopharmacol.* **196,** 643–648 (2008).
13. Shim, Y. S. *et al.* Effects of repeated dosing with Udenafil (Zydena) on cognition, somatization and erection in patients with erectile dysfunction: a pilot study. *Int. J. Impot. Res* **23,** 109–114 (2011).
14. Orejana, L., Barros-Miñones, L., Jordán, J., Puerta, E. & Aguirre, N. Sildenafil ameliorates cognitive deficits and tau pathology in a senescence-accelerated mouse model. *Neurobiol. Aging* **33,** 625.e11-625.e20 (2012).
15. Palmeri, A., Privitera, L., Giunta, S., Loreto, C. & Puzzo, D. Inhibition of phosphodiesterase-5 rescues age-related impairment of synaptic plasticity and memory. *Behav. Brain Res.* **240,** 11–20 (2013).
16. Yamamoto, M. *et al.* Hippocampal level of neural specific adenylyl cyclase type I is decreased in Alzheimer's disease. *Biochim. Biophys. Acta* **1535,** 60–8 (2000).
17. Teich, A. F. *et al.* Synaptic Therapy in Alzheimer's Disease: A CREB-centric Approach. *Neurotherapeutics* **12,** 29–41 (2015).
18. Baltrons, M. A., Pedraza, C. E., Heneka, M. T. & García, A. Beta-amyloid peptides decrease soluble guanylyl cyclase expression in astroglial cells. *Neurobiol. Dis.* **10,** 139–49 (2002).
19. Baltrons, M. A., Pifarré, P., Ferrer, I., Carot, J. M. & García, A. Reduced expression of NO-sensitive guanylyl cyclase in reactive astrocytes of Alzheimer disease, Creutzfeldt-Jakob disease, and multiple sclerosis brains. *Neurobiol. Dis.* **17,** 462–72 (2004).
20. Vitolo, O. V *et al.* Amyloid beta -peptide inhibition of the PKA/CREB pathway and long-term potentiation: reversibility by drugs that enhance cAMP signaling. *Proc. Natl. Acad. Sci. U. S. A.* **99,** 13217–21 (2002).
21. Cheng, Y.-F. *et al.* Inhibition of phosphodiesterase-4 reverses memory deficits produced by Aβ25-35 or Aβ1-40 peptide in rats. *Psychopharmacology (Berl).* **212,** 181–91 (2010).

22. Zhang, J. *et al.* Phosphodiesterase-5 inhibitor sildenafil prevents neuroinflammation, lowers beta-amyloid levels and improves cognitive performance in APP/PS1 transgenic mice. *Behav. Brain Res.* **250,** 230–7 (2013).
23. Lee, H. R. *et al.* Cilostazol suppresses β-amyloid production by activating a disintegrin and metalloproteinase 10 via the upregulation of SIRT1-coupled retinoic acid receptor-β. *J. Neurosci. Res.* **92,** 1581–1590 (2014).
24. Zhu, L. *et al.* A novel phosphodiesterase-5 Inhibitor: Yonkenafil modulates neurogenesis, gliosis to improve cognitive function and ameliorates amyloid burden in an APP/PS1 transgenic mice model. *Mech. Ageing Dev.* **150,** 34–45 (2015).
25. Puzzo, D., Gulisano, W., Arancio, O. & Palmeri, A. The keystone of Alzheimer pathogenesis might be sought in Aβ physiology. *Neuroscience* **307,** 26–36 (2015).
26. Ricciarelli, R. & Fedele, E. The Amyloid Cascade Hypothesis in Alzheimer's Disease: It's Time to Change Our Mind. *Curr. Neuropharmacol.* **15,** 926–935 (2017).
27. Puzzo, D. *et al.* Picomolar amyloid-beta positively modulates synaptic plasticity and memory in hippocampus. *J. Neurosci.* **28,** 14537–45 (2008).
28. Puzzo, D. *et al.* Endogenous amyloid-β is necessary for hippocampal synaptic plasticity and memory. *Ann. Neurol.* **69,** 819–30 (2011).
29. Puzzo, D., Privitera, L. & Palmeri, A. Hormetic effect of amyloid-β peptide in synaptic plasticity and memory. *Neurobiol. Aging* **33,** 1484.e15-24 (2012).
30. Morley, J. E. *et al.* A physiological role for amyloid-beta protein:enhancement of learning and memory. *J. Alzheimers. Dis.* **19,** 441–9 (2010).
31. Lawrence, J. L. M. *et al.* Regulation of presynaptic Ca2+, synaptic plasticity and contextual fear conditioning by a N-terminal betaamyloid fragment. *J Neurosci* **34,** 14210–14218 (2014).
32. Kamenetz, F. *et al.* APP processing and synaptic function. *Neuron* **37,** 925–37 (2003).
33. Cirrito, J. R. *et al.* Synaptic Activity Regulates Interstitial Fluid Amyloid-β Levels In Vivo. *Neuron* **48,** 913–922 (2005).
34. O'Brien, R. J. & Wong, P. C. Amyloid precursor protein processing and Alzheimer's disease. *Annu. Rev. Neurosci.* **34,** 185–204 (2011).
35. Das, U. *et al.* Visualizing APP and BACE-1 approximation in neurons yields insight into the amyloidogenic pathway. *Nat. Neurosci.* **19,** 55–64 (2016).
36. Kerppola, T. K. Design and implementation of bimolecular fluorescence complementation (BiFC) assays for the visualization of protein interactions in living cells. *Nat. Protoc.* **1,** 1278–1286 (2006).
37. Arancio, O., Kandel, E. R. & Hawkins, R. D. Activity-dependent long-term enhancement of transmitter release by presynaptic 3',5'-cyclic GMP in cultured hippocampal neurons. *Nature* **376,** 74–80 (1995).
38. Monfort, P., Muñoz, M.-D., Kosenko, E. & Felipo, V. Long-term potentiation in hippocampus involves sequential activation of soluble guanylate cyclase, cGMP-dependent protein kinase, and cGMP-degrading phosphodiesterase. *J. Neurosci.* **22,** 10116–22 (2002).
39. Ricciarelli, R. *et al.* A novel mechanism for cyclic adenosine monophosphate-mediated memory formation: Role of amyloid beta. *Ann. Neurol.* **75,** 602–7 (2014).
40. Morales-Corraliza, J. *et al.* In vivo turnover of tau and APP metabolites in the brains of wild-type and Tg2576 mice: greater stability of sAPP in the beta-amyloid depositing mice. *PLoS One* **4,** e7134 (2009).
41. Morales-Corraliza, J. *et al.* Immunization targeting a minor plaque constituent clears β-amyloid and rescues behavioral deficits in an Alzheimer's disease mouse model. *Neurobiol. Aging* **34,** 137–45 (2013).
42. Wesson, D. W., Morales-Corraliza, J., Mazzella, M. J., Wilson, D. A. & Mathews, P. M. Chronic anti-murine Aβ immunization preserves odor guided behaviors in an Alzheimer's β-amyloidosis model. *Behav. Brain Res.* **237,** 96–102 (2013).
43. Broadbent, N. J., Gaskin, S., Squire, L. R. & Clark, R. E. Object recognition memory and the rodent hippocampus. *Learn. Mem.* **17,** 5–11 (2010).
44. Puzzo, D. & Arancio, O. Amyloid-β peptide: Dr. Jekyll or Mr. Hyde? *J. Alzheimers. Dis.* **33 Suppl 1,** S111-20 (2013).

45. Fedele, E., Rivera, D., Marengo, B., Pronzato, M. A. & Ricciarelli, R. Amyloid β: Walking on the dark side of the moon. *Mech. Ageing Dev.* **152,** 1–4 (2015).
46. Tang, Y. *et al.* Early and selective impairments in axonal transport kinetics of synaptic cargoes induced by soluble amyloid β-protein oligomers. *Traffic* **13,** 681–93 (2012).
47. Canepa, E. *et al.* Cyclic adenosine monophosphate as an endogenous modulator of the amyloid-β precursor protein metabolism. *IUBMB Life* **65,** 127–33 (2013).
48. Thinakaran, G. & Koo, E. H. Amyloid precursor protein trafficking, processing, and function. *J. Biol. Chem.* **283,** 29615–9 (2008).
49. Wilkins, H. M. & Swerdlow, R. H. Amyloid precursor protein processing and bioenergetics. *Brain Res. Bull.* **133,** 71–79 (2017).
50. Sannerud, R. *et al.* Restricted Location of PSEN2/γ-Secretase Determines Substrate Specificity and Generates an Intracellular Aβ Pool. *Cell* **166,** 193–208 (2016).
51. Andoh, T., Chiueh, C. C. & Chock, P. B. Cyclic GMP-dependent protein kinase regulates the expression of thioredoxin and thioredoxin peroxidase-1 during hormesis in response to oxidative stress-induced apoptosis. *J. Biol. Chem.* **278,** 885–90 (2003).
52. Cai, Z.-X. *et al.* Double-Edged Roles of Nitric Oxide Signaling on APP Processing and Amyloid-β Production In Vitro: Preliminary Evidence from Sodium Nitroprusside. *Neurotox. Res.* **29,** 21–34 (2016).
53. Bonkale, W. L., Winblad, B., Ravid, R. & Cowburn, R. F. Reduced nitric oxide responsive soluble guanylyl cyclase activity in the superior temporal cortex of patients with Alzheimer's disease. *Neurosci. Lett.* **187,** 5–8 (1995).
54. Chalimoniuk, M. & Strosznajder, J. B. Aging modulates nitric oxide synthesis and cGMP levels in hippocampus and cerebellum. Effects of amyloid beta peptide. *Mol. Chem. Neuropathol.* **35,** 77–95 (1998).
55. Ugarte, A. *et al.* Decreased levels of guanosine 3', 5'-monophosphate (cGMP) in cerebrospinal fluid (CSF) are associated with cognitive decline and amyloid pathology in Alzheimer's disease. *Neuropathol. Appl. Neurobiol.* **41,** 471–82 (2015).
56. Huang, Y. Y., Nguyen, P. V, Abel, T. & Kandel, E. R. Long-lasting forms of synaptic potentiation in the mammalian hippocampus. *Learn. Mem.* **3,** 74–85 (1996).
57. Tyan, S.-H. *et al.* Amyloid precursor protein (APP) regulates synaptic structure and function. *Mol. Cell. Neurosci.* **51,** 43–52 (2012).
58. Li, Q. *et al.* Long-term administration of green tea catechins prevents age-related spatial learning and memory decline in C57BL/6 J mice by regulating hippocampal cyclic amp-response element binding protein signaling cascade. *Neuroscience* **159,** 1208–1215 (2009).
59. Xu, G. *et al.* Murine Aβ over-production produces diffuse and compact Alzheimer-type amyloid deposits. *Acta Neuropathol. Commun.* **3,** 72 (2015).

Chapter 3: Sub-efficacious doses of phosphodiesterase 4 and 5 inhibitors improve memory in a mouse model of Alzheimer's disease

Gulisano W[1], Tropea MR[1], Arancio O[2], Palmeri A[1], Puzzo D[3].

[1]Dept. Biomedical and Biotechnological Sciences, Section of Physiology, University of Catania, Catania, Italy. [2]Dept. of Pathology and Cell Biology, Taub Institute for Research on Alzheimer's Disease and the Aging Brain, Columbia University, New York, NY, USA. [3]Dept. Biomedical and Biotechnological Sciences, Section of Physiology, University of Catania, Catania, Italy.

In: Neuropharmacology. 2018 Aug;138:151-159.

doi: 10.1016/j.neuropharm.2018.06.002.

Abstract

Cyclic nucleotides cAMP and cGMP cooperate to ensure memory acquisition and consolidation. Increasing their levels by phosphodiesterase inhibitors (PDE-Is) enhanced cognitive functions and rescued memory loss in different models of aging and Alzheimer's disease (AD). However, side effects due to the high doses used limited their application in humans. Based on previous studies suggesting that combinations of sub-efficacious doses of cAMP- and cGMP-specific PDE-Is improved synaptic plasticity and memory in physiological conditions, here we aimed to study whether this treatment was effective to counteract the AD phenotype in APPswe mice. We found that a 3-week chronic treatment with a combination of sub-efficacious doses of the cAMP-specific PDE4-I roflumilast (0.01 mg/kg) and the cGMP-specific PDE5-I vardenafil (0.1 mg/kg) improved recognition, spatial and contextual fear memory. Importantly, the cognitive enhancement persisted for 2 months beyond administration. This long-lasting action, and the possibility to minimize side effects due to the low doses used, might open feasible therapeutic strategies against AD.

Introduction

Cyclic adenosine monophosphate (cAMP) and cyclic guanosine monophosphate (cGMP) are second messengers regulating signal transduction. Their levels are maintained thanks to a balance between their production, catalyzed by adenylyl cyclase and guanylyl cyclase, and their degradation, operated by phosphodiesterases (PDE)[1].

Because cAMP and cGMP are key molecules that cooperate to ensure memory acquisition and consolidation[2], increasing their levels results in cognitive-enhancing effects[3]. Several drugs acting on the cAMP- or the cGMP-pathway have been tested in pre-clinical studies, but the use of PDE inhibitors (PDE-Is) has received more attention for their better selectivity, specificity, and safety profile. Moreover, the presence of PDE in the brain, further supported by recent evidences confirming their availability in human neurons[4], have renewed the interest toward PDE-Is to treat a variety of neurodegenerative disorders[5].

In particular, considering that Alzheimer's disease (AD) and aging are characterized by an impairment of memory accompanied by a decrease of cyclic nucleotides[6], an increasing number of studies have proposed the use of PDE-Is to restore cAMP and cGMP levels in the brain to counteract cognitive deficits[3].

Previous studies have shown that cAMP- and cGMP-specific PDE-Is rescued synaptic plasticity and memory deficits in animal models of aging and AD[7–10], and might be beneficial in AD patients[11]. However, although several PDE-Is have been proposed to treat brain-related disorders, the resulting elevation of cyclic nucleotide levels in non-targeted areas has limited their use in patients[12]. For this reason, notwithstanding the remarkable potential of PDE-Is against age-related and neurodegenerative diseases, these drugs are so far indicated only to treat erectile dysfunction, pulmonary hypertension and chronic obstructive pulmonary disease (COPD).

Recently, we have demonstrated that combining sub-efficacious doses of the cAMP-specific PDE4-I rolipram and the cGMP-specific PDE5-I vardenafil improved recognition memory in wild type mice. Based on these findings, here, we have evaluated the effect of a combination therapy with sub-efficacious doses of PDE4-and

PDE5-Is in the APPswe animal model of AD. We have chosen the PDE4-I roflumilast and the PDE5-I vardenafil, well-tolerated drugs with a favorable safety profile, already in the market for other clinical applications in humans.

Results

A chronic but not acute treatment with sub-efficacious doses of roflumilast and vardenafil rescued recognition memory in APPswe mice

The experimental plan is described in Figure 1.

We first performed the NOR task, which has been demonstrated to be very useful to evaluate the therapeutic effects of drugs against the cognitive impairment in animal models of AD[13].

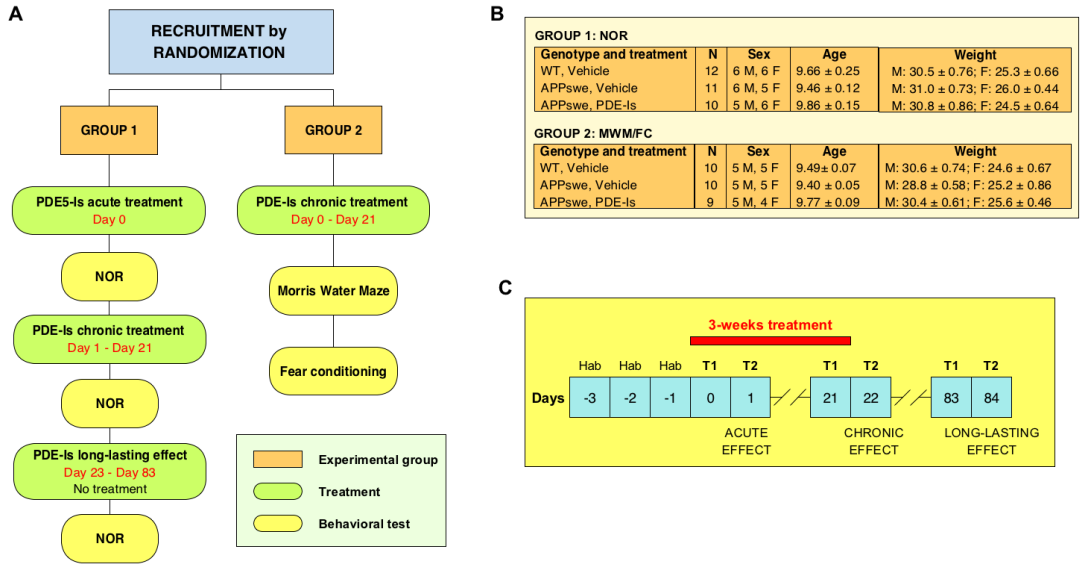

Fig. 1. Experimental plan. A) Scheme of treatment and behavioral studies performed on two different groups of mice selected by randomization. B) Detailed description of the characteristics of the two groups of mice. C) Time-line of novel object recognition test performed on mice after a single treatment (acute effect), a 3-weeks treatment (chronic effect), or two months withdrawal (long-lasting effect). Hab = habituation; T1 = training phase; T2 = memory test phase.

Based on previous studies[2,14], we first tested the effect of a single administration of sub-efficacious doses of a combination of the PDE4-I roflumilast and the PDE5-I vardenafil (Fig. 2A and B). Analyses of the D index (exploration of novel object minus exploration of familiar object/total exploration time) by one-way ANOVA showed a difference among the three groups of mice ($F(2,24) = 18.56$, $p < 0.0001$) and Bonferroni's post-hoc corrections indicated a difference between vehicle-treated WT and APPswe mice ($p < 0.0001$), as well as PDE-Is-treated APPswe mice ($p < 0.0001$), suggesting that the treatment was not able to revert the memory impairment in AD mice. Comparison of D with zero confirmed that APPswe mice treated with PDE-IS were not able to learn (one-sample t-test: $t(8) = 1.16$, $p = 0.27$; Fig. 2B). No sex differences were detected in D analyses (two-ways ANOVA for experimental condition and sex: $F(2,21) = 0.76$; $p = 0.48$).

Because it has been previously demonstrated that a 3-week treatment with the PDE5-I sildenafil or the PDE4-I rolipram was needed to rescue memory in mouse models of aging and AD[7,8,15,16], here we decided to administer the PDE-Is combination at sub-efficacious doses for 3 weeks. We found that the impairment of recognition memory in vehicle-treated APPswe mice was rescued after a 3-week i.p. treatment with roflumilast (0.01 mg/kg) + vardenafil (0.1 mg/kg). In fact, treated APPswe mice explored the novel object for a longer time comparable to vehicle-treated WT littermates suggesting that the treatment was able to rescue recognition memory (Fig. 2C). Analyses of the D index indicated a difference among groups (one-way ANOVA: $F(2,31) = 21.172$, $p < 0.0001$) and that the impairment of memory observed in vehicle-treated APPswe mice (Bonferroni's $p = 0.001$ vs. WT) was rescued by the PDE-Is treatment (Bonferroni's $p = 0.001$ between vehicle- and PDE-Is-treated APPswe mice; Fig. 2D). Comparison of single D with zero by one-sample t-test confirmed that PDE-Is-treated-APPswe mice ($t(11) = 8.79$, $p < 0.0001$) and WT control animals ($t(11) = 0.42$, $p < 0.0001$) were able to learn (Fig. 2D). No sex differences were detected in D analyses (two-ways ANOVA: $F(2,28) = 0.22$; $p = 0.8$).

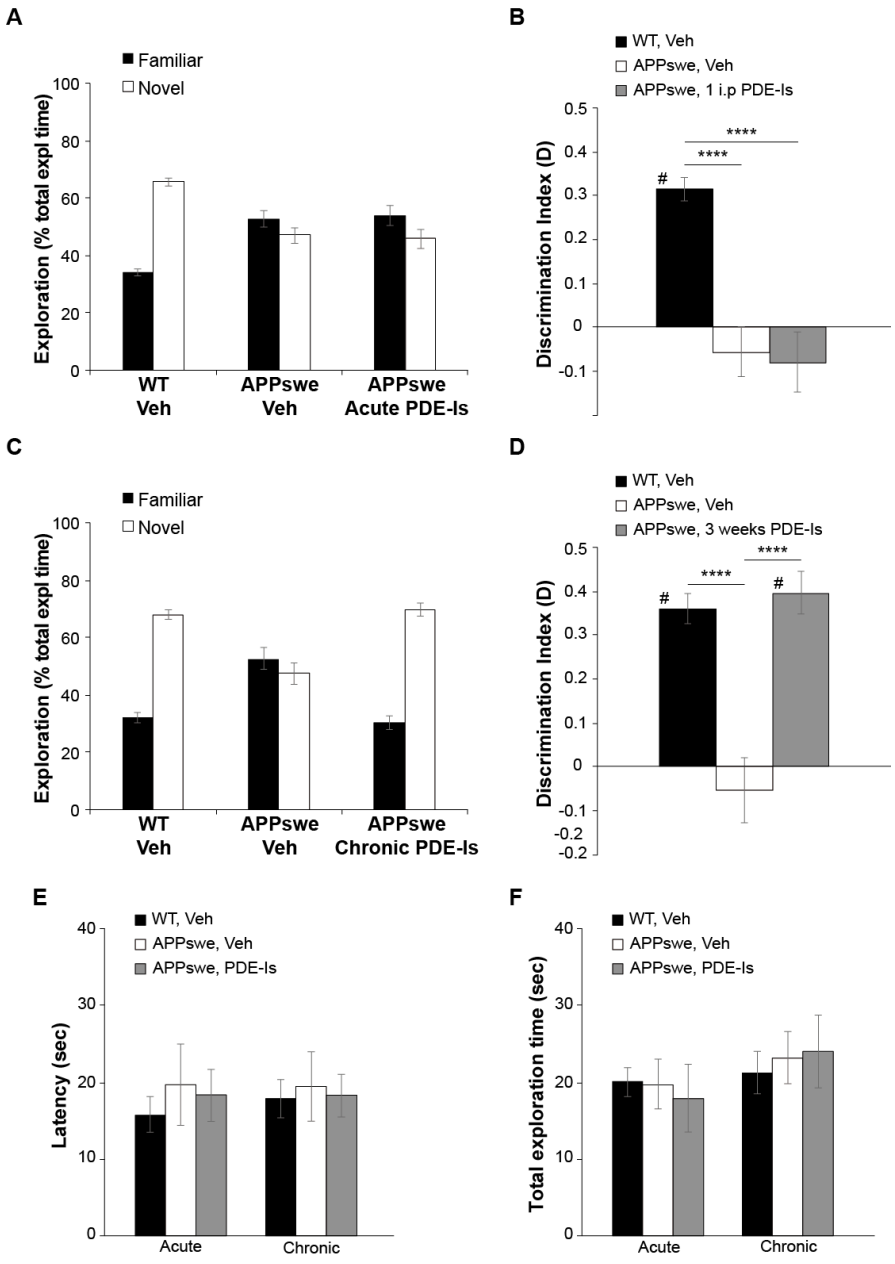

Fig. 2. Effects of an acute or chronic treatment with sub-efficacious doses of roflumilast and vardenafil in recognition memory of APPswe mice. A) Recognition memory is impaired in APPswe mice, since they spend a similar amount of time exploring the novel vs. the old object. An acute treatment (single i.p. injection) does not ffect exploration time of the novel vs. the familiar ovjet or B) discrimination index in APPsew mice. C) A chronic treatment (daily i.p. injections for 3 weeks) with sub-efficacious doses of roflumilast and vardenafil rescues recognition memory. D) Discrimination performance confirms the capability of this treatment to restore memory in APPswe mice. E) Latency to the first approach to novel object and F) total exploration time are not affected by treatment. ****$p < 0.0001$; #$p \neq 0$.

Either acute or chronic treatment did not modify latency to the first approach to novel object (acute: $F(2,31) = 0.06$, $p = 0.94$; chronic: $F(2,24) = 0.3$, $= 0.74$; Fig. 2E) as well as total exploration time (acute: $F(2,31) = 0.14$, $p = 0.86$; chronic: $F(2,24) = 0.12$, $p = 0.88$; Fig. 2F) among the three groups of mice.

A 3-week treatment with sub-efficacious doses of roflumilast and vardenafil rescued spatial learning, reference, and contextual fear memory in APPswe mice

Because the hippocampus is critical for spatial memory, and it is early damaged in AD, we decided to test whether sub-efficacious doses of roflumilast and vardenafil might rescue the typical impairment of hippocampal-dependent memory found in animal models of AD. For this, we used Morris Water Maze(MWM) to assess spatial learning and long-term memory, and Fear Conditioning to assess associative memory[17].

During the training phase of MWM, mice are required to find a hidden platform beneath the surface of the water. APPswe mice took longer to find the platform, thus confirming the AD-related learning impairment (ANOVA for repeated measures: $F(1,17) = 27.35$, $p < 0.001$ comparing vehicle-treated APPswe with vehicle-treated WT mice; Fig. 3A). APPswe mice previously treated with sub-efficacious doses of roflumilast + vardenafil for 3 weeks presented an overall latency comparable to WT animals ($F(1,15) = 4.11$, $p = 0.06$). When comparing the single sessions, the difference among groups was significant at the 5th ($F(2,24) = 3.46$, $p = 0.04$) and 6th trial ($F(2,24) = 5.70$, $p < 0.01$).

The probe trial (Fig. 3B), used to evaluate reference memory, evidenced that vehicle-treated APPswe mice failed to remember where the platform was located in the training sessions, since they spent a less amount of time in the target quadrant (TQ) compared to WT control mice (Bonferroni's $p = 0.01$). However, after a 3-week treatment with sub-efficacious doses of PDE-Is, the time spent in TQ was comparable between APPswe and WT control mice (Bonferroni's $p = 1$), indicating a rescue of reference memory. No sex differences were found when analyzing the escape latency during

spatial learning ($F(2,21) = 0.82$; $p = 0.45$) and the time spent in TQ ($F(2,21) = 1.55$; $p = 0.23$).

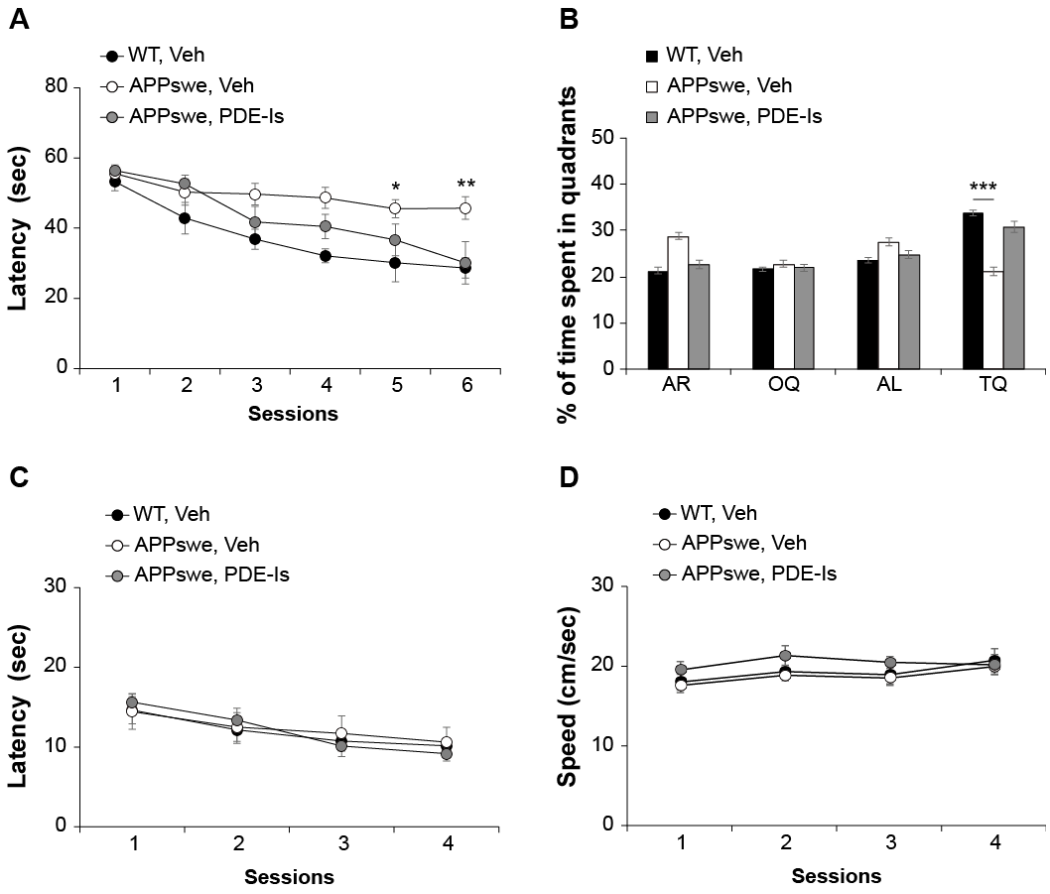

Fig. 3. Effects of a chronic treatment with sub-efficacious doses of roflumilast and vardenafil in spatial learning and reference memory in APPswe mice. A) Morris Water Maze task shows that a 3-week i.p. treatment with sub-efficacious doses of roflumilast + vardenafil rescue spatial learning in APPswe mice, since they spend less time to reach the hidden platform. B) Analyses of the probe trial indicate an improvement of reference memory after treatment, since the % time spent in the TQ increases. C) No differences were detected in latency and D) speed during the visible platform test. AR = adjacent right quadrant; OQ = opposite quadrant; AL = adjacent left quadrant; TQ = target quadrant. *$p < 0.05$; **$p < 0.01$; ***$p < 0.005$.

Finally, when performing a trial with a visible platform to exclude motor influences, no differences were found among groups in the latency to reach the platform ($F(2,24) = 0.02$, $p = 0.98$; Fig. 3C) and speed ($F(2,24) = 0.57$, $p = 0.22$; Fig. 3D).

Fear Conditioning experiments showed that freezing behavior measured during the training before the shock (baseline) was similar in the three groups of mice ($F(2,26) = 0.35$, $p = 0.7$; Fig. 4A). Analyses of contextual fear learning 24 h after training indicated a decrease of freezing behavior in vehicle-treated APPswe mice compared with vehicle-treated WT animals (ANOVA among all: $F(2,26) = 4.41$, $p = 0.02$; Bonferroni's $p < 0.05$ comparing APPswe and WT mice; Fig. 4A). Treatment with sub-efficacious doses of roflumilast + vardenafil for 3 weeks restored contextual fear learning in APPswe mice (Bonferroni's $p = 0.04$ comparing PDE-Is-treated vs. vehicle-treated APPswe mice and $p = 1$ comparing PDE-Is-treated APPswe vs. vehicle-treated WT mice; Fig. 4A). No sex differences were found in contextual fear memory ($F(2,22) = 0.6$, $p = 0.55$). Cued fear conditioning, mainly relying on amygdala, was similar among the three groups of mice in both the Pre-Cued ($F(2,26) = 0.08$, $p = 0.91$) and the Cued test ($F(2,26) = 0.89$, $p = 0.42$; Fig. 4B). No differences were found in the capability to perceive the electric shock during the sensory threshold assessment ($F(2,26) = 0.61$, $p = 0.55$; Fig. 4C).

Sub-efficacious doses of roflumilast and vardenafil exerted a long-lasting beneficial effect on recognition memory in APPswe mice

Finally, we evaluated the possible long-lasting effect of PDE-Is treatment. To this end, we used the same groups of mice that underwent a chronic treatment for 3 weeks and were tested for NOR. We suspended the treatment for 2 months and then NOR was performed again by using different objects (see Fig. 1A,C for experimental design). In AD mice previously treated with sub-efficacious doses of roflumilast + vardenafil the improvement of recognition memory persisted beyond the administration, as demonstrated by the increase of the time spent exploring the novel vs. the familiar object after two months of therapy withdrawal (Fig. 4A).

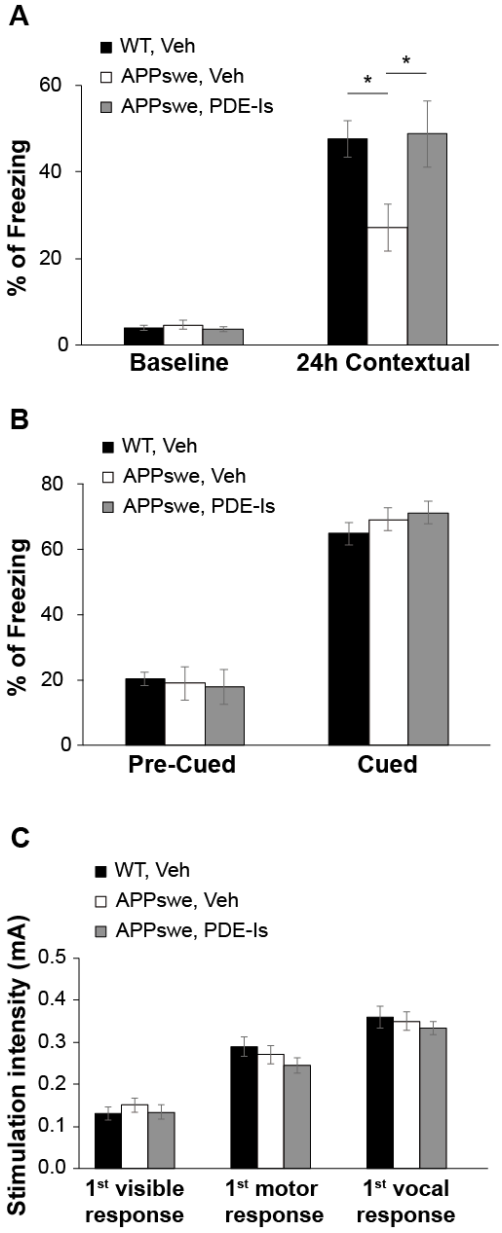

Fig. 4. Effects of a chronic treatment with sub-efficacious doses of roflumilast and vardenafil in fear memory in APPswe mice. A) APPswe mice treated with sub-efficacious doses of roflumilast + vardenafil show an increase of freezing behavior in the contextual task. B) Freezing behavior before (Pre) and after (Post) the auditory cue does not change among the three groups of mice. C) The sensory threshold assessment does not show differences among the three groups. *$p < 0.05$.

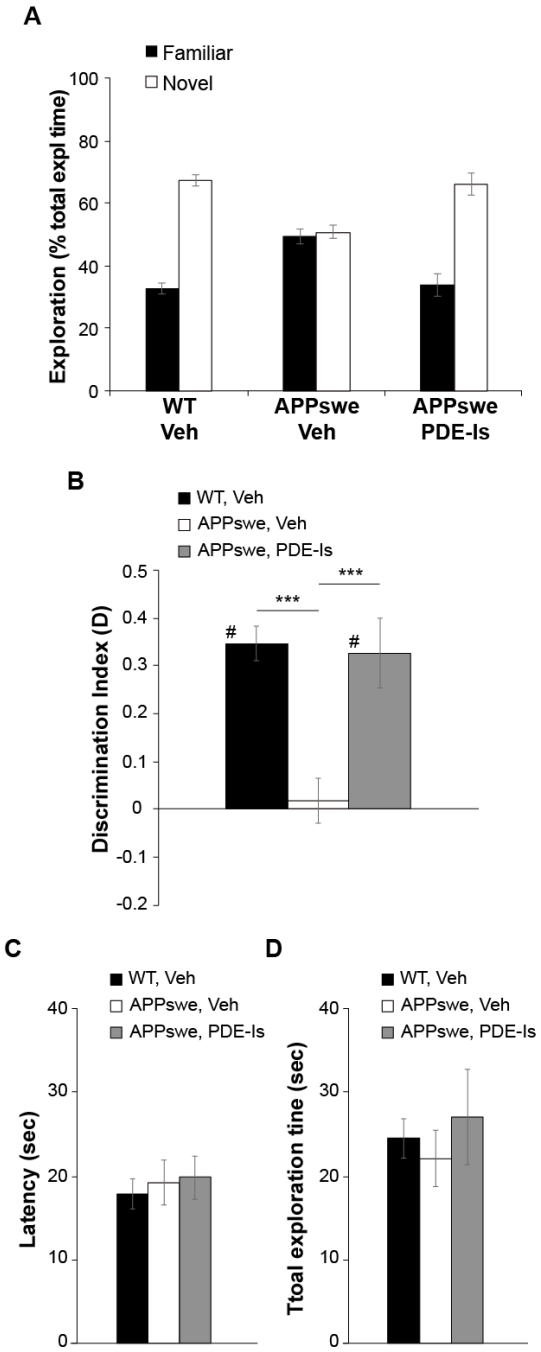

Fig. 5. Long-lasting beneficial effect of sub-efficacious doses of roflumilast and vardenafil in APPswe mice. A) After a 3-week administration, recognition memory was re-evaluated after 2 months of withdrawal. The higher time spent in exploring the novel object indicates that the improvement of recognition memory persisted in APPswe mice. B) Analyses of D index show a difference between vehicle-treated and PDE-Is-treated APPswe mice. One-sample t-test for D with zero confirms that PDE-Is-treated APPswe mice are able to learn. C) Latency to the first approach to novel object as well as D) total exploration time are not modified by treatment. ***$p < 0.005$; #$p \neq 0$.

Analyses of the D index ($F(2,27) = 11.64$, $p < 0.0001$ among groups) confirmed the impairment of memory in vehicle-treated APPswe mice (Bonferroni's $p = 0.001$ vs. WT) and the rescue by the PDE-Is treatment (Bonferroni's $p = 0.001$ between vehicle- and PDE-Is-treated APPswe mice; Fig. 4B). Indeed, D was different than zero PDE-Is-treated APPswe ($t(9) = 4.48$, $p = 0.002$; Fig. 4B). Latency to the first approach to novel object as well as total exploration time were similar in the three groups of mice ($F(2,27) = 0.16$, $p = 0.84$) and $F(2,27) = 0.35$, $p = 0.7$).

Thus, the cognitive-enhancing effect persisted beyond the administration of sub-efficacious doses of roflumilast and vardenafil.

Discussion

In this study we have demonstrated that a 3-week combined administration of sub-efficacious doses of the PDE4-I roflumilast and the PDE5-I vardenafil - that at the used concentration do not affect memory per se[14] - re-established memory in APPswe mice. In view of a translational approach on humans, we investigated recognition, spatial and contextual fear memory, known to depend upon the integrity of hippocampus, one of the first brain areas affected in AD[18,19]. These behavioral tasks are known to be impaired in different animal models of AD and reproduce the main cognitive dysfunction observed in AD patients[18,19]. More importantly, we have chosen drugs already approved for other clinical applications in humans, thus with available follow-up information. Vardenafil is a well-tolerated PDE5-I with a favorable safety profile and few transient side effects[20]. As for PDE4-Is, despite pre-clinical studies have frequently been performed with rolipram, clinical trials have failed due to severe emetic effects in humans[21]. Hence, here we preferred to use roflumilast, a PDE4-I approved for COPD, whose safety and effectiveness have been previously demonstrated in clinical studies[22]. Moreover, recent studies suggested that roflumilast improved cognition without emetic side effects in rodent models[23] and humans[24]. Notably, both compounds have been demonstrated to cross the blood-brain barrier when peripherally administered, and brain penetration was needed to exert cognitive effects in rodents[23,25,26]. Also, PDE-Is central effects have been demonstrated to be independent

of the increase of cerebral blood flow or glucose metabolism[27], suggesting a possible action on molecular mechanisms underlying synaptic plasticity, as previously shown[7,8,15,16]. In this context, it has been crucial to confirm the presence of PDE4 and PDE5 in the human brain. While PDE4 is known to be widely distributed in the rodent, monkey and human brain[26,28], and the specific localization of its isoforms has been previously described in humans[29], a number of studies failed at identifying PDE5 in the human brain tissue[28,30], leading to the conclusion that development of PDE5-Is for neurological disease would be a failure. However, it has been recently reported that PDE5 are expressed in human neurons at cortical, hippocampal and cerebellar level[4], renewing the interest towards PDE5-Is as therapeutic target.

Another finding reported in our study concerns the difference between an acute or chronic treatment. We have found that the beneficial effect on the AD phenotype is obtained only after a chronic 3-week administration. Although a single dose of a sub-efficacious PDE-Is combination was capable to enhance cognition in healthy rodents[14], it was insufficient to modify memory in APPswe mice. This is consistent with previous studies indicating that a prolonged treatment is needed to re-establish the increase in phosphorylationof the transcription factor CREB, which is crucial for memory formation, in mouse models of amyloid deposition or aging[8,15]. Interestingly, this also correlates with evidences that a chronic but not acute administration of PDE5-Is in humans was able to improve cognitive performances[31,32].

We have also shown that a contemporary delivery of the two drugs is efficacious. Indeed, according to our previous observations, sub-efficacious doses of PDE4-and PDE5-Is should be administered at different time windows, based on the specific effects exerted by cGMP and cAMP in memory formation and consolidation[2]. Therefore, the enhancement of memory in healthy rodents was obtained when separately administering vardenafil and rolipram during the early and late memory consolidation phases, respectively[14]. However, this therapeutic design might not be easily applicable on humans because, besides the difficulty to identify different phases of training in daily life, one should consider that the elderly already receive multiple

medications for chronic diseases. Here, we have verified that a concurrent administration of roflumilast and vardenafil reverted memory loss in AD mice, thus suggesting that these drugs could be administered together to improve patient compliance.

Another relevant result is that a 3-week treatment was beneficial for a prolonged period. In fact, when testing recognition memory 2 months after therapy suspension, the PDE-Is-induced protective action was maintained. This is consistent with previous observations indicating that higher doses of rolipram or sildenafil exerted a long-lasting cognitive-enhancing effect in animal models of AD[7,15].

In conclusion, we have shown that combining sub-efficacious doses of roflumilast and vardenafil, drugs already approved for other clinical applications in the elderly, might have several advantages compared to single PDE-Is administration at high doses, such as a possible long-standing human use and a perspective of a better compliance due to the possibility to minimize side effects due to the low doses used. Although an anisobolographic analysis would be necessary to clarify whether this combination therapy exerts a synergistic or additive action on memory, previous investigations have indicated that only when combined sub-efficacious doses of PDE-Is might enhance cognition[14]. This strengthen the idea that cAMP and cGMP, which are crucial for synaptic plasticity and memory and are known to decrease in AD and aged patients[6], cooperate to ensure memory formation[2,14], and that a contemporary intervention on both pathways improves the therapeutic effect. Even if we cannot exclude that testing wider dose ranges could reveal different relationship, here we have shown that a 3-week chronic treatment with roflumilast (0.01 mg/kg) and vardenafil (0.1 mg/kg) is able to counteract recognition, spatial and contextual fear memory impairment in pre-clinical models of AD. More importantly, the persistence of the effect beyond the administration suggests that this approach might have the potential of a disease-modifying therapy.

Authorship

W.G. and M.R.T. performed experiments and statistical analyses; A.P. and O.A. provided experimental resources; D.P. supervised the study and wrote the article.

Declaration of interest

None.

Acknowledgment

We thank Ottavio Arancio for providing the mice, who established a colony from a generous gift of Karen Hsiao-Ashe; Jos Prickaerts (Maastricht University, the Netherlands) for providing roflumilast. This work was supported by University of Catania intramural funds to A.P. and D.P.

Materials and methods

Animals

APP transgenic (Tg) mice (strain: B6; SJL-Tg(APPSWE)2576 Kha) overexpressing human APP (isoform 695) containing the double mutation K670N, M671L, also known as Swedish mutation, under the control of the hamster prion protein promoter were generated at Columbia University by crossing Tg males with B6SJLF1 wild type females. PCR on tail samples was used for genotyping, as previously described[15]. Animals (APP Tg and WT B6/SJL littermates) were maintained at the University of Catania in a conventional facility on a 12 h light/dark cycle, in a temperature (23 ± 1 °C) and humidity (57 ± 3%) controlled room. Each animal was housed in an individual IVC standard cage enriched with a plastic object used as a nest. Food (standard diet cubes) and water (filtered drinking water by particle filter, active carbon filter and UV light) were available ad libitum.

Mice were divided into three groups: APP Tg animals (named APPswe throughout the manuscript) treated with vehicle, APPswe treated with PDE-Is, and WT treated with vehicle as controls. Each group consisted of 10–12 animals, allocated to a specific treatment and behavioral paradigm by a randomization procedure (Fig. 1A). Researchers who performed the behavioral assessment were blind in respect to genotype and treatment. Pairing between raw data and the corresponding experimental group was performed at the end of each behavioral setting. Based on the recent NIH initiative to balance sex in preclinical research[33], both males and females were used (Fig. 1B), even if no sex differences were found in cognitive performances (see results for details). Mice were recruited at about 9–10 months of age (Fig. 1B), based on previous studies indicating a progressive impairment of cognition at this age[18].

The experiments complied with the ARRIVE guidelines, were carried out in accordance with the EU Directive 2010/63/EU for animal experiments, and received approval by the Institutional Animal Care and Use Committee (#327/2013-B).

Treatment

Roflumilast (generous gift of Dr. Jos Prickaerts from Maastricht University) and Vardenafil (Sigma Aldrich) were dissolved in DMSO to prepare stock solutions. The final concentration of PDE-Is (0.01 mg/kg roflumilast and 0.1 mg/kg vardenafil in a final DMSO concentration < 0.03%) was prepared immediately before use in 300 µl saline solution and administered via intraperitoneal injections for 3 weeks (Fig. 1A,C), based on previous works[8,14,15]. Vehicle-injected mice received the same amount of DMSO dissolved in saline solution.

Behavioral studies

As illustrated in the experimental design (Fig. 1A,C), we evaluated whether the PDE-Is treatment might rescue the AD phenotype through different behavioral tasks. In particular, we performed novel object recognition (NOR) to evaluate: i) the effect of a single acute administration of PDE-Is; ii) the effect of a chronic administration of PDE5-Is (daily at 9–10 a.m. for 3 weeks); iii) the possible long-lasting effect after 2 months from treatment suspension. Morris Water Maze(MWM) and Fear Conditioning (FC) were used to evaluate the effect of a chronic 3-weeks administration. Before starting the treatment, mice underwent a period of 1-week handling in the animal facility room.

For behavioral studies, mice were moved to the behavioral room (6 m2, white walls, soft illumination by two floor lamps located at the corners of the room to avoid shadows into the mazes) in their home cages and habituate to the new environment for about two hours before to start the experimental session.

Novel Object Recognition (NOR) was performed as previously described[34]. The arena was a plastic white box (50 × 35 × 45 cm) placed on a lab bench. A webcam, connected to the computer, was fixed on the wall. The NOR protocol was performed in 5 days: 3 days of habituation, 1 day of training (T1) and 1 day of testing (T2). Objects were designed by a computer aided design software (Solidworks, France) with the following characteristics: i) mean height of 54 ± 2.9 mm; ii) mean surface area of 95.24 ± 6.62 cm2; iii) mean volume of 43.07 ± 10.5 cm3; iv) different shapes (e.g. pyramid, cube, truncated sphere, cylinder, prism, star, etc.). The three-dimensional models were sliced and converted in g-code by a slicer software (Simplify3D, USA) and printed with a Prusa-inspired 3D printer of our design with a 100 µm resolution on z-axis and a printing nozzle diameter of 300 µm. Objects were printed in polylactic acid of different colors (blue, white, black, red, green). After each trial, the box and the objects were cleaned with 70% ethanol and dried with absorbent paper. During the first day (habituation to the arena), the mouse was put into the empty arena and allowed to explore it for 10 min. During the second and the third day (familiarization with objects), the mouse was put into the arena containing two different objects, randomly chosen among our object collection and changed from day to day, for 10 min. During the fourth day, NOR training session (T1) was performed. The mouse was put into the arena and allowed to explore for 10 min two identical objects placed in the central part of the box, equally distant from the perimeter and the center. During the fifth day (24 h after T1), the mouse underwent the second trial (T2) to test memory retention for 10 min. Mice were presented with two different objects, respectively a “familiar” (i.e. the one used for T1) and a “novel” object. Animal exploration - defined as the mouse pointing its nose toward the object from a distance not >2 cm – was measured in T2 to analyze: 1) percentage exploration of familiar vs. novel object; (2) discrimination (D) index, “exploration of novel object minus exploration of familiar object/total exploration time”; (3) latency to first approach to novel object; and (4) total exploration time. We excluded from the analyses mice with a total exploration time <5 s.

Morris Water Maze (MWM) was performed as previously described[35]. The apparatus consisted of: i) a plastic circular white tank (height: 80 cm, diameter: 110 cm) filled with warm water (25 °C) up to about 40 cm below the edge, made opaque to hide the submerged platform by the addition of nontoxic white paint; ii) a submerged platform (1.5–2 cm under the surface of the water) made in plexiglas (10 × 10 cm); iii) spatial cues made by objects (a weathercock, a colored hammer, a plastic ring, a plastic hand clapper) positioned on the 4 cardinal points of the maze; iv) a camera mounted on the ceiling and connected to a video tracking system and software for motion detection (customized software based on color differences between the maze and the mouse by Netsense srl, Catania, Italy). The MWM test was performed in 6 days. During the first three days spatial learning was evaluated by measuring time (escape latency) taken to reach the platform hidden beneath the surface of the water. Mice underwent 2 daily sessions, held 4 h apart, each consisting of three trials. Each trial the mouse was placed in the water from a different randomly chosen quadrant (that did not contain the platform), whereas the platform was always positioned in the same place (SW) during the three days. Each trial lasted the time needed to reach the platform or a maximum of 60 s. The inter-trial interval lasted 15 s during which the mouse was gently placed on the platform.

During the fourth day reference memory was evaluated by the probe test. The platform was removed and mice were allowed to freely swim. The probe test consisted of 4 trials lasting 60 s each, separated by a 20 s inter-trial interval. For each trial, the mouse started the test from a different cardinal point. The analysis of the percent time spent in each quadrant was performed (target quadrant TQ; i.e. the one previously containing the platform versus 3 non-target quadrants AL = adjacent left, AR = adjacent right, and OQ = opposite quadrant).

During the fifth and sixth day, a visible test was used to assess motivational, visual and motor abilities. The same protocol described in the hidden acquisition training was used (two daily session of three 1 min trials) and the time taken to reach a visible platform marked with a green plastic tree randomly positioned in a different place during each trial was measured. During the visible test swimming distance was measured to calculate swimming speed used to evaluate possible motor effects on the performance. We excluded from the analyses mice that due to thigmotaxis or passivity failed to perform 3 consecutive trials[17].

Fear Conditioning (FC) was performed as previously described[15]. The apparatus consisted in a conditioning chamber, connected to an interface (Kinder Scientific, USA), located in a sound-attenuating box (Campden Inst., UK) with a computer fan installed in one side to provide a background white noise. A webcam mounted on the top of the chamber allowed video recording of the experiment. The floor, made of 36-bar insulated shock grid, was removable and cleaned after each test with 70% ethanol and water. The protocol lasted 3 days. Mice were handled every day for about 5 min before the experiment. During the first day the animal was placed in the conditioning chamber for 2 min prior to the conditioned stimulus (CS) delivery. CS was a tone (2800 Hz and 85 dB) delivered for 30 s. In the last 2 s of the tone, the mouse received a foot shock as unconditioned stimulus (US), through the electrified grid floor (0.70 mA for 2 s). After the CS/US pairing, the mouse was left into the chamber for 30 s before to be placed in the home cage. Twenty-four hours after training (day 2), the mouse was placed back in the conditioning chamber to evaluate contextual fear memory for 5 min. Forty-eight hours after training (day 3) the mouse was replaced in the conditioning chamber to evaluate cued fear memory. To this end, a novel context was created by using a plastic black box with a smooth flat floor sprayed with vanilla odorant. After 2 min (pre-CS test), the mouse was exposed to the same tone used during the training for 3 min (CS test). Freezing (absence of movement except for that needed for breathing) was manually scored during the three days by two different operators and the averaged value was used to perform the analyses.

Sensory threshold assessment was then performed to exclude that results were influenced by sensory perception of the shock. The mouse was placed into the conditioning chamber and a sequence of single foot shocks (from 0.1 mA to 0.8 mA) was automatically delivered with a 30 s interval. The mouse behavior was evaluated by the operator and the minimum current value able to evoke flinching, jumping, and vocalization was recorded for each mouse.

Statistical analysis

Sample size was calculated by G power ($\alpha = 0.05$, power $1-\beta = 0.80$) suggesting a minimum of 8 mice for each condition to obtain an effect size = 0.62. Experimenters were "blind" with respect to genotype and treatment. All data were expressed as mean ± SEM. We used: i) one-way ANOVA with Bonferroni's post-hoc correction to analyze D index, latency to the first exploration in NOR, percentage of exploration time in NOR, escape latency during the 5thand the 6th trial, percentage time spent in TQ, freezing during contextual and cued fear conditioning, and sensory threshold assessment; ii) ANOVA for repeated measures to analyze the curve of escape latency during the hidden and visible test; iii) one-sample t-test to compare D index with ero; iv) two-ways ANOVA for experimental group and sex to evaluate sex differences. We used Systat 9 software (USA). Significance was set for $p < 0.05$.

References

1. Puzzo, D., Sapienza, S., Arancio, O. & Palmeri, A. Role of phosphodiesterase 5 in synaptic plasticity and memory. *Neuropsychiatr. Dis. Treat.* **4,** 371–87 (2008).
2. Bollen, E. *et al.* Improved long-term memory via enhancing cGMP-PKG signaling requires cAMP-PKA signaling. *Neuropsychopharmacology* **39,** 2497–505 (2014).
3. Heckman, P. R. A., Wouters, C. & Prickaerts, J. Phosphodiesterase inhibitors as a target for cognition enhancement in aging and Alzheimer's disease: a translational overview. *Curr. Pharm. Des.* **21,** 317–31 (2015).
4. Teich, A. F. *et al.* PDE5 Exists in Human Neurons and is a Viable Therapeutic Target for Neurologic Disease. *J. Alzheimers. Dis.* **52,** 295–302 (2016).
5. Bollen, E. & Prickaerts, J. Phosphodiesterases in neurodegenerative disorders. *IUBMB Life* **64,** 965–70 (2012).
6. Kelly, M. P. Cyclic nucleotide signaling changes associated with normal aging and age-related diseases of the brain. *Cellular Signalling* **42,** 281–291 (2018).
7. Gong, B. *et al.* Persistent improvement in synaptic and cognitive functions in an Alzheimer mouse model after rolipram treatment. *J. Clin. Invest.* **114,** 1624–34 (2004).
8. Palmeri, A., Privitera, L., Giunta, S., Loreto, C. & Puzzo, D. Inhibition of phosphodiesterase-5 rescues age-related impairment of synaptic plasticity and memory. *Behav. Brain Res.* **240,** 11–20 (2013).
9. Puzzo, D. *et al.* Phosphodiesterase 5 inhibition improves synaptic function, memory, and amyloid-beta load in an Alzheimer's disease mouse model. *J. Neurosci.* **29,** 8075–86 (2009).
10. Zhang, J. *et al.* Phosphodiesterase-5 inhibitor sildenafil prevents neuroinflammation, lowers beta-amyloid levels and improves cognitive performance in APP/PS1 transgenic mice. *Behav. Brain Res.* **250,** 230–7 (2013).
11. Prickaerts, J., Heckman, P. R. A. & Blokland, A. Investigational phosphodiesterase inhibitors in phase I and phase II clinical trials for Alzheimer's disease. *Expert Opin. Investig. Drugs* **26,** 1033–1048 (2017).
12. Prickaerts, J. *et al.* Physiological and pathological processes of synaptic plasticity and memory in drug discovery: Do not forget the dose-response curve. *Eur. J. Pharmacol.* **817,** 59–70 (2017).
13. Zhang, R. *et al.* Novel object recognition as a facile behavior test for evaluating drug effects in AβPP/PS1 Alzheimer's disease mouse model. *J. Alzheimers. Dis.* **31,** 801–12 (2012).
14. Bollen, E. *et al.* Object memory enhancement by combining sub-efficacious doses of specific phosphodiesterase inhibitors. *Neuropharmacology* **95,** 361–366 (2015).
15. Puzzo, D. *et al.* Phosphodiesterase 5 inhibition improves synaptic function, memory, and amyloid-b load in an Alzheimer's disease mouse model. *J. Neurosci* **29,** 8075–8086
16. Puzzo, D. *et al.* Effect of phosphodiesterase-5 inhibition on apoptosis and beta amyloid load in aged mice. *Neurobiol. Aging* **35,** 520–31 (2014).
17. Puzzo, D., Lee, L., Palmeri, A., Calabrese, G. & Arancio, O. Behavioral assays with mouse models of Alzheimer's disease: practical considerations and guidelines. *Biochem. Pharmacol.* **88,** 450–67 (2014).
18. Puzzo, D., Gulisano, W., Palmeri, A. & Arancio, O. Rodent models for Alzheimer's disease drug discovery. *Expert Opin. Drug Discov.* **10,** 703–11 (2015).
19. Vogel-Ciernia, A. & Wood, M. A. Examining object location and object recognition memory in mice. *Curr. Protoc. Neurosci.* **69,** 8.31.1-17 (2014).
20. Ashour, A. E., Rahman, A. F. M. M. & Kassem, M. G. Vardenafil dihydrochloride. *Profiles Drug Subst. Excip. Relat. Methodol.* **39,** 515–44 (2014).
21. Robichaud, A. *et al.* Assessing the emetic potential of PDE4 inhibitors in rats. *Br. J. Pharmacol.* **135,** 113–8 (2002).
22. Rabe, K. F. Update on roflumilast, a phosphodiesterase 4 inhibitor for the treatment of chronic obstructive pulmonary disease. *British Journal of Pharmacology* **163,** 53–67 (2011).
23. Vanmierlo, T. *et al.* The PDE4 inhibitor roflumilast improves memory in rodents at non-emetic doses. *Behav. Brain Res.* **303,** 26–33 (2016).

24. Van Duinen, M. A. *et al.* Acute administration of roflumilast enhances immediate recall of verbal word memory in healthy young adults. *Neuropharmacology* **131,** 31–38 (2017).
25. Jabaris, S. G. S. L. *et al.* Effects of rolipram and roflumilast, phosphodiesterase-4 inhibitors, on hypertension-induced defects in memory function in rats. *Eur. J. Pharmacol.* **746,** 138–47 (2015).
26. Reneerkens, O. A. H. *et al.* Phosphodiesterase type 5 (PDE5) inhibition improves object recognition memory: indications for central and peripheral mechanisms. *Neurobiol. Learn. Mem.* **97,** 370–9 (2012).
27. Rutten, K. *et al.* Phosphodiesterase inhibitors enhance object memory independent of cerebral blood flow and glucose utilization in rats. *Neuropsychopharmacology* **34,** 1914–25 (2009).
28. Lakics, V., Karran, E. H. & Boess, F. G. Quantitative comparison of phosphodiesterase mRNA distribution in human brain and peripheral tissues. *Neuropharmacology* **59,** 367–74 (2010).
29. Pérez-Torres, S. *et al.* Phosphodiesterase type 4 isozymes expression in human brain examined by in situ hybridization histochemistry and[3H]rolipram binding autoradiography. Comparison with monkey and rat brain. *J. Chem. Neuroanat.* **20,** 349–74 (2000).
30. Loughney, K. *et al.* Isolation and characterization of cDNAs encoding PDE5A, a human cGMP-binding, cGMP-specific 3',5'-cyclic nucleotide phosphodiesterase. *Gene* **216,** 139–47 (1998).
31. Grass, H. *et al.* Sildenafil (Viagra): is there an influence on psychological performance? *Int. Urol. Nephrol.* **32,** 409–12 (2001).
32. Shim, Y. S. *et al.* Effects of repeated dosing with Udenafil (Zydena) on cognition, somatization and erection in patients with erectile dysfunction: a pilot study. *Int. J. Impot. Res* **23,** 109–114 (2011).
33. McCullough, L. D. *et al.* NIH initiative to balance sex of animals in preclinical studies: generative questions to guide policy, implementation, and metrics. *Biol. Sex Differ.* **5,** 15 (2014).
34. Caraci, F. *et al.* A key role for TGF-β1 in hippocampal synaptic plasticity and memory. *Sci. Rep.* **5,** 11252 (2015).
35. Puzzo, D. *et al.* F3/Contactin promotes hippocampal neurogenesis, synaptic plasticity, and memory in adult mice. *Hippocampus* **23,** 1367–82 (2013).

Chapter 4: Extracellular tau oligomers produce an immediate impairment of LTP and memory

Fá M[1], Puzzo D[1,2], Piacentini R[3], Staniszewski A[1], Zhang H[1], Baltrons MA[1,4], Li Puma DD[3], Chatterjee I[1,5], Li J[1,6], Saeed F[1], Berman HL[1], Ripoli C[3], Gulisano W[2], Gonzalez J[7], Tian H[8], Costa JA[1], Lopez P[5], Davidowitz E[5], Yu WH[1], Haroutunian V[9], Brown LM[10], Palmeri A[2], Sigurdsson EM[11], Duff KE[1], Teich AF[1], Honig LS[1], Sierks M[7], Moe JG[5], D'Adamio L[12], Grassi C[3,13], Kanaan NM[14], Fraser PE[15], Arancio O[1].

[1]Department of Pathology and Cell Biology and Taub Institute for Research on Alzheimer's Disease and the Aging Brain, Columbia University, 630 W 168th St. New York, NY 10032 USA. [2]Department of Biomedical and Biotechnological Sciences, Section of Physiology, University of Catania, Catania, 95125 Italy. [3]Institute of Human Physiology, Università Cattolica del Sacro Cuore, Rome, 00168 Italy. [4]Department of Biochemistry and Molecular Biology, Institute of Biotechnology and Biomedicine, Universitat Autònoma de Barcelona, Bellaterra, 08193, Spain. [5]Oligomerix, Inc., Oligomerix, Inc., 7 Legion Drive, Suite 101, Valhalla, NY 10595, USA. [6]Department of Neurology, Third Military Medical University, Chongqing, 400042, China. [7]Translational Technology Core Laboratory, Rockefeller University, New York, NY 10065, USA. [8]Department of Chemical Engineering, ASU, Tempe, AZ 85281, USA. [9]Department of Psychiatry, The Mount Sinai School of Medicine, JJ-Peters VA Medical Center, Bronx, NY 10468, USA. [10]Department of Biological Sciences, Columbia University, New York, NY 10027, USA. [11]Department of Neuroscience and Physiology, NYU Langone Medical Center, New York, NY 10016, USA.[12]Department of Microbiology and Immunology, Einstein College of Medicine, Bronx, NY 10461, USA. [13]San Raffaele Pisana Scientific Institute for Research, Hospitalization and Health Care, Rome, 00163, Italy. [14]Department of Translational Science and Molecular Medicine, College of Human Medicine, MSU, Grand Rapids, MI, 49503, USA. [15]Tanz Centre for Research in Neurodegenerative Diseases and Department of Medical Biophysics, University of Toronto, 60 Leonard Avenue, Toronto, Ontario M5T 2S8 Toronto, Canada.

In: Sci Rep. 2016 Jan 20;6:19393.

doi: 10.1038/srep19393.

Abstract

Non-fibrillar soluble oligomeric forms of amyloid-β peptide (oAβ) and tau proteins are likely to play a major role in Alzheimer's disease (AD). The prevailing hypothesis on the disease etiopathogenesis is that oAβ initiates tau pathology that slowly spreads throughout the medial temporal cortex and neocortices independently of Aβ, eventually leading to memory loss. Here we show that a brief exposure to extracellular recombinant human tau oligomers (oTau), but not monomers, produces an impairment of long-term potentiation (LTP) and memory, independent of the presence of high oAβ levels. The impairment is immediate as it raises as soon as 20 min after exposure to the oligomers. These effects are reproduced either by oTau extracted from AD human specimens, or naturally produced in mice overexpressing human tau. Finally, we found that oTau could also act in combination with oAβ to produce these effects, as sub-toxic doses of the two peptides combined lead to LTP and memory impairment. These findings provide a novel view of the effects of tau and Aβ on memory loss, offering new therapeutic opportunities in the therapy of AD and other neurodegenerative diseases associated with Aβ and tau pathology.

Introduction

Amyloid-β (Aβ) was the focus of most of the studies on Alzheimer's disease (AD) in the last 20 years. However, Aβ is not the only pathological agent involved in AD. Microtubule Associated Protein Tau (MAPT) is also likely to play a major role in the disease. While Aβ species derive from APP processing, six tau isoforms are derived from alternative splicing of the MAPT gene transcript in the adult brain (Fig. S1A). Aβ forms extracellular amyloid plaques, whereas tau forms intracellular insoluble filaments and neurofibrillary tangles (NFTs). In addition, both Aβ and tau form intracellular and extracellular oligomeric species that are soluble pre-fibrillar aggregates[1–4] suggesting that the two proteins might share common mechanisms in AD etiopathogenesis.

The prevailing hypothesis in the AD field is that deleterious effects on synaptic function underlying memory loss caused by tau are initiated by Aβ [for a review see[5]]. As AD progresses, tau pathology spreads from the entorhinal cortex in a contiguous, highly selective and highly reproducible fashion, suggesting that extracellular soluble forms of tau transmit pathology from neuron to neighboring neuron [for a review see[6]]. Moreover, once Aβ triggers tau pathology, the disease would progress independent of Aβ[5]. Therefore, therapies targeting Aβ may not be effective once tau pathology is triggered. Nevertheless, tau toxicity does not involve Aβ pathology in tauopathies, suggesting that Aβ is not necessary for tau pathology to occur, and pointing at the need to better clarify the relationship between tau and Aβ.

Here, we investigated whether and how extracellular oligomeric forms of tau (oTau) affect memory and its cellular correlate, long-term potentiation (LTP), either by themselves or in combination with Aβ. Studies with recombinant forms of human tau showed oligomer specific inhibition of LTP and memory formation and were validated using tau derived from AD brains and mice expressing non-mutated forms of human tau (hTau). Collectively, the data demonstrate that a brief exposure to oTau and oAβ either alone or in combination produce an immediate impairment of LTP and memory.

Results

Tau is present in the extracellular space where it is released upon neuronal activity

Memory loss in AD is likely caused by the impairment of processes responsible for synaptic plasticity that are dependent upon neural activity. Given that tau is a major pathological component of AD, we studied the relationship between neuronal activity and tau. We assessed the release of tau into the extracellular medium of 12 day in vitro cultured mouse hippocampal neurons exposed for 15 min to vehicle or pharmacological agents that either increase (potassium chloride, KCl, or picrotoxin, PTx) or decrease (tetrodotoxin, TTx) neuronal activity. The treatment with KCl, which stimulates vesicular release, and PTx, which enhances neuronal activity by inhibiting GABA receptors, increased extracellular tau levels (Fig. 1A). By contrast, TTx, which reduces neuronal activity by blocking sodium channels, reduced extracellular tau level (Fig. 1A), suggesting a basal tonic release of tau in the extracellular space. These results confirm that the level of tau released from neurons increases with neuronal activity[7,8].

Soluble oligomeric forms of recombinant tau impair long-term potentiation (LTP)

The demonstration of activity-dependent tau secretion provided a rationale for investigating the effects of extracellular tau onto hippocampal LTP, an activity-dependent type of synaptic plasticity thought to underlie memory. Following production of purified recombinant tau 4R/2N (the longest adult human CNS isoform of tau, 441 amino acids), the preparation was oligomerized and assessed for oligomerization through non-reducing SDS-PAGE gel, and atomic force microscopy (AFM) (Fig. 1B,C). Additionally, we obtained preparations of oligomeric 4R/1N, oligomer-prone 4R C-terminal, 1N N-terminal tau which did not oligomerize, and monomeric 4R/1N (Fig. 1B).

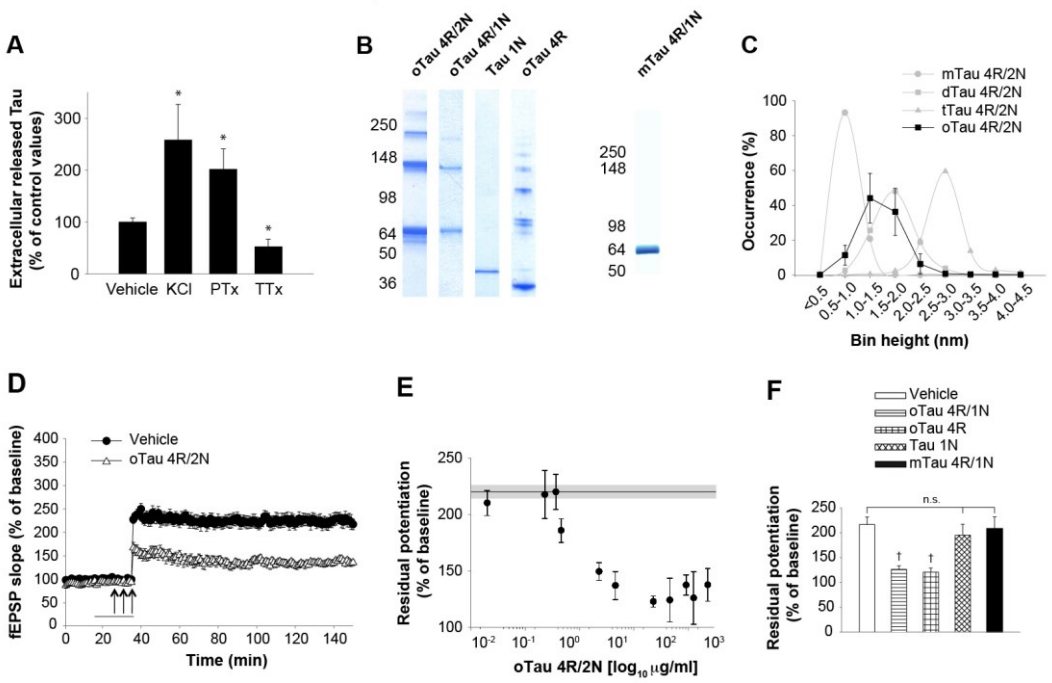

Figure 1: Extracellularly Applied oTau Impairs Hippocampal LTP. (A) Soluble tau is released onto the extracellular space upon activity. Neuronal activation by 50 mM KCl or 100 µM PTx increased extracellular tau in primary hippocampal cultures (Mann Whitney: *$p < 0.05$, $n = 7$ and $n = 4$, respectively), while neuronal inactivation by 1 µM TTx reduced it (Mann-Whitney *$p < 0.05$, $n = 10$) compared to vehicle ($n = 19$). All data shown are mean ± SEM. (B) Coomassie blue non-reducing SDS-PAGE gel of recombinant oTau 4R/2N, oTau 4R/1N, N-terminal tau (Tau 1N), C-terminal tau (oTau 4R), and monomeric Tau 4R/1N (mTau 4R/1N). (C) AFM histogram of recombinant oTau 4R/2N ($n = 4$). Purified monomeric (mTau), dimeric (dTau), and trimeric (tTau) tau 4R/2N are reported in the figure for comparison. (D) Perfusion with 2.29 µg/ml oTau 4R/2N reduced CA3-CA1 LTP ($n = 16$ slices, ANOVA $p < 0.0001$ vs. 18 vehicle treated slices). (E) Concentration-response curve for the effect of oTau 4R/2N on LTP ($n = 6$ to 10 slices per concentration). The shaded area corresponds to the average potentiation (continuous line) and the standard error range in vehicle-treated slices in this and the following figures. The residual potentiation was calculated by averaging the last 5 min of LTP at 120 min after the tetanus in this and the following graphs. (F) LTP was impaired by 4.29 µg/ml oTau 4R/1N, or equimolar concentrations of C-terminal tau 4R, but not N-terminal tau or mTau 4R/1N ($n = 6$ to 10 slices per construct; ANOVA $p < 0.005$, †$p < 0.005$ vs. vehicle). All data shown are mean ± SEM. See also Supplementary Figure S1.

We administered these preparations to mouse hippocampal slices and tested their effect on CA3-CA1 hippocampal LTP. A brief perfusion with oTau 4R/2N for 20 min prior to the theta-burst markedly reduced LTP (Fig. 1D) with an IC50 of 0.19 µg/ml (Fig.

1E) without affecting basal synaptic transmission (BST). We obtained similar results with the 4R/1N isoform, as well as the oligomerized C-terminal construct 4R (Fig. 1F). By contrast, monomeric N-terminal construct and monomeric tau 4R/1N did not reduce LTP (Fig. 1F). Together these experiments not only demonstrate that extracellular tau per se (without oAβ intervention) can impair synaptic plasticity, but also highlight a direct role for tau oligomerization in LTP impairment. Most importantly, the occurrence of LTP impairment after a brief tau exposure demonstrates that extracellular oTau has a rapid effect on neural activity that may impair plasticity.

oTau impairs memory formation

To extrapolate these electrophysiological findings to memory, we evaluated the effect of extracellular tau onto associative fear memory and spatial memory, two types of memory that are affected in AD patients. In these experiments, oTau 4R/2N (two injections at 180 and 20 min prior to the training) was infused via bilateral cannulas into the dorsal mouse hippocampi (Fig. 2A). This resulted in reduced freezing 24 hrs after the electric shock (IC50 = 11.06 μg/ml; Fig. 2B,C). The defect was due to hippocampal impairment as cued fear learning, a type of learning that depends upon amygdala function[9], was not affected (Fig. S2A). Moreover, the defect was not due to deficits in sensation, as sensory threshold assessment did not reveal any difference between vehicle-infused mice and mice infused with 4R/2N preparation (Fig. S2B). Finally, the defect was due to the presence of oligomers as tau 4R/1N and C-terminal tau 4R constructs which can oligomerize (Fig. 1B) reduced freezing 24 hrs after training, while monomeric N-terminal tau 1N or monomeric tau 4R/1N treatment did not affect freezing (Fig. 2D). This finding is consistent with the observation that accumulation of non-fibrillar soluble tau oligomeric species is associated with memory impairment[10,11].

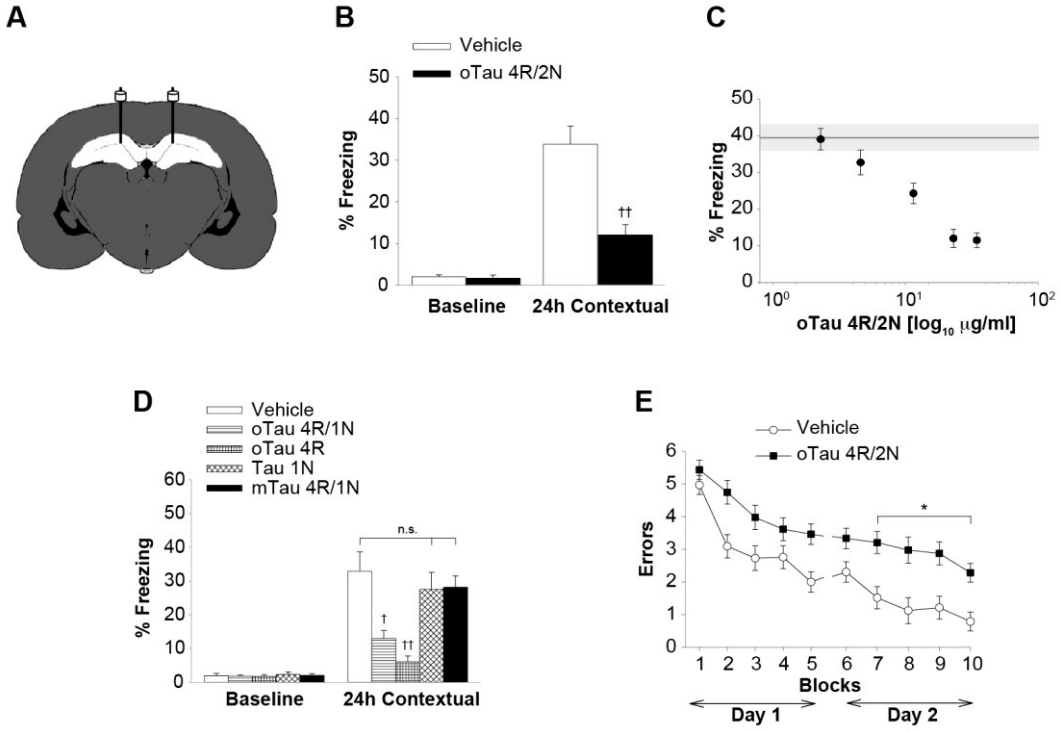

Figure 2 oTau Impairs Memory Formation (A) Schematic drawing of cannulas implanted into mouse dorsal hippocampi. Preparations were diluted in a final volume of 1 µl and administered over 1 min bilaterally, 180 and 20 min prior to the training. (B) oTau 4R/2N (22.95 µg/ml) impaired contextual memory. Freezing during the training phase (baseline) was not affected by the treatment. Vehicle: n = 18, oTau: n = 11, (24 hrs: ††$p < 0.001$). (C) Concentration-response curve for the effect of oTau 4R/2N on contextual memory (n = 10 to 18 mice per concentration). The shaded area corresponds to the average freezing (continuous line) and the standard error range in vehicle-infused mice. (D) 21.30 µg/ml oTau 4R/1N, or equimolar concentration of C-terminal tau 4R, but not N-terminal tau 1N or mTau 4R/1N, impaired contextual memory. Vehicle: n = 12, oTau 4R/1N: n = 10, Tau 4R: n = 11, Tau 1N: n = 10, mTau 4R/1N: n = 11, (24 hrs: ANOVA $p < 0.0001$, ††$p < 0.001$ for Tau 4R vs. vehicle, †$p < 0.005$ for oTau 4R/1N vs. vehicle). (E) oTau 4R/2N (22.95 µg/ml) impaired RAWM performance. 4R/2N: n = 13, vehicle: n = 11. ANOVA $p < 0.0001$; *$p < 0.05$ between groups. All data shown are mean ± SEM. See also Supplementary Figure S2.

Short-term spatial memory was tested with the 2-day radial arm water maze (RAWM). Mice infused with oTau 4R/2N (22.95 µg/ml) made a higher number of errors than vehicle-infused mice during the second day of RAWM testing (Fig. 2E). Control trials with a visible platform did not show any difference in speed or latency to reach the platform between the two groups, indicating that oTau infusion did not affect the motility, vision and motivation of mice during RAWM testing (Fig. S2C,D). Moreover,

open field testing did not reveal any difference between the two groups indicating that the oTau infusion did not alter mouse exploratory behavior, which might affect animal performance in the memory task (Fig. S2E,F). Collectively, these experiments indicate that a brief exposure to extracellular oTau produces immediate memory impairment.

The impairment of LTP and memory by recombinant oTau is reproduced by administration of a preparation enriched in soluble tau derived from human AD brain

As a first approach to establish whether the deleterious effects of recombinant oTau on LTP and memory occur with authentic AD tau species, we obtained preparations enriched in soluble tau from human AD brain specimens (AD-Tau) and control specimens from age-matched individuals (HC). The preparations were characterized prior to performing experiments. First, we confirmed the presence of tau using non-reducing SDS-PAGE and WB with a total tau antibody (Ab) (Fig. 3A,B, Subjects in Table S1). Second, we demonstrated that tau phosphorylation was preserved as shown by immunoblot at T217 and T231 (Fig. 3B), and Mascot database search of LC/MS/MS tandem mass spectrometry data indicating phosphorylation at T181 and S404 both in AD- and HC-Tau (Fig. S3, Table S2). Interestingly, proteomic analysis did not show the presence of amyloidogenic proteins, such as Aβ, synucleins, amylin. Third, we demonstrated the presence of oligomers through T22, a tau oligomer specific polyclonal Ab[12] (Fig. 3C), and the mouse monoclonal Ab specific for oTau TOC1[13] as the "capture" Ab in a sandwich ELISA (detection with R1, a rabbit polyclonal pan-tau Ab). TOC1 exhibited reactivity to AD- but not to HC-Tau (Fig. 3D, Table S1). The specificity of this result for tau oligomers was demonstrated by the control ELISA using capture Ab Tau5, a pan-tau antibody for total tau (detection with R1) that showed similar levels of tau in both sets of samples (Fig. 3E, Table S1). Similarly, strong reactivity to AD- but not to HC-Tau, was found with dot blots using TOC1 (Fig. 3F, Table S1) and T22 Ab (data not shown). Finally, when we examined the size of the structures present in our preparations through AFM, we found particles mostly with a

1.5–5 nm diameter, likely corresponding to oligomers, with very few particles <1.5 nm, likely corresponding to monomers, in AD-Tau, (Fig. 3G, Table S1), whereas HC-tau showed a high percentage of ~1 nm diameter structures, and a lower number of particles >1.5 nm (Fig. 3G, Table S1). Interestingly, AFM of both AD- and HC-Tau did not reveal particles >5 nm that might have suggested the presence of large tau aggregates. Collectively, these data confirm the presence of oligomeric tau in our AD-brain derived preparation.

To test the effects of AD-Tau on LTP we performed a concentration/response curve following 20 min perfusion with AD-Tau. Consistent with the observation that tau interstitial fluid (ISF) levels in healthy individuals have been shown to be 7–15 × 10−3 μg/ml[14], we found an IC50 = 0.02 μg/ml (Fig. 4A). By contrast, 0.23 μg/ml HC-Tau did not affect LTP (Fig. 4B). Moreover, if the AD-Tau preparation was incubated with dithiothreitol (DTT), to induce monomerization (mAD-Tau, 0.23 μg/ml), LTP was no longer affected (Fig. 4B). Taken together, these experiments suggest that extracellular oligomeric soluble tau from AD patients impairs LTP.

Similarly to oTau, AD-Tau reduced contextual memory (IC50 = 0.20 μg/ml; Fig. 4C), whereas HC-Tau (4.59 μg/ml) or mAD tau (both at 4.59 μg/ml and 22.95 μg/ml) did not (Fig. 4D). Neither amygdala-dependent cued learning nor sensory threshold were affected by AD-Tau, HC-Tau or mAD-Tau (Fig. S4A,B). Most importantly, the marked reduction of contextual learning was confirmed with preparations from 7 AD patients and 8 HC individuals, indicating a high degree of reproducibility across individuals (4.59 μg/ml; Fig. 4E). The similarity between recombinant tau and AD-Tau also held true in short-term spatial memory tasks. Mice that were infused with AD-Tau (4.59 μg/ml) made more errors than vehicle-infused mice during the second day of testing with the RAWM (Fig. 4F). The effect was caused by cognitive impairment because the same animals did not show behavioral differences in control experiments with the visible platform and open field tests that might have interfered with their cognitive assessment (Fig. S4C,F). The results using human tau are consistent with

behavioral findings with recombinant tau suggesting that the oligomeric structure is important for memory impairment.

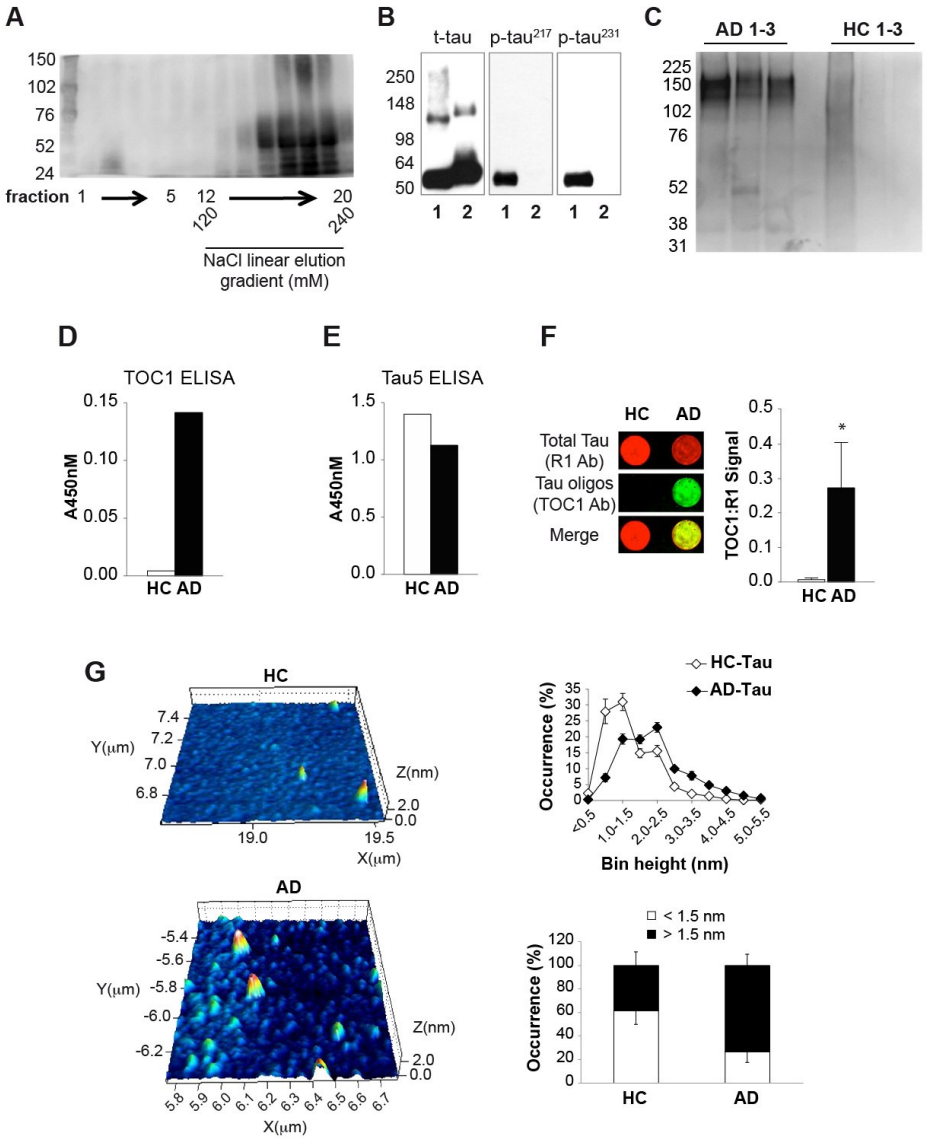

Figure 3: Characterization of Soluble Tau in Human AD Specimens. (A) A representative example of non-reducing SDS-PAGE analysis of human tau from AD brain tissue homogenized in a non-reducing buffer. Numbers at the bottom correspond to fraction samples obtained during chromatography. Specimen 15 (Table S1). (B) WB of AD-Tau (Lanes 1) vs. total tau (t-tau) by phospho-independent monoclonal Ab HT7, as well as tau phospho-epitope-specific Ab against threonine at amino acid positions 217 (p-tau217) and 231 (p-tau231). Lanes 2 display analysis from a control recombinant oTau 4R/2N, used as negative control for phospho-epitope specific tau Ab. Specimen 2 (Table S1). (C) Non-reducing WB probed with T22 Ab shows bands between 102 and 225 kDa in AD (but not HC) specimens confirming the presence of oligomers in our preparation (AD: 7, 9, 21; HC: 12, 16, 17; Table S1). (D–

E) Level of tau oligomers in representative HC and AD samples using sandwich ELISAs. Oligomer specific TOC1 Ab shows strong signal in AD, but not in an HC samples (D). Tau5 Ab measuring level of total tau shows substantial amounts of total tau protein both in HC and AD samples (E) (AD: 9; HC: 17; Table S1). (F) Representative TOC1 (green) & R1 (red, total tau) dual color dot blot of HC and AD samples. Results of TOC1 signal normalized to R1 signal, quantified in the graph, indicate significantly more oTau in AD samples compared to HCs ($p < 0.05$; AD; 7, 9, 21, 22; HC: 12, 13, 16, 17, 23; Table S1). (G) AFM suggests the presence of more oligomers in the AD-Tau preparation than in the HC one (bin height 0,5–1.0: $p = 0.04$; 1.0–1.5: $p = 0.06$; 2,0–2.5: $p = 0.08$; 2,5–3.0: $p = 0.008$). Representative tridimensional images for the two preparations are shown in the color panels. Occurrence of particles is displayed both by 0.5 nm bins (upper graph) and by separating <1.5 nm and >1.5 nm particles (lower graph). Note the absence of particles >5 nm in both preparations (AD: 6, 7, 9, 11, 18, 21, 22; HC: 8, 12-14, 16, 17, 19, 23; Table S1).

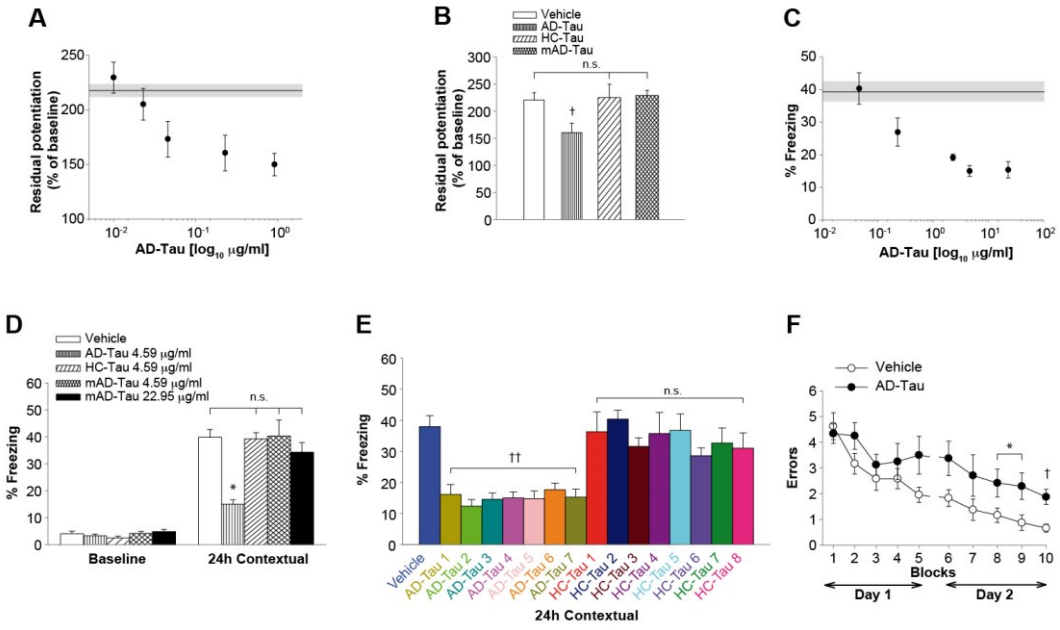

Figure 4: LTP and Memory Impairment by Recombinant oTau is Reproduced by a Preparation Enriched in Soluble Human Tau from AD Patients. (A) Concentration-response curve for the effect of AD-Tau on LTP (n = 7-34 slices per concentration). Specimen 15 (Table S1). (B) AD-Tau (0.23 µg/ml; n = 13), but not HC-Tau or monomeric AD-Tau (mAD-Tau, n = 8 for both) reduced LTP (vehicle n = 38; ANOVA $p < 0.0001$ †$p < 0.005$ vs. all other groups; AD: 15; HC: 13; Table S1). (C) Concentration-response curve for the effect of AD-Tau on contextual memory (n = 9 to 13 mice per concentration; specimens 2, 6, 11, Table S1). (D) AD-Tau (4.59 µg/ml, n = 9), but not mAD-Tau (both at 4.59 and 22.95 µg/ml; n = 11 and 9, respectively) or HC-Tau (4.59 µg/ml; n = 12), impaired contextual memory. Vehicle (n = 13) ANOVA $p < 0.0001$, *$p < 0.05$ vs. other groups (AD: 2, 6, 11; HC: 4, 17, 20; Table S1). (E) AD-Tau (4.59 µg/ml) impaired contextual memory [n = 9 for all the specimens except for AD7 (13), AD6 and HC7 (10) and vehicle (20); ANOVA $p < 0.0001$ ††$p < 0.001$ in AD-Tau groups compared to all other groups. AD: 2, 6, 10, 11, 15, 18, 24, 25; HC: 1, 3–5, 8, 14, 20, 25; Table S1). |(F)

AD-Tau (4.59 µg/ml) impaired RAWM performance. n = 8 per group, ANOVA $p < 0.05$, †$p < 0.005$, *$p < 0.05$ (Specimens 9, 18; Table S1). See also Supplementary Figure S4.

The impairment of LTP and memory by recombinant oTau is reproduced with 10–11 month old hTau mice, which form oligomers in the absence of NFTs

As an additional control method alternative to the use of soluble tau derived from human AD brain to further validate findings with recombinant oTau, we repeated the electrophysiological and behavioral studies in hTau mice naturally forming oTau from 6 months of age prior to NFT appearance and their control littermates lacking tau[15]. Neurons of 10–11 month old hTau mice showed hyper-phosphorylated tau by immunohistochemistry, but no NFTs were seen on Bielschowsky staining (Fig. S5A). However, aged (18 month) hTau mice had hyper-phosphorylated tau and NFTs (Fig. S5A), consistent with the interpretation that 10–11 month-old hTau mice were in a pre-tangle state. Interestingly, LTP and both contextual and spatial memory were impaired compared to control animals at 10–11 months (Fig. 5A–C). Furthermore, the two groups of animals did not show any difference in BST (Fig. S5B), cued conditioning, sensory threshold, visible platform and open field performance (Fig. S5C–H). Most importantly, a preparation enriched in soluble human tau obtained from the hTau mouse cortex (hTau-p), but not from tau-lacking control mice (C-p) (Fig. S5I), reduced LTP, contextual and spatial memory (Fig. 5D–F) without affecting cued conditioning, sensory threshold, visible platform and open field performance. Collectively, these experiments with endogenously produced oTau from a transgenic mouse model of AD confirm impairment of LTP and memory by exogenous recombinant human tau and human tau derived from AD brains.

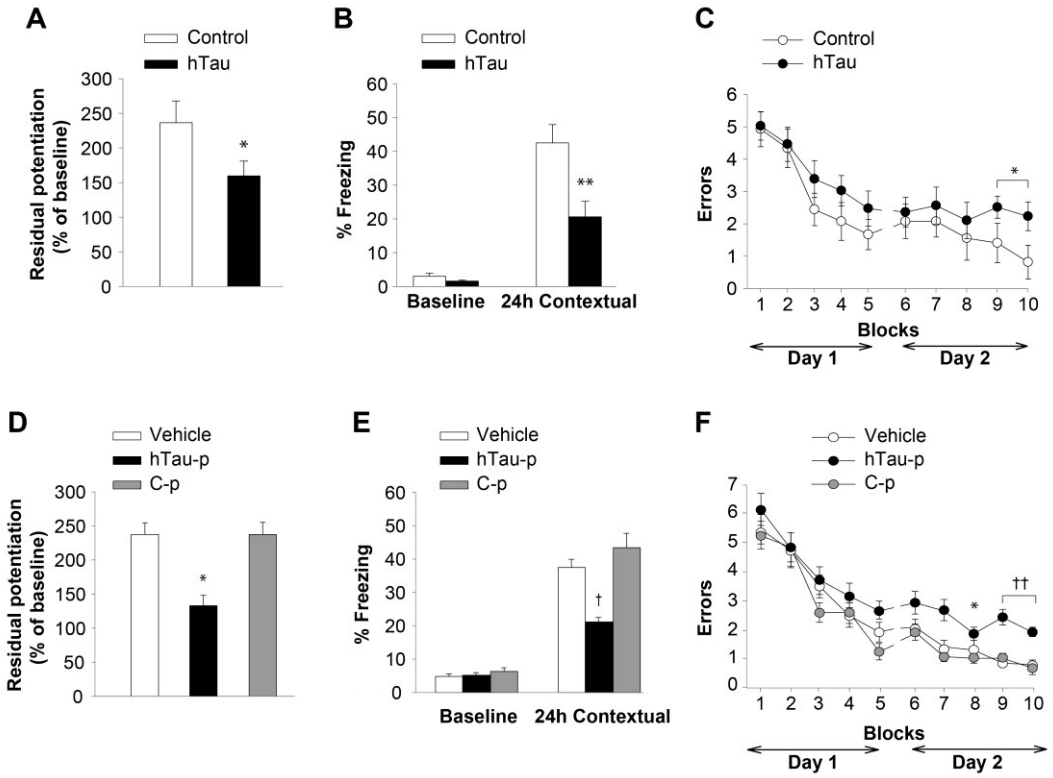

Figure 5: LTP and Memory Impairment by Recombinant oTau is Reproduced by Naturally Produced Human Tau from hTau Mice. (A) hTau mice have reduced LTP (hTau: 7 slices/6 mice; Controls: 9/7; ANOVA * $p < 0.05$). (B–C) hTau mice have reduced contextual memory (B) and RAWM performance (C) (hTau: $n = 9$, Control: $n = 13$, fear memory: **$p < 0.01$, RAWM: ANOVA $p = 0.09$ *$p < 0.05$). (D) Administration of hTau-p (0.46 µg/ml) reduced LTP, whereas C-p from control mice lacking tau did not (hTau-p: $n = 10$, C-p: $n = 11$; vehicle: $n = 10$ ANOVA *$p < 0.05$). (E–F) hTau-p (4.59 µg/ml) reduced contextual memory (E) and RAWM performance (F) whereas C-p did not (hTau-p: $n = 10$; C-p: $n = 11$, vehicle = 10 fear memory: ANOVA $p < 0.001$, †$p < 0.005$ vs. C-p, RAWM: ANOVA $p < 0.0001$ *$p < 0.05$ and ††$p < 0.001$ vs. C-p). All data shown are mean ± SEM. See also Supplementary Figure S5.

oTau acts concurrently with oAβ to impair LTP and memory

Both tau and Aβ are β-sheet forming proteins with propensity for oligomerization and close association with membranes suggesting a common toxicity mechanism[16]. Thus, we decided to determine if the combination of tau and Aβ oligomers - at subthreshold doses that give no significant impairment for LTP and memory for each alone according to their respective dose/response curves - impairs LTP and memory. Slices perfused for 20 min with subthreshold doses of oTau 4R/2N (0.05 µg/ml) plus oAβ42

(0.23 µg/ml) prior to inducing LTP revealed a marked reduction of potentiation compared to vehicle treated slices or slices treated with the same low doses of tau or Aβ alone (Fig. 6A). In interleaved experiments high amounts of oTau 4R/2N (2.29 µg/ml) or oAβ (0.90 µg/ml) alone were capable of affecting LTP (Fig. 6A). Similarly, the combination of 4.59 µg/ml oTau 4R/2N plus 0.34 µg/ml oAβ prior to electric shock for fear conditioning or training for RAWM affected the two forms of memory (Fig. 6B,C). The same low doses of oTau and oAβ alone did not affect memory, whereas high concentrations of oTau 4R/2N (22.95 µg/ml) or oAβ (0.90 µg/ml) alone reduced memory. Moreover, we did not observe any behavioral differences between groups of mice with cued conditioning, sensory threshold, visible platform and open field (Fig. S6A–F). Collectively, these experiments demonstrate that tau and Aβ oligomers can act concurrently.

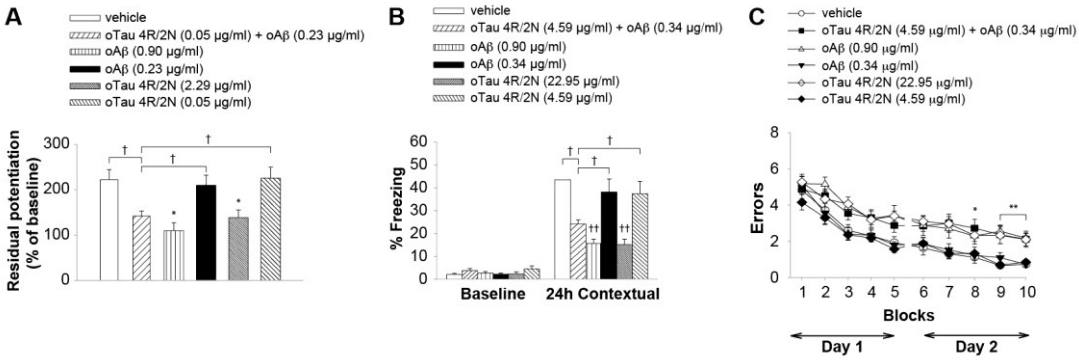

Figure 6: oTau can Act Concurrently with oAβ to Impair LTP and Memory. (A) Subthreshold doses of oTau 4R/2N (0.05 µg/ml) plus oAβ (0.23 µg/ml) reduced LTP (n = 11), whereas the same concentrations of the two oligomers alone did not. Vehicle n = 9, oTau (0.05 µg/ml), oAβ (0.23 µg/ml), and oTau (2.29 µg/ml) alone n = 8, oAβ (0.90 µg/ml) n = 7. ANOVA $p < 0.0001$; †$p < 0.005$, *$p < 0.05$ vs. vehicle. (B) Subthreshold doses of oTau 4R/2N (4.59 µg/ml) plus oAβ (0.34 µg/ml) impaired contextual memory (n = 13), whereas the same concentrations of the two oligomers alone did not. Vehicle n = 10, oTau (22.95 µg/ml) n = 13, oTau (4.59 µg/ml) n = 10, oAβ (0.90 µg/ml) n = 11, oAβ (0.34 µg/ml) n = 11 (24 hrs: ANOVA $p < 0.0001$; †$p < 0.005$, ††$p < 0.001$ vs. vehicle). (C) Subthreshold doses of oTau 4R/2N (4.59 µg/ml) plus oAβ (0.34 µg/ml) (n = 11), but not the same concentrations of the two oligomers alone, impaired RAWM performance (oTau n = 11, oAβ n = 10). Vehicle n = 11, oTau (22.95 µg/ml) n = 10, oAβ (0.90 µg/ml) n = 9. ANOVA $p < 0.0001$ *$p < 0.05$ **$p < 0.01$ vs. vehicle, or 4.59 µg/ml oTau 4R/2N, or 0.34 µg/ml oAβ). All data shown are mean ± SEM. See also Supplementary Figure S6.

oTau enters neurons

All our experiments have been performed through exogenous application of tau, yet molecular memory mechanisms affected by the protein are intracellular. Our next goal was therefore to establish a possible avenue between extracellular oTau and intracellular events. Misfolded tau has been shown to be internalized by cells in vitro[17]. For instance, uptake of low molecular weight tau species has been found in cultured neurons through endocytosis[18]. In light of the profound effect that tau exposure has on LTP and memory, we decided to perform optical measurements in mouse hippocampal cultures treated with 5 μg/ml oTau 4R/2N in order to determine whether also our tau 4R/2N preparation can be internalized in neurons. A time-lapse confocal imaging study demonstrated that oTau 4R/2N conjugated to IRIS-5 penetrates the cell membrane of cultured eGFP-expressing neurons after 20 min of exposure (yellow staining) (Fig. 7A, upper panels). By contrast, mTau 4R/2N conjugated to IRIS-5 could not be visualized up to the last time point investigated after 40 min of exposure (Fig. 7B, upper panels). We reached similar conclusions when we used immunocytochemistry on MAP-2 labeled neurons that were exposed to oTau 4R/2N conjugated to IRIS-5 for 3 or 6 hrs prior to fixation. Intracellular tau (yellow) was visible at 3 hrs, and the staining acquired a punctuated pattern at 6 hrs suggesting that tau localizes to vesicular structures[19] (Fig. 7A, lower panels). By contrast, there was no internalized tau after mTau 4R/2N exposure both at 3 and 6 hrs (Fig. 7B, lower panel). These findings demonstrate that oTau crosses cell membrane. By contrast, consistent with the previous study on primary mouse hippocampal cultures18 (but see also another study on SH-SY5Y cells[19]), tau monomers do no penetrate cells within the time frame investigated in the present study. Taken all together these findings support the possibility that oligomeric extracellular tau acts onto molecular mechanisms of learning and memory after penetration inside the cells.

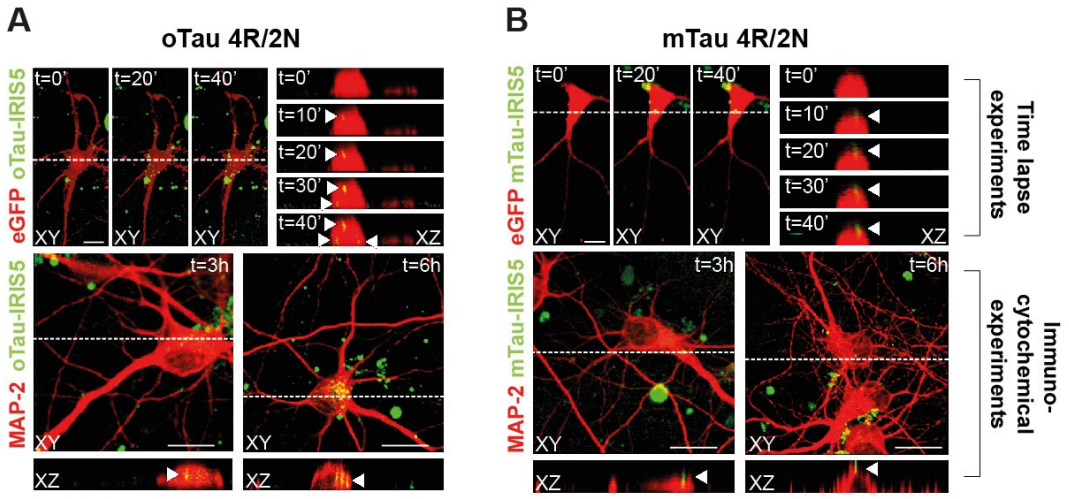

Figure 7: oTau, but not mTau, is internalized in neurons. (A,B) Representative examples of mouse hippocampal neurons exposed to 5 µg/ml oTau 4R/2N (A) or mTau 4R/2N (B). oTau or mTau were labeled at the N-terminus with the fluorescent dye IRIS-5-NHS. Upper panels show data obtained in time-lapse confocal experiments performed on eGFP-expressing neurons at DIV14. Data shown in the lower panels were obtained from immunocytochemical experiments performed after 3–6 hr tau application in neurons immunolabeled for the microtubule associated protein-2 (MAP-2). Colors of eGFP, MAP-2 and IRIS-5 were inverted to optimize image visualization. (A) oTau was clearly internalized (in yellow) within 30-min of application as shown in the XZ cross-sections from the Z-stack acquisitions (panels on the right). After 3 and 6 hrs, oTau internalization, but not mTau (B) was much more intense, as revealed by immunocytochemistry (lower panels, and XZ cross sections on the bottom). Time lapse confocal experiments: n = 10 both for oTau and mTau; Immunocytochemistry: n = 40 per each time point (3 and 6 hrs) and condition (oTau and mTau). Scale bars: 25 µM.

Discussion

The accumulation of protein aggregates in the brain is a common process in neurodegenerative diseases, each disease having its own specific aggregating proteins and distribution. Recently, the focus has shifted from large protein precipitates to small, very soluble aggregates called oligomers, as they appear more acutely toxic than large insoluble aggregates. Our studies establish a novel model through which oTau causes synaptic dysfunction and memory loss. Extracellular tau oligomers, recombinant or extracted from AD brains or naturally produced from hTau mice, effectively and consistently induce key features of AD including synaptic dysfunction and memory loss, whereas tau monomers produce no deleterious effects. These effects have a very

fast onset as they are present within a few minutes from the application of the oligomers. Additionally, they occur with tau alone, or in combination with oAβ as sub-toxic doses of oTau affect LTP and memory when paired with sub-toxic doses of oAβ. We found that recombinant extracellular oTau per se is capable of negatively affecting LTP and memory. This discovery was validated by our examination of soluble AD-Tau as well as experiments with hTau mice expressing non-mutated forms of human tau and forming oligomers prior to NFTs. Importantly, monomerized AD-Tau preparations containing post-translational modifications (PTMs), or purely monomeric tau recombinant forms, either in full length or as 255 amino acid long N-terminal fragment, failed to produce synaptic dysfunction and memory loss. In contrast, the oligomerized C-terminal fragment of recombinant protein impaired LTP and memory. This is consistent with the observation that tau multimer levels correlate with memory loss in the rTg4510 mouse model[10]. The C-terminal portion of tau containing the microtubule binding repeats is prone to aggregate as it has β-sheet forming hexapeptide motifs that self-interact, as well as cysteines that form disulfide linkages to stabilize the interactions. The N-terminal portion of tau used in our experiments does not have regions of tau self-interaction that have been characterized, and does not have a tendency to form aggregates upon incubation. Therefore, it was used as an additional control for non-aggregated tau. However, this does not exclude that other types of N-terminal fragments of a different length than the one used in our studies, either in a monomeric or oligomeric form, might be toxic. Consistent with this possibility, different effects have been reported according to the type of N-terminal fragment utilized. For instance, it has been found in cerebellar granule cells that the short N-fragment 1–44 is particularly toxic, whereas overexpression of longer fragments (1–230) and tau (1–441) blocks apoptosis[20]. Of note, our studies were performed with a 255 amino acid fragment that is consistent with lack of toxicity observed in cerebellar granule cells with tau fragments of similar length[20]. Moreover, an N-terminal motif in tau, called the phosphatase-activating domain (amino acids 2–18), can impair fast anterograde axonal transport when abnormally exposed in pathological forms of tau[21–23]. Together these data suggest that several routes of tau-mediated toxicity may exist

and that different parts of the protein are involved. The current studies suggest that the N-terminus (at least amino acids 1–255) is insufficient to disrupt LTP, but this part of the tau protein may be involved in other toxic mechanisms. Nevertheless, the observation that extracellular tau oligomers are likely to play a key role in synaptotoxicity is important for better understanding the role of tau in disease.

An important aspect of our studies is that the oTau effect on LTP and memory is rapid (i.e. as soon as 20 min after exposure). The implication of this observation is that memory loss in AD patients is likely to be due to a modification of the dynamic and fast processes underlying plasticity and memory formation that are being inhibited by oligomers. This is consistent with the widely accepted notion that synaptic strengthening is central to memory formation, and dementia could result from altered strengthening of synapses. As a consequence, our studies suggest that AD therapeutics acting on tau oligomers should produce beneficial effects on memory at any disease stage, as the most likely scenario for their action is that molecular mechanisms underlying plasticity and memory are continuously deranged by the oligomers as the disease evolves.

Both the C-terminal fragment and full-length oligomerized tau impaired LTP and memory. This begs the question of whether these forms of tau are secreted into the extracellular space, an essential requirement for our observations to be biologically relevant. To this end, secretion of different tau fragments has been investigated on synaptosomes prepared from cryopreserved human postmortem tissue[24]. This study showed that an extended tau form (~55 kDa), the truncated tau fragment (~20 kDa), as well as other N-terminal tau fragments (35–50 kDa) are released following depolarization. Only 15–25% of synaptosomes were immunoreactive for the tau 46 C-terminus antibody; however, the tau 46 antibody fails to recognize several secreted C-terminal tau fragments[25]. Of note, this study also showed a significant increase in C-terminal tau immunoreactivity in AD compared to aged normal synapses[24], suggesting that 4R tau cleavage fragments are efficiently secreted, especially in AD. In summary,

both full-length tau and C-terminal tau appear to be secreted outside cells, and therefore, our findings are biologically relevant.

We have found a marked reduction of LTP following slice perfusion with recombinant tau oligomers. This observation is consistent with the finding of an impaired long-term depression in hippocampal slices taken from an inducible mouse model expressing the tau repeat domain with the pro-aggregant mutation ΔK280[26]. Another study, in turn, showed a reduction of short-term potentiation with no significant effect on LTP by recombinant tau[27]. A possible explanation for the difference between our findings and those of this study that was also performed with recombinant tau[27] is linked to the different method of tau oligomerization. In the previous study[27], tau was oligomerized through seeding with Aβ, whereas our oligomerization method relied upon reduction and oxidation of cysteine residues. Tau oligomerization is typically achieved through different protocols such as addition of heparin, heparan sulfate, polyunsaturated fatty acids, RNA, or quinones[28–32] to drive it. These different protocols, although very efficient in producing tau oligomerization, are likely to result in a variety of species1 which in turn might be responsible for different levels of toxicity or no toxicity at all. Indeed, as reported[33], the kinetics of aggregation differs among protocols and the obtained tau species are not necessarily equivalent both in terms of size and biophysical properties. A standardized method is necessary for the production of tau. Although our current knowledge does not allow us to define the tau species that is/are toxic, our method offers the advantage of producing oligomers that efficiently and quickly affect both synaptic function and memory, two key features of the disease.

We have discovered that sub-toxic doses of oTau affect LTP and memory when paired with sub-toxic doses of oAβ. It is therefore possible that either the two oligomeric proteins act at the same level in the chain of molecular events leading to AD, or that they act on different targets that later converge on a common molecular downstream indirect target. This observation combined with the finding that the two peptides alone lead to LTP and memory impairment, independent of the presence of high concentrations of the other, suggests that it is not necessary to evoke the presence of elevated levels of Aβ to initiate the molecular mechanisms underlying synaptic

dysfunction and memory loss in AD. Consistent with this conclusion, tau toxicity does not involve Aβ pathology in tauopathies. In future experiments we will study whether other β-sheet forming proteins (i.e. synuclein, amylin) act concurrently with tau and/or Aβ to affect LTP and memory. We will also investigate whether the combined action of oTau and oAβ is synergistic or additive, with a mechanism dependent upon interaction between tau and Aβ oligomers prior to their binding with a common receptor, or as a consequence of their binding with the receptor. Nevertheless, the main observation of this manuscript showing that exogenous oTau and oAβ concurrently disrupt synaptic plasticity and memory formation is clear and has important implications for understanding AD pathology.

We have found another interesting parallelism between tau and Aβ. Similar to Aβ[34,35], tau can be secreted from hippocampal neurons in the extracellular space in a fashion that is regulated by neuronal activity via a Na+-channel dependent mechanism. This finding is consistent with the observation that tau is secreted into the extracellular space[25] in an activity-dependent fashion[7,8], and supports the concept that soluble oligomeric tau, whether secreted in oligomeric form per se or oligomerized outside the cells, can be detected in CSF. Furthermore, this finding is in agreement with the hypothesis that release of intracellular tau into the extracellular space promotes seeding in other brain cells[17,36–40]. Interestingly, our data unravel a tonic release of tau in the extracellular space, given that TTx-induced block of voltage-gated Na+-channels dramatically decreases tau secretion. This data is different from a study on ISF tau in which TTx failed to affect tau levels differently than Aβ levels[8]. However, this study used in vivo microdialysis, a technique that relies on protein turnover rate (half-life of ~11 days for tau vs. ~2 hrs for Aβ)[8], and therefore precluded the investigators from assessing the role of Na+ channels in tau release. One can speculate that the tonic release of tau performs a trophic action at the synapse. Future studies outside the scope of the present work will be necessary to demonstrate this.

In agreement with previous data showing tau internalization[17,18], we have found that tau oligomers enter neurons after 20 min of exposure. Consistent with these findings,

tau oligomers produce an immediate impairment of LTP and memory. Thus, a straightforward scenario that will be investigated in future experiments is that once oligomers are internalized they are detrimental to second messenger cascades involved in synaptic strengthening and memory formation.

Another important aspect of our studies is that synaptic and memory dysfunctions did not require the presence of NFTs. Indeed, we have shown that tau oligomer exogenous administration produced its deleterious effects in normal mice, and hTau mice display LTP and memory impairment in the presence of tau oligomers prior to the appearance of NFTs. This is consistent with work demonstrating that tau oligomer-specific antibodies (e.g. TOC1) label tau pathology in a pre-tangle state[41] prior to coalescing into NFTs[13,42,43]. Altogether, these findings suggest that tau oligomers precede the formation of NFTs, underlying subtle changes in synaptic function that are responsible for amnestic symptoms. However, this does not mean that insoluble tau precipitates have no pathogenic role in neuronal dysfunctions. Their invariant accumulation may signify that they serve as reservoirs of tau both in fragmented or low-n oligomeric forms, with NFTs serving as a protective mechanism sequestering toxic soluble tau species[44,45]. Alternatively, NFTs might play a role in other aspects of the disease (i.e. spread within the brain), independently of a direct effect on memory.

Our findings with recombinant tau were validated through two alternative sets of experiments performed either with a preparation enriched with tau derived from human specimens or with hTau mice. The method we used to extract tau from the specimens assured a high yield for the protein and preserved its phosphorylation status. Moreover, it excluded amyloidogenic proteins, such as Aβ, synucleins, amylin, as confirmed through proteomic analysis of the samples. However, it did not assure absolute purity of the preparations, in the hypothesis that other oligomerized proteins were responsible for the detrimental effects on LTP and memory. To overcome this drawback, we further purified our AD-Tau preparation via immunoaffinity in a limited set of LTP and fear conditioning experiments confirming our results from preparations obtained without the last immunoaffinity step. Most important, given that it is highly unlikely that one can obtain a human preparation absolutely devoid of any other molecule, regardless of

the method used, yet preserving the post-translational status of tau and the putative oligomeric toxic form of tau, we used hTau mice. These animals were useful for demonstrating the role of tau in the electrophysiological and behavioral defects because at 10–11 months they form tau oligomers in the absence of NFTs[15]. Thus, they can be used as a source of human tau oligomers, whereas their littermates lacking tau can be utilized as a negative control. Strikingly, either 10–11 month old hTau mice or a preparation enriched in human tau extracted from their brains reproduced the same findings as with AD-tau and recombinant tau. Obviously, one cannot exclude that expression of the tau human transgene generates other oligomeric proteins that might, in turn, be responsible for the effect onto LTP and memory. In this unlikely scenario, oTau would be still relevant to the disease etiopathogenesis.

Our preparations either derived from human specimens or from cortices of hTau mice were obtained by homogenizing cortical tissue. This prevented us from distinguishing between the intracellular and extracellular pool of tau. We chose using cortical tissue because the method assured sufficient amounts of tau for performing our experiments, whereas other sources of the protein such as CSF in which tau clearly belongs to the extracellular pool, would have not permitted to recover enough protein for performing our experiments. Moreover, our method did not allow us to distinguish between different forms of tau, some of which might be toxic and others not. To address these issues, we confirmed findings with exogenous tau using hTau mice that are likely to reproduce more faithfully than brain extracts what happens in the diseased brain, as these animals naturally produce human tau. Moreover, we obtained a similar finding using recombinant tau. In summary, we reached the same conclusions using four different methods, including human recombinant tau, tau derived from human specimens, human tau derived from hTau mice, and in vivo hTau mice. Thus, the main observations of this manuscript showing that exogenous tau oligomers impair LTP and memory are clear and have important implications for the treatment of diseases characterized by abnormal tau elevation.

Recombinant tau or tau extracted from a specimen might be different than tau released into the extracellular space in situ. To alleviate concerns regarding differences between

recombinant tau and extracted tau used in our experiments and secreted tau, it should be noted that release of aggregated forms of tau has already been shown[19]. Moreover, the same study reported results suggesting an uptake of monomeric and/or small oligomeric species formed by full-length tau or the C-terminus. Finally, tau aggregates formed in one cell were found to be released into the extracellular space, gain entry into neighboring or synaptically connected cells, and trigger further aggregate formation via templated conformational change[46]. Thus, it is reasonable to assume that our recombinant tau oligomers, as well as oligomers derived from human and hTau mouse brains, have relevance to human pathology, even if we could not use naturally secreted tau in the current studies.

While the present investigation is not aimed at evaluating the modalities and the extent of tau propagation, our data support and extend the notion that the presence and diffusion of extracellular tau is potentially harmful. The exact mechanism by which extracellular tau may potentially interact with exposed targets on the cell surface or after it enters inside the cell is still matter of intense debate and investigation[47]. Secretion of tau is not fully understood yet and there is no consensus regarding the mechanisms solely involved in physiological release or in pathological conditions. Evidence supports the release of both monomeric and oligomeric forms of tau, as well as tau fragments, with variegated levels of toxicity, depending on concentration, size of the oligomer or tau fragment, conformation, and prionoid activity upon internalization. Importantly, our data show a robust acute effect of tau oligomers onto synaptic plasticity and memory suggesting this phenomenon occurs independently of pathology propagation. In this instance, oligomerization seems important for plasticity and memory impairment, but it is not essential per se for secretion and propagation, and therefore cannot be generalized to all aspects of AD. Nevertheless, the process of tau spreading throughout the neural circuitry involved in memory would provide a means for extracellular oligomers to impair LTP and memory to a progressively growing extent.

Tau and Aβ oligomers produce common biochemical neuronal modifications relevant for molecular mechanisms of gene transcription involved in memory formation. This

is important in terms of translational significance because the most compelling and relevant outcome from our study is that we have highlighted a new model for oligomer-induced toxicity in AD, modifying the classical view that oAβ triggers molecular modifications responsible for amnesic changes in the disease via tau. A unifying hypothesis for the disease origin is that the oligomeric conformation of proteins involved in AD, such as Aβ and tau, is toxic, independent of the type of protein forming the oligomers. Therapies acting onto a common target (possibly in sites of interaction with the oligomers instead of the classical β- and γ-secretase sites), or downstream of it, might therefore represent a valid and effective strategy for developing therapeutics.

Acknowledgements

This work was supported by NIH grants NS049442 and AG049402 (OA), P50AG008702 (LSH), R01AG017761 (DPD), R43AG029777, R44AG029777, R44AG029777B and R44AG033474 (JGM), AG02219 (VH), R01NS082730 (NMK), AG041531, AG033007 and AG048971 (LD) (http://www.nih.gov). This work was also supported by BrightFocus Foundation A2013364S (NMK) (http://www.brightfocus.org), Università Cattolica Intramural Funds Linea D3.2-2103 (CG) (http://www.unicatt.it), Alzheimer's Association IIRG-11-205343 (MF), IIRG-09-134220 (DP), and ZEN-11-201425 (LD) (http://www.alz.org), Ministry of Science and Education, Spain PR2010-0297 (MAB) (http://www.mecd.gob.es), Canadian Institutes of Health Research MOP-115056 (PEF) (http://www.alzheimer.ca/en/on), ADDF 271209 (JGM and OA) (http://alzdiscovery.org). Brain specimens were provided by JP Vonsattel and EP Cortes of the NY Brain Bank of Columbia and Mt Sinai School of Medicine, NY. We also thank N. Hansmeier for assistance with AFM, Drs F. Mancia, L. Shapiro, S. Mannepalli, and G. Sciara for assistance with chromatography, Dr. Rong Cheng and Joseph Lee for assistance with statistical analysis of the AFM data, V. Kansara for help with cultures, L. Mammana and M.R. Tropea for help with behavioral studies.

Materials and methods

Animals

All protocols involving animals were approved by Columbia University, NYU and Università Cattolica del Sacro Cuore, and the respective Institutional Animal care and Use Committee (IACUC); experiments involving animals were performed in accordance with the relevant approved guidelines and regulations. C57BL/6J, hTau (Jackson Lab Stock #005491), eGFP (Jackson Lab Stock #07075) mice and their littermates were obtained from breeding colonies kept in the animal facility of Columbia University, NYU, and Università Cattolica del Sacro Cuore. They were 3–4 months of age except for hTau mice which were 10–11 months old, and newborn mice for cell cultures. The methods for genotyping the colonies have already been described[54,55]. All mice were maintained on a 12 hr light/dark cycle (with lights on at 6:00 A.M.) in temperature and humidity-controlled rooms of the animal facilities.

Measurement of Tau Release in Primary Neuronal Cultures

Cell cultures were prepared from hippocampi of 0- to 1-day old newborn mice (C57B6/JL) as described[56]. At 12 DIV, cell medium was discarded and the dishes were washed three times with warm HBSS medium to remove debris and neurotransmitters or proteins. Then cells were treated with either vehicle, or 50 mM KCl, or 100 μM picrotoxin (PTx), or 1 μM tetrodotoxin (TTx) in Artificial Cerebro-Spinal Fluid (ACSF) (NaCl 124 mM, KCl 4.4 mM, Na2HPO4 1 mM, NaHCO3 25 mM, Glucose 10 mM, CaCl2 2 mM, MgCl2 2 mM) for 15 minutes (37 °C) prior to harvesting both extracellular medium and cells. Cell death was assessed through trypan blue staining[57]. Upon collection, ACSF samples were flash frozen and stored at −80 °C until analysis through an innovative ELISA test coupled to a derivative of ruthenium which generates chemiluminescence by electrical pulses produced by the Sector Imager Reader (MSD, MesoScale, MD), as reported elsewhere[58,59]. Briefly, 96-well plate in the MesoScale Tau Kit was blocked by adding phosphate buffer containing 5% IgG-free bovine serum albumin and 1% Tween 20 for 1 hr. Anti-Tau antibody (4/53) was diluted in low cross buffer (MSD) containing 0.1% BSA and 0.1% Tween 20, and then incubated 1 hr at room temperature. The plates were then washed three times with PBS buffer containing 1% Tween. For detection of bound antibody, the anti-Tau SULFO-TAG-detection antibody was added after washing, at a final concentration of 10 nM and plates were incubated for 1 hr at room temperature. After addition of MSD reading buffer, tau signals were detected by electrochemoluminescence using the MSD SECTOR-Imager 2400 as described above. The intra-assay coefficient of variation (%) for total tau was 11.9.

Preparation of Recombinant Tau

The cDNA for tau 4R/1N (412 amino acid isoform) was purchased from OriGene and subcloned into the bacterial expression vector pET21B to produce the tau protein. Similarly, the amino (amino acids 1–255) and carboxyl-terminal tau fragments (amino acids 256–441) were subcloned from this cDNA. The tau 4R/1N construct and the derivative subclones have a C-terminal 6x His-tag. The tau 4R/2N construct was a gift of Dr. Furukawa (University of Yokohama, Japan)[60]. The plasmid was transfected in Escherichia coli (Rosetta), and cells were streaked on LB agar ampicillin plates and a single colony was picked and grown overnight in LB broth with glucose and 100 mg/ml carbenicillin. Protein expression was induced with 1 mM IPTG for 8 hrs at which time cells were pelleted at 4 °C by centrifugation at 6000 g. Pellets were stored overnight at −80 °C. After a freeze-thaw cycle, cells were lysed in a 2% Triton X-100 phosphate-buffered saline and with a protease inhibitor mixture (Complete, EDTA-free; Roche Diagnostics. Streptomycin sulfate was added to precipitate DNA. After centrifugation,

100 mM NaCl was added to the supernatant and heated at 100 °C for 15 min. The precipitate was removed by centrifugation. The first step of purification for the C-terminal anionic construct used a nickel column with His-bind resin. The supernatant was loaded on His-Spin Protein miniprep columns (Zymo Res.) and eluted with phosphate buffer containing 300 mM NaCl plus 250 mM imidazole. Eluted tau was then buffer exchanged for the protein preparations into 50 mM Tris-HCl pH 7.4 via Amicon Ultra Centrifugal Devices (Millipore). Protein concentration was determined with BCA assay (Thermo Sci.). Monomer, dimers and trimers were purified from the oligomer mixture by size fractionation and analyzed by non-reducing SDS-PAGE[61]. Size fractionation followed by SDS-PAGE was also used to separate monomers and oligomers from the Tau 4R/1N preparation[61].

Tau Oligomerization

Tau was monomerized by treatment with 5 mM dithiothreitol (DTT) and 5 mM EDTA. Oligomerization was achieved via introduction of disulfide bonds through incubation with 1 mM H2O2 at RT for 20 hrs. Upon oligomerization tau was buffer exchanged to remove excess chemicals. Any insoluble material was removed by ultracentrifugation at 110,000 × g at 4 °C for 30 min. Tau protein concentration was determined from the absorption at 280 nm with an extinction coefficient of 7450 cm−1 M−1. Given that tau preparations contain a mix of monomers and different size oligomers, and tau conformation may change between initial preparation and final experimental conditions, tau concentration was expressed in μg/ml.

Assessment of Immunoreactivity for Tau and Neuronal Proteins

oTau 4R/2N and human-specimen derived tau were run on precast 3–8% gradient polyacrylamide Tris-acetate gels (Invitrogen). Proteins were transferred to nitrocellulose membrane (Millipore). Tau immunoreactivity was detected using anti-total tau polyclonal antibody (1:2000; Epitomics), and phosphospecific polyclonal antibodies against tau [p-tau217] and [p-tau231] (Invitrogen). oTau was characterized through the conformational antibodies T22 (Millipore) and TOC-1[13,42,43,62]. Duplicate blots were first performed with the phosphorylated tau antibodies and re-used with for total tau analysis.

Atomic Force Microscopy (AFM)

AFM sample preparation and analysis was performed as previously described[61,63] (see Supplementary Methods for a detailed description).

Electrophysiological Studies

Hippocampal slices were cut with a tissue chopper and recorded as described[64] (see Supplementary Methods for a detailed description).

Behavioral Studies

Intracerebral tau or Aβ infusion, and behavioral tasks including fear conditioning, RAWM, sensory threshold, visible platform and open field were assessed as described[64–66] (see Supplementary Methods for a detailed description).

Extraction of Human Tau

For obtaining a preparation enriched in soluble human tau we used the prefrontal/frontal cortex of AD patients and HCs (Table S2), as well as cortices from hTau mice. Human tissue was provided by the New York Brain Bank–The Taub Institute, Columbia University, and the VAMC NY. The tissue was prepared as previously described[53] with the modification that tau solubilization was achieved without the use of detergents (allowing the selective recovery of

the soluble fraction), and immunoaffinity column for the final step (to achieve high quantities of protein: 0.006–0.1% mass of frozen brain tissue), except for a few control experiments in which we included immunoaffinity, confirming LTP and contextual memory impairment by the preparation. Furthermore, all molecules below 10 kDa were filtered out through Sartorius Vivaspin-Turbo-15 for the final purification step. Advantages of this method are that the acidic homogenization buffer containing 1% perchloric acid allows the removal of DNA and the vast majority of other proteins than tau, whereas it preserves the tau phosphorylation status[67]. Reductant was used during extraction and fractions containing monomeric tau were pooled, concentrated and buffer exchanged into 50 mM Tris-HCl pH 7.4. Then, the preparation was oligomerized according to the method for tau oligomerization described above.

Proteomic Analyses

Extracted tau protein[53] was prepared for mass spectrometry by alkylation of cysteines, digestion with trypsin and analyzed with a NanoAcquity UPLC and Synapt G2 quadrupole-time-of-flight HDMS mass spectrometer (Waters) as described previously[68]. Spectra were collected by data-dependent acquisition as previously[68], except that the survey scan time was 0.25 s, five ions were selected after a single survey scan, and advanced charge state peak detection was used with collision energy ramping (12–40 V start and 20–60 V end). The Mascot database search program (Vers. 2.4) (Matrix Science, London, UK) was used for protein and peptide identifications. Observed masses were searched by Mascot against the NCBI nr protein database of 08/14/13 (31,351,517 sequences; 10,835,265,410 residues) with Homo sapiens taxonomic filter (251,429 sequences). Search parameters included fixed modification of carbamidomethyl (C), variable modifications of oxidation (M), phospho (STY), peptide mass tolerance ± 0.01 Da and fragment mass tolerance ± 0.02 Da with decoy search enabled.

Enzyme-linked immunosorbent assay (ELISA)

Tau5 (total tau, human brain samples), or TOC1 (tau oligomers) were used as the capture antibody and R1 tau antibody (a polyclonal rabbit tau antibody) for detection of bound tau. All steps were performed at room temperature, 200 µl/well was used for rinsing and blocking steps, and 50 µl/well for all other steps. Capture antibodies were diluted (Tau5, 1 µg/ml; TNT1 and TOC1, 2 µg/ml) in borate saline (100 mM boric acid, 25 mM sodium tetraborate decahydrate, 75 mM NaCl, 250 µM thimerosal) and incubated in high binding ELISA microplates (Corning, #3590) for 1 hr. Plates are then rinsed twice with ELISA wash buffer (100 mM boric acid, 25 mM sodium tetraborate decahydrate, 75 mM NaCl, 250 µM thimerosal, 0.4% bovine serum albumin and 0.1% tween-20) and blocked with ELISA wash containing 5% non-fat dried milk for 1 hour. Each well was rinsed 2 times and samples added to the well for 1.5 hrs. In vitro tau aggregation samples were diluted in Tris Buffered Saline (TBS) to 25 nM and human brain extracts to a final total protein concentration of 20 µg/well for soluble tau fractions and 4 µg/well for insoluble tau fractions. Wells were rinsed twice, and then R1 was diluted (0.1 µg/ml) in blocking reagent and added to each well for 1.5 hours. Wells were rinsed 3 times and incubated for 1.5 hrs with goat anti-rabbit antibody conjugated to horseradish peroxidase (Vector Labs, PI-1000) diluted (0.2 µg/ml) in blocking reagent. The wells were rinsed 3 times, signal detected by developing with 3,3′,5,5′-tetramethylbenzidine (TMB) for 10–15 min and then the reaction was stopped using 3.5% sulfuric acid. The absorbance of TMB signal was measured at 450 nm.

Dot Blot
Brain extracts were analyzed as previously described[22] with the following exceptions. Samples were spotted onto the nitrocellulose membrane using a Whatman minifold I dot blot apparatus. The membranes were blocked, probed with TOC1 (oligomeric tau, diluted 1:5,000, Dr. Kanaan laboratory), and R1 (a pan-tau rabbit polyclonal antibody, diluted 1:20,000) and the appropriate Licor secondary antibodies (diluted 1:20,000), and imaged using the Licor Odyssey system. The signal intensity measurements for each dot were expressed as the ratio of oligomeric tau (TOC1 signal) per total tau (R1 signal). The Licor Odyssey system provides the advantages of dual-color quantitative blotting with a larger dynamic range and higher sensitivity than X-ray film and chemiluminescence. In a separate set of dot blots, the membranes were probed with either T22 antibody (1:1000, Millipore), and an anti-rabbit HRP conjugated secondary antibody diluted (1:20000) and detected using chemiluminescence and film.

Histopathology and Histochemistry
Immunohistochemistry was performed using the Ventana BenchMark Ultra automated platform (see Supplementary Methods for a detailed description).

Aβ Preparation
Aβ42 was prepared from synthetic peptide from the Teplow lab, as previously described[64,69] (see Supplementary Methods for a detailed description).

Assessment of Tau Entrance into Neurons
Primary cultures of hippocampal neurons were obtained from C57/BL6 mice, and eGFP-expressing mice, as previously described[70,71]. Before conjugation, monomeric tau was incubated with 1 mM dithiothreitol (DTT/PBS) for 10 min at 60 °C. Both oligomeric and monomeric preparations were purified with Amicon Ultra Centrifugal Filter (10 KDa). Tau preparations were then labeled with the IRIS 5-NHS active ester dye (IRIS 5; λex: 633 nm; λem: 650–700 nm; Cyanine Technology, Turin, Italy) according to manufacturer's protocol. Briefly, tau solutions (2 μM in PBS) were mixed with 6 mM IRIS 5 in dimethyl sulfoxide for 4 hrs in the dark under mild shaking conditions. After this time, labeled tau was purified with Vivacon 500 ultrafiltration spin columns (Sartorius Stedim Biotech GmbH, Goettingen, Germany) and then resuspended in PBS and used at final concentration of 100 nM. For time lapse confocal imaging experiment, hippocampal neurons from eGFP mice were cultured for 14 days in vitro (DIV) before being exposed to IRIS-5-labelled tau preparations for 40 min in Tyrode's solution at 37 °C. Immunocytochemistry was also performed in 14 DIV neurons treated with IRIS 5-labeled monomeric or oligomeric tau for 3, 6 and 18 hrs. After two washes in PBS, cells were fixed with paraformaldehyde (4% in PBS; Sigma) for 15 min at RT. After being permeabilized (15-min of incubation with 0.3% Triton X-100 [Sigma] in PBS), cells were incubated for 20 min with 0.3% bovine serum albumin in PBS to block nonspecific binding sites and then overnight at 4 °C with the antibody anti-microtubule associated protein-2 (MAP-2, Immunological Sciences, Rome, Italy). The next day, cells were incubated for 90 min at room temperature with the secondary antibodies Alexa Fluor 488 donkey anti-mouse (1:1,000; Invitrogen). Images (1024 × 1024 pixels) were acquired at 63× magnification with a confocal laser scanning system (TCS-SP2; Leica Microsystems) and an oil-immersion objective (numerical aperture 1.4; physical pixel size 233 nm). For time lapse imaging, confocal Z-stacks were acquired every 5 min in order to study tau internalization. All experiments were repeated at least 3 times. The operator was blind to the study conditions.

Statistical Analyses

Experiments were performed blinded with regards to vehicle or preparations. Results were expressed as the mean ± the standard error of the mean (SEM) (level of significance at $p < 0.05$). Results were analyzed by two-tailed Student's t test, or ANOVA plus post-hoc multiple comparisons test using Prism (GraphPad) software with treatment condition as main effect. Behavioral experiments were designed in a balanced fashion. For each condition, mice were trained and tested in three to four separate sets of experiments.

Supplementary Information

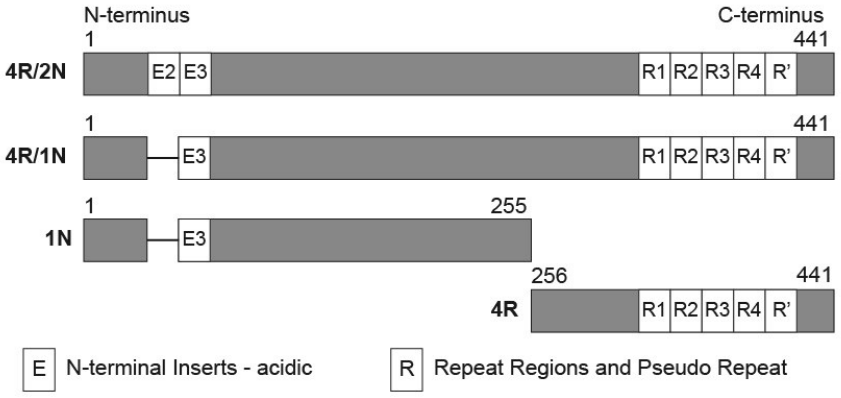

Supplementary Figure S1. Schematic of tau constructs used and their nomenclature. Six tau isoforms are encoded by the MAPT gene in the brain due to alternative splicing of exons 2 and 3 that encode N-terminal inserts (N) and exon 10 encoding the second microtubule binding repeat (R). The nomenclature is based on the domains included in the final protein that can have either zero, one or two N units, and three or four R units. The two longest tau isoforms, 4R/2N and 4R/1N, differ by the size of the inserts at the N-terminal (1N, 29 amino acids; 2N, 58 amino acids) and possess 4 repeats (4R) in the microtubule binding domain at their C-terminal side[48]. The numbering scheme is based on the longest isoform, 4R/2N, containing 441 amino acids.

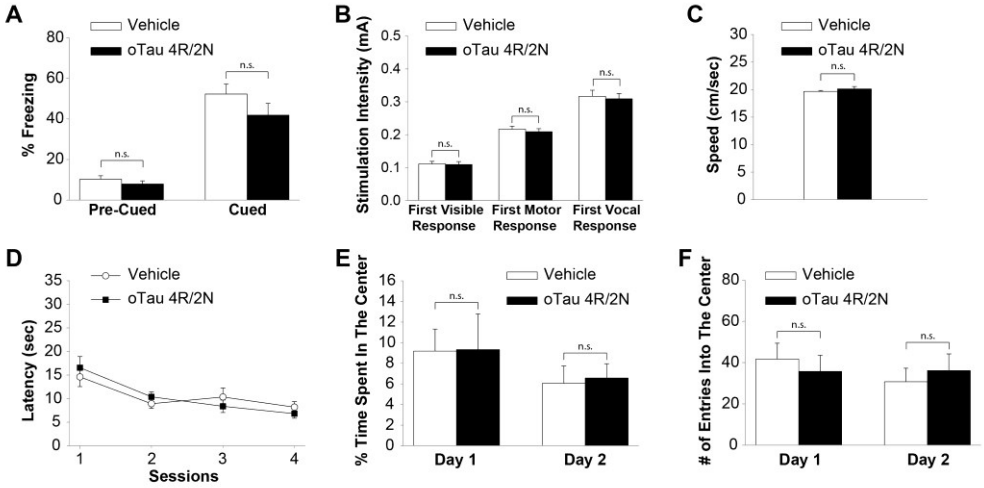

Supplementary Figure S2. Bilateral Injections of Recombinant Tau Oligomers into the Dorsal Hippocampi did not Affect Cued Fear Conditioning, Sensory Threshold, or Performance with the Visible Platform Task and Open Field Test. (A) Freezing responses before (Pre) and after (Post) the auditory cue were the same among vehicle- (n = 18), and 22.95 µg/ml oTau 4R/2N- (n = 11) infused

mice in the cued conditioning test. $p > 0.05$. (B) No difference was detected during assessment of the sensory threshold in vehicle (n = 18) and 22.95 µg/ml oTau 4R/2N-infused mice (n = 11). $p > 0.05$. (C-D) Testing with the visible platform task for assessment of visual-motor-motivational deficits did not reveal any difference for both speed (C) and time to the platform (D) between vehicle- (n = 11) and 22.95 µg/ml oTau 4R/2N-infused mice (n = 13). $p > 0.05$. (E-F) Open field testing in vehicle- and 22.95 µg/ml oTau 4R/2N-infused mice showed a similar percentage of time spent in the center compartment (E) and the number of entries into the center compartment (F) indicating that they had no differences in exploratory behavior (vehicle: n = 11, oTau 4R/2N: n = 13). $p > 0.05$. All data shown are mean ± SEM.

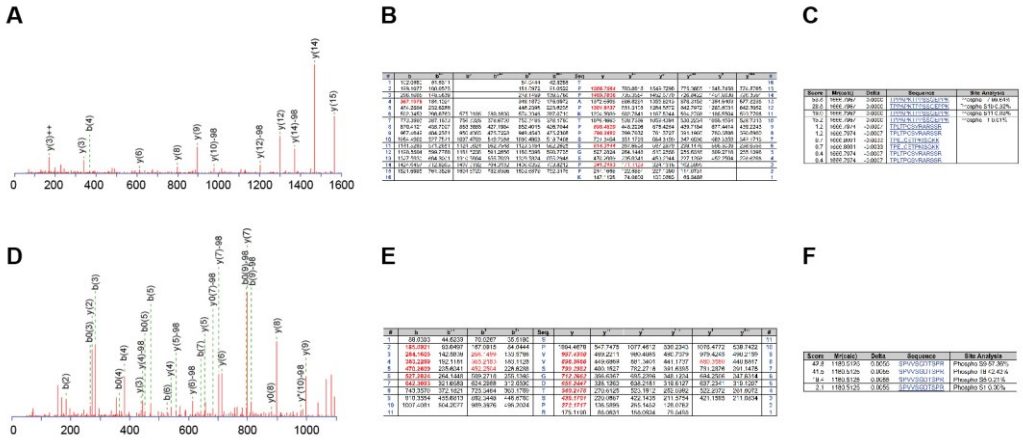

Supplementary Figure S3. Proteomic Assessment of Phosphorylation Sites in the AD-Tau Preparation. (A-C) Example MS/MS data for the peptide 175_TPPAPKpTPPSSGEPPK_190 from tau (identified in the NCBI non-redundant database as protein accession (gi) numbers 294862261, 6754638, 8400711, 8400715, 178557736, 294862258, 322303720, 32230374). Spectrum was acquired in data-dependent acquisition (DDA) mode on a Synapt G2 HDMS as analyzed by Mascot software. This peptide had a Mascot ion score of 54, precursor mass of 1666.79, charge state of +3, precursor mass error of 0.06 ppm, and product RMS error of 9 ppm. For this and the following panels, symbols (*) indicate loss of NH3, (0) indicates the loss of H2O, and ions were recorded as singly charged except if doubly charged (++). (A) Product ion spectrum with y-series and b-series ions labeled. Neutral losses of 98 indicated on the spectrum represent loss of H3PO4 from phosphorylated peptide fragment ions. (B) Table of detected masses as annotated by Mascot. Bold italic red indicates that the ion series contributed to the peptide score. Bold red indicates the number of matches in the ion series is greater than would be expected by chance alone, suggesting that the ion series is present in the spectrum. Non-bold red means that the number of matches in the ion series is no greater than would be expected by chance. Masses indicated in black type were not detected in the spectrum. (C) Alternate possible predicted sequence and Mascot site analysis indicating phosphorylation is probably on residue T7. (D-F) Example MS/MS data for the peptide 396_SPVVSGDTpSPR_406 from Microtubule-associated protein tau (sequence present in isoforms 1-8 represented by NCBInr gi numbers 294862261, 6754638, 8400711, 8400715, 178557736, 294862258, 322303720, 322303747). Spectrum was acquired in data-dependent acquisition (DDA) mode on a Synapt G2 HDMS as analyzed by Mascot software. This peptide had a Mascot ion score of 43, precursor mass of 1180.51, charge state of +2, precursor mass error of 4.6 ppm, and product RMS error of 6 ppm. (D) Product ion spectrum with y-series and b-series ions labeled. Neutral losses of 98 indicated on the spectrum represent loss of H3PO4 from phosphorylated peptide fragment ions. (E) Table of detected masses as annotated by Mascot. Bold italic red indicates that the ion series contributed to the peptide score. Bold red indicates the number of matches in the ion series is greater than would be expected by chance alone, suggesting that the ion series is present in the spectrum. Non-bold red means

that the number of matches in the ion series is no greater than would be expected by chance. Masses indicated in black type were not detected in the spectrum. (F) Mascot site analysis indicating phosphorylation is probably on residue S9 or T8.

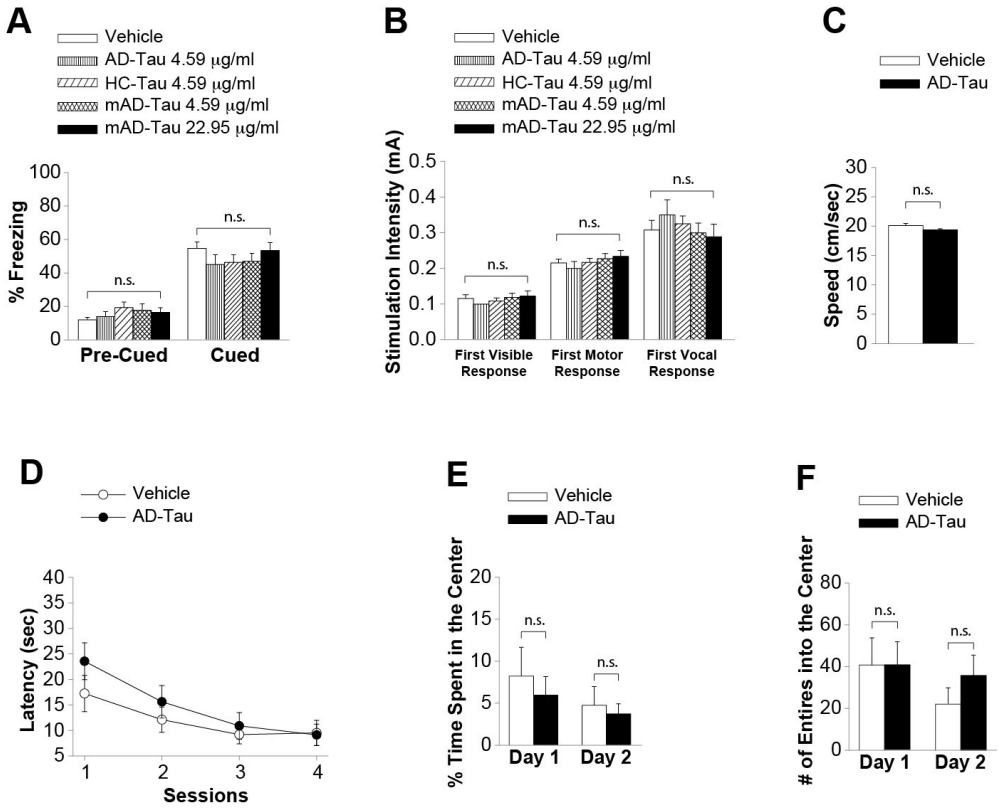

Supplementary Figure S4. Cued Fear Memory, Sensory Threshold, Performance with the Visible Platform Task and Open Field Test, and Basal Synaptic Transmission are Normal following Bilateral Injections of a Preparation Enriched in Soluble Human Tau Derived from AD Patients. (A) Freezing responses before (Pre) and after (Post) the auditory cue were the same among vehicle- (n = 13), AD-Tau- (4.59 μg/ml, n = 9), HC-Tau- (4.59 μg/ml; n = 12) or mAD-Tau- (both at 4.59 μg/ml and 22.95 μg/ml; n = 11 and 9 respectively) infused mice in the cued conditioning test. $p > 0.05$. Specimens from patients 34, 36 and 49 for AD and 28, 33 and 41 for HC (Table S1). (B) No difference was detected between groups during assessment of the sensory threshold in vehicle- and AD-Tau infused mice. Vehicle: n = 13, AD-Tau (4.59 μg/ml) n = 9, HC-Tau (4.59 μg/ml) n = 12, mAD-Tau (4.59 μg/ml and 22.95 μg/ml) n = 11 and 9, respectively, $p > 0.05$. Specimens from patients 34, 36 and 49 for AD and 28, 33 and 41 for HC (Table S1). (C-D) Testing with the visible platform task for assessment of visual-motor-motivational deficits did not reveal any difference in speed (C) and time to the platform (D) between vehicle- and AD-Tau infused mice (n = 8 per each group, respectively). $p > 0.05$. Specimens from patients 35, 37 (Table S1). (E-F) Open field testing in vehicle- and AD-Tau infused mice showed a similar percentage of time spent in the center compartment (E) and the number of entries into the center compartment (F) (n = 8 per each group; $p > 0.05$ for both), indicating that they had no differences in exploratory behavior. Specimens from patients 35, 37 (Table S1).

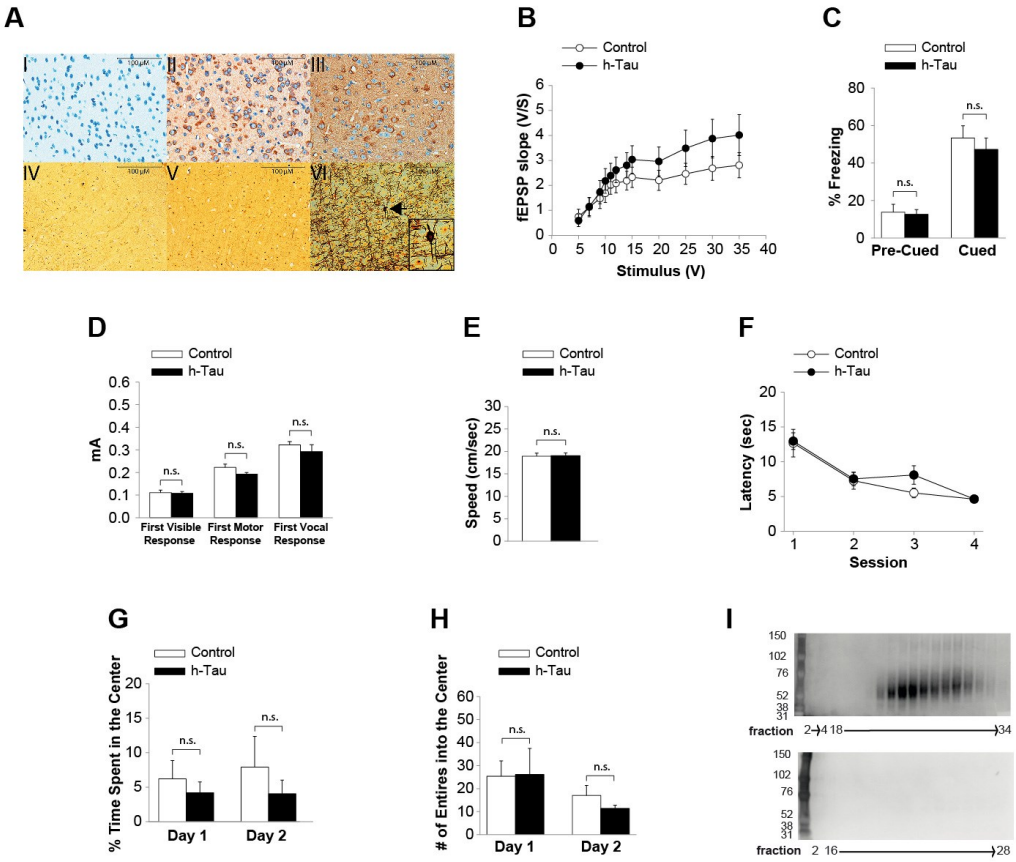

Supplementary Figure S5. Cued Fear Memory, Sensory Threshold, Performance with the Visible Platform Task and Open Field Test, and Basal Synaptic Transmission are Normal in Mice Expressing Non-Mutated Human Tau Gene. (A) Immunohistochemistry for hyper-phosphorylated human tau shows no staining in brain sections from adult (10-11 months of age) control mice (I). However, prominent staining was visible in adult (II) and aged (18 months) (III) hTau mice. A Bielschowsky silver stain (which highlights NFTs in AD patients) shows a normal staining pattern in adult control (IV) and hTau (V) mice. In contrast, aged hTau mice (VI) show occasional NFTs (arrow head - NFT is shown larger in magnified sub-panel). Interestingly, aged hTau mice also have neuronal processes that stain more prominently with the Bielschowsky stain. (B) BST at the CA3-CA1 connection of slices from 10- to 11-month-old hTau mice was similar to control littermates (n = 9 slices from 6 mice per group for hTau; and 7 slices from 6 mice for controls; ANOVA: $p > 0.05$). (C) Freezing responses before (Pre) and after (Post) the auditory cue were the same in controls (n = 9) and hTau (n = 13) mice in the cued conditioning test. $p > 0.05$. (D) No difference was detected between controls and hTau mice during assessment of the sensory threshold (n = 9 for controls and 13 for hTau mice). $p > 0.05$. (E-F) Testing with visible platform task for assessment of visual-motor-motivational deficits did not reveal any difference in speed (E) and time to the platform (F) between controls and hTau mice (n = 9 for controls and 13 for hTau mice). $p > 0.05$. (G-H) Open field testing in controls and hTau mice showed a similar percentage of time spent in the center compartment (G) and the number of entries into the center compartment (H) ($p > 0.05$ for both), indicating that they had no differences in exploratory behavior (n = 8 for controls and 9 for hTau mice). (I) Representative examples of non-reducing SDS-PAGE analysis of hTau-p and C-p. Numbers at the bottom of the WB correspond to fraction samples obtained during chromatography. All data shown are mean ± SEM.

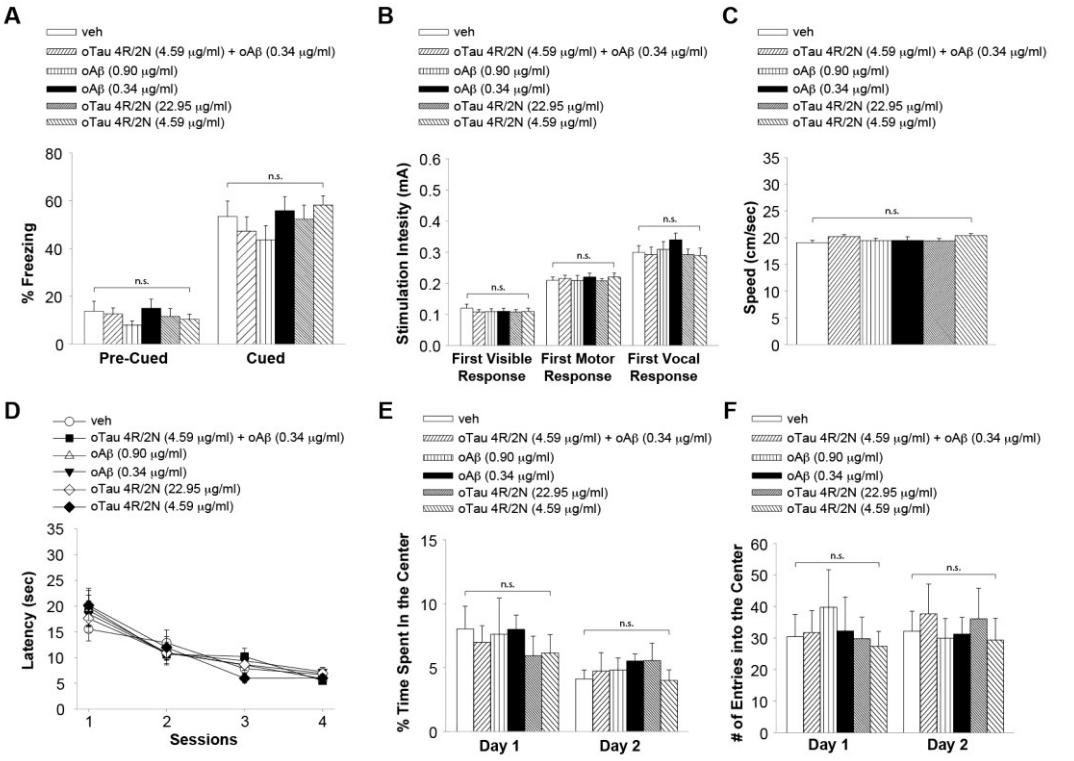

Supplementary Figure S6. Bilateral Injections of oTau Concurrently with oAβ into the Dorsal Hippocampi did not Affect Cued Fear Conditioning, Sensory Threshold, or Performance with the Visible Platform Task and Open field Test. (A) Freezing responses before (Pre) and after (Post) the auditory cue were the same among vehicle- (n = 10), 4.59 μg/ml oTau 4R/2N + 0.34 μg/ml oAβ (n = 13), 0.90 μg/ml oAβ (n = 11), 0.34 μg/ml oAβ (n=11), 22.95 μg/ml oTau 4R/2N (n = 13), and 4.59 μg/ml oTau 4R/2N (n = 10) infused mice in the cued conditioning test. ANOVA: $p > 0.05$. (B) No difference was detected between groups during assessment of the sensory threshold in vehicle- (n = 10), 4.59 μg/ml oTau 4R/2N + 0.34 μg/ml oAβ- (n = 13), 0.90 μg/ml oAβ- (n = 11), 0.34 μg/ml oAβ- (n=11), 22.95 μg/ml oTau 4R/2N- (n = 13), and 4.59 μg/ml oTau 4R/2N- (n = 10) infused mice. ANOVA: $p > 0.05$. (C-D) Testing with the visible platform task for assessment of visual-motor-motivational deficits did not reveal any difference in speed (C) and time to the platform (D) between vehicle- (n=11), 4.59 μg/ml oTau 4R/2N + 0.34 μg/ml oAβ- (n=11), 0.90 μg/ml oAβ- (n=9), 0.34 μg/ml oAβ- (n=13), 22.95 μg/ml oTau 4R/2N- (n = 9) and 4.59 μg/ml oTau 4R/2N- (n = 11) infused mice. ANOVA: $p > 0.05$. (E-F) Open field testing showed a similar percentage of time spent in the center compartment (E) and the number of entries into the center compartment (F) in vehicle- (n = 10), 4.59 μg/ml oTau 4R/2N + 0.34 μg/ml oAβ- (n = 9), 0.90 μg/ml oAβ- (n = 9), 0.34 μg/ml oAβ- (n = 7), 22.95 μg/ml oTau 4R/2N- (n = 9), and 4.59 μg/ml oTau 4R/2N- (n = 9) infused mice in the cued conditioning test. ANOVA: $p > 0.05$, indicating that they had no differences in exploratory behavior. All data shown are mean ± SEM.

subject #	diagnosis	age	gender	PMI	Braak #	CERAD #	NIA-R #
1	HC	36	M	9:00	0	0	0
2	AD	44	M	20:08	VI	C	HIGH
3	HC	54	F	15:40	0	0	0
4	HC	57	F	9:40	0	0	0
5	HC	57	M	6:50	0	0	0
6	AD	61	M	5:00	VI	C	HIGH
7	AD	62	F	23:40	VI	undetermined	HIGH
8	HC	64	F	11:30	0	0	0
9	AD	65	M	9:50	VI	undetermined	HIGH
10	AD	67	M	25:20	VI	C	HIGH
11	AD	68	M	7:40	VI	C	HIGH
12	HC	70	M	23:50	0	0	undetermined
13	HC	71	M	21:37	0	0	undetermined
14	HC	72	M	4:30	0	0	0
15	AD	72	M	9:00	VI	C	HIGH
16	HC	73	F	3:00	0	0	undetermined
17	HC	74	M	11:50	0	0	undetermined
18	AD	74	F	23:09	VI	C	HIGH
19	HC	78	M	8:00	0	0	0
20	HC	78	M	8:00	0	0	0
21	AD	78	F	41:30	VI	undetermined	HIGH
22	AD	79	F	11:40	VI	undetermined	HIGH
23	HC	83	M	16:50	0	0	undetermined
24	AD	83	F	5:00	VI	B	HIGH
25	HC	89	M	9:30	III	A	LOW

Supplementary Table S1 Brain Bank Sample Characteristics. A list of frozen post-mortem tissue samples from healthy control individuals (HCs) or neuropathologically confirmed AD cases. All individuals were characterized for their Braak and Braak stage (Braak # 0-VI), Consortium to Establish a Registry for Alzheimer's Disease (CERAD) Neuropsychological Battery score (C for AD patients, not evaluable for HCs), and National Institute of Aging – Reagan Institute rating (NIA-R) (high for the AD patients, 0 for HCs). AD patients had no other diseases that might have contributed to the clinical deficits. De-identified specimens include AD and HCs. HC: range 36-89 yrs, average: 68.28 ± 3.65; probable AD: range: 44-83 yrs, average: 68.45 ± 3.25 yrs. PMI: post-mortem interval.

Phosphorylation site	Phosphopeptide	m/z	Measured Mass (Da)	Mascot site analysis score (%)	Mascot peptide ion score	Reference
181	175_TPPAPKpTPPSSGEPPK_190	556.61[3]+	1666.80	99.6	54	This study
181	175_TPPAPKpTPPSSGEPPK_190	556.61[3]+	1666.80	-	-	[2]
404	396_SPVVSGDTpSPR_406	591.27[2]+	1180.52	57.4	43	This study
404	396_SPVVSGDTpSPR_406	591.26[2]+	1180.51	-	-	[2]

Supplementary Table S2 Some Phosphorylation Sites Detected, their Putative Locations and a Comparison to Data Previously Reported in the Literature. Tau was identified in the NCBI non-redundant database as protein accession (gi) numbers 294862261, 6754638, 8400711, 8400715, 178557736, 294862258, 322303720, 32230374. Our purification technique preserves the phospho-epitopes of adult human tau suggesting that our extraction method produces samples amenable to analysis by mass spectrometry and provides usable spectra of phosphorylated peptides, as shown on Figure S3A-F. The table compares our results with data in the literature and demonstrates that our results are essentially identical to those published by other groups. The sites identified, their assignment to particular residues, the m/z values and charge states were all identical to those reported by other groups[49]. These results demonstrate the effectiveness of a technique simpler than previous protocols[50], yet still allowing efficient detection of phosphosites. The mass spectra collected compared favorably with spectra for these same peptides in public databases[51,52]. These spectra demonstrated the potential for using this technique for studying phosphorylation in future more comprehensive studies. We also demonstrate that tau phosphorylation survived this perchloric acid treatment in a manner that retained compatibility with mass spectrometric identification. Finally, these findings confirm the stability of phosphosites to this extraction method, already shown with immunologic data[53], through the use of mass spectrometry.

Supplementary Methods

Atomic Force Microscopy (AFM)

For AFM sample preparation, a 10 µl aliquot of 10 µg/µl tau protein solution was deposited on a freshly cleaved mica substrate (Spruce Pine, NC), incubated for 5 min at room temperature, rinsed extensively with 0.2 µm filtered deionized water (18.1 MΩ, Millipore, MA), and dried under a gentle stream of N2 gas. All AFM height images were recorded in tapping mode with scan rates of 2.5 Hz and 512x512 pixels resolution with commercial AFMs in air at room temperature. AFM images for height distribution calculations were acquired using the Nanoscope IIIa AFM (Veeco, Santa Barbara, CA) equipped with oxide sharpened Si3N4 AFM tips (k = 40 N/m, fo ~ 300kHz) (Model: OTESPA, Veeco, Santa Barbara, CA) and analyzed with the Scanning Probe Imaging Processor software (SPIP, Image Metrology) to generate

height distribution plots, as previously described 7. Presented topographic AFM images were recorded using the MFP-3D AFM (Asylum Research, Santa Barbara, CA) equipped with commercial microcantilevers (k = 2 N/m, fo ~ 70kHz) (OMCL-AC240TS-W2, Olympus, Japan). Images are displayed 3-dimensionally without further processing using the implemented ARgyle Light 3D imaging module (Asylum Research, Santa Barbara, CA).

Electrophysiological Studies

Hippocampal slices (400 μm) were cut with a tissue chopper and maintained in an interface chamber at 29° C for 90 minutes prior to recording, as previously described[64]. Following assessment of basal synaptic transmission by plotting the stimulus voltages against slopes of field Excitatory Post-Synaptic Potentials (fEPSP); baseline was recorded every minute at an intensity that evoked a response 35% of the maximum evoked response, baseline was recorded every minute at an intensity that evoked a response 35% of the maximum evoked response. Slices were perfused for 20 min with different tau and Aβ preparations or vehicle, and LTP was induced using a theta-burst stimulation (4 pulses at 100 Hz, with the bursts repeated at 5 Hz and each tetanus including 3 ten-burst trains separated by 15 sec). Responses were measured as fEPSP slopes expressed as percentage of baseline.

Behavioral Studies

Intracerebral tau and Aβ infusion. After 5-7 days from the implant of cannulas onto dorsal hippocampi[64] , mice were bilaterally infused with tau or Aβ preparations or vehicle in a final volume of 1 μl over 1 minute with a microsyringe connected to the cannulas via polyethylene tubing. Tau was infused at 180 and 20 minutes prior to the foot shock, whereas Aβ was infused at 20 minutes prior the foot shock. During infusion animals were handled gently to minimize stress. After infusion, the needle was left in place for another minute to allow diffusion. Mice were handled once a day for 3 days before behavioral assessment. After behavioral testing, a solution of 4% methylene blue was infused into the cannulas to check for the position of the cannulas, as described[64].

Fear conditioning (FC) 8. Mice were placed in a conditioning chamber for 2 minutes before the onset of a tone (Conditioning Stimulus, CS) (a 30 sec, 85 dB sound at 2800 Hz). In the last 2 sec of the CS, mice were given a 2 sec, 0.6 mA foot shock (Unconditioning Stimulus, US) through the bars of the grid-floor and left in the conditioning chamber for additional 30 sec. Freezing behavior (the absence of all movements except for those needed for breathing) was scored using FreezeView software. Contextual fear learning was evaluated 24 hrs after training by measuring freezing for 5 min in the chamber in which mice were trained. Cued fear learning, a type of memory depending upon amygdala function[9], was assessed 24 hrs after contextual testing by placing mice in a novel context for 2 minutes (pre-CS test), after which they were exposed to the CS for 3 min (CS test). To determine whether the treatments affected sensory perception of the mice, threshold assessment was conducted as previously described[64].

2-day Radial Arm Water Maze (RAWM)[65,66]. During the first day of the protocol mice were trained to identify the platform location by alternating between a visible and a hidden platform in a goal arm, except that during the last 3 trials in which the platform was hidden. On the second day, in turn, all 15 trials were hidden. Entries to arms with no platform were counted as an error, and the animal was gently pulled back to the start arm. Failure to select an arm after 15 sec was also counted as an error and the mouse was returned to the start arm. The duration of each trial was up to 1 min. At the end of each trial mouse rested on the platform for 15 sec. The platform location was different for each mouse. Data were analyzed and displayed as

averages of blocks of 3 trials per mouse. Controls for this task were performed with the visible platform and open field test[64].

Histopathology and Histochemistry

Immunohistochemistry was performed using the Ventana BenchMark Ultra automated platform. Tissue sections were first deparaffinized using Ventana's "ez-prep" solution. Antigen retrieval was performed by treatment at 95°C for 54 minutes using Ventana's CC1 (pH7.3) solution, followed by treatment with 0.3% hydrogen peroxide to block endogenous peroxidase. Tissue sections were then incubated in protein-free block (Biocare's background sniper) for 15 min to inhibit the nonspecific binding of primary. Primary antibody (AT8 at 1:200, Thermo Scientific) was incubated for 32 min at room temperature. Detection was performed using Ventana's ultraview DAB kit, and counterstaining with the Gill hematoxylin solution. For Bielschowsky staining, slides were first deparaffinized and hydrated with distilled water. They were then placed in 20% Silver Nitrate at 60° C for 15 min, rinsed, and then stained in ammoniacal silver solution for 30 min. Slides were then rinsed in tap water, washed in sodium thiosulfate solution for 2 min, rinsed in tap water, and then dehydrated and mounted with synthetic resin.

Aβ Preparation

Aβ42 was prepared from synthetic peptide from the Teplow lab, as previously described 8. Briefly, lyophilized Aβ42 was resuspended in cold 1,1,1,3,3,3-hexafluoro-2-propanol (HFIP, Sigma) and aliquoted in polypropylene vials. After 24 hrs, the HFIP solution was allowed to evaporate in a fume hood until formation of a thin film of monomeric peptide at the bottom of the vials. Peptide films, dried under gentle vacuum, were stored in sealed vials at –20°C. Prior to use, following monomerization of Aβ through DMSO (Sigma), the peptide was sonicated for 10 minutes 12. Aβ42 oligomers were obtained by incubating an aliquot of monomeric Aβ/DMSO solution in sterile phosphate buffer at 4°C overnight. Oligomerized Aβ peptide was diluted to the final concentration with vehicle immediately before the experiments.

References

1. Sahara, N. *et al.* Assembly of two distinct dimers and higher-order oligomers from full-length tau. *Eur. J. Neurosci.* **25,** 3020–9 (2007).
2. Lasagna-Reeves, C. A., Castillo-Carranza, D. L., Guerrero-Muoz, M. J., Jackson, G. R. & Kayed, R. Preparation and characterization of neurotoxic tau oligomers. *Biochemistry* **49,** 10039–41 (2010).
3. Xu, S., Brunden, K. R., Trojanowski, J. Q. & Lee, V. M.-Y. Characterization of tau fibrillization in vitro. *Alzheimers. Dement.* **6,** 110–7 (2010).
4. Chromy, B. A. *et al.* Self-assembly of Abeta(1-42) into globular neurotoxins. *Biochemistry* **42,** 12749–60 (2003).
5. Morris, M., Maeda, S., Vossel, K. & Mucke, L. The many faces of tau. *Neuron* **70,** 410–426 (2011).
6. Clavaguera, F., Grueninger, F. & Tolnay, M. Intercellular transfer of tau aggregates and spreading of tau pathology: Implications for therapeutic strategies. *Neuropharmacology* **76 Pt A,** 9–15 (2014).
7. Pooler, A. M., Phillips, E. C., Lau, D. H. W., Noble, W. & Hanger, D. P. Physiological release of endogenous tau is stimulated by neuronal activity. *EMBO Rep.* **14,** 389–394 (2013).
8. Yamada, K. *et al.* Neuronal activity regulates extracellular tau in vivo. *J. Exp. Med.* **211,** 387–393 (2014).
9. Phillips, R. G. & LeDoux, J. E. Differential contribution of amygdala and hippocampus to cued and contextual fear conditioning. *Behav. Neurosci.* **106,** 274–85 (1992).
10. Berger, Z. *et al.* Accumulation of pathological tau species and memory loss in a conditional model of tauopathy. *J. Neurosci.* **27,** 3650–62 (2007).
11. Brunden, K. R., Trojanowski, J. Q. & Lee, V. M.-Y. Evidence that non-fibrillar tau causes pathology linked to neurodegeneration and behavioral impairments. *J. Alzheimers. Dis.* **14,** 393–9 (2008).
12. Lasagna-Reeves, C. A. Identification of oligomers at early stages of tau aggregation in Alzheimer's disease. *FASEB J.* **26,** 1946–1959 (2012).
13. Patterson, K. R. *et al.* Characterization of prefibrillar Tau oligomers in vitro and in Alzheimer disease. *J. Biol. Chem.* **286,** 23063–76 (2011).
14. Magnoni, S. *et al.* Tau elevations in the brain extracellular space correlate with reduced amyloid-β levels and predict adverse clinical outcomes after severe traumatic brain injury. *Brain* **135,** 1268–80 (2012).
15. Castillo-Carranza, D. L. *et al.* Specific targeting of tau oligomers in Htau mice prevents cognitive impairment and tau toxicity following injection with brain-derived tau oligomeric seeds. *J. Alzheimers. Dis.* **40 Suppl 1,** S97–S111 (2014).
16. Gendreau, K. L. & Hall, G. F. Tangles, Toxicity, and Tau Secretion in AD - New Approaches to a Vexing Problem. *Front. Neurol.* **4,** 160 (2013).
17. Frost, B., Jacks, R. L. & Diamond, M. I. Propagation of Tau Misfolding from the Outside to the Inside of a Cell. *J. Biol. Chem.* **284,** 12845–12852 (2009).
18. Wu, J. W. *et al.* Small Misfolded Tau Species Are Internalized via Bulk Endocytosis and Anterogradely and Retrogradely Transported in Neurons. *J. Biol. Chem.* **288,** 1856–1870 (2013).
19. Michel, C. H. Extracellular monomeric tau protein is sufficient to initiate the spread of tau protein pathology. *J. Biol. Chem.* **289,** 956–967 (2014).
20. Amadoro, G. *et al.* Role of N-terminal tau domain integrity on the survival of cerebellar granule neurons. *Cell Death Differ.* **11,** 217–30 (2004).
21. LaPointe, N. E. *et al.* The amino terminus of tau inhibits kinesin-dependent axonal transport: implications for filament toxicity. *J. Neurosci. Res.* **87,** 440–51 (2009).
22. Kanaan, N. M. Pathogenic forms of tau inhibit kinesin-dependent axonal transport through a mechanism involving activation of axonal phosphotransferases. *J. Neurosci.* **31,** 9858–9868 (2011).
23. Kanaan, N. M. *et al.* Phosphorylation in the amino terminus of tau prevents inhibition of

anterograde axonal transport. *Neurobiol. Aging* **33,** 826.e15-30 (2012).
24. Sokolow, S. *et al.* Pre-synaptic C-terminal truncated tau is released from cortical synapses in Alzheimer's disease. *J. Neurochem.* **133,** 368–79 (2015).
25. Kim, W., Lee, S. & Hall, G. F. Secretion of human tau fragments resembling CSF-tau in Alzheimer's disease is modulated by the presence of the exon 2 insert. *FEBS Lett.* **584,** 3085–8 (2010).
26. Decker, J. M. Pro-aggregant Tau impairs mossy fiber plasticity due to structural changes and Ca++ dysregulation. *Acta Neuropathol. Commun.* **3,** 23 (2015).
27. Lasagna-Reeves, C. A. *et al.* Alzheimer brain-derived tau oligomers propagate pathology from endogenous tau. *Sci. Rep.* **2,** 700 (2012).
28. Goedert, M. Assembly of microtubule-associated protein tau into Alzheimer-like filaments induced by sulphated glycosaminoglycans. *Nature* **383,** 550–553 (1996).
29. Kampers, T., Friedhoff, P., Biernat, J., Mandelkow, E. M. & Mandelkow, E. RNA stimulates aggregation of microtubule-associated protein tau into Alzheimer-like paired helical filaments. *FEBS Lett.* **399,** 344–9 (1996).
30. Pérez, M., Valpuesta, J. M., Medina, M., Montejo de Garcini, E. & Avila, J. Polymerization of tau into filaments in the presence of heparin: the minimal sequence required for tau-tau interaction. *J. Neurochem.* **67,** 1183–90 (1996).
31. Wilson, D. M. & Binder, L. I. Free fatty acids stimulate the polymerization of tau and amyloid beta peptides. In vitro evidence for a common effector of pathogenesis in Alzheimer's disease. *Am. J. Pathol.* **150,** 2181–95 (1997).
32. Santa-María, I., Hernández, F., Martín, C. P., Avila, J. & Moreno, F. J. Quinones facilitate the self-assembly of the phosphorylated tubulin binding region of tau into fibrillar polymers. *Biochemistry* **43,** 2888–97 (2004).
33. Kumar, S. *et al.* Stages and conformations of the Tau repeat domain during aggregation and its effect on neuronal toxicity. *J. Biol. Chem.* **289,** 20318–32 (2014).
34. Kamenetz, F. *et al.* APP processing and synaptic function. *Neuron* **37,** 925–37 (2003).
35. Cirrito, J. R. *et al.* Synaptic Activity Regulates Interstitial Fluid Amyloid-β Levels In Vivo. *Neuron* **48,** 913–922 (2005).
36. Clavaguera, F. Transmission and spreading of tauopathy in transgenic mouse brain. *Nat. Cell Biol.* **11,** 909–913 (2009).
37. de Calignon, A. *et al.* Propagation of tau pathology in a model of early Alzheimer's disease. *Neuron* **73,** 685–97 (2012).
38. Kfoury, N., Holmes, B. B., Jiang, H., Holtzman, D. M. & Diamond, M. I. Trans-cellular propagation of Tau aggregation by fibrillar species. *J. Biol. Chem.* **287,** 19440–51 (2012).
39. Kim, W. *et al.* Interneuronal transfer of human tau between Lamprey central neurons in situ. *J. Alzheimers. Dis.* **19,** 647–64 (2010).
40. Liu, L. *et al.* Trans-Synaptic Spread of Tau Pathology In Vivo. *PLoS One* **7,** e31302 (2012).
41. Braak, E., Braak, H. & Mandelkow, E. M. A sequence of cytoskeleton changes related to the formation of neurofibrillary tangles and neuropil threads. *Acta Neuropathol.* **87,** 554–567 (1994).
42. Ward, S. M. *et al.* TOC1: characterization of a selective oligomeric tau antibody. *J. Alzheimers. Dis.* **37,** 593–602 (2013).
43. Mufson, E. J., Ward, S. & Binder, L. Prefibrillar tau oligomers in mild cognitive impairment and Alzheimer's disease. *Neurodegener. Dis.* **13,** 151–3 (2014).
44. Spires-Jones, T. L., Stoothoff, W. H., de Calignon, A., Jones, P. B. & Hyman, B. T. Tau pathophysiology in neurodegeneration: a tangled issue. *Trends Neurosci.* **32,** 150–9 (2009).
45. Kopeikina, K. J., Hyman, B. T. & Spires-Jones, T. L. Soluble forms of tau are toxic in Alzheimer's disease. *Transl. Neurosci.* **3,** 223–233 (2012).
46. Mirbaha, H., Holmes, B. B., Sanders, D. W., Bieschke, J. & Diamond, M. I. Tau Trimers Are the Minimal Propagation Unit Spontaneously Internalized to Seed Intracellular Aggregation. *J. Biol. Chem.* **290,** 14893–903 (2015).
47. Holmes, B. B. & Diamond, M. I. Prion-like properties of Tau protein: the importance of extracellular Tau as a therapeutic target. *J. Biol. Chem.* **289,** 19855–19861 (2014).

48. Himmler, A., Drechsel, D., Kirschner, M. W. & Martin, D. W. Tau consists of a set of proteins with repeated C-terminal microtubule-binding domains and variable N-terminal domains. *Mol. Cell. Biol.* **9,** 1381–8 (1989).
49. Hanger, D. P. *et al.* Novel Phosphorylation Sites in Tau from Alzheimer Brain Support a Role for Casein Kinase 1 in Disease Pathogenesis. *J. Biol. Chem.* **282,** 23645–23654 (2007).
50. Hanger, D. P., Betts, J. C., Loviny, T. L., Blackstock, W. P. & Anderton, B. H. New phosphorylation sites identified in hyperphosphorylated tau (paired helical filament-tau) from Alzheimer's disease brain using nanoelectrospray mass spectrometry. *J. Neurochem.* **71,** 2465–76 (1998).
51. Bodenmiller, B. *et al.* PhosphoPep—a database of protein phosphorylation sites in model organisms. *Nat. Biotechnol.* **26,** 1339–1340 (2008).
52. Craig, R., Cortens, J. P. & Beavis, R. C. Open Source System for Analyzing, Validating, and Storing Protein Identification Data. *J. Proteome Res.* **3,** 1234–1242 (2004).
53. Ivanovova, N., Handzusova, M., Hanes, J., Kontsekova, E. & Novak, M. High-yield purification of fetal tau preserving its structure and phosphorylation pattern. *J. Immunol. Methods* **339,** 17–22 (2008).
54. Polydoro, M., Acker, C. M., Duff, K., Castillo, P. E. & Davies, P. Age-dependent impairment of cognitive and synaptic function in the htau mouse model of tau pathology. *J. Neurosci.* **29,** 10741–9 (2009).
55. Andorfer, C. *et al.* Hyperphosphorylation and aggregation of tau in mice expressing normal human tau isoforms. *J. Neurochem.* **86,** 582–90 (2003).
56. Ninan, I. & Arancio, O. Presynaptic CaMKII is necessary for synaptic plasticity in cultured hippocampal neurons. *Neuron* **42,** 129–41 (2004).
57. Antonova, I. *et al.* Rapid increase in clusters of presynaptic proteins at onset of long-lasting potentiation. *Science* **294,** 1547–50 (2001).
58. Schipke, C. G., Prokop, S., Heppner, F. L., Heuser, I. & Peters, O. Comparison of immunosorbent assays for the quantification of biomarkers for Alzheimer's disease in human cerebrospinal fluid. *Dement. Geriatr. Cogn. Disord.* **31,** 139–45 (2011).
59. Mattsson, N. *et al.* The Alzheimer's Association external quality control program for cerebrospinal fluid biomarkers. *Alzheimers. Dement.* **7,** 386–395.e6 (2011).
60. Furukawa, Y., Kaneko, K. & Nukina, N. Tau protein assembles into isoform- and disulfide-dependent polymorphic fibrils with distinct structural properties. *J. Biol. Chem.* **286,** 27236–46 (2011).
61. Tian, H. Trimeric tau is toxic to human neuronal cells at low nanomolar concentrations. *Int. J. Cell Biol.* **2013,** 260787 (2013).
62. Ward, S. M., Himmelstein, D. S., Lancia, J. K. & Binder, L. I. Tau oligomers and tau toxicity in neurodegenerative disease. *Biochem. Soc. Trans.* **40,** 667–71 (2012).
63. Wang, M. S., Zameer, A., Emadi, S. & Sierks, M. R. Characterizing antibody specificity to different protein morphologies by AFM. *Langmuir* **25,** 912–8 (2009).
64. Puzzo, D. *et al.* Picomolar amyloid-beta positively modulates synaptic plasticity and memory in hippocampus. *J. Neurosci.* **28,** 14537–45 (2008).
65. Alamed, J., Wilcock, D. M., Diamond, D. M., Gordon, M. N. & Morgan, D. Two-day radial-arm water maze learning and memory task; robust resolution of amyloid-related memory deficits in transgenic mice. *Nat. Protoc.* **1,** 1671–9 (2006).
66. Fiorito, J. *et al.* Synthesis of quinoline derivatives: discovery of a potent and selective phosphodiesterase 5 inhibitor for the treatment of Alzheimer's disease. *Eur. J. Med. Chem.* **60,** 285–94 (2013).
67. Csokova, N. *et al.* Rapid purification of truncated tau proteins: model approach to purification of functionally active fragments of disordered proteins, implication for neurodegenerative diseases. *Protein Expr. Purif.* **35,** 366–72 (2004).
68. Moran, D., Cross, T., Brown, L. M., Colligan, R. M. & Dunbar, D. Data-independent acquisition (MSE) with ion mobility provides a systematic method for analysis of a bacteriophage structural proteome. *J. Virol. Methods* **195,** 9–17 (2014).
69. Fa, M. *et al.* Preparation of oligomeric beta-amyloid 1-42 and induction of synaptic plasticity

impairment on hippocampal slices. *J. Vis. Exp.* (2010). doi:10.3791/1884
70. Piacentini, R. *et al.* HSV-1 promotes Ca2+ -mediated APP phosphorylation and Aβ accumulation in rat cortical neurons. *Neurobiol. Aging* **32,** 2323.e13-26 (2011).
71. Ripoli, C. *et al.* Intracellular accumulation of amyloid-β (Aβ) protein plays a major role in Aβ-induced alterations of glutamatergic synaptic transmission and plasticity. *J. Neurosci.* **34,** 12893–903 (2014).

Chapter 5: LTP and memory impairment caused by extracellular Aβ and tau oligomers is APP-dependent

Puzzo D[1], Piacentini R[2], Fá M[3], Gulisano W[1], Li Puma DD[2], Staniszewski A[3], Zhang H[3], Tropea MR[1], Cocco S[2], Palmeri A[1], Fraser P[4], D'Adamio L[5], Grassi C[2], Arancio O[6].

[1]Department of Biomedical and Biotechnological Sciences, University of Catania, Catania, Italy. [2]Institute of Human Physiology, Università Cattolica del Sacro Cuore, Rome, Italy. [3]Department of Pathology and Cell Biology and Taub Institute for Research on Alzheimer's Disease and the Aging Brain, Columbia University, New York, United States. [4]Tanz Centre for Research in Neurodegenerative Diseases and Department of Medical Biophysics, University of Toronto, Toronto, Canada. [5]Department of Microbiology and Immunology, Albert Einstein College of Medicine, New York, United States. [6]Department of Pathology and Cell Biology and Taub Institute for Research on Alzheimer's Disease and the Aging Brain, Columbia University, New york, United States.

In: Elife. 2017 Jul 11;6. pii: e26991.
doi: 10.7554/eLife.26991.

Abstract

The concurrent application of subtoxic doses of soluble oligomeric forms of human amyloid-beta (oAβ) and Tau (oTau) proteins impairs memory and its electrophysiological surrogate long-term potentiation (LTP), effects that may be mediated by intra-neuronal oligomers uptake. Intrigued by these findings, we investigated whether oAβ and oTau share a common mechanism when they impair memory and LTP in mice. We found that as already shown for oAβ, also oTau can bind to amyloid precursor protein (APP). Moreover, efficient intra-neuronal uptake of oAβ and oTau requires expression of APP. Finally, the toxic effect of both extracellular oAβ and oTau on memory and LTP is dependent upon APP since APP-KO mice were resistant to oAβ- and oTau-induced defects in spatial/associative memory and LTP. Thus, APP might serve as a common therapeutic target against Alzheimer's Disease (AD) and a host of other neurodegenerative diseases characterized by abnormal levels of Aβ and/or Tau.

Introduction

Protein aggregation and deposition have been considered key pathogenetic processes in several neurodegenerative disorders, including Alzheimer's Disease (AD), tauopathies, Parkinson's Disease, Huntington disease and many others[1,2]. More recently, soluble small aggregates of these proteins have gained a lot of attention in studies aimed at understanding the etiopathogenesis of these diseases. This is particularly evident in AD, in which the abnormal increases of the levels of amyloid-beta (Aβ) and Tau proteins and their aggregation are crucial steps in the chain of events leading to dementia[3,4].

The importance of soluble oligomeric forms of Aβ (oAβ) and Tau (oTau) has been corroborated by numerous evidences demonstrating their presence in human cerebrospinal fluid in healthy individuals and, in higher amounts, in AD patients[5,6]. oAβ and oTau are also toxic to cell-to-cell communication, as they disrupt synaptic plasticity, paving the way to the subsequent cognitive impairment[7–9]. Interestingly, we have recently demonstrated that a brief exposure to a combination of subtoxic doses of extracellular oAβ and oTau dramatically reduces memory and its electrophysiological surrogate long-term potentiation (LTP)[9]. These findings beg the question of whether they act through a common pathway when they impair memory and LTP.

Aβ and Tau share numerous common biochemical features. Both proteins can form insoluble deposits: that is, extracellular amyloid plaques due to the accumulation of Aβ, and intracellular insoluble filaments and neurofibrillary tangles formed by Tau. In addition, Aβ and Tau are present as non-fibrillar soluble monomeric and oligomeric species[7,9,10]. They can be secreted at the synapse in an activity-dependent fashion[9,11–13], and enter neurons[9,14–16]. Moreover, both Aβ and Tau can bind to amyloid precursor protein (APP)[17–21], a protein with a central role in AD pathogenesis that might act as a cell surface receptor[22].

APP, the precursor of Aβ, which derives from sequential cleavage of APP by β-secretase (also known as BACE1) and γ-secretase[23,24], has a central role in AD pathogenesis and might act as both an Aβ precursor and a cell surface receptor[22]. Here

we have postulated that oAβ and oTau involve APP as a common mechanism of action when they impair memory and LTP. This has been investigated through a series of experiments in which we have used APP knock-out (APP-KO) mice and assayed whether suppression of APP function blocks the deleterious effects of both oAβ and oTau onto memory and LTP.

Results

Similar to oAβ, oTau binds to APP

APP has been shown to bind both Aβ and Tau[17–21]. The interaction between oAβ and APP has been thoroughly investigated in studies demonstrating that different species of Aβ (monomers, dimers, oligomers and fibrils) bind to APP[17–20]. However, there is no proof that oTau binds to APP, as previous studies on Tau-APP binding did not use oligomers but fibrils[21,25–27]. We therefore decided to investigate whether the interaction between Tau and APP can be extended to oTau. This was accomplished through two different approaches. In the first one, we utilized membrane fractions from HEK293 cells stably transfected with human APP with the Swedish mutation (APPSw) and incubated with/out oTau derived from recombinant 4R/2N Tau protein. After incubation APP was immuno-precipitated (IP) and the IPs were tested for oTau binding. As shown in Figure 1A, APP co-IPed oTau. In the second approach, as an alternative method to analyze protein-protein interaction dependent upon the presence of endogenous APP, we performed far-WB (fWB) on cultured hippocampal neurons from either wild type (WT) or APP-KO animals. We found that, in lysates from WT cultures, oTau (used as the bait protein) was detected at the molecular weight of APP (~110 KDa) by an anti-Tau antibody (Tau 5). Conversely, this band was not observed in lysates from control APP-KO cultures (Figure 1B), supporting the interaction between murine APP and oTau. Collectively, these experiments demonstrate that oTau is able to bind APP.

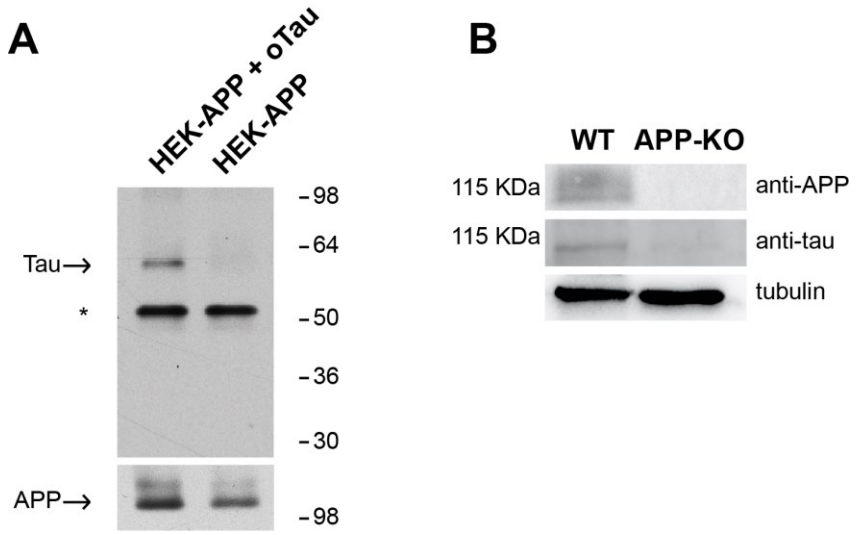

Figure 1. APP binds to oTau. (A) WB with anti-Tau antibodies Tau5 showing oTau co-IPed with APP in HEK293 cells stably transfected with human APP with the Swedish mutation. * corresponds to the heavy chain of the antibody used for IP. (B) Representative data from fWB experiments performed on hippocampal neurons from WT and APP-KO mice, showing interaction between APP and Tau. Tau binding to APP is demonstrated by the presence of bands recognized by Tau5 antibodies at 110 KDa (the molecular weight of APP). Tubulin was used as loading control. n = 3.

Expression of APP is required for efficient intra-neuronal uptake of oAβ and oTau

The similarity between Aβ and Tau can be extended to the entrance of their oligomers into neurons from the extracellular space[9,14–16]. Given that both Aβ and Tau can bind to APP, our next goal was to establish whether APP is needed for oligomer internalization. To address this issue, we treated cultured hippocampal neurons obtained from WT and APP-KO mice with either 200 nM oAβ labeled with HiLyte Fluor 555 (oAβ−555) or 100 nM oTau labeled with IRIS-5 ester dye (oTau-IRIS5) for 20 min and we studied their cellular internalization by high-resolution confocal microscopy using an automated algorithm to detect and count intraneuronal spots. We found that WT neurons internalized much more Aβ and Tau than APP-KO cells. In fact, after extracellular oAβ−555 application, a higher percentage of WT neurons

exhibited Aβ accumulation compared to APP-KO cultures (Figure 2A). Aβ accumulation was found in 91 ± 3% of WT MAP2-positive cells (Figure 2B) and the mean number of intracellular fluorescent spots/neuron was 5.3 ± 0.4 (Figure 2C). When the same treatment was applied to APP-KO cultures we found that 73 ± 5% of total cells internalized Aβ (Figure 2B) and the mean number of fluorescent spots was 2.9 ± 0.2 (Figure 2C). Similar results were obtained when WT and APP-KO neurons were treated with extracellular oTau-IRIS5 (Figure 2D) which was found in 80 ± 6% of WT cells containing 2.7 ± 0.2 fluorescent spots and in 47 ± 6% of APP-KO neurons exhibiting 1.4 ± 0.1 spots (Figure 2E–F). Moreover, to provide a global estimate of the protein uploading into neurons, we performed quantitative analysis of these data through the 'internalization index', which showed a 61% reduction in APP-KO neurons compared to WT cells for oAβ (Figure 2G), and a 69% reduction for oTau (Figure 2H). Notably, the amounts of Aβ and tau oligomers attached to neuronal surface did not significantly differ between WT and APP-KO cells. Specifically, fluorescent Aβ spots were 6.9 ± 0.5 and 6.5 ± 0.6 for WT and APP-KO, respectively (Figure 2I); whereas for Tau they were 4.3 ± 0.4 and 4.0 ± 0.4, respectively (Figure 2J). Collectively, these data show that APP suppression reduces the entrance of extracellular oligomers of both Aβ and Tau into neurons.

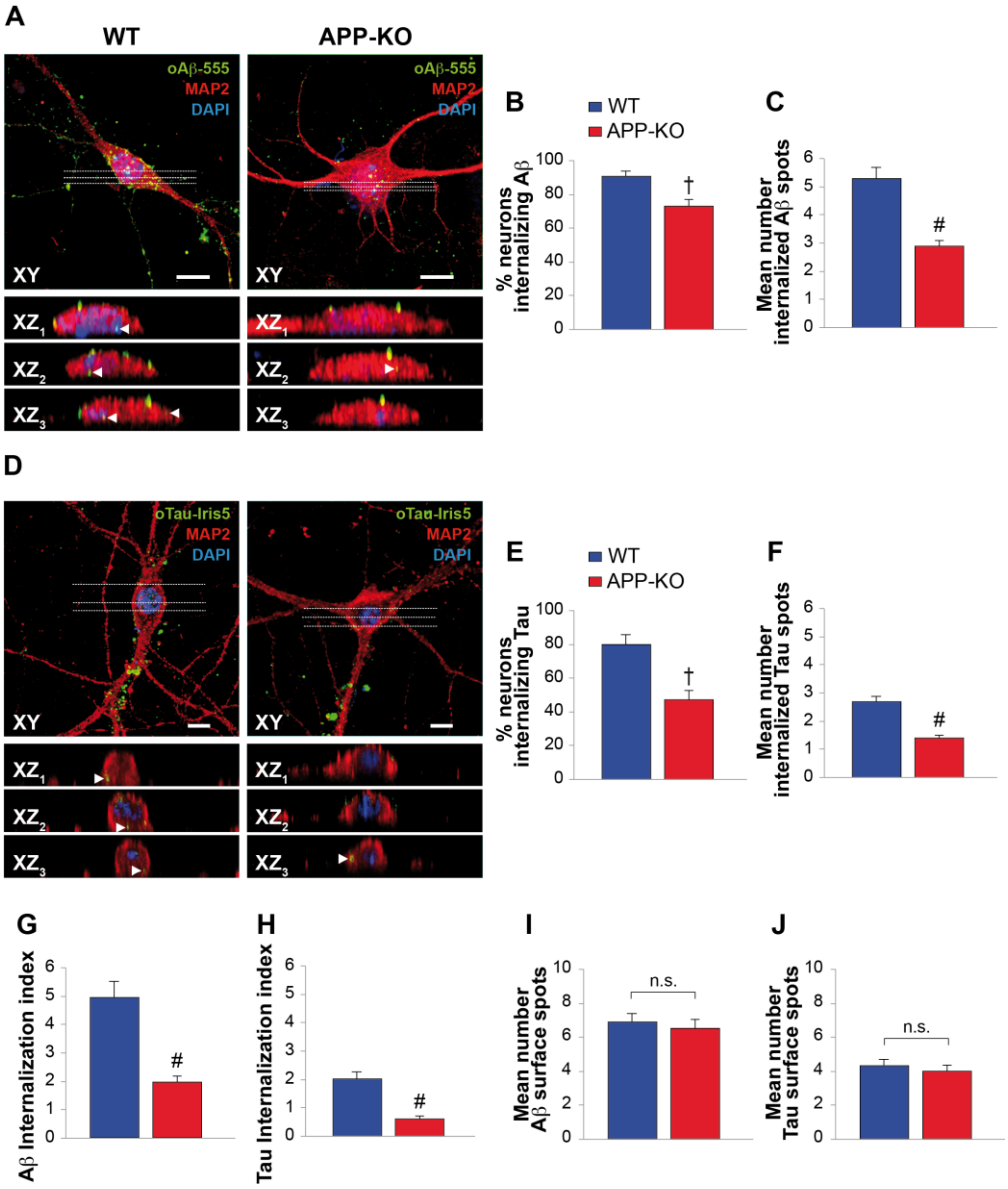

Figure 2. APP suppression reduces internalization of oAβ and oTau into neurons. (A) Representative images of cultured hippocampal neurons (microtubule associated protein-2 (MAP2) positive cells) obtained from either WT or APP-KO mice and treated with 200 nM human oligomeric Aβ42 labeled with HiLyteTM Fluor 555 (oAβ−555) for 20 min and immunostained for MAP-2. Lower images show different XZ cross-sections from the acquired confocal Z-stack referring to the dotted lines numbered as 1–3 in each panel. Arrowheads indicate internalized proteins. Scale bars: 10 µm. (B–C) After 20 min of extracellular oAβ−555 application, the percentage of WT neurons exhibiting Aβ accumulation was 91 ± 3% of total cells (n = 127) and the mean number of intracellular fluorescent spots/neuron was 5.3 ± 0.4. When the same treatment was applied to APP-KO cultures we found that 73 ± 5% of total cells internalized Aβ (n = 112; t test: t(98) = 2.734; p=0.007 comparing APP-KO vs. WT cells) and a markedly lower mean number of fluorescent spots (2.9 ± 0.2; t(191) = 4.508; p<0.0001 comparing APP-KO vs. WT cells). (D) Representative images of WT and APP-KO cultured hippocampal neurons treated with 100 nM IRIS-5-labeled human recombinant oligomeric Tau (oTau-IRIS5) for 20 min. Lower images show different XZ cross-sections from the acquired confocal Z-stack

referring to the dotted lines numbered as 1–3 in each panel. Arrowheads indicate internalized proteins. Scale bars: 10 μm. (E–F) After 20 min of extracellular Tau-IRIS5, the percentage of WT neurons exhibiting Tau was 80 ± 6% of WT cells (n = 88) with 2.7 ± 0.2 fluorescent spots, whereas 47 ± 6% of APP-KO neurons showed Tau internalization (n = 84; $t(71) = 3.945$; $p=0.0002$) with a mean number of fluorescent spots equal to 1.4 ± 0.1 ($t(92) = 4.331$; $p<0.0001$). (G–H) The 'internalization index' shown on the graph was 4.9 ± 0.6 in WT neurons treated with Aβ−555 vs. 1.9 ± 0.2 of APP-KO cells ($t(98) = 5.246$; $p<0.0001$), and 2.0 ± 0.3 in WT neurons treated with Tau-IRIS5 vs. 0.6 ± 0.1 of APP-KO cells ($t(71) = 5.013$; $p<0.0001$). (I) Fluorescent Aβ spots attached to neuronal surface were 6.9 ± 0.5 and 6.5 ± 0.6 for WT and APP-KO, respectively ($t(170) = 0.576$; $p=0.56$). (J) Fluorescent Tau spots attached to neuronal surface were 4.3 ± 0.4 and 4.0 ± 0.4 for WT and APP-KO, respectively ($t(93) = 0.363$; $p=0.72$).

The effect of extracellular oAβ onto memory depends upon the presence of endogenous APP

Neuronal uploading of oAβ from the extracellular space reduces LTP[28], a cellular surrogate of memory. Interestingly, both associative fear memory and spatial memory, two types of memory that are altered in AD patients, are impaired by oAβ[29]. Thus, these effects may require intra-neuronal uptake of oAβ. Since APP is required for efficient uptake of oAβ, we evaluated the effect of oAβ onto two types of memory, assessed through Fear Conditioning and 2 day Radial Arm Water Maze (RAWM), respectively, in the presence or absence of functional APP expression using 3–4 month-old WT and APP-KO mice. Consisting with previous results[30,31], high doses of oAβ (200 nM in a final volume of 1 μl, one injection 20 min prior to the training) infused via bilateral cannulas into the dorsal mouse hippocampi, resulted in reduced freezing 24 hr after the electric shock in WT mice (Figure 3A), confirming that contextual fear memory is altered by high amounts of oAβ. By contrast, in interleaved experiments, memory was spared by the deleterious effects of oAβ in APP-KO mice (Figure 3A). Similarly, APP-KO mice that were infused with vehicle displayed normal memory, as previously shown in KO animals of this age[32] (Figure 3A). We also confirmed that the defect in contextual memory found in WT mice was due to an oAβ-induced hippocampal impairment, whereas cued fear learning, a type of learning depending upon amygdala function[33], was not affected in both WT and APP-KO animals treated with vehicle or oAβ (Figure 3B). Moreover, we excluded that the defect was due to

deficits in mouse capability to perceive the electric shock, as sensory threshold assessment did not reveal any difference among the four groups of mice (Figure 3C).

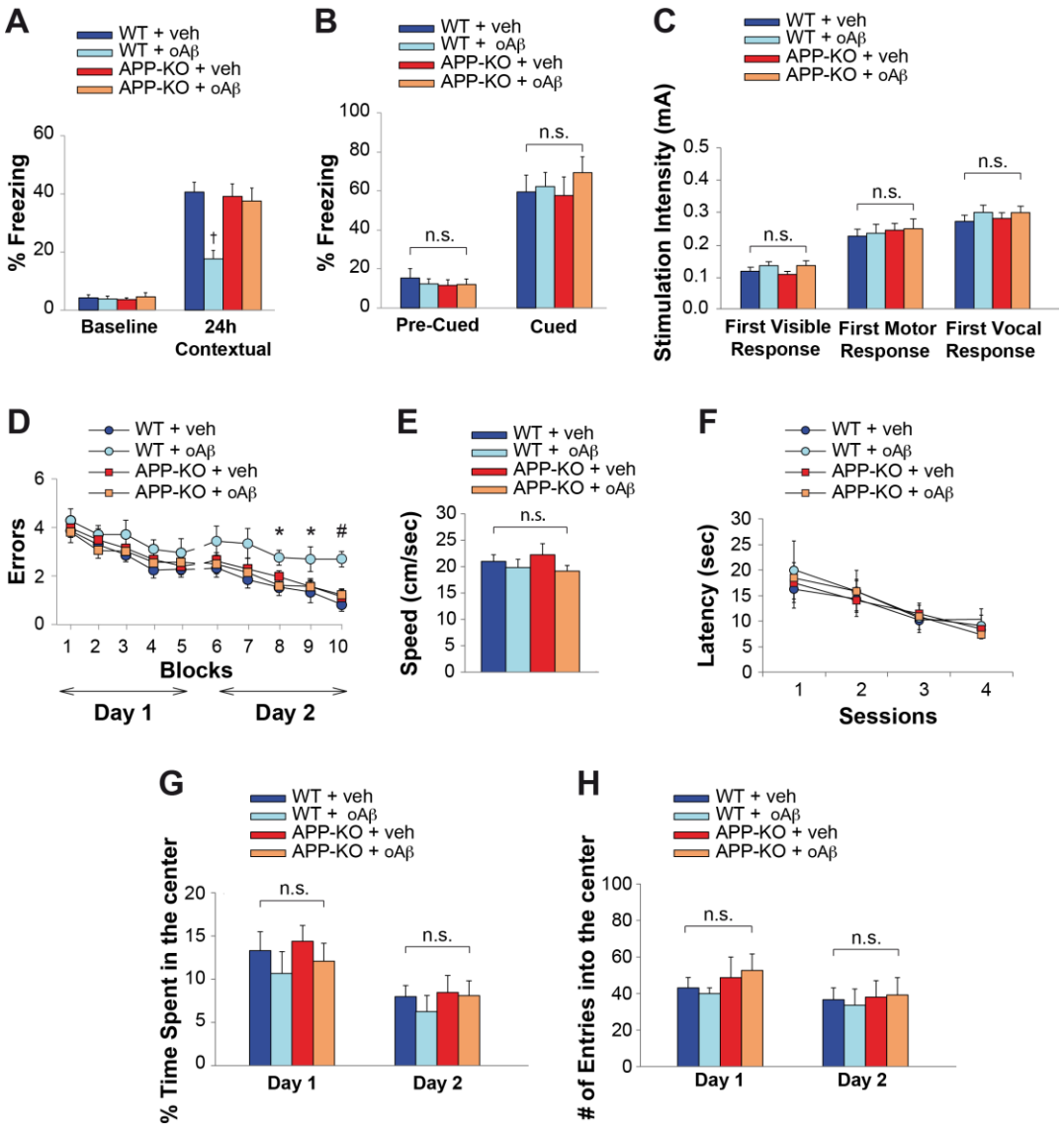

Figure 3. APP is necessary for extracellular oAβ to reduce memory. (A) oAβ (200 nM) impaired contextual memory in WT mice, whereas it did not impair memory in APP-KO mice. n = 11 per condition in this and the following panels. 24 hr: ANOVA $F(3,40) = 8.047$, $p<0.0001$; Bonferroni: WT + vehicle vs. WT + oAβ: † $p<0.001$. (B) Freezing responses before (Pre) and after (Post) the auditory cue were the same among vehicle- and oAβ-infused APP-KO mice as well as vehicle- and oAβ-infused WT littermates in the cued conditioning test. ANOVA Pre-Cued: $F(3,40) = 0.242$, $p=0.867$; Cued: $F(3,40) = 0.372$, $p=0.774$. (C) No difference was detected among the four groups during assessment of the sensory threshold. ANOVA for repeated measures $F(3,40) = 0.626$, $p=0.602$. (D) oAβ (200 nM) impaired the RAWM performance in WT mice whereas it did not impair the performance in APP-KO mice. ANOVA for repeated measures (day 2) $F(3,40) = 5.297$, $p=0.004$. WT + vehicle vs. WT + oAβ: *$p<0.05$ for block 8 and 9, and # $p<0.0001$ for block 10. (E–F) Testing with the visible platform task for

assessment of visual-motor-motivational deficits did not reveal any difference in average speed [ANOVA: $F(3,40) = 0.899$, $p=0.450$] (E), and time to reach the visible platform [ANOVA for repeated measures $F(3,40) = 0.05$, $p=0.985$] (F) among the four groups. (G–H) Open field testing showed a similar percentage of time spent in the center compartment [ANOVA for repeated measures $F(3,40) = 0.692$ $p=0.489$] (G) and the number of entries into the center compartment [ANOVA for repeated measures $F(3,40) = 0.332$, $p=0.802$] (H) in vehicle- and oAβ-infused APP-KO mice as well as vehicle- and oAβ-infused WT littermates, indicating that they had no differences in exploratory behavior.

We then evaluated short-term spatial memory with the RAWM. As previously shown[31], WT mice infused with oAβ (200 nM in a final volume of 1 µl, one injection 20 min prior to the first trial of RAWM training in day one and two, bilaterally) made a higher number of errors than vehicle-infused WT littermates during the second day of RAWM testing (Figure 3D). By contrast, the performance of APP-KO mice, which was normal when these animals were infused with vehicle, was not affected by the Aβ infusion (Figure 3D). Control trials with a visible platform did not show any difference in speed or latency to reach the platform among the four groups, indicating that oAβ infusion did not affect the motility, vision and motivation of mice during RAWM testing (Figure 3E–F). Moreover, open field testing did not reveal any difference among WT and APP-KO mice treated with vehicle or oAβ, indicating that mouse exploratory behavior, which might affect animal performance in the memory task, was not affected by treatment or genotype (Figure 3G–H). Collectively, these experiments indicate that the deleterious effect exerted by oAβ on memory is dependent upon the presence of endogenous APP.

The effect of extracellular oTau onto memory depends upon the presence of endogenous APP

Both associative fear memory and spatial memory are impaired not only by oAβ, but also by oTau[9]. As shown before, oTau binds APP and needs APP for an efficient entrance into neurons, just like oAβ. Thus, we tested if, similar to oAβ, exogenous oTau requires APP to alter memory. As previously demonstrated[9], oTau infusion (500 nM in a final volume of 1 µl, two injections bilaterally at 180 and 20 min prior to the electric shock for fear conditioning or the first trial of the RAWM training in day one and two)

affected the two forms of memory in WT animals (Figure 4A and Figure 4D). By contrast, APP-KO mice displayed normal performance when they were infused with oTau both in the fear conditioning and RAWM tests (Figure 4A and Figure 4D). Moreover, we did not observe any behavioral differences between groups of mice tested for cued conditioning (Figure 4B), sensory threshold (Figure, Figure 4), visible platform (Figure 4E and F) or open field (Figure 4G and H). Thus, as for oAβ, the impairment of memory induced by oTau was dependent upon the presence of APP.

APP is necessary for extracellular oAβ and oTau to reduce LTP

LTP represents a cellular correlate of learning and memory[34]. It is reduced after treatment with both high amounts of oAβ and/or oTau[9]. Hence, we checked whether APP is needed for oAβ and oTau to impair LTP at the CA3-CA1 synapses. Following recording of basal synaptic transmission (BST), which did not reveal any difference between WT and APP-KO slices (Figure 5A), slices were perfused with oAβ, or oTau, or vehicle prior to eliciting LTP through a theta-burst stimulation. As previously demonstrated[35], perfusion with oAβ (200 nM for 20 min before the tetanus) reduced LTP in slices from WT mice (Figure 5B). However, consistent with the behavioral results, the peptide did not impair LTP in slices from APP-KO littermates (Figure 5B). Similarly, oTau (100 nM for 20 min before tetanus) reduced LTP in WT slices but not in APP-KO slices (Figure 5C).

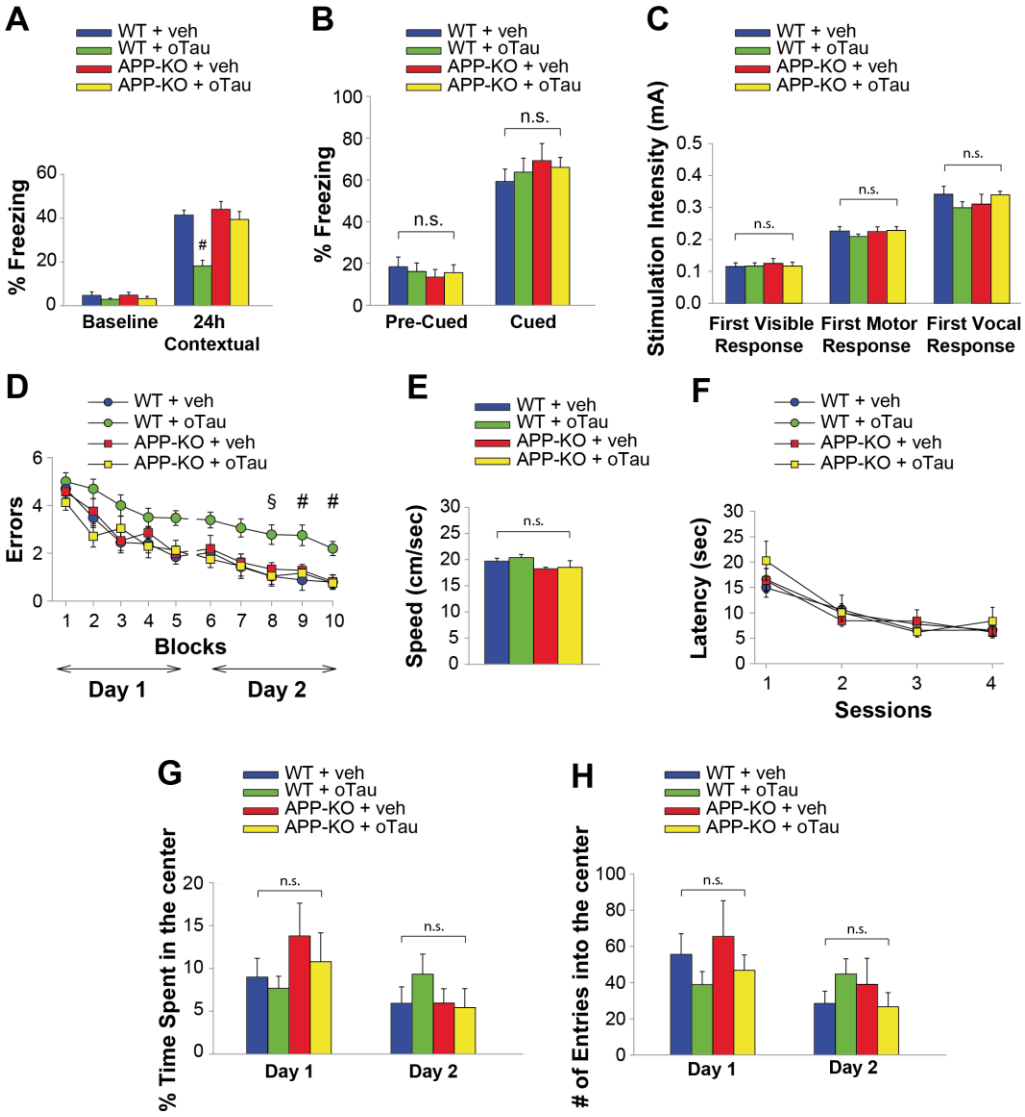

Figure 4. APP is necessary for extracellular oTau to reduce memory. (A) oTau (500 nM) impaired contextual memory in WT mice, whereas it did not impair contextual memory in APP-KO mice. 24 hr: ANOVA $F(3,38) = 18.472$, $p<0.0001$; Bonferroni: WT + vehicle vs. WT + oTau: # $p<0.0001$. WT + vehicle: n = 11, WT + oTau: n = 12, APP-KO + vehicle: n = 8, APP-KO + oTau: n = 11. (B) Freezing responses before (Pre) and after (Post) the auditory cue were the same among the four groups shown in A in the cued conditioning test. ANOVA Pre-cued: $F(3,38) = 0.215$, $p=0.885$; Cued: $F(3,38) = 0.410$, $p=0.747$. (C) No difference was detected among the four groups shown in A during assessment of the sensory threshold. ANOVA for repeated measures $F(3,38) = 0.643$, $p=0.592$. (D) oTau (500 nM) impaired the RAWM performance in WT mice whereas it did not impair the performance in APP-KO mice. ANOVA for repeated measures (day 2) $F(3,34) = 11.309$, $p<0.0001$. WT + vehicle vs. WT + oTau: § $p<0.005$ for block 8, and # $p<0.001$ for block 9 and 10. WT + vehicle: n = 11, WT + oTau: n = 12, APP-KO + vehicle: n = 7, APP-KO + oTau: n = 8. (E–F) Testing with the visible platform task for assessment of visual-motor-motivational deficits for animals shown in D did not reveal any difference in average speed [ANOVA: $F(3,34) = 1.532$, $p=0.224$] (E) and time to reach the visible platform

[ANOVA for repeated measures: F(3,34) = 0.221, p=0.881] (F) among the four groups. (G–H) Open field testing for the same animals as in D showed a similar percentage of time spent in the center compartment [ANOVA for repeated measures F(3,34) = 0.190, p=0.902] (G) and the number of entries into the center compartment [ANOVA for repeated measures F(3,34) = 0.354, p=0.787] (H) in vehicle- and oTau-infused APP-KO mice as well as vehicle- and oTau-infused WT littermates, indicating that they had no differences in exploratory behavior.

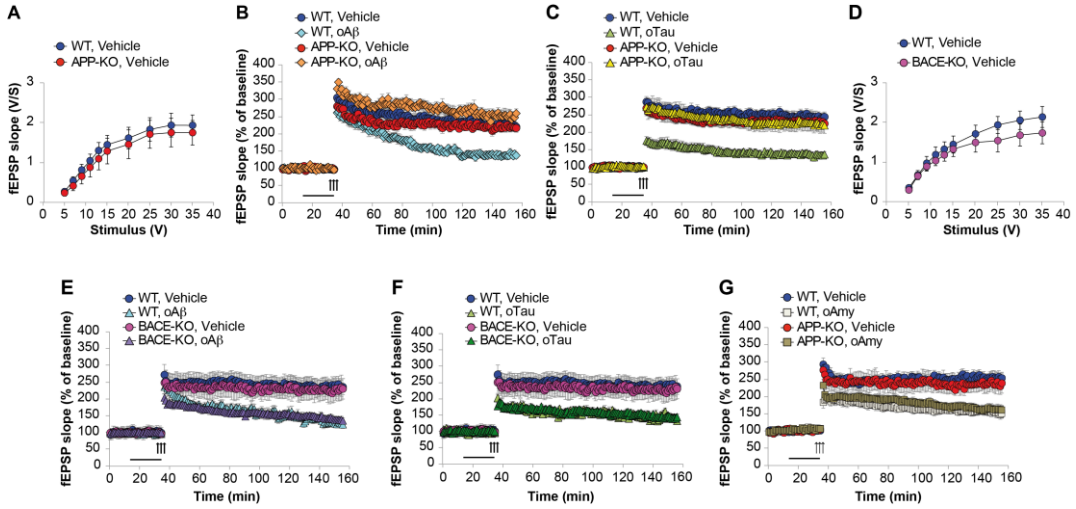

Figure 5. APP is necessary for extracellular oAβ and oTau to reduce LTP. (A) Basal synaptic transmission (BST) at the CA3-CA1 connection in slices from 3- to 4-month-old APP-KO mice was similar to WT littermates (n = 18 slices from WT vs. 18 slices from APP-KO; ANOVA for repeated measures F(1,34) = 0.416, p=0.524). (B) LTP was impaired in hippocampal slices from WT mice perfused with oAβ (200 nM), whereas there was no impairment in slices from APP-KO littermates. ANOVA for repeated measures F(3,30) = 19.738, p<0.0001. WT + vehicle vs. WT + oAβ: F(1,16) = 29.393, p<0.0001. WT + vehicle vs. APP-KO + oAβ: F(1,13) = 3.297, p=0.093. WT + vehicle: n = 9, WT + oAβ: n = 9, APP-KO + vehicle: n = 10, APP-KO + oAβ: n = 6. (C) LTP was impaired in hippocampal slices from WT mice perfused with oTau (100 nM), whereas there was no impairment in slices from APP-KO littermates. ANOVA for repeated measures F(3,35) = 11.033, p<0.0001. WT + vehicle vs. WT + oTau: F(1,16) = 50.543, p<0.0001. WT + vehicle vs. APP-KO + oTau: F(1,16) = 0.382, p=0.575. WT + vehicle: n = 8, WT + oTau: n = 10, APP-KO + vehicle: n = 11, APP-KO + oTau: n = 10. (D) CA3-CA1 BST in slices from 3- to 4-month-old BACE1-KO mice was similar to WT littermates (n = 24 slices from WT vs. 26 slices from BACE-KO; ANOVA for repeated measures F(1,48) = 0.714, p=0.402). (E) LTP was impaired in hippocampal slices from both WT and BACE-KO mice perfused with oAβ (200 nM). ANOVA for repeated measures F(3,29) = 5.738, p=0.003. WT + vehicle vs. WT + oAβ: F(1,14) = 23.663, p<0.0001. WT + vehicle vs. BACE-KO + oAβ: F(1,14) = 38.295, p<0.0001. WT + vehicle: n = 8, WT + oAβ: n = 8, BACE-KO + vehicle: n = 9, BACE-KO + oAβ: n = 8. F) LTP was impaired in hippocampal slices from both WT and BACE-KO mice perfused with oTau (100 nM). ANOVA for repeated measures F(3,30) = 6.919, p=0.001. WT + vehicle vs. WT + oTau: F(1,14) = 33.230, p<0.0001. WT + vehicle vs. BACE-KO + oTau: F(1,15) = 36.9961, p<0.0001. WT + oTau: n = 8, BACE-KO + oTau: n = 9. G) LTP was impaired in hippocampal slices from both WT and APP-KO

mice perfused with oAmy (200 nM). ANOVA for repeated measures $F(3,38) = 8.900$, $p<0.0001$. WT + vehicle vs. WT + oAmy: $F(1,21) = 34.694$, $p<0.0001$. WT + vehicle vs. APP-KO + oAmy: $F(1,19) = 19.277$, $p<0.0001$. WT + vehicle: n = 11, WT + oAmy: n = 12, APP-KO + vehicle: n = 9, APP-KO + oAmy: n = 10.

Next, we checked whether the amyloidogenic processing of APP is required for oAβ and oTau toxicity. This was determined by using mice deficient in BACE1[36]. In previous WB analysis of these mice we had confirmed that they do not express BACE1 protein and have impaired β-processing of APP[37]. BST recording did not reveal any difference between WT and BACE1-KO slices (Figure 5D). Slices perfusion with oAβ (200 nM for 20 min before the tetanus), or oTau (100 nM for 20 min before tetanus), or vehicle showed that, similar to WT mice, oAβ and oTau reduced LTP in slices from BACE1-KO mice (Figure 5E). Thus, these experiments demonstrate that APP processing is not involved in the toxicity of extracellularly-applied Aβ and Tau.

Finally, we asked whether the APP-dependence for the negative effects of oAβ and oTau onto LTP is specific to these oligomers, or a broader property of APP with β-sheet, oligomer forming proteins. To address this question, we selected human amylin (Amy), an amyloid protein of 37 amino-acids differing from Aβ42 in its primary sequence, but sharing with it the ability to form β-sheets and oligomerize[38]. Amy crosses the blood brain barrier[39], and has a profile of neurotoxicity that is strikingly similar to that of Aβ[40], including the marked reduction of LTP[41]. As previously demonstrated[41], perfusion of hippocampal slices for 20 min with 200 nM oligomeric Amy (oAmy) produced a marked reduction of LTP in WT slices (Figure 5G). The same impairment of LTP was observed in slices from APP-KO mice (Figure 5G); thus, different than oTau and oAβ, oAmy does not require APP for its negative effect on synaptic plasticity. Collectively, these experiments suggest that a brief exposure to both oAβ or oTau, but not oAmy, needs the presence of endogenous APP to impair LTP.

Discussion

Protein aggregate accumulation in the brain is a common feature to neurodegenerative diseases, each disease displaying specific aggregating proteins and aggregate distribution. Oligomers of these proteins are gaining a lot of attention because they are likely to be involved in the cell-to-cell propagation of the pathology, and look more acutely toxic than large insoluble aggregates. For instance, in AD, oligomers of both Aβ and Tau have been shown to produce an immediate reduction of synaptic plasticity and memory when extracellularly applied[9]. Intriguingly, the negative effects of oAβ and oTau occurred not only with high concentrations of Aβ or Tau alone, but also when sub-toxic doses of oAβ were combined with sub-toxic doses of oTau[9]. These observations inspired the experiments shown in this manuscript. Here, we demonstrate that the suppression of APP, to which both oAβ and oTau can bind, causes a marked reduction of the oligomer entrance into neurons. Most importantly, we have found a common mechanism of action for extracellular Aβ and Tau oligomers, whose deleterious effect on LTP and memory depends upon the presence of endogenous APP. Our finding that extracellular oAβ requires APP to impair synaptic plasticity and memory is consistent with previous studies showing that Aβ neurotoxicity might be mediated by APP, as suggested by the reduced vulnerability towards Aβ of cultured APP null neurons or mutated APP cells[17,19]. This finding is also consistent with the observation that the presence of APP is likely to contribute to hippocampal hyperactivity, which has been suggested as a key mechanism of disease etiopathogenesis both in AD animal models and patients[42–46]. Along with these studies, APP has been demonstrated to bind Aβ monomers and dimers leading to activity-dependent APP-APP conformational changes that enhance neurotransmitter release[20]. When Aβ is accumulating in the brain, this increase of release probability might induce hippocampal hyperactivity resulting in failure of synaptic plasticity and memory loss[47]. Another interesting finding in our studies is that extracellular oTau requires APP to impair synaptic plasticity and memory. In support of this observation a few studies published several years ago, prior to the introduction of the concept of Tau oligomers,

supported a direct interaction between APP and Tau[25–27]. Moreover, recently, APP has been involved in the uptake of Tau fibrils into cells influencing Tau intracellular aggregation and spreading in the brain[21].

The dependence for the presence of APP shared by both oAβ and oTau in order to impair synaptic plasticity, suggests that APP is a key molecule involved in a common mechanism by which extracellular oAβ and oTau interfere with second messenger cascades relevant to memory formation. Indeed, Aβ and Tau share numerous biochemical characteristics and previous studies have suggested a possible common toxicity mechanism[48]. Both peptides are β-sheet forming proteins, which explains their propensity for oligomerization and close association with membrane. Furthermore, both peptides can bind APP, a protein with structural similarities to type I transmembrane receptors, that might act as a cell surface receptor.

APP is also the precursor of Aβ[49], which derives from sequential cleavage by γ- and β-secretases. We have therefore asked whether the toxicity of extracellular Aβ and Tau oligomers depends upon this amyloidogenic processing of APP. To this end we have used mice deficient in BACE1, the enzyme that initiates the amyloidogenic cascade. We found that BACE1-deficient mice are susceptible to the synapto-toxicity of oAβ and oTau in a similar fashion as WT littermates. Thus, amyloidogenic APP cleavage is not required for the impairment of LTP by the oligomers.

We also found that the APP dependence for the negative effect of oAβ and oTau onto LTP is specific to these proteins. This observation is consistent with the fact that both proteins are involved in AD. This conclusion derived from the experiments in which oAmy was capable of reducing LTP in APP-KO slices. Nevertheless, one cannot exclude that other β-sheet forming proteins besides Aβ and Tau require APP to impair synaptic plasticity. Regardless, the finding that Aβ and Tau share APP as a common mechanism for impairing LTP and memory is relevant and provides a common etiopathogenetic mechanism for their involvement in AD.

Our data are consistent with the hypothesis that APP serves as a common, direct molecular target for extracellular oAβ and oTau to impair LTP and memory. This is supported by the demonstration that both oAβ and oTau bind to APP. However, our

experiments do not conclusively demonstrate that oligomer binding to APP is the cause of LTP and memory reduction, nor we can rigorously exclude the possibility that the two types of oligomers act on additional targets. For instance, it has been demonstrated that heparan sulfate and heparin sulphate proteoglycans bind with Aβ and Tau[50,51] and mediate their internalization and neurotoxicity[50,52,53]. Given that APP and heparan sulfate proteoglycans are likely to interact at the plasma membrane[54] and proteoglycans are rapidly degraded in the absence of proteins belonging to the APP superfamily[55] proteoglycan degradation in the absence of APP might block the toxic action of oAβ and oTau. Nevertheless, the main observation of this manuscript showing that extracellular oAβ and oTau disrupt molecular mechanisms of synaptic plasticity and memory via APP is clear and has relevant implications for understanding AD etiopathogenesis.

We have found that suppression of APP reduces oAβ and oTau entrance into cells. This observation combined with the finding that intracellular perfusion with 6E10 antibodies recognizing the sequence 1–16 of human Aβ42, rescues the LTP block by extracellular human oAβ[28], supports the hypothesis that, at least for oAβ, APP-dependent uploading of extracellular oligomers plays a critical role the impairment of synaptic plasticity, and presumably memory. APP might permit the entrance of the peptides into cells either directly into the cytosol or within vesicles during endocytosis, after which molecular mechanisms of learning and memory are impaired. A direct entrance into the cytosol might occur if APP functions as a channel through which the two oligomers both with a diameter in the low nm range[9,56] enter cells. In agreement with this hypothesis, it has been reported that APP forms a non-selective channel when injected in Xenopus oocytes[57]. A variant on this hypothesis is that APP permits the formation of pores/channels by the oligomers, as ion conductance across lipid bilayers is increased by oligomers of several different amyloids[58], which affect the permeability of the plasma membrane, leading to elevation of intracellular [Ca2+] and toxic changes. With this regard, Aβ has been reported to form large conductance, non-specific ion channels[59]. The endocytotic mechanism, in turn, is supported by the demonstration that

full-length APP is a transmembrane protein, which is endocytosed from the cell surface into endosomes[60] and by studies showing endocytosis of Tau[16].

Another aspect of our experiments is that APP suppression does not appear to dramatically affect the number of MAP2-positive cells taking up Aβ (only ~80% of WT cells), but does reduce the number of intracellular aggregates for the peptide per neuron (~55% of WT cells), whereas APP suppression clearly affects both the number of cells taking up Tau (~50%) and the number of intracellular aggregates for oTau (~52%). These findings open the question of whether the number of cells taking up oligomers and the amount of intracellular aggregates may reflect two different processes, i.e., uptake and degradation/clearance of aggregates. This is an interesting possibility that might explain our observations. Of note, to date there is no data showing that APP is involved in modulation of Aβ/Tau clearance. Nevertheless, it would be interesting in future experiments to explore whether mechanisms controlling protein degradation/clearance in neurons are regulated by APP.

Albeit the experiments on oligomer entrance support the hypothesis that APP serves as a Trojan horse for oAβ and oTau to enter neurons prior to impairing second messenger cascades relevant to synaptic plasticity and memory formation, they do not exclude an alternative scenario in which oligomer interaction with APP activates the intracellular segment of APP, AID/AICD, triggering a cascade of events leading to derangement of memory mechanisms. In support of this hypothesis, it has been shown that phosphorylation of the intracellular threonine 668 of APP mediates synaptic plasticity deficits and memory loss[61]. Moreover, the AID/AICD fragment of APP could form a multimeric complex with the nuclear adaptor protein Fe65 and the histone acetyltransferase Tip60, potentially stimulating transcription[62]. If so, the entrance of the oligomers might serve other purposes rather than impairing synaptic plasticity and memory. For instance, it has been suggested that Tau entrance leads to propagation of Tau misfolding[14]. Nevertheless, our findings that APP is necessary for impairment of LTP and memory following elevation of Aβ and Tau is still relevant, as it sheds light into how the oligomers cause memory loss in AD and other neurodegenerative disorders.

The prevailing hypothesis in the AD field is that Aβ triggers Tau pathology. Our data, however, do not support this hypothesis in which Aβ and Tau are placed in series but suggest a different scenario in which extracellular Aβ and Tau oligomers act in parallel, both through APP. Interestingly, this hypothesis would also explain why tauopathies result in neuronal loss similar to AD but in the absence of Aβ. The identification of the common biochemical neuronal modifications occurring after the APP involvement and underlying the derangement of the molecular mechanisms of gene transcription involved in memory formation, is beyond the scope of the present manuscript. Nevertheless, our findings are translationally significant, as they have permitted the identification of a common molecule, APP, which might be therapeutically targeted at sites serving for direct interaction with Aβ and Tau oligomers or, alternatively, with proteins downstream of such oligomers, other than the classical β- and γ-secretase sites.

Materials and methods

Animals

All protocols involving animals were approved by Columbia University (#AC-AAAO5301), Università di Catania (#327/2013-B, #119–2017-PR), Università Cattolica del Sacro Cuore (#626–2016-PR), Albert Einstein College of Medicine (#20160407), and the respective Institutional Animal care and Use Committee (IACUC); experiments involving animals were performed in accordance with the relevant approved guidelines and regulations. C57BL/6J (RRID:IMSR_JAX:000664) and App-KO (Jackson Lab B6.129S7-Apptm1Dbo/J; RRID:IMSR_JAX:004133) mice and their littermates were obtained from breeding colonies kept in the animal facility of Columbia University, Università di Catania, and Università Cattolica del Sacro Cuore. Bace1-KO mice[36] and their WT littermates were obtained from a breeding colony kept at Albert Einstein College of Medicine which derived from mice that were originally donated by Dr. Vassar at Northwestern University. They were 3–4 months of age except newborn mice for cell cultures. Both sexes were used. All mice were maintained on a 12 hr light/dark cycle (lights on at 6:00 AM) in temperature and humidity-controlled rooms; food and water were available ad libitum.

Oligomer preparation

Tau oligomers

Human Tau preparation and oligomerization was obtained as described previously with slight modifications[9]. Briefly, a recombinant Tau 4R/2N construct containing C-terminal 6x His-tag was transfected in Escherichia coli (Rosetta). Cells were streaked on LB agar ampicillin plates and a single colony was picked and grown overnight in a shaker at 37°C in 100 ml Expansion Broth (Zymo Research) and 300 ml Overexpression Broth (Zymo Research). Cells were pelleted at 4 ˚C by centrifugation at 6000 × g. After a freeze-thaw cycle, cells were lysed in a 2% Triton X-100 PBS and with a protease inhibitor mixture (Complete, EDTA-free; Roche Diagnostics). Streptomycin sulfate was added to precipitate DNA. After incubation for 5 min

at 4°C followed by sonication, the preparation was heated at 100°C for 15 min, and centrifuged to remove the precipitate. TCEP-HCl (ThermoScientific) and 1% perchloric acid were added to the supernatant prior to neutralizing it with 1N NaOH, and placing it in a Pierce protein concentrator (PES, 30K MWCO) (ThermoScientific) to be centrifuged at 4000 × g. The resulting supernatant was loaded on His-Spin Protein Miniprep columns (Zymo Res.) and eluted with phosphate buffer containing 300 mM NaCl plus 250 mM imidazole. Eluted tau was then treated with TCEP-HCl and EDTA, and incubated at room temperature (RT) for 1 hr. Oligomerization buffer was next added to the treated eluted Tau prior to centrifuging it in a PES at 4000 × g. Oligomerization was achieved via introduction of disulfide bonds through incubation with 1 mM H2O2 at room RT for 20 hr, followed by centrifugation in a PES at 4000 × g. The resulting material was used for our experiments. Tau protein concentration was determined from the absorption at 280 nm with an extinction coefficient of 7450 cm−1 M−1.

Aβ oligomers

Human Aβ42 oligomerization was obtained as described previously[31,35]. Briefly, a protein film was prepared by dissolving Aβ42 lyophilized powder (Biopolymer Laboratory, UCLA, CA, USA or American Peptide, CA, USA) in 1,1,1,3,3,3-Hexafluoro-2-Propanol (HFIP) and subsequent incubation for 2 hr at RT to allow complete monomerization. The Aβ film was dissolved in dimethylsulfoxide (DMSO), sonicated for 15 min, aliquoted, and stored at −20°C. To oligomerize the peptide, phosphate buffered saline (PBS) was added to an aliquot of DMSO-Aβ to obtain a 5 mM solution that was incubated for 12 hr at 4°C. This oligomerized Aβ solution was then diluted to the final concentration of 200 nM in artificial cerebrospinal fluid (ACSF) composed as following: 124.0 NaCl, 4.4 KCl, 1.0 Na2HPO4, 25.0 NaHCO3, 2.0 CaCl2, 2.0 MgCl2 in mM.

Amylin oligomers

Human Amy oligomerization was obtained as described previously[28]. Briefly, a protein film was prepared by dissolving Amy lyophilized powder (Anaspec, CA, USA) in HFIP and subsequent incubation for 2 hr at RT to allow complete monomerization. The Amy film was dissolved in DMSO, sonicated for 15 min, aliquoted, and stored at −20°C. To oligomerize the peptide, PBS was added to an aliquot of DMSO-Amy to obtain a 5 mM solution that was incubated for 12 hr at 4°C. This oligomerized Amy solution was then diluted to the final concentration of 200 nM in ACSF.

Co-Immunoprecipitation

WT and APP695 with the Swedish mutation (APPSw) overexpressing human embryonic kidney (HEK293; RRID:CVCL_0045) cells were used to examine the molecular interaction between Tau oligomers and APP. HEK293 cells were originally obtained from ATCC and verification of the cell line was validated by STR profiling (see; https://www.atcc.org/Products/All/CRL-1573.aspx#specifications). Testing for potential mycoplasma was performed using Hoechst 33258 as a marker for indirect DNA fluorescent staining (protocol described at: http://www.sigmaaldrich.com/technical-documents/protocols/biology/testing-for-mycoplasma0.html).

APPSw and untransfected cells were maintained in DMEM supplemented with 10% fetal bovine serum. Membrane fractions were prepared by homogenizing cells in buffer (5 mM HEPES pH 7.4, 1 mM EDTA, 0.25 M sucrose, protease inhibitor cocktail). Extracts were clarified by centrifugation (1000 × g, 5 min, 4°C) and membrane fractions were obtained by centrifuging supernatant (100,000 × g, 1 hr, 4°C). Membranes from control (endogenous APP only) and APPSw expressing cells were solubilized under mild conditions (25 mM HEPES pH

7.4, 150 mM NaCl, 2 mM EDTA, 1% CHAPSO, protease inhibitor cocktail), diluted to 0.5% CHAPSO - to maintain normal lipidation of APP and native protein conformation - and incubated with Tau 4R/2N oligomers (10 µg, 3–4 hr, 4°C). Samples (1.11 mg total protein) were incubated with a monoclonal antibody directed to the APP C-terminal domain (C1/6.1[63]); 5 µg, 2 hr) and immunoprecipitated using Protein G-Sepharose. Non-specific bound proteins were removed by successive washing with lysis buffer. Immunoprecipitated APP complexes were eluted with Laemmli buffer, resolved by SDS-PAGE (4–12% Bis-Tris gels, BioRad) and probed for Tau using Tau-5 antibodies (1:1,000) and APP-CTF (C1/6.1) to confirm the immunoprecipitation efficiency as well as the interaction.

Far western blotting (fWB)

APP-Tau interaction was detected performing fWB as previously described[64]. Hippocampal neurons were lysed in cold RIPA buffer containing 1 mM phenylmethylsulfonyl fluoride, phosphatase and protease inhibitor mixtures (Sigma) and 0.1% sodium dodecyl sulfate. After incubation for 30 min on ice and centrifugation (10,000 × g for 30 min at 4°C), the supernatant was removed and protein concentration was determined using the Bio-Rad protein assay. Each protein sample (30 µg) was separated on 8% SDS-polyacrylamide gel and blotted onto nitrocellulose membranes (Millipore Co., Bedford, MA). The blotted proteins were then denatured with guanidine–HCl and then renatured by gradually reducing guanidine concentration (from 6 to 0 M). The last renaturing step with the guanidine-HCl-free buffer was maintained overnight at 4°C. The membrane was blocked with 5% nonfat dry milk in TBS, 1% tween-20 (TBST) for 1 hr at RT and then incubated overnight at 4°C with 10 µg of purified 'bait' protein oTau. After three washes with TBST, the membrane was incubated with one of the following primary antibodies for 1 hr a RT in 3% milk in the TBST buffer: anti Tau Ab-2 (clone Tau-5, Thermo Fisher Scientific, Waltham, MA). Membranes were then stripped by heating at 56°C in 62.5 mM Tris-HCl, pH 6.7, with 100 mM 2-mercaptoethanol and 2% SDS and re-incubated with anti APP-C terminus (Sigma) to check whether Tau and APP are on the same position on the membrane. Blots were developed with the Pierce ECL Plus Western Blotting Substrate (Thermo Fisher Scientific) and visualized using UVItec Cambridge Alliance. The BenchMark Pre-Stained Protein Ladder (Invitrogen) was used as molecular mass standards.

Assessment of oligomers entrance into neurons

Primary hippocampal neuronal cultures

Primary cultures of hippocampal neurons were obtained from C57BL/6J mice (WT), and B6.129S7-Apptm1Dbo/J (APP KO) mice as previously described[65,66]. Briefly, hippocampi dissected from the brain of E18 mice embryos were incubated for 10 min at 37°C in PBS containing trypsin-ethylenediaminetetraacetic acid (0.025%/0.01% wt/vol; Biochrom AG, Berlin, Germany), and the tissue was then mechanically dissociated at RT with a fire-polished Pasteur pipette. The cell suspension was harvested and centrifuged at 235 × g for 8 min. The pellet was suspended in 88.8% Minimum Essential Medium (Biochrom), 5% fetal bovine serum, 5% horse serum, 1% glutamine (2 mM), 1% penicillin-streptomycin-neomycin antibiotic mixture (Invitrogen, Carlsbad, CA), and glucose (25 mM). Cells were plated at a density of 105 cells on 20 mm coverslips (for immunocytochemical studies) and 106 cells/well on 35 mm six-well plates (for fWB studies), precoated with poly-L-lysine (0.1 mg/mL; Sigma, St. Louis, MO). Twenty-four hours later, the culture medium was replaced with a mixture of 96.5% Neurobasal medium (Invitrogen), 2% B-27 (Invitrogen), 0.5% glutamine (2 mM), and 1% penicillin streptomycin- neomycin antibiotic mixture. After 72 hr, this medium was

replaced with a glutamine free version of the same medium, and the cells were grown for 10 more days before experiments.

Preparation of labeled Aβ

Freeze-dried human synthetic Aβ42 labeled with HiLyteTM Fluor 555 at the C-terminus (oAβ−555) was purchased from AnaSpec (Fremont, CA). Protein solution was prepared as previously described[67]. Briefly, peptide was diluted to 1 mM in 1,1,1,3,3,3,-hexafluoro-2-propanol to disassemble preformed aggregates and stored as dry films at −20°C before use. The film was dissolved at 1 mM in DMSO, sonicated for 10 min, diluted to 100 μM in cold PBS, and incubated for 12 hr at 4°C to promote protein oligomerization. Aβ42-555-labeled preparation was purified with Amicon Ultra Centrifugal Filter (2 KDa) and then was resuspended in PBS at a concentration of 100 mM before final dilution in the culture medium.

Preparation of labeled Tau

oTau preparations were labeled with the IRIS-5-NHS active ester dye (IRIS-5; λex: 633 nm; λem: 650–700 nm; Cyanine Technology Turin, Italy) as previously described[9]. Briefly, Tau solutions (2 μM in PBS) were mixed with 6 mM IRIS-5 in DMSO for 4 hr in the dark under mild shaking conditions. After this time, labeled Tau was purified with Vivacon 500 ultrafiltration spin columns (Sartorius Stedim Biotech GmbH) and then resuspended in PBS and used at final concentration of 100 nM in the culture medium.

Assessment of oAβ and oTau entrance into neurons

WT and APP KO hippocampal neurons at 14 days in vitro were treated with either 200 nM Aβ42-555 or 100 nM oTau-IRIS5 for 20 min. After treatment cells were fixed with 4% paraformaldehyde in PBS for 10 min at RT, permeabilized for 15 min with 0.3% Triton X-100 [Sigma] in PBS, and incubated for 30 min with 0.3% BSA in PBS to block nonspecific binding sites. The primary antibody rabbit anti microtubule associated protein 2 (MAP2, Immunological Sciences, Rome, Italy; 1:200 overnight at 4°C for 90 min) and the corresponding secondary antibody Alexa Fluor 488 donkey anti-rabbit (Invitrogen 1:1000 for 90 min at RT) were then used to recognize neurons. Nuclei were counterstained with 4′,6-diamidino-2-phenylindole (DAPI, 0.5 μg/ml for 10 min; Invitrogen) and cells were coverslipped with ProLong Gold anti-fade reagent (Invitrogen), before being studied through high-resolution confocal microscopy. Confocal stacks made of images (512 × 512 pixels) were acquired with a confocal laser scanning system (Nikon A1 MP) and an oil-immersion objective (60× magnification; N.A. 1.4). Additional 2.5× magnification was applied to obtain a pixel size of 90 nm. Fluorescent dyes were excited with diode lasers (405, 488, 546 and 633 nm). The following criteria were used for spot detection: XY area ≥200 nm2; Z height ≥1.5 μm. The studied proteins were considered internalized when the overlapping of MAP2 fluorescence with the height of the fluorescent spots was greater than 65% (~1 μm). Conversely, they were considered attached to the neuronal surface when the fluorescence signals were close to each other, but with less than 30% overlap. Spots internalized in neurons were detected and counted by the Image J software, through an algorithm that automatically detects co-localization between MAP2 fluorescence and either Aβ555 or Tau-IRIS5. MAP2 fluorescence was binarized to form a mask of the fluorescence pattern for every single XY plane of the Z stacks, and this mask was multiplied plane-by-plane for the corresponding fluorescence of Aβ or Tau stacks. This operation selected only Aβ and Tau signals associated with MAP2-positive areas by deleting any Aβ and Tau signals unrelated to MAP-2 immunoreactivity. The resulting fluorescence signals gave an unbiased estimate of Aβ or Tau oligomers internalized in neurons within each microscopic field. The number of fluorescent spots were then counted by the

'analyze particle' macro of Image J after having done a maximum intensity projection of every Z stacks. To provide a global estimate of the protein uploading into neurons, internalization of oAβ and oTau was also quantified through the 'internalization index' obtained by multiplying the percentage of neurons internalizing fluorescent proteins by the mean number of fluorescent spots inside neurons. Assessment of fluorescent protein oligomers attached to the neuronal surface was carried out by spanning the XZ-YZ planes from Z stacks for every microscopic field acquired.

Behavioral studies

Intrahippocampal administration of oAβ and oTau

To perform intrahippocampal infusions of oligomers, mice underwent stereotaxic surgery for cannulas implantation. After anesthesia with Avertin (500 mg/Kg), mice were implanted with a 26-gauge guide cannula into the dorsal part of the hippocampi (coordinates from bregma: posterior = 2.46 mm, lateral = 1.50 mm to a depth of 1.30 mm). After 6–8 days of recovery, mice were bilaterally infused with oAβ or oTau preparations or vehicle in a final volume of 1 μl over 1 min with a microsyringe connected to the cannulas via polyethylene tubing. During infusion, animals were handled gently to minimize stress. After infusion, the needle was left in place for another minute to allow diffusion. In some animals, after behavioral studies, a solution of 4% methylene blue was infused for localization of infusion cannulas.

Fear conditioning

Fear conditioning was performed as previously described[30,31]. Our conditioning chamber, equipped with a camera placed on the top of the cage, was in a sound-attenuating box. The conditioning chamber had a bar insulated shock grid floor, removable. After each experimental test the floor was cleaned with 75% ethanol. Mice were handled once a day for 3 days before behavioral experiments. Only one animal at a time was present in the experimentation room. During the first day, mice were placed in the conditioning chamber for 2 min before the onset of a discrete tone [conditioned stimulus (CS)] (a sound that lasted 30 s at 2800 Hz and 85 dB). In the last 2 s of the CS, mice were given a foot shock [unconditioned stimulus (US)] of 0.80 mA for 2 s through the bars of the floor. After the CS/US pairing, the mice were left in the conditioning chamber for 30 s and then they were placed back in their home cages. Freezing behavior, defined as the absence of all movement except for that necessitated by breathing, was manually scored. During the second day, we evaluated the contextual fear learning. Mice were placed in the conditioning chamber and freezing was measured for five consecutive min. During the third day, we evaluated the cued fear learning. Mice were placed in a novel context (rectangular black cage with vanilla odorant) for 2 min (pre-CS test), after which they were exposed to the CS for 3 min (CS test), and freezing was measured. Sensory perception of the shock was determined 24 hr after the cued test through threshold assessment. Foot shock intensity started at 0.1 mA and increased by 0.1 mA every 30 s. We recorded the first visible, motor and vocal response.

2 day radial arm water maze (RAWM)

RAWM was performed as previously described[31]. During the first day, mice were trained in 15 trials to identify the platform location in a goal arm by alternating between a visible and a hidden platform from trial 1 to 12 (beginning with the visible platform in the assigned arm). In the last four trials (trial 13–15) only a hidden platform was utilized. During the second day the same procedure was repeated by using only the hidden platform from trial 1 to 15. An entrance into an arm with no platform, or failure to select an arm after 15 s was counted as an error and the mouse was gently pulled back to the start arm. The duration of each trial was up to 1 min.

At the end of each trial, mouse rested on the platform for 15 s. The goal arm was kept constant for all trials, with a different starting arm on successive trials. Data were analyzed and displayed as averages of blocks of 3 trials per mouse. A visible platform test was performed to control for possible motivational, visual and motor deficits. This consisted in a two-day test, with two sessions/day (each consisting of three 1 min trials), in which we recorded the time taken to reach a visible platform (randomly positioned in a different place each time) marked with a green flag.

Open field

Open Field was performed as previously described[9]. Our arena consisted in a white plastic bow divided into sectors (periphery and center) by black lines. Each mouse started the test randomly from one of the border, and was permitted to freely explore the arena for 5 min in two consecutive days. The test was performed in a quiet, darkened room and one light bulb provided a bright illumination. We scored the % time spent into the center and the number of entries into the center.

Electrophysiological recordings

Electrophysiological recordings were performed as previously described[35]. Briefly, transverse hippocampal slices (400 μm) were cut and transferred to a recording chamber where they were maintained at 29°C and perfused with ACSF (flow rate 2 ml/min) continuously bubbled with 95% O2 and 5% CO2. Field extracellular recordings were performed by stimulating the Schaeffer collateral fibers through a bipolar tungsten electrode and recording in CA1 stratum radiatum with a glass pipette filled with ACSF. After evaluation of basal synaptic transmission, a 15 min baseline was recorded every minute at an intensity eliciting a response approximately 35% of the maximum evoked response. LTP was induced through a theta-burst stimulation (4 pulses at 100 Hz, with the bursts repeated at 5 Hz and three tetani of 10-burst trains administered at 15 s intervals). Responses were recorded for 2 hr after tetanization and measured as field excitatory post-synaptic potentials (fEPSP) slope expressed as percentage of baseline.

Statistical analyses

All experiments were in blind with respect to treatment. All data were expressed as mean ± standard error mean (SEM). For experiments on oligomer entrance into cultured neurons pairwise comparisons were performed through Student's t test. Behavioral experiments were designed in a balanced fashion and, for each condition mice were trained and tested in three to four separate sets of experiments. Freezing, latency, time spent in the center of the arena and number of entries in the center were manually scored by an expert operator by using a video-tracking recording system. We used one-way ANOVA with Bonferroni post-hoc correction or ANOVA with repeated measures for comparisons among the four groups of mice. For electrophysiological recordings on slices, results were analyzed in pClamp 10 (Molecular Devices; RRID:SCR_011323) and compared by ANOVA with repeated measures considering 120 min of recording after tetanus or the 26th-30th recording points. Statistical analysis was performed by using Systat 9 software (Chicago, IL, USA; RRID:SCR_010455). For protein entrance into neurons we used Student's t-test to compare the internalization index between WT and APP KO neurons. The level of significance was set at $p<0.05$.

References

1. Shelkovnikova, T. A. *et al.* [Proteinopathies--forms of neurodegenerative disorders with protein aggregation-based pathology]. *Mol. Biol. (Mosk).* **46,** 402–15
2. Takalo, M., Salminen, A., Soininen, H., Hiltunen, M. & Haapasalo, A. Protein aggregation and degradation mechanisms in neurodegenerative diseases. *Am. J. Neurodegener. Dis.* **2,** 1–14 (2013).
3. Irvine, G. B., El-Agnaf, O. M., Shankar, G. M. & Walsh, D. M. Protein aggregation in the brain: the molecular basis for Alzheimer's and Parkinson's diseases. *Mol. Med.* **14,** 451–64 (2008).
4. Kopeikina, K. J., Hyman, B. T. & Spires-Jones, T. L. Soluble forms of tau are toxic in Alzheimer's disease. *Transl. Neurosci.* **3,** 223–233 (2012).
5. Hölttä, M. *et al.* Evaluating amyloid-β oligomers in cerebrospinal fluid as a biomarker for Alzheimer's disease. *PLoS One* **8,** e66381 (2013).
6. Sengupta, U. *et al.* Tau oligomers in cerebrospinal fluid in Alzheimer's disease. *Ann. Clin. Transl. Neurol.* **4,** 226–235 (2017).
7. Selkoe, D. J. Soluble oligomers of the amyloid β-protein impair synaptic plasticity and behavior. *Behavioural Brain Research* **192,** 106–113 (2008).
8. Lasagna-Reeves, C. A. *et al.* Alzheimer brain-derived tau oligomers propagate pathology from endogenous tau. *Sci. Rep.* **2,** 700 (2012).
9. Fa, M. *et al.* Extracellular tau oligomers produce an immediate impairment of LTP and memory. *Sci Rep* **6,** 39 (2016).
10. Lasagna-Reeves, C. A., Castillo-Carranza, D. L., Guerrero-Muoz, M. J., Jackson, G. R. & Kayed, R. Preparation and characterization of neurotoxic tau oligomers. *Biochemistry* **49,** 10039–41 (2010).
11. Kamenetz, F. *et al.* APP processing and synaptic function. *Neuron* **37,** 925–37 (2003).
12. Pooler, A. M., Phillips, E. C., Lau, D. H. W., Noble, W. & Hanger, D. P. Physiological release of endogenous tau is stimulated by neuronal activity. *EMBO Rep.* **14,** 389–394 (2013).
13. Yamada, K. *et al.* Neuronal activity regulates extracellular tau in vivo. *J. Exp. Med.* **211,** 387–393 (2014).
14. Frost, B., Jacks, R. L. & Diamond, M. I. Propagation of Tau Misfolding from the Outside to the Inside of a Cell. *J. Biol. Chem.* **284,** 12845–12852 (2009).
15. Lai, A. Y. & McLaurin, J. Mechanisms of amyloid-Beta Peptide uptake by neurons: the role of lipid rafts and lipid raft-associated proteins. *Int. J. Alzheimers. Dis.* **2011,** 548380 (2010).
16. Wu, J. W. *et al.* Small Misfolded Tau Species Are Internalized via Bulk Endocytosis and Anterogradely and Retrogradely Transported in Neurons. *J. Biol. Chem.* **288,** 1856–1870 (2013).
17. Lorenzo, A. *et al.* Amyloid beta interacts with the amyloid precursor protein: a potential toxic mechanism in Alzheimer's disease. *Nat. Neurosci.* **3,** 460–464 (2000).
18. Van Nostrand, W. E. *et al.* Localization of a fibrillar amyloid beta-protein binding domain on its precursor. *J. Biol. Chem.* **277,** 36392–8 (2002).
19. Shaked, G. M. *et al.* Abeta induces cell death by direct interaction with its cognate extracellular domain on APP (APP 597-624). *FASEB J.* **20,** 1254–1256 (2006).
20. Fogel, H. *et al.* APP homodimers transduce an amyloid-β-mediated increase in release probability at excitatory synapses. *Cell Rep.* **7,** 1560–1576 (2014).
21. Takahashi, M. *et al.* Extracellular association of APP and tau fibrils induces intracellular aggregate formation of tau. *Acta Neuropathol.* **129,** 895–907 (2015).
22. Deyts, C., Thinakaran, G. & Parent, A. T. APP Receptor? To Be or Not To Be. *Trends Pharmacol. Sci.* **37,** 390–411 (2016).
23. Cole, S. L. & Vassar, R. The Alzheimer's disease beta-secretase enzyme, BACE1. *Mol. Neurodegener.* **2,** 22 (2007).
24. De Strooper, B. Loss-of-function presenilin mutations in Alzheimer disease. Talking Point on the role of presenilin mutations in Alzheimer disease. *EMBO Rep.* **8,** 141–6 (2007).
25. Giaccone, G. *et al.* beta PP and Tau interaction. A possible link between amyloid and neurofibrillary tangles in Alzheimer's disease. *Am. J. Pathol.* **148,** 79–87 (1996).

26. Islam, K. & Levy, E. Carboxyl-terminal fragments of beta-amyloid precursor protein bind to microtubules and the associated protein tau. *Am J Pathol* **151,** 265–271 (1997).
27. Smith, M. A. *et al.* Tau protein directly interacts with the amyloid beta-protein precursor: implications for Alzheimer's disease. *Nat. Med.* **1,** 365–9 (1995).
28. Ripoli, C. *et al.* Intracellular accumulation of amyloid-β (Aβ) protein plays a major role in Aβ-induced alterations of glutamatergic synaptic transmission and plasticity. *J. Neurosci.* **34,** 12893–903 (2014).
29. Puzzo, D., Lee, L., Palmeri, A., Calabrese, G. & Arancio, O. Behavioral assays with mouse models of Alzheimer's disease: practical considerations and guidelines. *Biochem. Pharmacol.* **88,** 450–67 (2014).
30. Fiorito, J. *et al.* Synthesis of quinoline derivatives: discovery of a potent and selective phosphodiesterase 5 inhibitor for the treatment of Alzheimer's disease. *Eur. J. Med. Chem.* **60,** 285–94 (2013).
31. Watterson, D. M. *et al.* Development of Novel In Vivo Chemical Probes to Address CNS Protein Kinase Involvement in Synaptic Dysfunction. *PLoS One* **8,** e66226 (2013).
32. Senechal, Y., Kelly, P. H. & Dev, K. K. Amyloid precursor protein knockout mice show age-dependent deficits in passive avoidance learning. *Behav. Brain Res.* **186,** 126–32 (2008).
33. Phillips, R. G. & LeDoux, J. E. Differential contribution of amygdala and hippocampus to cued and contextual fear conditioning. *Behav. Neurosci.* **106,** 274–85 (1992).
34. Bliss, T. V & Collingridge, G. L. A synaptic model of memory: long-term potentiation in the hippocampus. *Nature* **361,** 31–9 (1993).
35. Puzzo, D. *et al.* Amyloid-beta peptide inhibits activation of the nitric oxide/cGMP/cAMP-responsive element-binding protein pathway during hippocampal synaptic plasticity. *J. Neurosci.* **25,** 6887–97 (2005).
36. Luo, Y. *et al.* Mice deficient in BACE1, the Alzheimer's beta-secretase, have normal phenotype and abolished beta-amyloid generation. *Nat. Neurosci.* **4,** 231–2 (2001).
37. Del Prete, D., Lombino, F., Liu, X. & D'Adamio, L. APP is cleaved by Bace1 in pre-synaptic vesicles and establishes a pre-synaptic interactome, via its intracellular domain, with molecular complexes that regulate pre-synaptic vesicles functions. *PLoS One* **9,** e108576 (2014).
38. Wineman-Fisher, V., Tudorachi, L., Nissim, E. & Miller, Y. The removal of disulfide bonds in amylin oligomers leads to the conformational change of the 'native' amylin oligomers. *Phys. Chem. Chem. Phys.* **18,** 12438–42 (2016).
39. Banks, W. A., Kastin, A. J., Maness, L. M., Huang, W. & Jaspan, J. B. Permeability of the blood-brain barrier to amylin. *Life Sci.* **57,** 1993–2001 (1995).
40. Jhamandas, J. H. *et al.* Actions of β-amyloid protein on human neurons are expressed through the amylin receptor. *Am. J. Pathol.* **178,** 140–9 (2011).
41. Kimura, R., MacTavish, D., Yang, J., Westaway, D. & Jhamandas, J. H. Beta amyloid-induced depression of hippocampal long-term potentiation is mediated through the amylin receptor. *J. Neurosci.* **32,** 17401–6 (2012).
42. Bakker, A. *et al.* Reduction of Hippocampal Hyperactivity Improves Cognition in Amnestic Mild Cognitive Impairment. *Neuron* **74,** 467–474 (2012).
43. Busche, M. A. *et al.* Critical role of soluble amyloid-β for early hippocampal hyperactivity in a mouse model of Alzheimer's disease. *Proc. Natl. Acad. Sci. U. S. A.* **109,** 8740–5 (2012).
44. Palop, J. J. *et al.* Aberrant Excitatory Neuronal Activity and Compensatory Remodeling of Inhibitory Hippocampal Circuits in Mouse Models of Alzheimer's Disease. *Neuron* **55,** 697–711 (2007).
45. Verret, L. *et al.* Inhibitory interneuron deficit links altered network activity and cognitive dysfunction in alzheimer model. *Cell* **149,** 708–721 (2012).
46. Vossel, K. A. *et al.* Seizures and Epileptiform Activity in the Early Stages of Alzheimer Disease. *JAMA Neurol.* **70,** 1158 (2013).
47. Koppensteiner, P. *et al.* Time-dependent reversal of synaptic plasticity induced by physiological concentrations of oligomeric Aβ42: an early index of Alzheimer's disease. *Sci. Rep.* **6,** 32553 (2016).
48. Gendreau, K. L. & Hall, G. F. Tangles, Toxicity, and Tau Secretion in AD - New Approaches

to a Vexing Problem. *Front. Neurol.* **4,** 160 (2013).
49. Muller, U. C. & Zheng, H. Physiological Functions of APP Family Proteins. *Cold Spring Harb. Perspect. Med.* **2,** a006288–a006288 (2012).
50. Holmes, B. B. *et al.* Heparan sulfate proteoglycans mediate internalization and propagation of specific proteopathic seeds. *Proc. Natl Acad. Sci. USA* **110,** E3138–E3147 (2013).
51. Lindahl, U. & Li, J. Interactions between heparan sulfate and proteins-design and functional implications. *Int. Rev. Cell Mol. Biol.* **276,** 105–59 (2009).
52. Mirbaha, H., Holmes, B. B., Sanders, D. W., Bieschke, J. & Diamond, M. I. Tau Trimers Are the Minimal Propagation Unit Spontaneously Internalized to Seed Intracellular Aggregation. *J. Biol. Chem.* **290,** 14893–903 (2015).
53. Sandwall, E. *et al.* Heparan sulfate mediates amyloid-beta internalization and cytotoxicity. *Glycobiology* **20,** 533–41 (2010).
54. Reinhard, C., Borgers, M., David, G. & De Strooper, B. Soluble amyloid-β precursor protein binds its cell surface receptor in a cooperative fashion with glypican and syndecan proteoglycans. *J. Cell Sci.* **126,** 4856–61 (2013).
55. Cappai, R. *et al.* The amyloid precursor protein (APP) of Alzheimer disease and its paralog, APLP2, modulate the Cu/Zn-Nitric Oxide-catalyzed degradation of glypican-1 heparan sulfate in vivo. *J. Biol. Chem.* **280,** 13913–20 (2005).
56. Cizas, P. *et al.* Size-dependent neurotoxicity of beta-amyloid oligomers. *Arch. Biochem. Biophys.* **496,** 84–92 (2010).
57. Fraser, S. P., Suh, Y. H., Chong, Y. H. & Djamgoz, M. B. A. Membrane Currents Induced In Xenopus Oocytes By the C-Terminal Fragment Of the Beta-Amyloid Precursor Protein. *J. Neurochem.* **66,** 2034–2040 (1996).
58. Kayed, R. *et al.* Permeabilization of lipid bilayers is a common conformation-dependent activity of soluble amyloid oligomers in protein misfolding diseases. *J. Biol. Chem.* **279,** 46363–46366 (2004).
59. Fraser, S. P., Suh, Y. H. & Djamgoz, M. B. Ionic effects of the Alzheimer's disease beta-amyloid precursor protein and its metabolic fragments. *Trends Neurosci.* **20,** 67–72 (1997).
60. Nordstedt, C., Caporaso, G. L., Thyberg, J., Gandy, S. E. & Greengard, P. Identification of the Alzheimer beta/A4 amyloid precursor protein in clathrin-coated vesicles purified from PC12 cells. *J. Biol. Chem.* **268,** 608–12 (1993).
61. Lombino, F., Biundo, F., Tamayev, R., Arancio, O. & D'Adamio, L. An intracellular threonine of amyloid-β precursor protein mediates synaptic plasticity deficits and memory loss. *PLoS One* **8,** e57120 (2013).
62. Cao, X. & Südhof, T. C. A transcriptionally [correction of transcriptively] active complex of APP with Fe65 and histone acetyltransferase Tip60. *Science* **293,** 115–20 (2001).
63. Mathews, P. M. *et al.* Calpain activity regulates the cell surface distribution of amyloid precursor protein. Inhibition of calpains enhances endosomal generation of beta-cleaved C-terminal APP fragments. *J. Biol. Chem.* **277,** 36415–24 (2002).
64. Wu, Y., Li, Q. & Chen, X.-Z. Detecting protein-protein interactions by Far western blotting. *Nat. Protoc.* **2,** 3278–84 (2007).
65. Piacentini, R. *et al.* Herpes Simplex Virus type-1 infection induces synaptic dysfunction in cultured cortical neurons via GSK-3 activation and intraneuronal amyloid-β protein accumulation. *Sci. Rep.* **5,** 15444 (2015).
66. Scala, F. *et al.* Intraneuronal Aβ accumulation induces hippocampal neuron hyperexcitability through A-type K+ current inhibition mediated by activation of caspases and GSK-3. *Neurobiol. Aging* **36,** 886–900 (2015).
67. Ripoli, C. *et al.* Effects of different amyloid β-protein analogues on synaptic function. *Neurobiol. Aging* **34,** 1032–1044 (2013).

Concluding remarks

"We have to remember that what we observe is not nature herself,
but nature exposed to our method of questioning."
Werner Heisenberg

Aβ and tau share several features leading to common mechanisms of toxicity, regardless of their different sequence (Table 1). This was predicted by a study showing that all of the soluble oligomers tested including α-synuclein, islet amyloid polypeptide, polyglutamine, lysozyme, human insulin, and prion peptide, display a common conformation-dependent structure that is unique to soluble oligomers[1].

	AMYLOID-β PEPTIDE	TAU PROTEIN
Physiological functions	• Neuronal growth • Neurotransmitter release • Synaptic transmission and plasticity • Memory formation • Immune response • Anti-oxidant properties	• Microtubule assembly and stabilization • Axon elongation • Synaptic plasticity • Nuclear function
Isoforms	Aβ40, Aβ42, other fragments	3R-4R, 1N-2N
Aggregation sequence	Monomers → Oligomers → Fibrils → Senile plaques	Tau hyperphosphorylation → PHFs → NFTs
Insoluble and soluble forms	• Poor correlation between senile plaques and cognitive impairment • High correlation between oligomers and cognitive impairment • Oligomers increase in brains and CSF of AD patients vs. controls	• Poor correlation between NFTs and cognitive impairment • High correlation between oligomers and cognitive impairment • Oligomers increase in brains and CSF of AD patients vs. controls
Genetic mutations	APP, PS1 and PS2 linked to FAD	MAPT linked to FTDP-17, PSP, CBD
Synaptic target	CREB, CamKII, BDNF among others	CREB, CamKII, BDNF among others
Extra- and intracellular dynamic	• Activity dependent secretion • Neuronal and glia uptake • Extracellular toxicity • Intracellular toxicity	• Neuronal activity dependent • Neuronal and glia uptake • Extracellular toxicity • Intracellular toxicity
Spreading	EC → Hippocampus → Cortex	EC → Hippocampus → Cortex
APP-dependent mechanism	• APP binding • Neuronal and glial uptake • Synaptic plasticity impairment • Memory impairment	• APP binding • Neuronal and glial uptake • Synaptic plasticity impairment • Memory impairment

Table 1. PHFs, paired helical filaments; NFTs, neurofibrillary tangles; CSF, cerebrospinal fluid; AβPP, amyloid-β protein precursor; PS, presenilin; FAD, familiar Alzheimer's disease; MAPT, microtubule-associated protein tau; FTPD-17, frontotemporal dementia with parkinsonism-17; PSP, progressive supranuclear palsy; CBD, corticobasal degeneration; CREB, cAMP response element binding protein; CaMKII, Ca2+/calmodulin-dependent protein kinase II; BDNF, brain-derived neurotrophic factor; EC, entorhinal cortex.

By now, a variety of studies have demonstrated that soluble oligomeric forms of Aβ and tau, more than their aggregates, are increased in the diseased brain, are detectable in the CSF, and are highly correlated with cognitive impairment. The deleterious effect of Aβ and tau occurs at the synapse, where they interfere with molecular pathways needed for synaptic plasticity and memory. The capability of neuronal and glial cells to release and internalize Aβ and tau contributes to spread of the disease from specific areas, such as EC and the hippocampus, to the entire brain. Despite these studies have certainly clarified several aspects of AD onset and progression, the crosstalk between Aβ and tau in the diseased brain is still a matter of debate. The most common view in the AD field is based on the "Amyloid Cascade Hypothesis" and suggests that the initial increase of Aβ induces amyloid and tau pathology over time (Fig. 1).

This temporal sequence derives from studies in patients with FAD, where the genetic-driven increase of Aβ is followed by NFT accumulation[2], whereas the increase of tau, as in tauopathies, is not associated with Aβ deposition. Preclinical studies have confirmed that oligomers of Aβ can trigger tau pathology[3] and, conversely, when knocking down tau, Aβ toxic effects are prevented[4,5]. Interestingly, recent work has demonstrated that Aβ acutely induces tubulin post-translational modifications and stabilizes dynamic microtubules promoting tau-dependent loss of dendritic spines and tau hyperphosphorylation[6]. Thus, Aβ has been thought to act upstream of tau in the pathogenesis of the disease. However, our recent works have challenged this scenario. We have demonstrated that oligomers of both Aβ and tau produce an immediate reduction of synaptic plasticity and memory when extracellularly applied and that these detrimental effects occur not only with high concentrations of Aβ or tau alone, but also when sub-toxic doses of oligomeric Aβ are combined with sub-toxic doses of oligomeric tau[7].

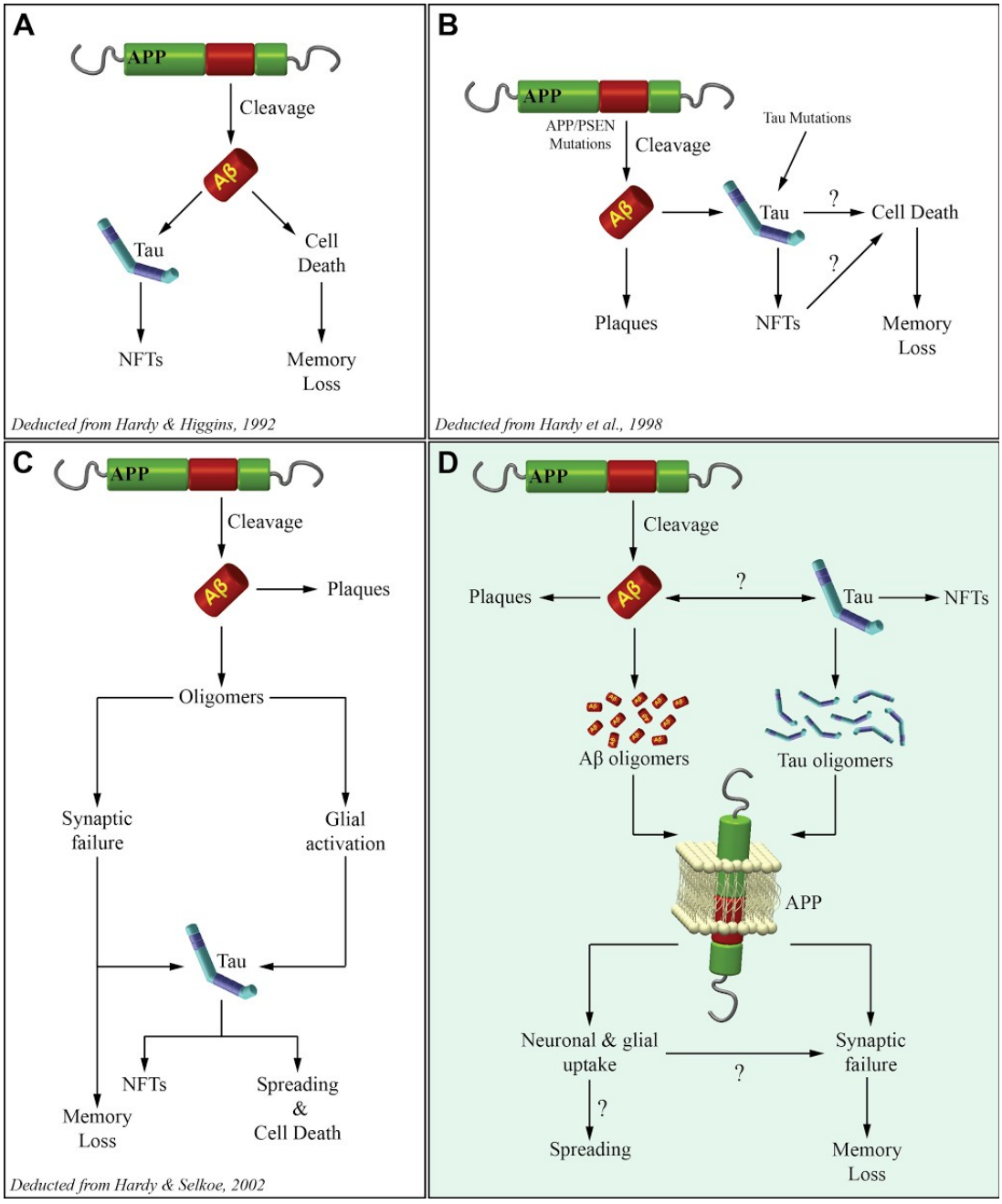

Fig.1 Different views of Aβ and tau interaction in AD pathogenesis. The Amyloid Cascade Hypothesis has dominated the AD field for several years. This picture describes how it has been updated over time from the beginning (A), to the discovery of genetic mutations involving both Aβ and tau production (B), to a more complex vision recognizing oligomers as the toxic Aβ species (C). Notably, in A-C Aβ acts upstream tau. D) According to our novel vision, both oligomers of Aβ and tau exert a neurotoxic effect mediated by AβPP leading to synaptic and memory dysfunction. AβPP also mediates oligomers entrance into neurons and glial cells, a mechanism probably contributing to the spreading of the disease throughout the brain.

These observations suggested that: 1) Aβ and tau might act at the same level or on different targets that later converge on a common molecular mechanism; 2) the two proteins are able to impair synaptic plasticity and memory per se, i.e., regardless of the presence of high concentrations of one another; and 3) elevated levels of Aβ are not needed to initiate the tau-mediated toxic events leading to synaptic dysfunction. Inspired by these data, we have recently focused on the possible common mechanism of action for extracellular Aβ and tau oligomers to impair LTP and memory. We found that both oligomers of Aβ and tau require APP to exert their deleterious effect at the synapse[8], in agreement with previous observations indicating that APP mediates extracellular Aβ neurotoxicity[9–11], and a recent study showing that APP is required for binding of human brain-derived oligomers to synapses and disruption of synaptic plasticity[12]. Our findings are also consistent with the observation that APP is involved in AD hippocampal hyperactivity[13–17]. Previous papers have already shown that oligomeric Aβ is able to bind APP[18], whereas APP and tau interaction was studied several years ago in the context of NFTs[19–21]. We have now provided evidence that soluble oligomeric tau is able to bind APP[8]. This binding might be related to the APP-mediated uptake of Aβ and tau, since APP influences accumulation of tau fibrils in cultured cells[22] and is needed for the entrance of oligomeric Aβ and tau into neurons[8] and astrocytes[23]. Based on these findings, we hypothesize that APP-mediated oligomer uptake plays a role in AD pathogenesis. Indeed, because Aβ and tau do not impair synaptic plasticity and memory in APP KO mice, APP binding and/or APP-mediated internalization of the two proteins should lead to LTP and memory reduction, even if one cannot exclude the possibility that Aβ and tau act on other targets, or that their intraneuronal accumulation does not directly inhibit the synaptic machinery. However, a previous observation indicating that blocking intracellular Aβ rescues the LTP impairment induced by administration of extracellular Aβ[8] supports the hypothesis that Aβ intraneuronal uptake is critical for the impairment of synaptic plasticity. On the other hand, recent studies have evidenced that the APP-dependent accumulation of extracellular tau oligomers in astrocytes induces a disruption of calcium signaling

which in turn disrupts synaptic function in neighboring neurons[23]. Interestingly, while it has been previously demonstrated that extracellular Aβ requires APP cleavage to permit intraneuronal Aβ accumulation[24], our results have excluded that the toxicity of extracellular Aβ and tau oligomers on LTP depends upon amyloidogenic processing of APP since BACE KO mice still present the impairment of LTP induced by the two oligomeric proteins[8]. The requirement for APP to lead to intracellular entrance of Aβ and tau oligomers to produce synaptic dysfunction and memory loss begs the question of how this occurs. Whether APP acts as a channel permeable to the oligomers[25,26], or induces the formation of pores across the membrane to let oligomers enter the cell[27], or promotes endocytosis of the oligomers[28], is still under investigation. Another possibility is that when Aβ and tau oligomers bind APP, they lead to the activation of its intracellular portion, AID/AICD, triggering either a structural change, for example inducing a different APP conformation, or a functional effect, for example activating or inhibiting molecular cascades involved in synaptic plasticity and memory. Interestingly, it is known that AID/AICD might stimulate transcription by forming a multimeric complex with the nuclear adaptor protein Fe65 and the histone acetyltransferase Tip60[29]. It has been also shown that APP-dependent transcription mediated by Fe65 is blocked by the cell death mediator p75, which is able to bind APP altering its processing[30]. Another possible mechanism might involve APP phosphorylation at specific intracellular sites. For example, it has been demonstrated that APP phosphorylation of Thr668, which regulates docking sites for intracellular proteins that interact with APP, is increased in AD cases[31] and knock-in mouse bearing a Thr(668)Ala mutation preventing phosphorylation at this site protects against abnormal synaptic plasticity and memory when crossed with a mouse model of dementia[32]. Our model placing extracellular Aβ and tau in parallel and upstream of APP does not exclude the possibility that the two proteins involve other molecules to produce detrimental effects in addition to synaptic plasticity and memory impairment, nor the possibility that some deleterious effects need the other protein for the effect itself to be present (i.e., Aβ might require tau for some of the pathologies to occur). Consistent with this scenario, AD is a complex condition involving multiple aspects in

addition to memory, a phenomenon that is likely dependent upon synaptic activity and that has greatly influenced our critical analysis of the current literature because it represents the clinical hallmark of AD. Furthermore, as shown in Table 1, some of the physiological functions of the two proteins are different with Aβ playing a major role in neuronal growth and synaptic plasticity and tau in axonal elongation and microtubule assembly and stabilization. Then, in light of the different affinities that Aβ has towards its multiple targets, it is likely that as the concentration of the peptide increases with worsening of the pathology new pathways are affected by the disease. In any case, demonstrating that APP serves as a Trojan horse to mediate synaptic plasticity and memory impairment by extracellular oligomers of both Aβ and tau, challenges the prevailing hypothesis in the AD field stating that Aβ triggers tau pathology. According to our findings, Aβ and tau do not act in series but in parallel, both through APP (Fig. 1). Now, it would be desirable to understand whether and how the involvement of APP is limited to Aβ and tau entrance into cells or also underlies the derangement of molecular mechanisms involved in synaptic plasticity and memory. In any case, this new player might be taken into consideration when studying the pathogenesis of AD. For example, further studies should be performed to understand the exact mechanisms of APP-mediated entrance of oligomers inside neurons and glial cells and whether this might initially represent a compensatory mechanism aimed at clearing toxic oligomers from the synaptic cleft. The consequences of the model underlying AD pathology proposed in the current review are notable from a drug discovery point of view. The first thought is that therapies targeting tau might notwork similarly to the failure of anti-Aβ therapies, as Aβ might still exercise its detrimental effects independent of tau and vice versa. Most important, given the convergence of Aβ and tau onto APP, a fascinating possibility is that therapies acting onto APP might be more efficacious than those acting solely against Aβ or tau. Furthermore, an approach directed against APP would have the advantage of overcoming obstacles offered by the physiological functions of Aβ and tau that might occur independently of their action onto APP and might still be present if one decides to simultaneously target Aβ and tau, an approach that is also suggested by our model. A strategy directed against APP will likely have

its own drawbacks including physiological functions of full length APP[33]. Nevertheless, APP offers the flexibility of having multiple sites undergoing post-translational modifications that could be exploited as a tool to selectively affect a putative APP-dependent toxicity of Aβ and tau oligomers[34]. To this end, the APP phosphorylation at Thr668 is very interesting because it has been suggested that averting its noxious role in synaptic plasticity and memory might serve as a therapeutic strategy for human dementias[32]. Consistent with this finding it has been shown that overexpression of the protein phosphatase 2A (PP2A) methyltransferase, leucine carboxyl methyltransferase-1, leads to a decrease in APP phosphorylation at the PP2Asensitive Thr-668 site and protects mice against Aβ-induced damage of synaptic plasticity and memory[35]. Certainly, our hypothesis paves the way to an increased interest toward APP, a molecule that has been taken into account mostly for its role as an Aβ generator, being, in our opinion, unfortunately overshadowed by its own child, Aβ.

In conclusion, after more than one century of research in the AD field, several questions remain to be answered especially on the role of the two main actors, Aβ and tau, in the pathogenesis of the disease. It is certain that their interactions at the synapse need to be further elucidated and new players such as APP should enter the stage to get a clearer picture of this intricate disease.

References

1. Kayed, R. *et al.* Common structure of soluble amyloid oligomers implies common mechanism of pathogenesis. *Science* **300,** 486–9 (2003).
2. Bateman, R. J. *et al.* Clinical and Biomarker Changes in Dominantly Inherited Alzheimer's Disease. *N. Engl. J. Med.* **367,** 795–804 (2012).
3. Shankar, G. M. *et al.* Amyloid-β protein dimers isolated directly from Alzheimer's brains impair synaptic plasticity and memory. *Nat. Med.* **14,** 837–842 (2008).
4. Jin, M. *et al.* Soluble amyloid -protein dimers isolated from Alzheimer cortex directly induce Tau hyperphosphorylation. in *and neuritic degeneration. Proc Natl Acad Sci U S A 108* **108,** 5819–5824 (2011).
5. Roberson, E. D. *et al.* Reducing endogenous tau ameliorates amyloid [beta]-induced deficits in an Alzheimer's disease mouse model. *Science (80-.).* **316,** 750–754 (2007).
6. Qu, X. *et al.* Stabilization of dynamic microtubules by mDia1 drives Tau-dependent Aβ1-42synaptotoxicity. *J. Cell Biol.* **216,** 3161–3178 (2017).
7. Fa, M. *et al.* Extracellular tau oligomers produce an immediate impairment of LTP and memory. *Sci Rep* **6,** 39 (2016).
8. Puzzo, D. *et al.* LTP and memory impairment caused by extracellular Aβ and Tau oligomers is APP-dependent. *Elife* **6,** (2017).
9. Tampellini, D. *et al.* Synaptic Activity Reduces Intraneuronal A , Promotes APP Transport to Synapses, and Protects against A -Related Synaptic Alterations. *J. Neurosci.* **29,** 9704–9713 (2009).
10. Lorenzo, A. *et al.* Amyloid beta interacts with the amyloid precursor protein: a potential toxic mechanism in Alzheimer's disease. *Nat. Neurosci.* **3,** 460–464 (2000).
11. Shaked, G. M. *et al.* Abeta induces cell death by direct interaction with its cognate extracellular domain on APP (APP 597-624). *FASEB J.* **20,** 1254–1256 (2006).
12. Wang, Z. *et al.* Human Brain-Derived Aβ Oligomers Bind to Synapses and Disrupt Synaptic Activity in a Manner That Requires APP. *J. Neurosci.* **37,** 11947–11966 (2017).
13. Vossel, K. A. *et al.* Seizures and Epileptiform Activity in the Early Stages of Alzheimer Disease. *JAMA Neurol.* **70,** 1158 (2013).
14. Bakker, A. *et al.* Reduction of Hippocampal Hyperactivity Improves Cognition in Amnestic Mild Cognitive Impairment. *Neuron* **74,** 467–474 (2012).
15. Busche, M. A. *et al.* Critical role of soluble amyloid-β for early hippocampal hyperactivity in a mouse model of Alzheimer's disease. *Proc. Natl. Acad. Sci. U. S. A.* **109,** 8740–5 (2012).
16. Palop, J. J. *et al.* Aberrant Excitatory Neuronal Activity and Compensatory Remodeling of Inhibitory Hippocampal Circuits in Mouse Models of Alzheimer's Disease. *Neuron* **55,** 697–711 (2007).
17. Verret, L. *et al.* Inhibitory interneuron deficit links altered network activity and cognitive dysfunction in alzheimer model. *Cell* **149,** 708–721 (2012).
18. Fogel, H. *et al.* APP homodimers transduce an amyloid-β-mediated increase in release probability at excitatory synapses. *Cell Rep.* **7,** 1560–1576 (2014).
19. Smith, M. A. *et al.* Tau protein directly interacts with the amyloid beta-protein precursor: implications for Alzheimer's disease. *Nat. Med.* **1,** 365–9 (1995).
20. Giaccone, G. *et al.* beta PP and Tau interaction. A possible link between amyloid and neurofibrillary tangles in Alzheimer's disease. *Am. J. Pathol.* **148,** 79–87 (1996).
21. Islam, K. & Levy, E. Carboxyl-terminal fragments of beta-amyloid precursor protein bind to microtubules and the associated protein tau. *Am J Pathol* **151,** 265–271 (1997).
22. Takahashi, M. *et al.* Extracellular association of APP and tau fibrils induces intracellular aggregate formation of tau. *Acta Neuropathol.* **129,** 895–907 (2015).
23. Piacentini, R. *et al.* Reduced gliotransmitter release from astrocytes mediates tau-induced synaptic dysfunction in cultured hippocampal neurons. *Glia* **65,** 1302–1316 (2017).
24. Tampellini, D. Synaptic activity and Alzheimer's disease: A critical update. *Front. Neurosci.* **9,** 1–7 (2015).

25. Fraser, S. P., Suh, Y. H., Chong, Y. H. & Djamgoz, M. B. A. Membrane Currents Induced In Xenopus Oocytes By the C-Terminal Fragment Of the Beta-Amyloid Precursor Protein. *J. Neurochem.* **66,** 2034–2040 (1996).
26. Fraser, S. P., Suh, Y. H. & Djamgoz, M. B. Ionic effects of the Alzheimer's disease beta-amyloid precursor protein and its metabolic fragments. *Trends Neurosci.* **20,** 67–72 (1997).
27. Kayed, R. *et al.* Permeabilization of lipid bilayers is a common conformation-dependent activity of soluble amyloid oligomers in protein misfolding diseases. *J. Biol. Chem.* **279,** 46363–46366 (2004).
28. Xu, W. *et al.* Amyloid precursor protein-mediated endocytic pathway disruption induces axonal dysfunction and neurodegeneration. *J. Clin. Invest.* **126,** 1815–1833 (2016).
29. Cao, X. A Transcriptively Active Complex of APP with Fe65 and Histone Acetyltransferase Tip60. *Science (80-.).* **293,** 115–120 (2001).
30. Fombonne, J., Rabizadeh, S., Banwait, S., Mehlen, P. & Bredesen, D. E. Selective vulnerability in Alzheimer's disease: amyloid precursor protein and p75(NTR) interaction. *Ann. Neurol.* **65,** 294–303 (2009).
31. Shin, R.-W. *et al.* Amyloid precursor protein cytoplasmic domain with phospho-Thr668 accumulates in Alzheimer's disease and its transgenic models: a role to mediate interaction of Abeta and tau. *Acta Neuropathol.* **113,** 627–36 (2007).
32. Lombino, F., Biundo, F., Tamayev, R., Arancio, O. & D'Adamio, L. An intracellular threonine of amyloid-β precursor protein mediates synaptic plasticity deficits and memory loss. *PLoS One* **8,** e57120 (2013).
33. Muller, U. C. & Zheng, H. Physiological Functions of APP Family Proteins. *Cold Spring Harb. Perspect. Med.* **2,** a006288–a006288 (2012).
34. Saito, Y., Matsushima, T. & Suzuki, T. Mechanism of Alzheimer Amyloid β-Protein Precursor Localization to Membrane Lipid Rafts. in *Understanding Alzheimer's Disease* (ed. Zerr, I.) (InTech, 2013). doi:10.5772/54096
35. Nicholls, R. E. *et al.* PP2A methylation controls sensitivity and resistance to β-amyloid–induced cognitive and electrophysiological impairments. *Proc. Natl. Acad. Sci.* **113,** 3347–3352 (2016).